# Studies on the regulation of Hypoxia Inducible Factor 1 (HIF-1) in normoxia

Sarah F. Smart

July 2014

Department of Biological Sciences
Royal Holloway, University of London
Egham
Surrey
TW20 0EX

A thesis submitted for the degree of
Master of Philosophy of the University of London.

# Declaration of Authorship

I Sarah Smart hereby declare that this thesis and the work presented in it is entirely my own. Where I have consulted the work of others, this is always clearly stated.

Signed:

Date:

# Abstract

Hypoxia, the state of low levels of oxygen concentration in tissue, results in the up-regulation of heterodimeric transcription factors called hypoxia inducible factors (HIFs) of which HIF-1, consisting of the sub-units HIF-1α and ARNT, is the most globally expressed. HIF up-regulation results in the transcriptional activation of genes whose protein products participate in the cellular adaptation to hypoxia. In normoxia, HIF-1α is targeted for proteasomal degradation by a ubiquitin ligase complex containing the tumour suppressor pVHL. VHL disease, an inherited cancer syndrome, results in inactivation of the gene encoding pVHL, and thus disregulation of HIF-α degradation. Altered HIF function has also been identified as a major contributory factor in several major diseases including ischaemia and tumourigenesis.

In order to modulate HIF function in normoxia, RNA aptamers were targeted to the HIF-1α oxygen dependent degradation domain and their effect on the transcription of a hypoxia responsive target gene was assessed. RNA aptamers were successfully produced but appeared to have little or no effect on a hypoxia responsive target gene possibly as a result of the mixed aptamer pool containing aptamers that increased transcriptional activity as well as those that decreased transcriptional activity which resulted in the observation of little or no effect on an a hypoxia responsive target gene .

Pheochromocytoma, a tumour associated with VHL disease, also occurs as a result of inactivating mutations in *SDH B, SDH C* and *SDH D*, three of the four sub-units of mitochondrial complex II/succinate dehydrogenase (SDH). Similarities in tumour type suggested that inactivation of *SDH B-D* would have an impact on HIF-1α regulation. Cells were treated with an SDH inhibitor: 3-NPA, which resulted in increased HIF-1α protein levels, yet unexpectedly decreased ARNT and PTEN protein levels. Specific targeting of *SDH B* with siRNA resulted in the suppression of HIF-1α and GLUT-1 protein levels that were not due to an off target effect of the siRNA. The discovery that regulation of HIF is a factor in a metabolic cancer

syndrome emphasises the need for research into new therapeutic strategies such as those that could be offered by small molecule technologies.

# Acknowledgements

Thanks must go to the BBSRC as my sponsor and to Oxford BioMedica for providing financial support for the project and use of their facilities. I would particularly like to thank Stuart Naylor, Katie Binley and Sharifah Iqball of Oxford Biomedica for their assistance and helpful discussions. I am indebted to Mark Crompton, my original supervisor, who provided so much support and whose insightful discussions and probing scientific questions have helped me to become the scientist I am today. I am particularly grateful to Mark for continuing to support me when his career took him onto pastures new. I would like to thank Chris Rider for becoming my supervisor and also for helping to clarify some of my written work for those not familiar with the project.

On a more personal note I would like to thank Amanda Harvey and Joanna Tupper (the rest of the lab), for their support and endless offers to read anything to do with 'the book'. Thanks must also go to my vast array of friends who have been so supportive and have known just when not to ask anything by the look on my face. Last and by no means least, I must thank my husband David Bolton for supporting me through both the good and bad writing days and for continuing to believe that no matter how long it takes, I am capable of completing my thesis.

# Table of Contents

# List of Figures

**Figure** **Page**

# List of Tables

# Abbreviations

| | |
|---|---|
| °C | degrees Celsius |
| µg | micrograms |
| µl | microlitres |
| µM | micromolar |
| •NO | NO radical |
| 17-AAG | 17-allylamino-17-demethoxygeldanamycin |
| 2OG | 2-oxoglutarate |
| 3-NPA | 3-nitropropionic acid |
| A | alanine |
| aa | amino acid |
| AD-1 | transcriptional activation domain 1 |
| ADM | adrenomedullin |
| AhR | aryl hydrocarbon receptor |
| AMF | autocrine motility factor |
| AP | associated protein |
| AP-1 | activator protein-1 |
| ARD-1 | arrest defective-1 |
| ARNT | aryl hydrocarbon receptor nuclear translocator |
| ASK1 | apoptosis signal-regulating kinase 1 |
| ASPs | apparently sporadic pheochromocytomas |
| ATCC | American type culture collection |
| ATF | activating transcription factor |
| ATP | adenosine triphosphate |
| BAD | BCL2 antagonist of cell death |
| BB-BSA | binding buffer containing BSA |
| bHLH | basic-helix-loop-helix |
| BMAL1 | brain-muscle-ARNT-like protein 1 |
| BMAL2 | brain-muscle-ARNT-like protein 2 |
| bp | base pairs |
| BSA | bovine serum albumin |
| BTM | basal transcription machinery |
| C | cystine |
| *C. elegans* | *Caenhorabditis elegans* |
| CB | carotid body |
| CBP | CREB binding protein |
| CH | cysteine-histidine rich region |
| CITED2 | CBP/p300 interacting transactivator with ED-rich tail 2 |
| CITED4 | CBP/p300 interacting transactivator with ED-rich tail 4 |
| CMV | cytomegalovirus |
| $CO_2$ | carbon dioxide |
| CP | core particle |
| CREB | cyclic adenosine monophosphate response element transcription factor |
| C-TAD/CAD | C-terminal transactivation domain |
| Cul2 | cullin 2 |
| D | aspartic acid |
| DCF | highly fluorescent 2,7-dichlorofluorescein |
| DCFH | 2,7-dichlorofluorescein |

| | |
|---|---|
| DCFH-DA | 2,7-dichlorofluorescein-diacetate |
| DEC1 | deleted in esophageal cancer 1 |
| DEC2 | deleted in esophageal cancer 2 |
| DFO | desferrioxamine/deferoxamine mesylate |
| $dH_2O$ | distilled water |
| DMEM | Dulbecco's modified eagle medium |
| *dmHPH* | *Drosophila melanogaster* HIF prolyl hydroxylase |
| DNA | deoxyribonucleic acid |
| dNTP | deoxynucleotide triphosphate |
| DUB | de-ubiquitinating enzyme |
| E | glutamic acid |
| *E. coli* | *Escherichia coli* |
| E1 | ubiquitin activating enzyme |
| E2 | ubiquitin conjugating enzyme |
| E3 | ubiquitin ligase |
| ECL | enhanced chemiluminescence |
| EDTA | ethylenediaminetetraacetic acid |
| EGF | epidermal growth factor |
| EG-VEGF | endocrine gland derived vascular endothelial growth factor |
| ELISA | enzyme linked immunosorbent assay |
| ENG | endoglin |
| ENO1 | enolase 1 |
| eNOS | endothelial nitric oxide synthase |
| EPAS | endothelial PAS protein |
| EPO | erythropoietin |
| ERK | extracellular signal related kinases |
| ES | embryonic stem |
| ETC | electron transport chain |
| ETS1 | v-ets avian erythroblastsosis virus e26 oncogene homolog1 |
| F | phenylalanine |
| FAD | flavin adenine dinucleotide |
| FCS | foetal calf serum |
| Fe | iron |
| FGF | fibroblast growth factor |
| FH | fumarate hydratase |
| FIH | factor inhibiting HIF |
| FITC | fluoroisothiocyanate |
| FIXa | coagulation factor IXa |
| FMN | flavin mononucleotide |
| FN1 | fibronectin 1 |
| FSH | follicle stimulating hormone |
| G | glycine |
| g | grams |
| GA | geldanamycin |
| GAP | GTPase-activating protein |
| GAPDH | glyceraldehyde-3-phosphate dehydrogenase |
| GDP | guanine diphosphate |
| GEO | GST-EPAS-ODDD |
| GHO | GST-HIF-1$\alpha$-ODDD |
| GLUT 1 | glucose transporter 1 |

| | |
|---|---|
| GPI | glucose-6-phosphate isomerise |
| GSK3 | glycogen synthase kinase 3 |
| GSNO | S-nitroso-glutathione |
| GST | glutathione-S-transferase |
| GTP | guanine triphosphate |
| GTPase | guanine triphosphatase |
| H | histidine |
| $H_2O$ | Water |
| $H_2O_2$ | Hydrogen peroxidase |
| HAS | HIF ancillary sequence |
| HAT | histone acetyl transferase |
| HBx | hepatitis B virus X protein |
| HDAC | histone deacetylases |
| HDM2 | human double minute 2 homologue |
| HECT | homologous to E6-AP C-terminus |
| HEK293 | human embryonic kidney 293 cells |
| HEPES | N-(2-hydroxyethyl)piperazine-N'-(2-ethanesulphonic acid) |
| HGF | hepatocyte growth factor |
| HIF | hypoxia inducible factor |
| HIF-PH/HPH | hypoxia inducible factor prolyl hydroxylase |
| HK1 | hexokinase 1 |
| HK2 | hexokinase 2 |
| HKO | HIF-1α knockout mouse embryonic fibroblasts |
| HLF | HIF-1α like factor |
| HLRCC | hereditary leiomyomatosis and renal cell cancer |
| HNF4 | hepatocyte Nuclear Factor 4 |
| HNP | head and neck paragangliomas |
| hnrnpa2 | heterogeneous nuclear ribonucleoprotein A2 homolog 2 |
| HRE | hypoxia responsive element |
| HRF | mouse HIF related factor |
| HRP | horse radish peroxidase |
| hrs | hours |
| Hsp70 | heat shock protein 70 |
| HSP90 | heat shock protein 90 |
| Hyp | hydroxyproline |
| I | isoleucine |
| IDH1 | isocitrate dehydrogenase 1 |
| IDH2 | isocitrate dehydrogenase 2 |
| IGF-1 | insulin like growth factor 1 |
| IGF-2 | insulin like growth factor 2 |
| IGFBP -1 | insulin-like growth factor binding protein 1 |
| IGFBP -2 | insulin-like growth factor binding protein 2 |
| IGFBP -3 | insulin-like growth factor binding protein 3 |
| IgG | immunoglobulin |
| IL-1β | interleukin-1β |
| iNOS | inducible nitric oxide synthase |
| IPAS | inhibitory PAS protein |
| IPTG | isopropyl β-D galactopyranoside |
| IVS | intervening sequence |
| JNK | c-Jun N-terminal kinase |

| | |
|---|---|
| KAP-1 | KRAB associated protein 1 |
| kb | kilobases |
| kbp | kilobase pairs |
| kDa | kilodaltons |
| KOH | potassium hydroxide |
| KRAB | kruppel associated box |
| KRT14 | keratin 14 |
| KRT18 | keratin 18 |
| KRT19 | keratin 19 |
| L | leucine |
| LB | Lennox B broth base |
| LDH | lactate dehydrogenase |
| LDHA | lactate dehydrogenase A |
| LEP | leptin |
| LOH | loss of heterozygosity |
| LRP1 | lipoprotein receptor-related protein 1 |
| Lys | lysine |
| M | Methionine |
| M | Molar |
| mA | milliAmps |
| MAP | mitogen activated protein |
| MAPK | mitogen activated protein kinase |
| MAPKK | mitogen activated protein kinase kinase |
| MAPKKK | mitogen activated protein kinase kinase kinase, |
| MDR1 | multidrug resistance protein 1 |
| mEFs | mouse embryonic fibroblasts |
| MEK | mitogen activated protein kinase kinase |
| MEKK | mitogen activated protein kinase kinase kinase |
| mg | milligrams |
| $MgCl_2$ | magnesium chloride |
| min | minute(s) |
| miRNA | microRNA |
| ml | millilitres |
| mM | millimolar |
| MMP2 | matrix metalloproteinase 2 |
| MOP1 | member of PAS superfamily 1 |
| MOP2 | member of PAS superfamily 2 |
| MOP3 | member of PAS superfamily 3 |
| MOP9 | member of PAS superfamily 9 |
| mRNA | messenger RNA |
| mTOR | mammalian target of rapapamycin |
| N | asparagine |
| NaCl | sodium chloride |
| $NAD^+$ | nicotinamide adenine dinucleotide |
| NADP+ | nicotinamide adenine dinucleotide phosphate |
| NADPH | nicotinamide adenine dinucleotide phosphate |
| NaOH | sodium hydroxide |
| NEMO | NF – κB essential modulator |
| NFDM | non-fat dried milk |
| ng | nanograms |

| | |
|---|---|
| NIP3 | BCL2/adenovirus E1B 19kDa interacting protein 3 |
| NIX | BCL2/adenovirus E1B 19kDa interacting protein 3 like |
| NLS | nuclear localisation signal |
| nNOS | neuronal nitric oxide synthase |
| NO | nitric oxide |
| NOS | nitric oxide synthase |
| NOS2 | nitric oxide synthase 2 |
| NP40 | Nonidet-P40 |
| N-TAD/NAD | N-terminal transactivation domain |
| o/n | overnight |
| $O_2$ | Oxygen |
| OBM | Oxford Biomedica |
| ODDD | oxygen dependent degradation domain |
| ORF | open reading frame |
| P | Proline |
| p300 | adenovirus E1A associated 300kDA protein |
| PAI1 | plasminogen activator inhibitor 1 |
| PAS | Per-Arnt-Sim motif |
| PBS | phosphate buffered saline |
| PBS-T | phosphate buffered saline containing triton X-100 |
| PCR | polymerase chain reaction |
| PDGF | platelet derived growth factor |
| PDK-1 | phosphatidylinositol dependent kinase-1 |
| PFK | phosphofructokinase |
| PFKL | phosphofructokinase liver type |
| PGK1 | phosphoglycerate kinase 1 |
| PGL | hereditary paraganglioma |
| $pH_2O$ | HPLC grade water |
| PHD | prolyl hydroxylase domain containing protein |
| PI | phosphoinosite |
| PI3K | phosphatidylinositol 3-kinase |
| PIC | pre-initiation complex |
| $PIP_2$ | phophatidylinositol 4,5 bisphosphate |
| $PIP_3$ | phosphatidylinositol 3,4,5 triphosphate |
| PKCδ | protein kinase C delta |
| PKCλ | protein kinase C lambda |
| PKCζ | protein kinase C zeta |
| PKM | pyruvate kinase muscle |
| PRMT1 | protein arginine methyltransferase 1 |
| Pro | proline |
| PtdIns | phosphatidylinositol |
| PTEN | phosphatase and tensin homologue deleted on chromosome ten |
| pVHL | von Hippel Lindau tumour suppressor protein |
| Q | glutamine |
| R | arginine |
| $r_0$ | starting RNA aptamer pool |
| $r_1$ | $1^{st}$ selected RNA aptamer pool |
| $r_2$ | $2^{nd}$ selected RNA aptamer pool |
| $r_3$ | $3^{rd}$ selected RNA aptamer pool |

| | |
|---|---|
| $r_4$ | $4^{th}$ selected RNA aptamer pool |
| Rbx | RING box protein |
| RCC | renal cell carcinoma |
| Ref-1 | pedox-effector factor-1 |
| RING | really interesting new gene |
| RNA pol II | RNA polymerase II |
| RNA | ribonucleic acid |
| RNAi | RNA interference |
| RNI | reactive nitrogen intermediates |
| rNTP | ribonucleotide triphosphate |
| ROS | reactive oxygen species |
| RP | regulatory particle |
| Rpb1 | RNA polymerase II sub-unit 1 |
| Rpb6 | RNA polymerase II sub-unit 6 |
| Rpb7 | RNA polymerase II sub-unit 7 |
| rpm | revolutions per minute |
| RT | reverse transciptase |
| rt | room temperature |
| RTP801 | HIF-1 responsive protein 801 |
| RT-PCR | reverse transcription PCR |
| S | serine |
| SCF | Skp-Cul-F box complex |
| SDH | succinate dehydrogenase |
| SDHA | succinate dehydrogenase sub-unit A |
| SDHAF2 | succinate dehydrogenase assembly factor 2 |
| SDHB | succinate dehydrogenase sub-unit B |
| SDHC | succinate dehydrogenase sub-unit C |
| SDHD | succinate dehydrogenase sub-unit D |
| SDS | sodium dodecyl sulphate |
| SDS-PAGE | SDS polyacrylamide gel electrophoresis |
| sec | second(s) |
| SELEX | systematic evolution of ligands by exponential enrichment procedure |
| SFQ | serum free media containing glutamine |
| Siah | mammalian homologue of *Drospohila* seven in absentia |
| siRNA | small interfering RNAs |
| SphK1 | sphingosine kinase 1 |
| SQR | succinate: ubiquinone oxidoreductase |
| SRC-1 | steroid receptor co-activator 1 |
| T | threonine |
| TAD | transactivation domain |
| TAE | tris acetate EDTA |
| TAFs | TBP associated factors |
| TAK-1 | transforming growth factor-β activating kinase |
| TBP | TATA box binding protein |
| TBS | tris-buffered saline |
| TBS-T | tris buffered saline containing Tween-20 |
| TCA | tricarboxylic acid cycle |
| TCP-1 | T-complex polypeptide 1 |
| TGF-β | transforming growth factor β |
| TGF-β3 | transforming growth factor β3 |

| | |
|---|---|
| TGF-α | transforming growth factor α |
| TIF2 | transcriptional intermediary factor 2 |
| TLR | toll like receptor |
| TNF-α | tumour necrosis factor α |
| TPI | triosephosphate isomerise |
| TRiC | TCP-1 ring complex |
| Tris | trizma base |
| Trx-1 | thioredoxin-1 |
| U2OS | human osteosarcoma cells |
| Ub | ubiquitin |
| Uba | ubiquitin activating enzyme |
| UBA | ubiquitin pathway associated domain |
| Ubc | ubiquitin conjugating enzyme |
| UBL | ubiquitin like domain |
| UIM | ubiquitin interacting motif |
| UPAR | urokinase-type plasminogen activator receptor |
| UV | ultraviolet |
| V | valine |
| V | Volts |
| v/v | volume per volume |
| VBC | pVHL-Elongin B-Elongin C complex |
| VDU1 | von Hippel Lindau protein interacting deubiquitinating enzyme-1 |
| VDU2 | von Hippel Lindau protein-interaction deubiquitinating enzyme-2 |
| VEGF | Vascular endothelial growth factor |
| VEGFR1 | vascular endothelial growth factor receptor 1 |
| VEGFR2 | vascular endothelial growth factor receptor 2 |
| VHL | von Hippel Lindau |
| VHLaK | pVHL associate KRAB-A domain containing protein |
| VIM | vimentin |
| W | tryptophan |
| w/v | weight per volume |
| WAF1 | wild-type p53-activated fragment 1 |
| Wnt | wingless – type MMTV integration site |
| X | unknown amino acid |
| XRE | xenobiotic response element |
| Y | tyrosine |
| YC-1 | 3-(5’-hydroxymethyl-2’-furyl)-1-benzylindazole |

# Chapter 1: Introduction

## 1.1 Oxygen Homeostasis

Oxygen ($O_2$) homeostasis is tightly controlled in order to maintain intracellular oxygen levels in a steady state. This steady state represents a balance between $O_2$ consumption by metabolic processes and the risk of oxidative damage if too much $O_2$ were available (reviewed by Semenza, 2001). Normal tissue oxygen levels range from 14% in pulmonary alveoli to 3% in most other organs of the body (Sharp and Bernaudin, 2004). To maintain these optimum tissue oxygen levels, mammalian tissues have developed a range of responses that help to prevent metabolic demise due to hypoxia (low $O_2$ concentration) or oxidative damage due to hyperoxia (high $O_2$ concentration).

The primary site of oxygen sensing is the carotid body (CB), an organ located at the bifurcation of the carotid artery, near the heart. The CB senses the level of $O_2$ in arterial blood and this sensory information is then relayed to the areas of the brain responsible for regulating the respiratory and cardiovascular reflex systems. This is an almost instantaneous response (a few seconds) which in the case of intermittent hypoxia results in increased heart rate and hyperventilation without related protein synthesis. In sustained hypoxia, such as individuals experience at high altitude, the morphology and function of the CB is altered. Sustained hypoxia also results in cellular adaptation to hypoxia which is regulated by hypoxia inducible factors (HIFs, section 1.2 onwards). Activation of hypoxia inducible factors results in the up-regulation of anaerobic metabolic pathways, stress proteins involved in cell death and survival, red blood cell production (erythropoiesis) and new blood vessel formation (angiogenesis). All of the mechanisms activated during hypoxia contribute to the recovery of a cell from mechanisms that may induce apoptosis (Semenza, 2001; Prabhakar and Semenza, 2012). Unbalanced oxygen homeostasis leading to hypoxia is a feature of many diseases including ischaemia, pulmonary hypertension, and cancer (section 1.6).

The excess levels of oxygen present in hyperoxia lead to the development of reactive oxygen species (ROS) such as superoxide. Mammalian tissues prevent any oxidative

damage to lipids, proteins and DNA, by up-regulating antioxidant enzymes, such as superoxide dismutase, to scavenge excess ROS (D'angio and Finkelstein, 2000).

## 1.2 Hypoxia inducible factor (HIF)

The most prominent transcription factor that regulates oxygen homeostasis and the founding member of the hypoxia inducible factor (HIF) family is HIF-1, a heterodimeric transcription factor comprised of the subunits HIF-1α and HIF-1β/ ARNT (aryl hydrocarbon nuclear receptor translocator, Wang *et al.*, 1995). HIF-1 was originally identified through studying the hypoxic induction of erythropoietin. Several HIF-1 target genes have since been identified that are involved in angiogenesis, oxygen transport, iron metabolism, glycolysis, growth factor signalling, apoptosis and invasion and metastasis (Semenza *et al*, 1991, Semenza and Wang, 1992). Homologues of HIF-1α and ARNT have also been identified and include HIF-2α, HIF-3α, ARNT2, ARNT3/BMAL1 and ARNT4/BMAL2 (figures 1.1 and 1.2, sections 1.2.2 and 1.2.3, respectively).

### *1.2.1 bHLH-PAS domains*

All HIF-α and ARNT subunits are members of the basic-helix-loop-helix-Per/Arnt/Sim (bHLH-PAS) family of transcription factors. The term PAS is derived from the first letters of the founding members of the family: PER (the protein product of the *Drosophila period* gene), ARNT and SIM (the protein product of the *Drosophila simple-minded* gene). Accordingly, all members of the HIF family, apart from three splice variants of HIF-3α, contain a conserved basic DNA binding sequence adjacent to a helix-loop-helix domain at the N-terminal end of the protein (Bardos and Ashcroft, 2005). The PAS domain also located at the N-terminal end of the HIF proteins is between 250-300 amino acids in length and contains two sub-regions termed the A and B repeats (figures 1.1 and 1.2). The bHLH domain allows homo or heterodimerisation with other bHLH proteins in the formation of functional complexes and is also a requirement in DNA binding. For dimerisation to occur between HIF-α and ARNT subunits the bHLH and part of the PAS A domains are

required (Jiang *et al* 1996; Chapman-Smith *et al.,* 2004). Therefore, the PAS domain confers an additional level of regulation in the dimerisation process and is also involved in the binding of cellular chaperones (reviewed by Gu *et al.,* 2000).

### *1.2.2 The HIF α subunit family: structure and function*

There are three known HIF-α subunits (figure 1.1); HIF-1α/MOP1 (member of PAS superfamily 1), HIF-2α, more commonly known as EPAS-1 (endothelial PAS protein 1), but also known as HRF (mouse HIF related factor), HLF (HIF-1α like factor) and MOP2 (member of PAS superfamily 2) and HIF-3α (Wang *et al.,* 1995; Iyer *et al.,* 1998; Tian *et al.,* 1997; Ema *et al.,* 1997; Hogenesch *et al.,* 1997; Gu *et al.,* 1998). Splice variants of HIF-1α and HIF-3α have also been identified (Chun *et al.,* 2001; Maynard *et al.,* 2003).

HIF-1α is the most well studied of the three homologues and is the most global regulator of oxygen homeostasis. In normoxia HIF-1α is targeted for proteasomal degradation via an oxygen dependent degradation domain (ODDD). Within the *ODDD* domain are two conserved proline residues that are hydroxylated in normoxia by prolyl hydroxylases (PHDs). Prolyl hydroxylated HIF-α subunits are recognised by the von Hippel Lindau tumour suppressor protein (pVHL). pVHL is a component of an E3 ubiquitin ligase complex which targets HIF-α subunits for degradation via the proteasomal pathway (section 1.3).

In hypoxia HIF-1α is up-regulated and translocates to the nucleus where it dimerises with ARNT via a bHLH-PAS domain (see section 1.2.1). The HIF-1 complex then binds to a consensus sequence in the target gene called a hypoxia responsive element (HRE). HIF-1 then recruits several co-activators, such as CREB binding protein/ adenovirus E1A associated 300kDA protein, steroid receptor co-activator 1 and transcriptional intermediary factor 2 (CBP/p300, SRC-1 and TIF2, respectively), in order to activate the expression of target genes. Both transcriptional activation and the recruitment of co-activators are mediated via the N-terminal and C-terminal transactivation domains (N-TAD and C-TAD, respectively, section 1.4).

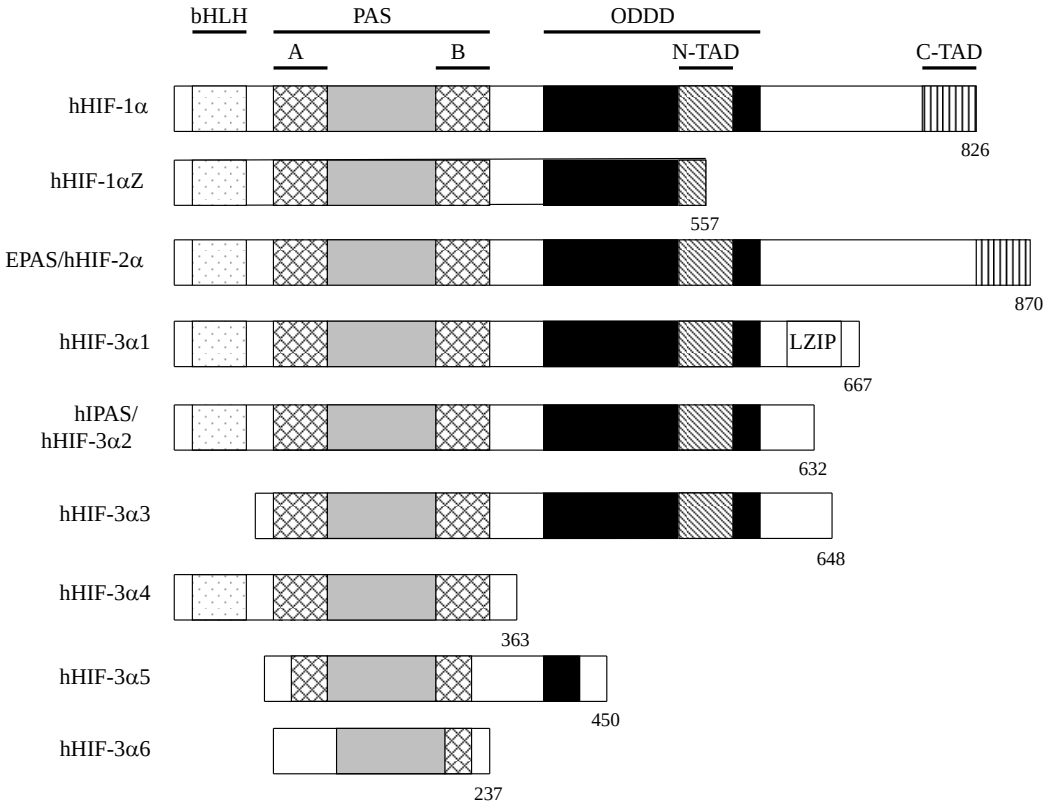


**Figure 1.1 A schematic representation of the human HIF-α sub-units (hHIF-α).**

There are three known human HIF-α subunits; HIF-1α, HIF-2α/EPAS and HIF-3α. All are members of the bHLH-PAS family of transcription factors and are regulated in normoxic conditions via their oxygen dependent degradation domain. Transcriptional activation and recruitment of co-activators is mediated via the C-TAD domains of HIF-1α and EPAS. Splice variants of HIF-1α (hHIF-1) and HIF-3α (HIF -3α2-6) have been identified and are shown above.

**Key:** A/B, A and B repeats; bHLH, basic-helix-loop helix domain; C-TAD, C-terminal activation domain; EPAS, Endothelial Pas protein; hHIF, human Hypoxia Inducible Factor protein; LZIP, leucine zipper domain; N-TAD, N-terminal activation domain; ODDD, oxygen dependent degradation domain; PAS, Per/Arnt/Sim domain.

A splice variant of HIF-1α was discovered during studies into the effect of zinc ions on HIF-1α induction. The splice variant, named HIF-1αZ, was identical to HIF-1α apart from a deletion of 434 base pairs of coding sequence corresponding to the loss of exon 12. HIF-1αZ had a dominant-negative effect on HIF function by sequestering ARNT in the cytosol, preventing its translocation into the nucleus (Chun *et al.*, 2001).

EPAS-1 only shares 48% homology with HIF-1α, however, the pVHL binding site is conserved and in normoxia EPAS-1 is targeted for proteasomal degradation in the same manner as HIF-1α (section 1.3, Tian *et al.,* 1997). Under hypoxic conditions EPAS-1 is up-regulated and, like HIF-1α, binds to ARNT (Wiesener *et al.,* 1998 and Tian *et al.,* 1997, respectively). Under these conditions EPAS-1 recognises a hypoxia responsive element (HRE) in target genes before initiating transcription (section 1.4).

Analysis of HIF-1α and EPAS-1 mRNA expression patterns revealed that HIF-1α and EPAS-1 were expressed in all the tissues investigated which included heart, brain, smooth muscle, kidney, lung and liver, the only exception being leukocytes where HIF-1α mRNA alone was expressed. Tissues that were of a highly vascularised nature e.g. lungs, heart and placenta, exhibited higher levels of EPAS-1 mRNA than HIF-1α mRNA (Tian *et al.,* 1997). Research into the protein expression patterns of HIF-1α and EPAS-1 in hypoxic samples or samples treated with hypoxia mimetics has provided increasing amounts of evidence that these proteins have different roles within the body. For example, the accumulation of HIF-1α and EPAS-1 protein in rat kidney was selective with respect to cell type. HIF-1α was predominantly expressed in tubular cells, whereas EPAS-1 was predominantly expressed in endothelial cells (Rosenberger *et al.,* 2002). A difference in function between HIF-1α and EPAS-1 was also supported by studies in *hif-1α*$^{-/-}$ and *EPAS-1*$^{-/-}$ mouse embryos. The *hif-1α*$^{-/-}$ phenotype was lethal by embryonic day 10, with embryos exhibiting gross morphological and vascular abnormalities, whereas *EPAS-1*$^{-/-}$ embryos did not exhibit gross morphological abnormalities but did exhibit grossly disorganised vasculature (Iyer *et al.,* 1998; Kotch *et al.,* 1999; Peng *et al.,* 2000, respectively). The *EPAS*$^{-/-}$ genotype was lethal in all embryos by embryonic day 11.5 (Peng *et al.,* 2000).

The final known member of the HIF-α family is HIF-3α, which was originally identified in mice (Gu *et al.,* 1998). A human homologue of HIF-3α (hHIF-3α) was later identified in human kidney and shown to share a high degree of sequence similarity with HIF-1α and EPAS-1 in the N-terminal region, but lacked the C-terminal region of the protein. hHIF3α, like HIF-1α and EPAS-1, was up-regulated in hypoxic conditions and able to bind to ARNT. However, unlike HIF-1α and

EPAS-1, hHIF-3α was able to repress HRE driven transcription of a reporter gene (Hara *et al.,* 2001). Database searches identified six splice variants of hHIF-3α (figure 1.1). The first three splice variants, hHIF3α1-3, contained *ODDD* domains closely resembling those of HIF-1α and EPAS-1 and were targeted for pVHL mediated proteasomal degradation (Maynard *et al.,* 2003). The inhibitory PAS (IPAS) domain protein identified in mice is an alternative HIF-3α splice variant, with hHIF-3α4 exhibiting the closest sequence similarity (Makino *et al.,* 2002; Maynard *et al.,* 2003). In mice, experimentally overexpressed IPAS bound to HIF-1α under hypoxic conditions and exhibited a dominant negative effect on HIF-1 mediated gene expression. This resulted in retarded tumour growth and vascular density *in vivo* (Makino *et al.,* 2001). In humans HIF-3α4 suppresses the transcriptional activity of HIF-1 thereby acting as a dominant negative regulator (Maynard *et al.,* 2005). Both IPAS and hHIF-3α4 are oxygen regulated suggesting the existence of other mechanisms that contribute towards the control of HIF-1 transcriptional activity.

The existence of three HIF-α homologues indicates their distinct functional roles. However, in certain situations it is possible that there is a functional overlap between the three homologues (Bardos and Ashcroft, 2005).

### *1.2.3 The ARNT subunit family*

There are two known ARNT subunits and two ARNT like subunits (ARNTL). These are; - ARNT/ HIF-1β, ARNT 2, ARNTL 1/ ARNT 3/ MOP3 (more commonly referred to as Brain-Muscle-ARNT-Like protein-1 [BMAL-1]) and ARNTL 2/ ARNT 4/ MOP9 (more commonly referred to as BMAL2) (figure 1.2, Wang *et al.,* 1995; Hirose *et al.,* 1996; Ikeda *et al.,* 1997; Ikeda *et al.,* 2000; Okano *et al.,* 2001).

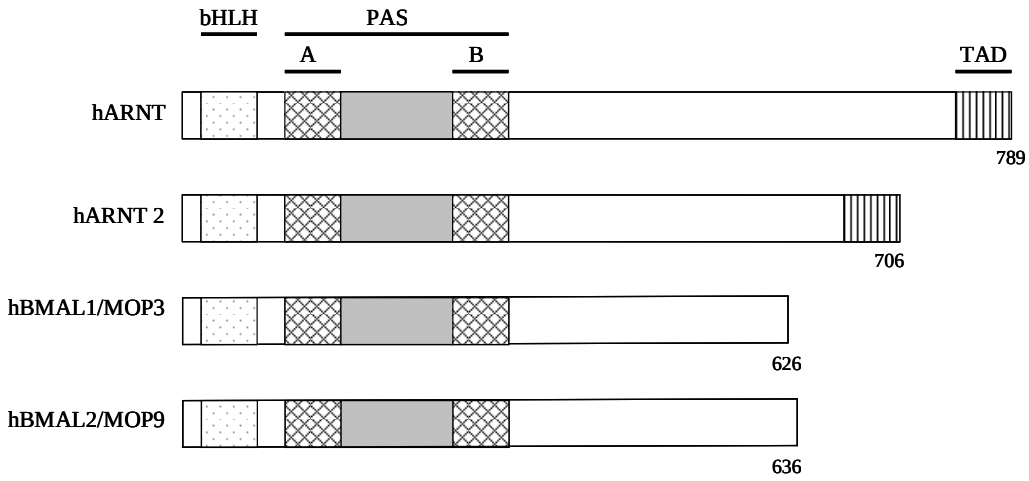


**Figure 1.2 A schematic representation of the human ARNT related sub-units (hARNT).**

Two ARNT and two ARNT like sub-units have been identified. All sub-units are members of the bHLH-PAS family of transcription factors. ARNT is the main dimerization partner for HIF-α subunits. The TAD domains of ARNT and ARNT2 mediate the transcription of HIF target genes. The protein length of each ARNT related subunit (in amino acids), is indicated.

**Key:** A/B, A and B repeats; bHLH, basic-helix-loop helix domain; hARNT, human aryl hydrocarbon receptor nuclear translocator; hBMAL, human, brain-muscle-ARNT-like protein; MOP, Member of PAS superfamily; PAS, Per/Arnt/Sim domain; TAD, transactivation domain

ARNT is ubiquitously expressed and is the main dimerisation partner for HIF-α subunits in hypoxia. Dimerisation occurs via the bHLH-PAS domain (section 1.2.1) and the transactivation (TAD) domain of ARNT is involved in the HIF-1 mediated transcription of target genes. The importance of the HIF-α-ARNT dimerisation partnership in hypoxic conditions has been illustrated by *Arnt* gene knockout studies performed in embryonic stem cells and mice (Maltepe *et al.*, 1997). These studies particularly focussed on vasculogenesis and angiogenesis, processes regulated by HIF-1, due to the knowledge that ARNT has other functions within the cell. The *Arnt*$^{-/-}$ genotype was embryonically lethal, with death occurring at embryonic day 10.5. These embryos exhibited normal vasculogenesis and organ development, but angiogenesis of the yolk sac and branchial arches was impaired and embryos showed stunted development. Loss of ARNT rendered embryonic stem (ES) cells unable to activate genes normally up-regulated in low oxygen, indicating ARNT is an essential

component of the hypoxic response. *Arnt*$^{-/-}$ ES cells also failed to respond to a decrease in glucose concentration, showing ARNT is also essential in the response to hypoglycaemia (Maltepe *et al.,* 1997). Altered *Arnt* gene expression has also been identified as a potential factor in the development of human type II diabetes. Individuals with type II diabetes exhibit marked defects in their pancreatic β cell function and multiple alterations in gene expression. One of the genes which showed a marked decrease in expression was *Arnt.* Follow up experiments, which used siRNA to inhibit *Arnt* mRNA expression, resulted in severe impairment of glucose–stimulated insulin secretion and alterations in mRNA expression levels. Pancreatic β cell specific deletion of *Arnt* in mice mirrored the results from *in vitro* studies. This data suggested that ARNT is a likely upstream regulator of many of the changes associated with type II diabetes (Gunton *et al.,* 2005).

ARNT has other functions within the cell in addition to its role in hypoxia signalling; in particular ARNT is involved in xenobiotic metabolism. Dioxin (2,3,7,8-tetrachlorodibenzo-p-dioxin, TCDD) and other halogenated aromatic compounds are environmental pollutants. The metabolic response to these chemicals is mediated via the aryl hydrocarbon receptor (AhR), also known as the dioxin receptor, a bHLH-PAS protein. Prior to ligand binding, the AhR is localised to the cytoplasm and is bound by two molecules of heat shock protein 90 (HSP90). Following ligand binding, the AhR/HSP90 complex translocates to the nucleus where HSP90 is exchanged for ARNT. The AhR-ARNT heterodimer mediates the transcription of xenobiotic metabolising enzymes from genes containing a xenobiotic response element (XRE) consensus sequence (reviewed by Gu *et al.,* 2000; Kewley *et al.,* 2004). ARNT is also capable of forming homodimers however the functions of these have yet to be determined *in vivo* (Hirose *et al.,* 1996).

ARNT2 is the most similar protein to ARNT, sharing 57% sequence homology. The expression of ARNT2 is tightly regulated and to date has only been detected in the brain and kidney (Hirose *et al.,* 1996; Drutel *et al.,* 1996). ARNT2 was able to dimerise with HIF-1α and form a functional complex *in vivo*. ARNT2 was also able to restore hypoxia induced gene expression in *Arnt*$^{-/-}$ ES and hepatocyte cells (Maltepe *et al.,* 2000). Expression of *Arnt2* in *Arnt*-defective c4 mutant Hepa-1 cells was able to rescue XRE driven reporter gene activity. This evidence suggests that

ARNT2 is able to functionally replace ARNT in the tissues in which it is expressed (Hirose *et al.*, 1996).

BMAL1 and BMAL2 share 49% sequence homology between them and exhibit a lower level of sequence homology with ARNT and ARNT2 (Ikeda *et al.*, 2000). The highest degree of similarity between the BMAL and ARNT proteins is observed in the bHLH-PAS domains. Both BMAL1 and BMAL2 bind to HIF-1α *in vitro*, however in the case of BMAL1 this was a weak interaction (Takahata *et al.*, 1998; Gu *et al.*, 2000; Hogenesch *et al.*, 2000). Due to BMAL proteins binding HIF-1α *in vitro*, it was originally speculated that they may function in the hypoxia sensing pathway. However, more detailed research has revealed that both BMAL1 and BMAL2 are involved in the regulation of the circadian clock (Ikeda *et al.*, 2000; Hogenesch *et al.*, 2000; Gekakis *et al.*, 1998). Both BMAL proteins have tightly restricted mRNA expression patterns with BMAL1 predominantly expressed in the brain and skeletal and cardiac muscle and BMAL2 expression occurs in adult brain and liver (Ikeda *et al.*, 1997; Ikeda *et al.*, 2000).

## 1.3 The oxygen dependent regulation of HIF activity

In normoxia HIF-α subunits are subjected to two types of hydroxylation, prolyl hydroxylation of the ODDD and asparaginyl hydroxylation of the C-TAD (figure 1.3).

HIF-1α protein stability is regulated by the prolyl hydroxylation of Proline 564 ($P^{564}$), located in the C-terminal ODDD (CODDD) and/or Proline 402 ($P^{402}$), located in the N-terminal ODDD (NODDD, Ivan *et al.*, 2001; Jaakkola *et al.*, 2001; Masson *et al.*, 2001). Maximal regulation of HIF-1α subunits is achieved when both proline residues are hydroxylated (Masson *et al.*, 2001). This reaction is catalysed by prolyl hydroxylase domain containing proteins (PHDs) and is a pre-requisite for pVHL recognition and binding to HIF-α subunits, resulting in HIF-α proteasomal degradation (Epstein *et al.*, 2001; Bruick and McKnight, 2001, sections 1.3.1-1.3.5). Hydroxylation of asparagine 803 ($N^{803}$), located in the C-TAD, is carried out by factor inhibiting HIF (FIH-1), an asparaginyl hydroxylase (section 1.3.2).

Asparaginyl hydroxylation abrogates HIF-1α C-TAD interaction with the transcriptional co-activator p300 and its paralogue CBP, thereby introducing a level of control that prevents the transcription of HIF regulated genes (section 1.3.2). Both PHDs and FIH-1 are oxygen dependent hydroxylases, therefore in hypoxia, neither prolyl or asparaginyl hydroxylation occurs, resulting in up-regulation of HIF-α subunits, HIF-α/ARNT dimerisation and the subsequent transcription of HIF/EPAS target genes (section 1.4).

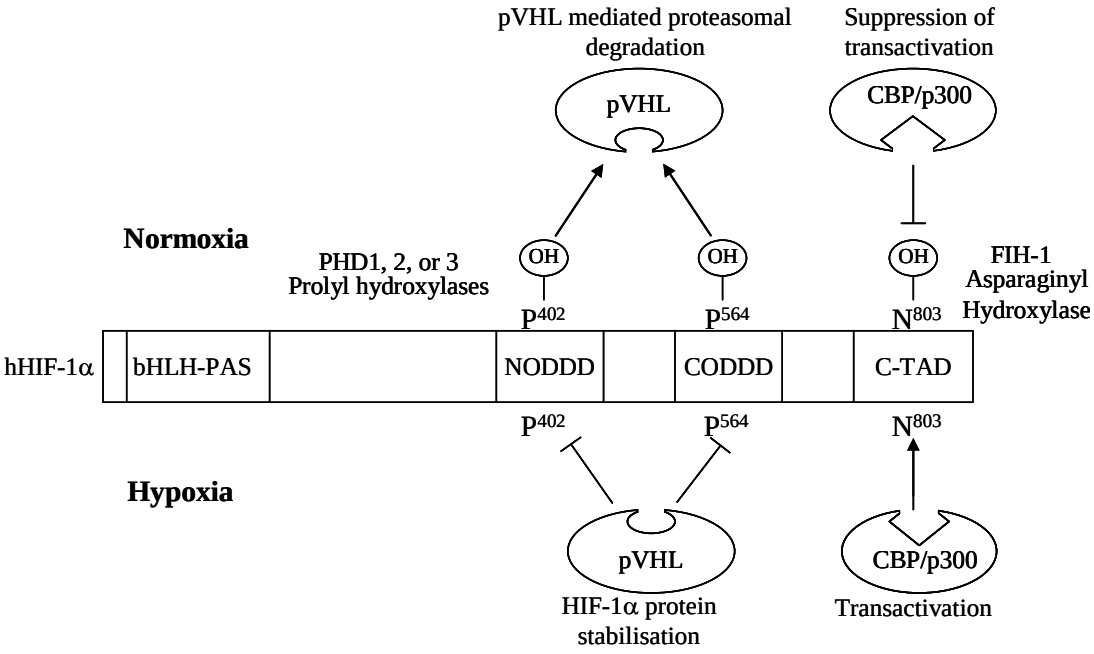


**Figure 1.3 Regulation of HIF-1α by prolyl and asparaginyl hydroxylases**

In normoxia HIF-1α is subjected to prolyl and asparaginyl hydroxylation by prolyl hydroxylases (PHDs) and asparaginyl hydroxylases (FIH-1). The PHDs and FIH-1 are members of a family of iron and 2-oxoglutarate dependent dioxygenases. Hydroxylation of proline residues 402 and 564 of HIF-1α by PHDs1-3 is responsible for regulation of protein stability, while hydroxylation of asparagine residue 803 by FIH-1 reduces the transcriptional regulation of target genes by HIF-1.

**Key:** bHLH-PAS, basic helix loop helix Per ARNT Sim domain; CBP, CREB binding protein; CODDD, C-terminal oxygen dependent degradation domain; C-TAD, C-terminal transactivation domain; FIH-1- factor inhibiting HIF; HIF, hypoxia inducible factor; N, asparagine; NODDD, N-terminal oxygen dependent degradation domain; OH, hydroxyl; P, proline; pVHL – von Hippel Lindau protein; PHD- prolyl hydroxylase domain containing protein.

### *1.3.1 The prolyl hydroxylase domain containing protein (PHD) family*

HIF prolyl hydroxylase (HPH) was originally identified as the protein product of the *egl 9* gene in *Caenhorabditis elegans* (*C. elegans)*. Database analysis of *egl 9* identified a family of three homologous genes, *phd 1-3* in humans and mice (Epstein *et al.,* 2001). Several other researchers also identified the protein products of these genes and PHD1, PHD2 and PHD3 are also referred to as HPH3, HPH2 and HPH1 and homologue of EGL nine 2 (EGLN2), EGLN1 and EGLN3, respectively (Bruick and McKnight, 2001).

The PHDs belong to a superfamily of iron and 2-oxoglutarate dependent dioxygenases (McNeill *et al.*, 2002). Recruitment of PHD2 (and presumably PHD1 and 3, although no data is currently available) is dependent on the presence of leucine 574 ($L^{574}$) of HIF-1α (Kageyama *et al.*, 2004). This leucine residue is conserved between all three HIF-α subunits. Once the HIF-α subunit has been identified by the PHD, hydroxylation of the proline residue located at the end of an LXXLAP motif, corresponding to proline residues 402 and 564 in HIF-1α, occurs. The LXXLAP motif has also been identified in EPAS and some splice variants of HIF-3α. To date no evidence has been published to show prolyl hydroxylation of the HIF-3α isoform. However, it has been hypothesised that those HIF-3α splice variants with functional ODDD are targeted for pVHL mediated proteasomal degradation. This infers prolyl hydroxylation must occur for pVHL recognition of the ODDD containing HIF-3α splice variants. *In vitro* studies have determined the relative activities of the PHD proteins as PHD2>PHD3>PHD1. However, these results differ from other published findings where PHD2 and 3 showed similar specific activities and PHD1 exhibited a lower specific activity (Berra *et al.*, 2006).

All three PHDs are capable of hydroxylating $P^{564}$ of HIF-1α but only PHD1 and PHD2 are able to hydroxylate $P^{402}$ of HIF-1α. The same trend is also observed in EPAS-1 (Appelhoff *et al.*, 2004). Prolyl hydroxylation and subsequent proteasomal degradation of HIF-α subunits is enhanced by the ubiquitously expressed protein, OS9, a protein with previously undefined function. OS9 binds to residues of HIF-1α in both normoxic and hypoxic conditions and is also able to associate with PHD2 and

PHD3. OS9 binding to both PHD 2/3 and HIF-1α occurs in such a way as to allow the formation of a stable trimeric complex that does not prevent PHD hydroxylation of HIF-α subunits (figure 1.4, Baek *et al.,* 2005).

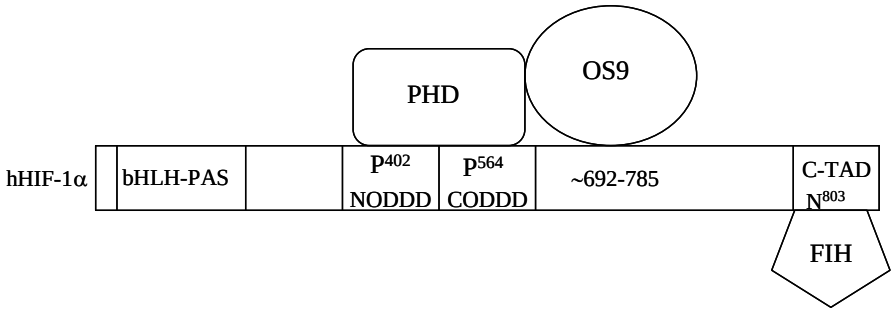


**Figure 1.4 PHD and OS9 interaction with hHIF-1α.**

HIF-1α, PHD/PHD3 and OS9 form a ternary protein complex in normoxia. Formation of this complex enhances prolyl hydroxylation of $P^{402}$ and $P^{564.}$ OS9 binding to HIF-1α occurs between HIF-1α residues 692 and 785 (approximately) and does not obstruct binding of either PHD2 or 3 to HIF-1α.

**Key:** bHLH-PAS, basic-helix-loop-helix Per ARNT Sim domain; CODDD/NODDD, C-terminal/N-terminal oxygen dependent degradation domain; C-TAD- C-terminal transactivation domain; FIH- Factor inhibiting HIF; HIF, hypoxia inducible factor; P, proline; PHD, prolyl hydroxylase domain containing protein; N, asparagine

Based on a figure by Flashman *et al,* 2005.

In addition to the role of OS9 in HIF-α hydroxylation, studies using human homologues of OS9 have indicated a role in HIF-α transport (Flashman *et al.,* 2005).

The presence of three PHD proteins led to further research to determine the contribution each protein makes towards HIF-α regulation. Overall, all three PHDs were shown to regulate HIF-1α and EPAS-1. However the degree of regulation is dependent on the relative abundance of each PHD protein. In the range of cell types investigated PHD2 is present in greater abundance than PHD1 and PHD3 (Appelhoff *et al.,* 2004). This data would explain why PHD2 has been shown to be the major regulator of HIF-1α activity in normoxia, an observation that appears to be confirmed by the discovery that knockdown of *phd2,* but not *phd1* or *phd3,* is lethal in mice (Berra *et al.,* 2003 and 2006). However, evidence for differential roles of the

three proteins has been identified. PHD3 appears to preferentially regulate EPAS-1 protein levels over HIF-1α. PHD3 also appears to have a role in the regulation of HIF-α subunits in hypoxia (Appelhoff *et al.*, 2004).

Differential roles for the three PHD proteins are also supported by the differences in intracellular localisation of the proteins. All three PHD proteins are expressed at different levels in all tissue types (Soilleux *et al.*, 2005). However, differences are observed when expression levels within the cell are investigated. PHD1 is exclusively localised to the nucleus, PHD2 is mainly localised in the cytoplasm and PHD3 is distributed between the nucleus and the cytoplasm (Metzen *et al.*, 2003). Despite the mainly cytoplasmic localisation of PHD2, it has been reported that it can shuttle between the cytoplasm and the nucleus of a cell (Berra *et al.*, 2006).

Several mechanisms have been identified that regulate the expression of the PHD proteins. In hypoxia there is an increase in both the mRNA and protein levels of PHD2 and PHD3, suggesting a feedback mechanism to prevent hypoxic responses in re-oxygenated cells (Epstein *et al.*, 2001; Berra *et al.*, 2003; Appelhoff *et al.*, 2004). This increase in PHD2 and PHD3 expression is largely regulated by HIF-1, However, EPAS is also thought to be able to increase the expression of PHD3 (del Peso *et al.*, 2003 and reviewed by Berra *et al.*, 2006). Further regulation of PHD1 and PHD3 is achieved by proteasomal degradation (section 1.3.3). Siah1a and Siah2 (mammalian homologues of *Drosophila* seven in absentia) are specific E3 ubiquitin ligases for PHD1 and PHD3. In hypoxia Siah1a and Siah2 are upregulated in a HIF-dependent manner (Nakayama *et al.*, 2004).

### *1.3.2 HIF asparaginyl hydroxylation by factor inhibiting HIF (FIH-1)*

The transcriptional activity of HIF-α subunits is regulated, in normoxia, by the hydroxylation of asparagine residues 803, of HIF-1α and 851 of HIF-2α, which are located ion the C-TAD of each protein (Lando *et al.*, 2002a). This hydroxylation prevents the association of the C-TAD with the cysteine-histidine rich region (CH-1) domain of the transcriptional co-activators CBP/p300 (figure 1.3, Lando *et al.*, 2002b). Asparaginyl hydroxylation is carried out by factor inhibiting HIF-1α (FIH-

1), a protein originally identified, in a yeast two hybrid screen, as binding to HIF and later confirmed as the HIF asparaginyl hydroxylase (Mahon *et al.,* 2001; Lando *et al.,* 2002b; Hewitson *et al.,* 2002). Like the PHDs, FIH-1 is a dioxygen, iron and 2-oxoglutarate dependent protein (Lando *et al.,* 2002b). However, unlike the PHDs, only one isoform has been identified. FIH-1 has been shown to be localised in the cytoplasm in all analysed tissues and cell types (Metzen *et al.,* 2003; Linke *et al.,* 2004; Soilleux *et al.,* 2005). This is similar to the cellular localisation of PHD2, the prolyl hydroxylase predominantly responsible for HIF-1α prolyl hydroxylation (section 1.3.1). FIH-1 has at least two distinct sites of interaction with HIF-1α or HIF-2α and the active site is predicted to be located in a pocket at the C-terminal end of the protein. Both Fe (II) and 2-oxoglutarate are bound in the active site (Dann III *et al.,* 2002). The amino acid residue adjacent to $N^{803}$, $V^{802}$, is conserved throughout HIF-α sequences and is crucial for optimal asparagine hydroxylation by FIH-1. Molecular modelling has predicted that $V^{802}$ is essential for the correct positioning of $N^{803}$ in relation to the active site of FIH-1 (Linke *et al.,* 2004). FIH-1 interacted with VHL at a distinct site from HIF interactions (Lee *et al.,* 2003). This association facilitates HIF-1α recruitment to VHL for ubiquitination and subsequent degradation (section 1.3.5).

### *1.3.3 The proteasomal degradation pathway*

It is now well established that HIF-α subunits are degraded in normoxia via the ubiquitin proteasome degradation pathway which consists of ubiquitin (Ub), an ubiquitin activating protein (Uba/E1), an ubiquitin conjugating protein (Ubc/E2), an ubiquitin ligase protein/protein complex (E3 ligase), the 26S proteasome and a deubiquitylating enzyme (DUB, figure 1.5). Additionally, an E4 enzyme may be required for efficient multi-ubiquitin chain assembly (reviewed by Glickman and Ciechanover, 2002).

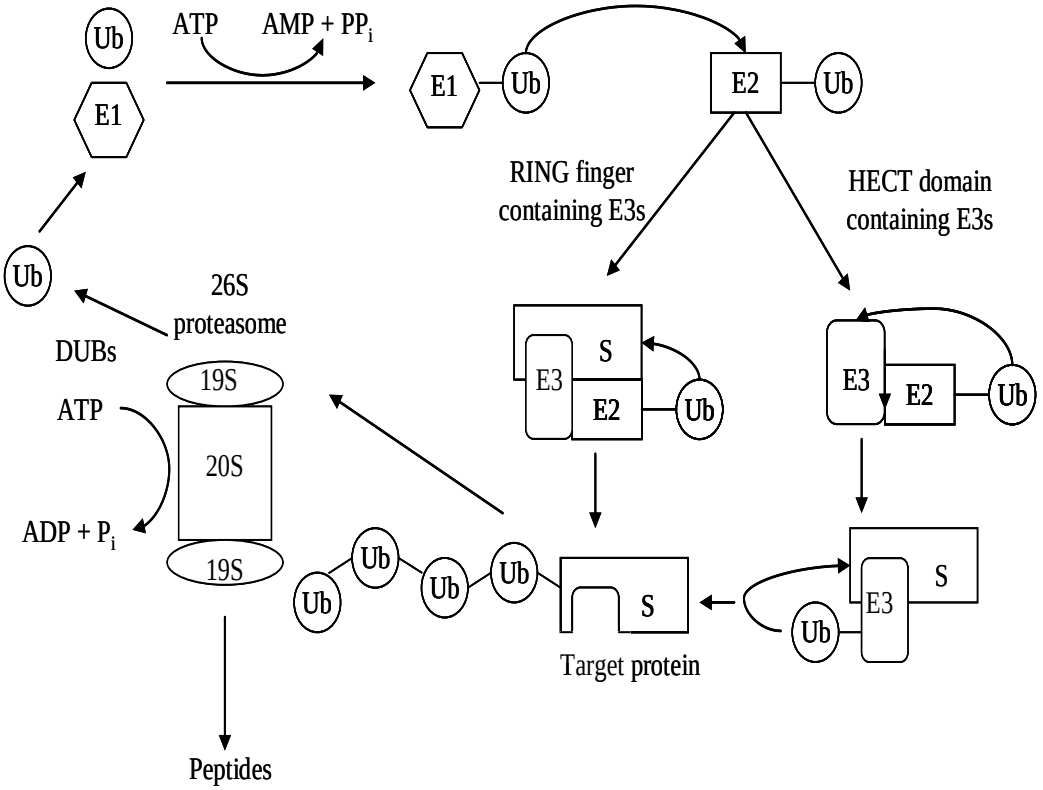


**Figure 1.5 The ubiquitin proteasome pathway**

Ub is activated in an ATP dependent manner by E1. Activated Ub is then transferred to an E2 enzyme. From E2, Ub can either be transferred directly to S which is bound to an E3 belonging to the RING finger family of ligases. Alternatively, Ub is transferred from an E2 to an E3 belonging to the HECT domain containing family of ligases which is associated with the substrate. HECT E3s then transfer Ub to S. Additional Ub can then bind to the substrate associated Ub, generating a polyubiquitin chain. Polyubiquitinated substrate binds to the 26S proteasome (comprised of two 19S and a 20S sub-units) where the substrate is degraded into short peptides. Ub is released in a re-usable form from the 26S proteasome by de-ubiquitinating enzymes.

ATP, adenosine triphosphate; DUBs, de-ubiquitinating enzymes; E1, Ub activating enzyme; E2, Ub conjugating enzyme; E3, Ub ligase; HECT, homologous to E6-AP C-terminus; $PP_i$, Pyrophosphate; $P_i$, inorganic phosphate; RING, really interesting new gene; S, substrate; Ub, ubiquitin.

The polyubiquitin chain acts as a signal that targets the substrate towards the 26S proteasome. The 26S proteasome is highly conserved among eukaryotes and is the predominant mediator of selective proteolysis (Miller and Gordon, 2005). The 26S proteasome is comprised of approximately 30 subunits that form a 20S core particle

(20S CP) and two flanking 19S regulatory complexes (19S RP, figure 1.6). The 20S subunit is a cylindrical pore particle consisting of 14 subunits, α 1-7 and β 1-7, that form a barrel shaped complex of four stacked heptameric rings. Two narrow channels at either end of the pore feed a central cavity comprised of β 1-7 subunits, some of which have protease activity. These pores are gated by two 19S RP. The 19S RP are comprised of at least 19 different subunits that can be broken down into two sub-complexes, the 'lid' and the 'base'. The lid consists of approximately nine subunits. The base directly contacts the α rings of the 20S CP and is comprised of approximately 10 subunits including six ATPases whose role is to gate the 20S CP and unfold the protein substrates before translocating them into the 20S proteolytic chamber.

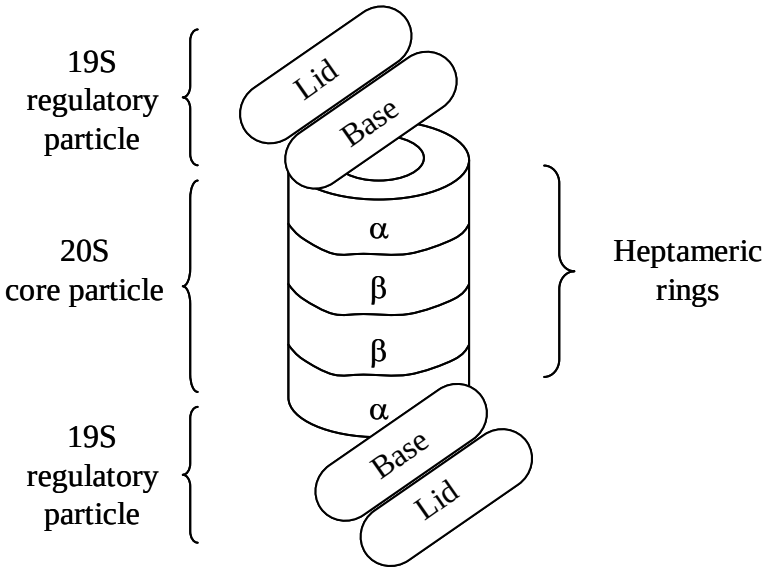


**Figure 1.6 The structure of the 26S proteasome**

The 26S proteasome is comprised of a 20S core particle capped with two 19S regulatory particles. The 20S core particle is formed of four heptameric rings which are comprised from either α 1-7 or β 1-7 subunits, arranged as indicated above. The 19S regulatory particles are formed of two sub-complexes, the lid and the base.

Based on figures by Glickman and Ciechanover, 2002 and Miller and Gordon, 2005).

The lid is composed of eight non-ATPase subunits many of which have undefined roles. However, at least one of the subunits, POH1, has de-ubiquitinating activity and two other subunits, Pus1/Rpn10/S5a and Rpt5/S6', have ubiquitin interacting motifs (UIMs) that recognise poly-ubiquitin tags.

Not all ubiquitinated proteins are recognised by the 19S RP or by chaperone proteins. In these instances, proteins with ubiquitin pathway associated domains (UBA domains) or ubiquitin like domains (UBL domains) have been implicated in the recognition of poly-ubiquitinated proteins and their delivery to the 26S proteasome.

Once the substrate has been delivered to the 26S proteasome, the ubiquitin chain is removed and the protein unfolded before being fed into the 20S CP where it is degraded into short peptide sequences. The ubiquitin is recycled by de-ubiquitinating enzymes (DUBs) which reverse the ubiquitin conjugation process (reviewed by Glickman and Ciechanover, 2002; Hartmann-Petersen *et al.,* 2003; Miller and Gordon, 2005; Navon and Ciechanover, 2009).

### *1.3.4 pVHL as a component of an E3 ubiquitin ligase complex*

von Hippel-Lindau (VHL) disease is a rare inherited cancer syndrome where affected individuals exhibit a pre-disposition to retinal, spinal and cerebellar hemangioblastoma, clear cell renal carcinoma and pheochromocytoma (section 1.6.5 reviewed by Bryant *et al.,* 2003). Individuals affected by VHL disease inherit a single mutated gene and develop the above tumours if there is loss of expression or mutational inactivation of the second *vhl* allele (Pugh and Ratcliffe, 2003).

The *vhl* tumour suppressor gene encodes for a protein which is ubiquitously expressed (Latif *et al.,* 1993). Two different protein products, $pVHL_{19}$ and $pVHL_{30}$, are expressed from the *vhl* gene with apparent molecular weights of 19 and 30kDa, respectively (Schoenfeld *et al.,* 1998; Iliopoulos *et al.,* 1995, respectively). The smaller form is translated from an alternative in-frame initiation site. Both forms have tumour suppressor function and form the same complexes. The only differences between $pVHL_{19}$ and $pVHL_{30}$ that have been identified are in the cellular localisation

of the proteins. $pVHL_{19}$ is equally distributed between the nucleus and the cytosol and does not associate with cell membranes, whereas $pVHL_{30}$ is mainly localised to the cytoplasm with small amounts of the protein localised to the nucleus or found in association with cell membranes (Iliopoulos *et al.,* 1998).

pVHL ($pVHL_{19}$ and $pVHL_{30}$), is one component of a complex that acts as an E3 ubiquitin ligase (Lisztwan *et al.,* 1999; Iwai *et al.,* 1999). The other members of the complex are elongin B, elongin C, Cullin 2 and Rbx1 (RING box protein 1, Duan *et al.,* 1995; Kibel *et al.,* 1995; Pause *et al.,* 1997; Kamura *et al.,* 1999, respectively). Crystallisation of the pVHL- elongin B-elongin C (VBC) complex (also referred to as the VHL E3 ligase, VBCC complex [pVHL-elongin B-elongin C-Cul2], VBC-CR {VBC-Cul2-Rbx1} or the HIF ubiquitin ligase) revealed pVHL has two domains, the α domain and the β domain (Stebbins *et al.,* 1999). The α domain binds components of the E3 ligase complex and the β domain is mainly involved in substrate recognition. The α domain along with a small portion of the β domain interact with elongin C which in turn binds to elongin B. Folding of pVHL and incorporation into the VBC complex is assisted by chaperone proteins, in particular heat shock protein 70 (Hsp70) or TCP-1 ring complex (TriC where TCP represents T-complex polypeptide), thus protecting pVHL from auto-ubiquitination (Czyzyk-Krzeska and Meller, 2004; Schoenfeld *et al.,* 2000). Once the trimeric VBC complex is formed Cul2 can associate followed by Rbx1 (figure 1.7 Pause *et al.,* 1999; Kamura *et al.,* 1999). Rbx1 is a RING finger protein and facilitates polyubiquitination of the substrate. Cul2 regulates the pVHL E3 ligase complex by undergoing neddylation. Nedd8 is a small ubiquitin like molecule that is covalently attached to lysine 689 of Cul2 (Czyzyk-Krzeska and Meller, 2004). This process enhances the ubiquitin ligase activity of the complex and is also thought to aid recruitment of the E2 enzyme to the pVHL E3 ligase complex (Kim and Kaelin Jr, 2003).

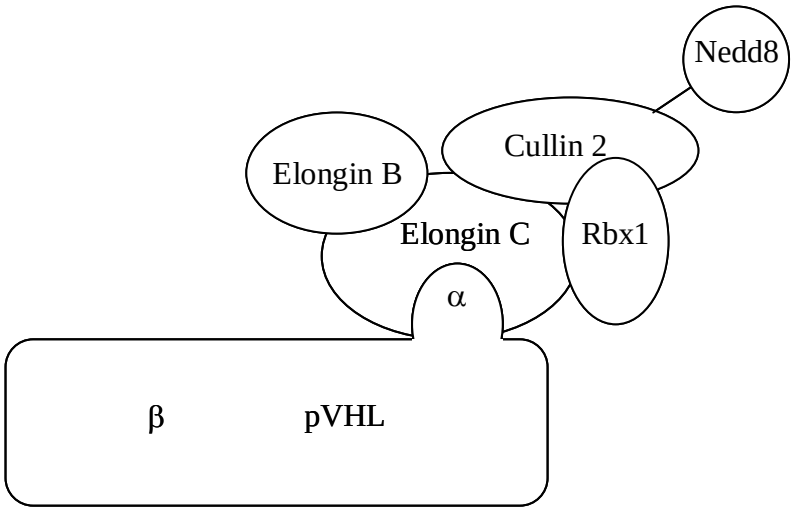


**Figure 1.7 The pVHL E3 ubiquitin ligase complex**

pVHL binds to Elongin C through its α and part of its β domains. Elongin B then binds to Elongin C. The pVHL-Elongin B-Elongin C complex then recruits Cullin 2 and Rbx1. Neddylation of Cullin 2 enhances the ubiquitin ligase activity of the complex.

### *1.3.5 The pVHL mediated ubiquitination and degradation of HIF-α subunits*

The best documented pVHL E3 ligase targets are the HIF-α family of proteins. This interaction was discovered following observations that pVHL-defective tumours were highly vascular and frequently overproduced angiogenic proteins e.g. vascular endothelial growth factor (VEGF; Semenza, 2000). *VEGF* was known to be a hypoxia responsive gene and it was also known that many hypoxia responsive genes were under the control of HIFs. This information, combined with the fact that HIF-1α was polyubiquitinated and degraded in normoxia, led to the discovery that HIF-1α bound to pVHL and was ubiquitinated by the pVHL E3 ligase complex (Salceda and Caro, 1997; Maxwell *et al.*, 1999; Ohh *et al.*, 2000; Kamura *et al.*, 2000; Tanimoto *et al.*, 2000; Cockman *et al.*, 2000).

In normoxia HIF-1α subunits containing an LXXLAP motif in the NODDD or CODDD are hydroxylated on conserved proline residues by one of three HIF specific PHDs (section 1.3.1). In a process aided by the association of FIH with pVHL, HIF-

1α is recruited to the pVHL E3 ligase complex. Hydroxyproline residue 564 ($Hyp^{564}$) is then recognised by the pVHL substrate recognition site, located in the β-domain (Mahon *et al.,* 2001). The presence of $L^{574}$ in HIF-1α is essential for pVHL recognition (Huang *et al.,* 2002). Structural studies of HIF-1α-pVHL complexes have revealed that, once recognised, hydroxylated $P^{564}$ is inserted into a hydrophobic pocket of pVHL. Inside the hydrophobic pocket hydroxylated $P^{564}$ interacts with $W^{88}$, $Y^{98}$, $W^{117}$, $H^{115}$ and $Ser^{111}$ of pVHL (Min *et al.,* 2002; Hon *et al.,* 2002). Mutations in three of these residues, $Y^{98}$, $S^{111}$ and $W^{117}$, abrogate HIF-1α binding to pVHL and are often found in VHL disease associated tumours (Ohh *et al.,* 2000). To prevent HIF-1α transcriptional activity while bound to the pVHL E3 ligase complex, pVHL associates with histone deacetylases 1-3 (HDAC1-3; Mahon *et al.,* 2001). pVHL recognition of HIF-1α is assisted further by activator of RNA decay 1 (ARD-1), which acetylates $Lysine^{532}$ ($K^{532}$) of HIF-1α. This modification not only enhances HIF-1α interaction with pVHL but also stimulates ubiquitination of HIF-1α (Jeong *et al.,* 2002). SSAT2 (Spermine/ Spermidine -*N*- Acetyltransferase 2) is another protein which assists in the HIF-1α degradation process. SSAT2 binds not only pVHL and Elongin C, in a process which stabilises this interaction, but also HIF-1α, promoting its ubiquitination (Baek *et al.,* 2007). After substrate recognition Rbx1 facilitates the transfer of ubiquitin from the E2 enzyme, Ubc5, to HIF-1α. A second ubiquitin is then conjugated to $K^{48}$ of the first ubiquitin and so on. A minimum of four ubiquitin proteins must be conjugated to HIF-1α for degradation to occur (Pickart C., 2000). The β domain of pVHL also associates with Tat binding protein 1 (TBP-1). This association occurs while pVHL is complexed with the other components of the E3 ubiquitin ligase and also with HIF-1α (Corn *et al.,* 2003). TBP-1 is one of the six ATPases that are present in the 19S regulatory particle of the 26S proteasome (Tanahashi *et al.,* 1998). It is hypothesised that the association of TBP-1 with the β domain of pVHL (as part of the E3 ligase complex) allows for the efficient recruitment and degradation of HIF-1α by the 26S proteasome (figure 1.8). Once HIF-1α has been recruited to the 26S proteasome the polyubiquitin chain is removed and the protein unfolded before entry into the 20S core particle where degradation occurs (figure 1.8).

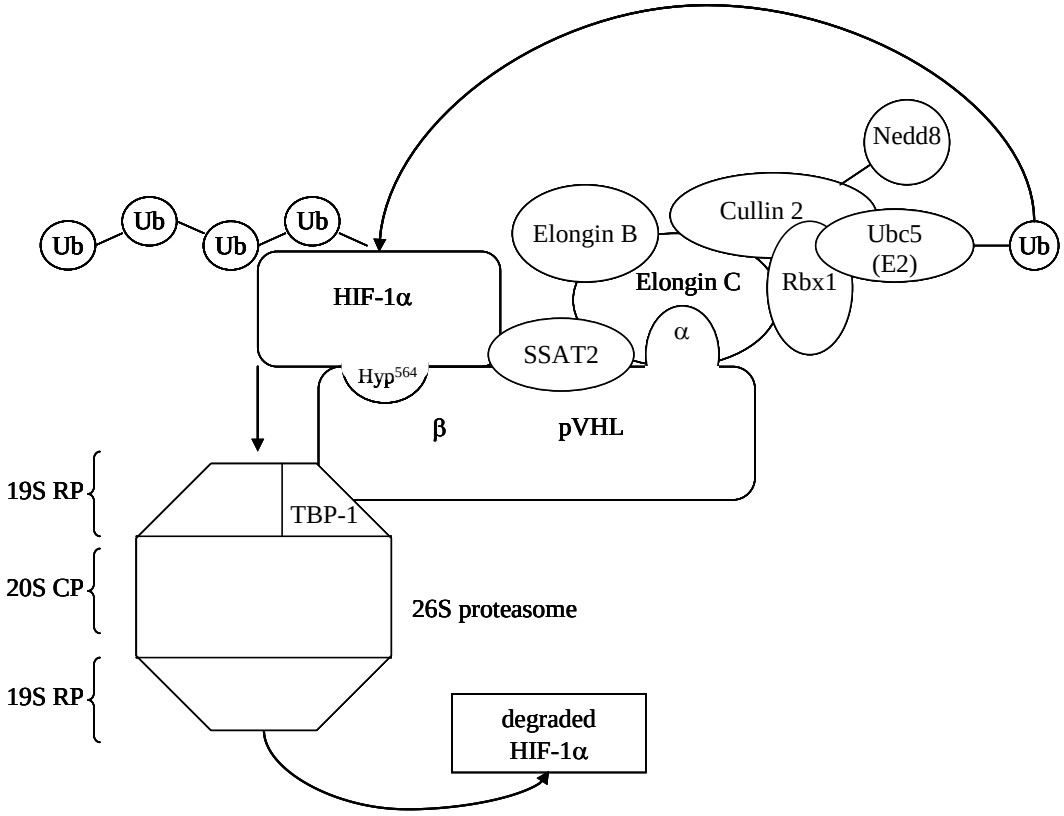


**Figure 1.8 The HIF-1α degradation pathway.**

In normoxia HIF-1α is hydroxylated by a prolyl hydroxylase on proline 564 ($Hyp^{564}$). $Hyp^{564}$ is recognised by pVHL which is a component of an E3 ubiquitin ligase complex also comprised of Elongins B and C, Cullin 2, Rbx-1 and SSAT2. Once HIF-1α has been recognised, Rbx-1 of the pVHL E3 ligase complex assists in the transfer of ubiquitin from the ubiquitin conjugating enzyme, Ubc5, to a lysine residue of HIF-1α. Subsequent ubiquitination occurs on the previously attached Ub to form a poly-ubiquitin chain on HIF-1α.

pVHL as part of the E3 ligase complex also binds with TBP-1 an ATPase of the 19S regulatory particle. This assists in poly-ubiquitinated HIF-1α recognition and recruitment to the 26S proteasome. Once recruited to the proteasome, HIF-1α is de-ubiquitinated and unfolded before entering the 20S core particle where protein degradation occurs.

**Key**: ATP, adenosine triphosphate; CP, core particle; HIF, hypoxia inducible factor; Hyp, hydroxyproline; pVHL, von Hippel-Lindau protein; Rbx1, RING box protein 1; RP, regulatory particle; SSAT, Spermidine N1-Aceytltransferase 2; TBP-1, Tat binding protein-1; Ub, ubiquitin; Ubc5, ubiquitin conjugating enzyme 5.

EPAS-1/HIF-2α is degraded in the same manner as HIF-1α. Presumably, HIF-3α splice variants with LXXLAP motifs that are capable of binding to pVHL are also

degraded in the same manner however, no data is currently available to support this hypothesis.

### *1.3.6 Additional pVHL E3 ligase complex substrates and alternative functions of pVHL.*

The role of pVHL as part of an E3 ubiquitin ligase is well documented and largely focuses on pVHL's interaction with the HIF-α proteins. However, other pVHL binding partners have been identified, some as potential ubiquitination targets, others that indicate pVHL involvement in other signalling pathways and some that still require more research in order to understand their physiological relevance (Table 1.1, Leonardi *et al.*, 2009; Kaelin, 2007).

pVHL as part of the E3 ubiquitin ligase complex has been shown to regulate the ubiquitination of several other proteins. Interaction with some of these proteins involves pVHL recognition of a hydroxylated proline residue in a similar manner to the pVHL-HIF-α interaction however, some interactions occur without proline hydroxylation. Two subunits of the RNA polymerase II complex, the main enzyme that synthesises cellular mRNA, have been identified as pVHL E3 ubiquitin ligase substrates. pVHL directly binds to the seventh subunit of RNA polymerase II (Rpb7) via its β domain. This interaction is not dependent on the hydroxylation of a proline residue but does result in the ubiquitination, proteasomal degradation and nuclear depletion of Rpb7 (Na *et al.*, 2003). Rpb7 is found at high levels in the kidney suggesting a role for Rpb7 in the development of renal clear cell carcinoma, a tumour type often found in patients with von Hippel-Lindau disease (section 1.6.5). Rpb7 regulates the transcription of VEGF, a protein often found up-regulated in tumours associated with VHL disease. Thus, loss of pVHL could cause up-regulation of VEGF in a HIF-independent manner (Czyzyk-Krzeska and Meller, 2004).

**Table 1.1 pVHL protein association**

| pVHL associated proteins | Interacting protein function | pVHL action (where known) | Reference |
|---|---|---|---|
| Elongin B (p14) | pVHL stabilisation; ubiquitin ligase component | Formation of E3 Ub ligase complex | Duan *et al.*, 1995; Kibel *et al.*, 1995; Iwai *et al.*, 1999; Lisztwan *et al.*, 1999 |
| Elongin C (p18) | pVHL stabilisation; ubiquitin ligase component | Formation of E3 Ub ligase complex | Duan *et al.*, 1995; Kibel *et al.*, 1995; Iwai *et al.*, 1999; Lisztwan *et al.*, 1999 |
| Cullin 2 | Ubiquitin ligase component | Formation of E3 Ub ligase complex | Pause *et al.*, 1997; Iwai *et al.*, 1999; Lisztwan *et al.*, 1999 |
| SSAT2 | Stabilisation of pVHL:Elongin C interaction | Formation of E3 Ub ligase complex | Baek *et al.*, 2007 |
| Rbx1 (ROC1) | Ubiquitin ligase component | Not Applicable | Kamura *et al.*, 1999 |
| Hsp70 | Folding of pVHL and VCB complex | Not Applicable | Melville *et al.*, 2003 |
| TRiC | Folding of pVHL and VCB complex | Not Applicable | Melville *et al.*, 2003 |
| HIF-α sub-units | Regulation of hypoxia responsive genes | Ubiquitination of HIF-α sub-units | Maxwell *et al.*, 1999; Cockman *et al.*, 2000 |
| FIH-1 | HIF-α recruitment to pVHL E3 ligase complex/asparaginyl hydroxylation of HIF-α | Not Applicable | Mahon *et al.*, 2001 |
| TBP-1 | Recruitment of pVHL ubiquitination targets to 26S proteasome | Not Applicable | Corn *et al.*, 2003 |
| VHLaK | Repression of HIF-1α mediated transcription | Recruits VHLaK to the HIF binding promotor | Li *et al.*, 2003 |
| VDU-1 and 2 | HIF de-ubiquitinating enzymes | Ubiquitination of VDU – 1 and VDU-2 | Li *et* al., 2002; Li *et al., 2003;* Li *et al.*, 2005 |
| Rpb7 | Transcription regulation | Ubiquitination of Rpb7 | Na *et al.*, 2003 |
| Rpb1 | Transcription regulation/ possible DNA repair | Ubiquitination of Rpb1 | Kuznetsova *et al.*, 2003 |
| Sp1 | Transcriptional activator | Repression of Sp1-dependent transcription | Pal *et al.*, 1998 |
| PKCλ, PKCζ | Immune response | Inhibition of aPKCλ and ζ kinase activity; possible ubiquitination of these proteins | Okuda *et al.*, 1999 |
| PKCδ | Tumour suppressor protein; Cell cycle progression; Apoptosis | Inhibition of PKCδ kinase activity | Pal *et al.*, 1997 |

| pVHL associated proteins | Interacting protein function | pVHL action (where known) | Reference |
|---|---|---|---|
| Jade-1 | Possible tumour suppressor function; | Jade-1 stabilisation leading to Wnt pathway regulation | Zhou *et al.,* 2005 |
| HuR (RNA binding protein) | mRNA stabilisation | Possible HuR regulation | Danilin *et al.,* 2009 |
| α-tubulin | Microtubule protein | Microtubule stabilisation | Hergovich *et al.,* 2003 |
| β - tubulin | Microtubule protein | Microtubule stabilisation | Hergovich *et al.,* 2003 |
| Fibronectin | Extracellular matrix protein | Possible involvement in extracellular matrix assembly | Ohh *et al.,* 1998 |

pVHL also targets subunit one of the RNA polymerase II complex (Rpb1) for ubiquitin mediated proteasomal degradation. This interaction requires hydroxylation of $P^{1465}$, located at the end of an LXXLAP motif and hyperphosphorylation of the C-terminal domain of Rpb1. The functional reason for pVHL mediated Rpb1 degradation is still unknown (Kuznetsova *et al.,* 2003). However, following findings that pVHL protects cells from UV induced apoptosis, it is hypothesised that pVHL mediated ubiquitination of Rpb1 may be involved in transcription regulation and DNA repair (Czyzyk-Krzeska and Meller, 2004).

Two other proteins have been identified as potential targets of the pVHL E3 ubiquitin ligase complex, atypical protein kinase C delta (aPKCδ) and VHL interacting de-ubiquitylating enzyme-1 (VDU-1). Both of these proteins interact with the β domain of pVHL but they do not contain prolyl hydroxylation motifs. The pVHL mediated interaction with VDU-1 may cause the ubiquitin mediated degradation of other proteins by inhibiting de-ubiquitination of specific pathways. pVHL interacts with the regulatory domain of aPKCδ. However this interaction only occurs when aPKCδ is in an active conformation as the regulatory domain is masked when aPKCδ is inactive. Loss of pVHL complex activity with regard to aPKCδ could lead to cytoskeletal disorganisation and affect cell-cell interactions (Czyzyk-Krzeska and Meller, 2004).

Further experimental findings have implicated a role for pVHL in microtubule stabilisation, fibronectin matrix assembly, cell cycle control, PKC-dependent signalling, urokinase-type plasminogen activator system regulation and transcription repression in certain tissues (reviewed by Ivan and Kaelin Jr, 2001; Czyzyk-Krzeska and Meller, 2004). Of particular interest is the pVHL dependent repression of HIF-1α transactivation by pVHL associated KRAB-A domain containing protein (VHLaK, KRAB, Kruppel associated box, Li *et al.*, 2003). VHLaK appears to be recruited, by pVHL, to HIF bound to the hypoxia response element (HRE) of target genes. VHLaK also interacts with the transcriptional repressor KRAB associated protein 1 (KAP-1)/ KRAB interacting protein 1 (KRIP-1)/ transcription intermediary factor 1β which enhances the transcriptional repression conferred by the KRAB-A domain (figure 1.9). Once formed the pVHL-VHLaK-KAP-1 complex represses HIF-1α transcriptional activity and HIF-1α induced VEGF expression in HEK 293 cells (Li *et al.*, 2003).

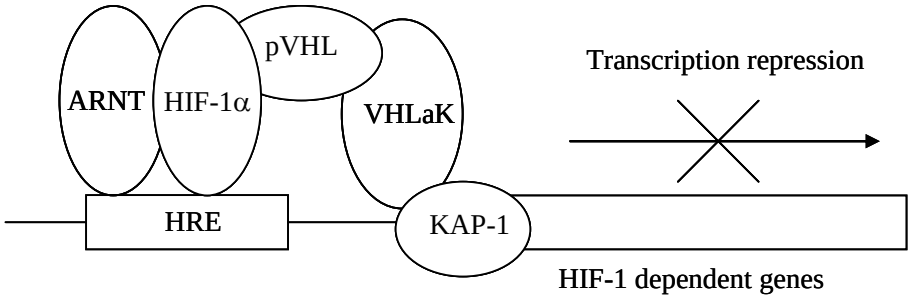


**Figure 1.9 The proposed mechanism of HIF transcriptional repression by pVHL and VHLaK.**

pVHL recruits VHLaK to the HIF-1 transcription complex (dimerised HIF-1α and ARNT bound to the HRE of a target gene). In turn VHLaK recruits KAP-1 a well known transcriptional repressor to inhibit HIF-1 dependent transcription.

**Key:** ARNT, aryl hydrocarbon receptor nuclear translocator; HIF, hypoxia inducible factor, HRE, hypoxia response element; KAP-1, KRAB associated protein 1; KRAB, Kruppel associated box VHLaK, pVHL associated KRAB-A domain containing protein; pVHL, von Hippel Lindau protein

## 1.4 The effect of hypoxia on HIFs and the HIF transcriptional response

In hypoxia HIF-1α and EPAS-1 are no longer hydroxylated by the PHDs due to lack of oxygen, a requirement for PHD activity. Un-hydroxylated proline residues are not recognised by pVHL and thus pVHL mediated HIF-1α/EPAS-1 protein degradation cannot occur, resulting in HIF-1α/EPAS-1 protein up-regulation. Whether hypoxia has a similar effect on the protein levels of HIF-3α remains to be determined.

After the hypoxic stabilisation of HIF-1α/EPAS-1 the proteins translocate to the nucleus in a process that occurs irrespective of the presence of ARNT (Chilov *et al.,* 1999). This process is mediated by the presence of a nuclear localisation signal (NLS) residing in the C-terminal portion of all three HIF-α subunits (Kallio *et al.,* 1998; Luo and Shibuya, 2001). Once in the nucleus HIF-1α/EPAS-1 subunits bind their dimerisation partner, ARNT/HIF-1β, to form HIF-1 and EPAS, respectively. In certain cell types, dimerisation with ARNT2 may occur instead of ARNT (Maltepe *et al.,* 2000). Dimerisation of HIF-1α/EPAS-1 with ARNT occurs via the bHLH domain and the PAS domain appears to stabilise this interaction (section 1.2.1). Once ARNT has bound, a conformational change in HIF-1α/EPAS-1 occurs that induces activation of the protein (Kallio *et al.,* 1997). The activated HIF-1/EPAS transcription factor recognises a hypoxia response element (HRE) with the DNA consensus sequence; 3' RCGTG 5' (where R generally represents an A or G) in HIF target genes and binds to these sequences via the bHLH domain. The lack of available oxygen in a hypoxic environment also abrogates the function of FIH resulting in a decrease of HIF-1α/EPAS-1 asparagine hydroxylation. Lack of asparagine hydroxylation activates the C-TAD of HIF-1α/EPAS-1 resulting in increased transcriptor co-activator recruitment such as CBP/p300, SRC-1 and TIF2 (section 1.4.1). The transcriptional co-activators then recruit components of the basal transcription machinery (BTM) to ensure efficient transcription by HIF-1/EPAS of their target genes (figure 1.10, sections 1.4.2 and 1.4.3).

The transcriptional response of HIF-1/EPAS can be further influenced by phosphorylation of HIF-1α, methylation of the HIF-1/EPAS binding site, the

sequence of the HRE and the presence of additional transcription factors such as activator protein-1 (AP-1, Wenger *et al.*, 2005).

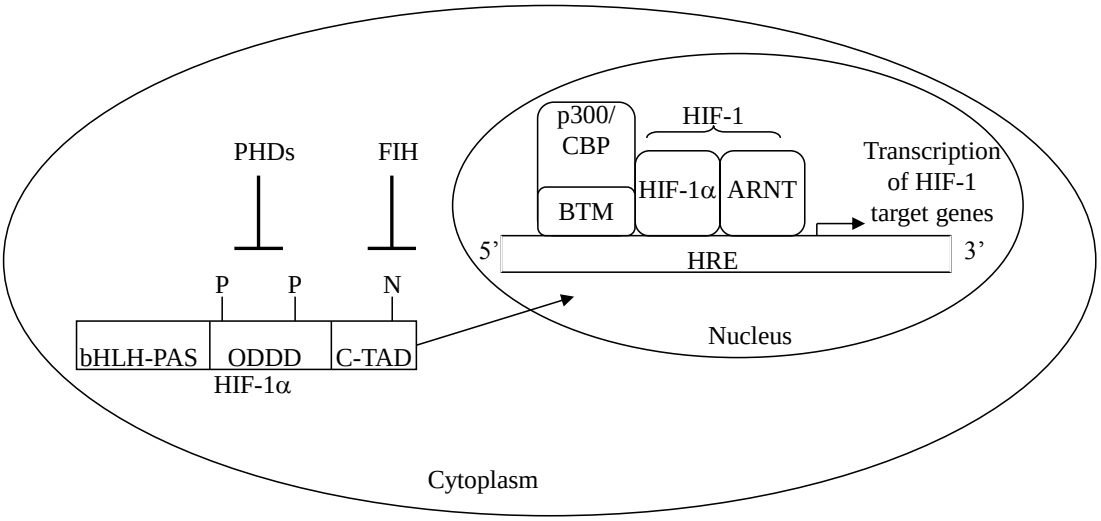


**Figure 1.10 HIF-1α in hypoxia**

In hypoxia the PHDs and FIH are no longer capable of hydroxylating HIF-1α. Abrogated prolyl hydroxylation prevents pVHL mediated proteasomal degradation of HIF-1α resulting in increased HIF-1α protein levels. HIF-1α then translocates to the nucleus where it dimerises with ARNT to form HIF-1. HIF-1 recognises a DNA consensus sequence known as the HRE in target genes. The C-TAD of HIF-1α is no longer hydroxylated by FIH in hypoxia and becomes activated, resulting in the recruitment of p300/CBP, a transcriptional co-activator. p300/CBP then recruits other proteins that form the BTM and transcription of HIF-1 target genes occurs.

**Key:** ARNT, Aryl Hydrocarbon Nuclear Translocator; bHLH-PAS, basic helix-loop-helix-Per-ARNT-Sim domain; BTM, basal transcription machinery; C-TAD, C-terminal transactivation domain; CBP, CREB binding protein; FIH, Factor inhibiting HIF; HIF, hypoxia inducible factor; HRE, hypoxia response element; ODDD, oxygen dependent degradation domain; PHDs, prolyl hydroxylase domain containing proteins

### *1.4.1 HIF transcriptional co-activators and transcriptional activity enhancers*

CBP/p300 were the original transcriptional co-activators identified that bound to HIF-1α and increased the transcriptional activation of HIF target genes e.g. VEGF (section 1.4.4, Arany *et al.*, 1996). CBP and p300 are ubiquitiously expressed, nuclear localised proteins, belonging to the CBP/p300 family of proteins. This family also includes the proteins p270 and p400 however, these have not been associated with HIF transcriptional activity (Giles *et al.*, 1998).

There is a high degree of homology between p300 and CBP which suggests a high degree of functional redundancy. CBP was originally identified as a binding partner for cyclic adenosine monophosphate response element transcription factor (CREB) while p300 was discovered through its interaction with the adenoviral E1A protein. Further experiments showed that each protein was interchangeable for these functions. Due to the interchangeable nature of the two proteins they are generally referred to as CBP/p300 (Kalkhoven, 2004).

CBP/p300 have several cellular functions, they act as transcriptional co-activators, forming a bridge between transcription factors like HIF-1/EPAS and the transcription initiation complex containing RNA polymerase II (section 1.4.3). The second important aspect of CBP/p300 co-activator function is their intrinsic histone acetyltransferase (HAT) activity. This allows CBP/p300 to acetylate nucleosomal histones that are in close proximity to gene promoters. It is thought that the acetylation of histones neutralises their positive charge thus loosening the histone:DNA interaction resulting in increased accessibility to the DNA for the transcription complex (section 1.4.3). CBP/p300 is also involved in multiple events that are central to cell growth, differentiation, transformation and apoptosis (Goodman and Smolik, 2000). Both CBP and p300 are essential in embryogenesis however, despite their high homology and interchangeable nature, in this role at least, they have some unique functions. *In vivo* studies have shown that homozygous CBP and p300 knockout mice die before birth and both sets of mice display open neural tube defects indicating CBP and p300 share some common functions. However, the phenotypes of the mice also show CBP and p300 have some unique functions. $p300^{-/-}$ mice display heart defects which $CBP^{-/-}$ mice do not exhibit, while $CBP^{+/-}$ mice exhibit craniofacial abnormalities and growth retardation, which is not observed in the $p300^{+/-}$ counterparts (reviewed by Kalkhoven, 2004). In addition, CBP and p300 are thought to be tumour suppressor proteins due to their inactivation by the adenoviral E1A oncoprotein (Mazure *et al* 2004).

The physical interaction between HIF-1α/EPAS-1 and CBP/p300 occurs via the activated C-TAD and CH1 domain of each protein, respectively (Kallio *et al.,* 1998; Arany *et al.,* 1996; Kung *et al.,* 2000). The basis of this interaction is the hypoxic inhibition of FIH function. This results in asparagine 803 of HIF-1α being left

unhydroxylated (Sang *et al.,* 2002). The CH 1 domain of CBP/p300 can then form a clamp around the unhydroxylated asparagine residue, in an energetically favourable reaction (Freedman *et al.,* 2002). The CBP/p300:HIF-1α interaction is enhanced by s-nitrosation of cysteine 800 of HIF-1α. $L^{795}$, $L^{818}$ and $L^{822}$ of HIF-1α are also crucial for CBP/p300 recruitment (Yasinka and Sumbayev, 2003; Freedman *et al.,* 2002).

Several proteins have been identified that interact with both CBP/p300 and HIF-1α. Some of these proteins have transcriptional co-activator function e.g. SRC-1 and TIF-2 while others appear to enhance HIF-1 transcriptional activity in processes that still need to be determined e.g. c-Jun. SRC-1 and TIF2/SRC-2 are transcriptional co-activators belonging to the p160 steroid receptor co-activator family (Xu and Li, 2003). Both SRC-1 and TIF2 act in a synergistic manner with CBP/p300 to enhance transcriptional activation by HIF-1 (Carrero *et al.,* 2000). SRC-1 does not interact directly with HIF-1α but is recruited by CBP to form a HIF-1α/ARNT/CBP/SRC-1 complex via its AD-1 domain (transcriptional activation domain 1, Ruas *et al.,* 2005 and Xu and Li, 2003). The mechanism by which SRC-1 and TIF2 enhance the transcriptional activation of HIF-1 responsive genes has yet to be elucidated but it may involve the recruitment of histone methyltransferases, such as protein arginine methyltransferase 1 (Xu and Li, 2003).

The increase in HIF-1 transcriptional activity induced by SRC-1 or TIF2 was greatly potentiated by Ref-1 (redox-effector factor-1, Carrero *et al.,* 2000). Ref-1 is involved in base excision repair, oxidative DNA damage repair and is known to stimulate the DNA binding activity of several transcription factors, including EPAS (Evans *et al.,* 2000). In pancreatic and prostate carcinomas, HIF-1α, STAT3, CBP/p300 and Ref-1 form a transcriptional complex to regulate Src-dependent hypoxia-induced expression of VEGF. This finding suggests Ref-1 may form the same complex in hypoxic cells (Gray *et al.,* 2005).

c-Jun is another transcription factor whose interaction with HIF-1 potentiates the transcriptional activity of HIF responsive genes (Alfranca *et al.,* 2002). However, c-Jun does not act as a transcription factor in this case and therefore does not bind to

DNA in order to increase the transcriptional activity of HIF responsive genes. Instead, c-Jun binds to the ODDD domain of HIF-1α, preventing HIF-1α ubiquitination and proteasome mediated degradation and resulting in an accumulation of functional HIF-1 (Yu *et al.,* 2009).

In addition, several transcriptional co-activators have been identified that are specific for either HIF-1α or HIF-2α. For example; HNF4 (hepatocyte nuclear factor 4), a liver and kidney specific transcriptional co-activator, acting in conjunction with HIF-1, but not HIF-2/EPAS, has been reported to be essential for *epo* transcription. NF-κB essential modulator (NEMO) and the transcription factor Ets1 interact exclusively with HIF-2α. NEMO enhances HIF-2α mediated transcription in normoxia while Ets1 interacts with HIF-2α to enhance the transcription of VEGF receptor 2 (reviewed by Loboda *et al.,* 2010).

### *1.4.2 Regulation of HIF transcriptional activity by CITED2 (CBP/p300 interacting transactivator with ED rich tail).*

Although CBP/p300 are the central transcriptional co-activators of HIF-1/EPAS, a protein that can negatively regulate the CBP/p300:HIF-1/EPAS interaction has been identified, p35srj/CITED2 (CBP/p300 interacting transactivator with ED rich tail 2). All endogenous CITED2 binds to the CH1 domain of CBP/p300, thus competing with HIF-1 for CBP/p300 binding and inhibiting HIF-1 transactivation (Bhattacharya *et al.,* 1999; Freedman *et al.,* 2003). CITED2 protein levels are up-regulated by hypoxia, suggesting CITED2 participates in a negative feedback loop to down-regulate HIF-1 mediated transcription. However, the low levels of endogenous CITED2, when compared to endogenous CBP/p300 levels, would not seem to support the competitive model hypothesis. Another hypothesis suggests that the availability of functional CH1 sites to HIF is limited by the binding of other transcription factors and other members of the CITED family (e.g. NFkB and CITED4, respectively) to the CH-1 domain of CBP/p300. This adds a level of complexity to the competitive model hypothesis (Bhattacharya and Ratcliffe, 2003; Fox *et al.,* 2004). In support of a competitive model hypothesis are the findings in CITED2$^{-/-}$ mice embryos where inactivation of CITED2 results in the heightened expression of HIF target genes (Yin *et al.,* 2002).

### *1.4.3 HIF dependent transcriptional regulation.*

Following HIF-α/HIF-β binding to form HIF-1/EPAS, translocation to the nucleus occurs. HIF-1/EPAS then binds to the HRE. Dissection of the *epo* enhancer identified two sequences essential for reporter activity the core HRE consensus sequence (A/G)CGTG and the HIF ancillary sequence (HAS), an imperfect repeat sequence that recruits transcription factor complexes other than HIF. Once HIF/EPAS has assembled on the HRE transcriptional co-activators are recruited by the C-TAD and N-TAD of HIF-1/EPAS (section 1.4.1) Once CBP/p300 have been recruited, they acetylate the histone octamers forming the nucleosomes that mask the appropriate gene promoter (reviewed by Lisy and Peet, 2008). Histone acetylation relaxes the histone:DNA interaction therefore making gene promoters more accessible for recruitment of the transcription factors that comprise the basal transcription machinery binding (BTM). The BTM is comprised of the general transcription factors (GTFs) TFIIA, TFIIB, TFIID, TFIIE, TFIIF and TFIIH (transcription factor for type II genes A, B, D-F and H, respectively), which are essential for RNA polymerase II (RNA pol II) mediated transcription. Once all of the TFII factors have assembled into the transcription initiation complex, RNA polymerase II mediated transcription of HIF-1/EPAS responsive genes can occur (Cosma, 2002).

### *1.4.4 HIF target genes*

Microarray analysis has shown that there are over 200 hypoxia responsive genes. However, not all of these genes are HIF regulated. Approximately 70 genes are known to be HIF-1 targets. The majority of these are involved in oxygen supply, cellular metabolism, cell growth and apoptosis. Other gene products regulated by HIFs include transcriptional co-factors, transcriptional repressors, chaperone proteins and proteins involved in oxygen sensing. Figure 1.11 shows the majority of known HIF-1/EPAS regulated genes.

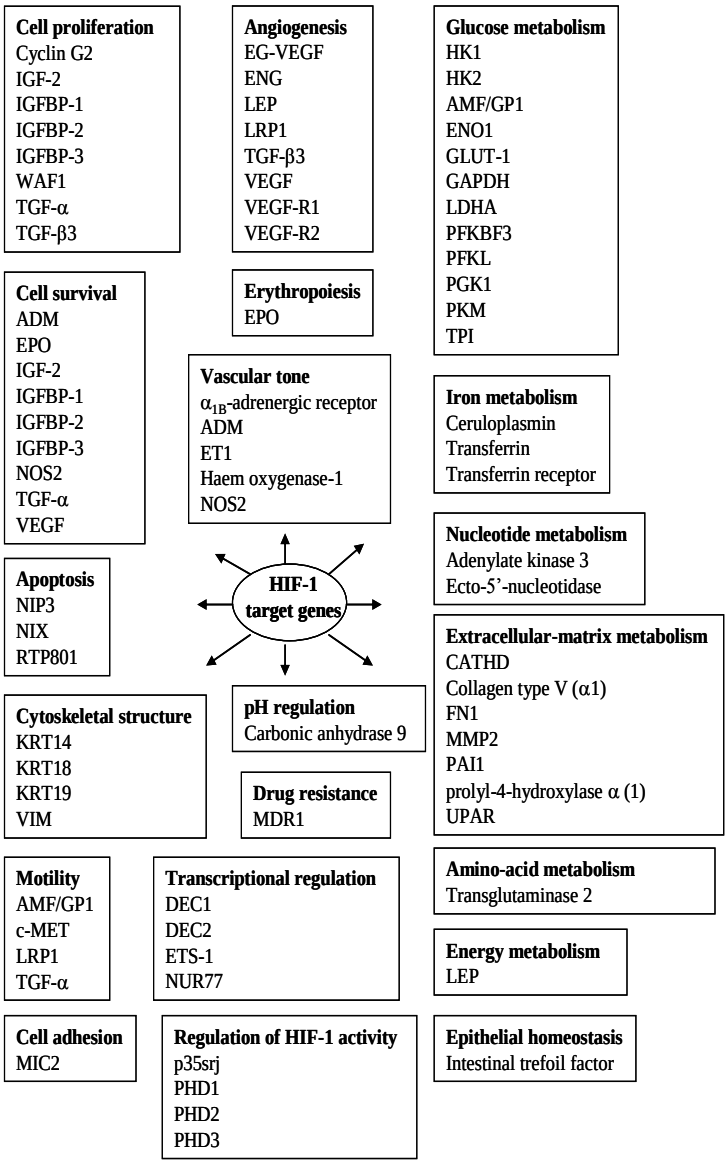


**Figure 1.11 Genes that are transcriptionally up-regulated following HIF activation.**

Based on information from Semenza, 2002; Lee *et al.*, 2004; Bardos and Ashcroft, 2005.

**Key:** ADM, adrenomedullin; AMF, autocrine motility factor; DEC1, deleted in esophageal cancer 1; DEC2, deleted in esophageal cancer 2; EG-VEGF, endocrine gland derived vascular endothelial growth factor; ENG, endoglin; ENO1, enolase 1; EPO, erythropoietin; ETS1, v-ets avian erythroblastsosis virus e26 oncogene homolog1; FN1, fibronectin 1; GAPDH, glyceraldehyde-3-phosphate dehydrogenase; GLUT 1 , glucose transporter 1; HIF, hypoxia inducible factor; HK1, hexokinase 1; HK2, hexokinase 2; IGF-2, insulin like growth factor 2; IGFBP -1, insulin-like growth factor binding protein 1; IGFBP -2, insulin-like growth factor binding protein 2; IGFBP -3, insulin-like growth factor binding protein 3; KRT14, keratin 14; KRT18, keratin 18; KRT19, keratin 19; LDHA, lactate dehydrogenase A; LEP, leptin; LRP1, lipoprotein receptor-related protein 1; MDR1, multidrug resistance protein 1; MMP2, matrix metalloproteinase 2; NIP3, BCL2/adenovirus E1B 19kDa interacting protein 3; NIX, BCL2/adenovirus E1B 19kDa interacting protein 3 like; NOS2, nitric oxide synthase 2; PAI1, plasminogen activator inhibitor 1; PFKL, phosphofructokinase liver type; PGK1, phosphoglycerate kinase 1; PHD, prolyl hydroxylase domain containing protein; PKM, pyruvate kinase muscle; RTP801, HIF-1 responsive protein 801; TGF-β3, transforming growth factor β3; TGF-α, transforming growth factor α; TPI, triosephosphate isomerise; UPAR, urokinase-type plasminogen activator receptor; VEGF, Vascular endothelial growth factor; VEGFR1, vascular endothelial growth factor receptor 1; VEGFR2, vascular endothelial growth factor receptor 2; VIM, vimentin; WAF1, wild-type p53-activated fragment 1

### *1.4.5 Regulation of HIF activity in hypoxia by other signalling pathways.*

Although hypoxia is the major mechanism through which HIF proteins are regulated, regulation by other signalling pathways also plays a role. This regulation can occur under both hypoxic and normoxic conditions (section 1.5). In hypoxia the MAPK signalling pathway (section 1.5.2), reactive oxygen species (ROS), p53 and heat shock protein 90 (HSP90) have all been identified as playing a role in HIF regulation (reviewed by Bardos and Ashcroft, 2005).

## 1.5 Regulation of HIF activity in normoxia by other signalling pathways.

Various stimuli induce the up-regulation of HIF-α subunits in normoxic conditions. These include transition metals, nitric oxide (NO), reactive oxygen species (ROS), growth factors, cytokines and oncogenic activation (Semenza, 2002b; Bardos and Ashcroft, 2005). In particular the following growth factors and cytokines have been shown to up-regulate HIF-1α in normoxia: epidermal growth factor (EGF), insulin like growth factor 1 (IGF-1), insulin like growth factor 2 (IGF-2), insulin, heregulin, interleukin-1β, follicle stimulating hormone (FSH), androgens, hepatocyte growth factor (HGF), tumour necrosis factor-α (TNF-α), angiotensin II, platelet derived growth factor (PDGF), transforming growth factor β (TGF-β) and thrombin. Similar observations have also been made for induction of EPAS-1 (Bardos and Ashcroft, 2005). Many of these stimuli can regulate HIF activity either by using reactive oxygen species as part of their signalling pathway or via the phosphatidylinositol 3-kinase (PI3K) or the mitogen- activated protein kinase (MAPK) signalling pathways (sections 1.5.3, 1.5.1 and 1.5.2, respectively). Signalling via the PI3K or MAPK pathways can be dependent on a number of factors that include the nature of the signal, cell type and the targeted pathway that results in increased HIF-α up-regulation (Semenza, 2002b).

### *1.5.1 HIF-1α and the PI3K signalling pathway in normoxia*

The PI3Ks are a family of lipid kinases that phosphorylate the 3' hydroxyl group of phosphatidylinositols and phosphoinositides. PI3Ks are classified into three groups (class I, II and III) based on their structure, substrate specificity, distribution and mechanism of activation. Of the three classes, the most information is known about Class I. Class I PI3Ks are further subdivided into Class IA and Class IB. Members of these groups are activated by receptor tyrosine kinases (RTKs) and G-protein coupled receptors, respectively.

Growth factor signalling via the PI3K pathway is largely mediated via class IA PI3Ks. Growth factors known to stimulate Class IA PI3Ks include EGF, PDGF and IGF-1. Once a growth factor has bound to the relative RTK, this results in the recruitment of the appropriate PI3K from the cytoplasm to the cell membrane where the PI3K phosphorylates phosphatidylinositol 4,5 bisphosphate ($PIP_2$) to generate phosphatidylinositol 3,4,5 trisphosphate ($PIP_3$). Proteins with high affinity binding sites for these lipids are subsequently recruited by $PIP_3$. Important downstream effectors of $PIP_3$ are phosphoinositide dependent kinase 1 and Akt,, which is fully activated by PDK-1. Recruitment of these proteins to the cell membrane brings them into close contact with their substrates or target proteins, thus potentiating further downstream signalling (figure 1.12, reviewed by Chalhoub and Baker, 2009; Jiang and Liu, 2009).

Class I PI3K signalling is antagonised by the action of dual specificity phosphatases/ 3'-phosphoinositide phosphatases which have protein phosphatase and lipid phosphatase activity. Phosphatase and tensin homologue deleted on chromosome 10 (PTEN) is one such dual specificity phosphatase and is able to specifically dephosphorylate $PIP_3$ to $PIP_2$. This means PTEN is a negative regulator of the PI3K pathway and is important in maintaining phosphatidylinositol homeostasis (Fry, 2001; Chalhoub and Baker, 2009).

The PI3K signalling pathway can regulate HIF-1α protein levels in normoxia. Several groups have published findings showing that growth factors mediated the up-regulation of HIF-1α protein levels. This up-regulation was abrogated by PI3K

inhibitors thus supporting the hypothesis that the PI3K/Akt pathway is involved in normoxic HIF-1 activation (Jiang *et al.*, 2001; Zhou *et al.*, 2004; Fukuda *et al.*, 2002; Zundel *et al.*, 2000). Similarly, PTEN inactivating mutations or loss of PTEN results in high levels of HIF dependent VEGF expression and this can be inhibited by the reintroduction of wild type PTEN (Zundel *et al.*, 2000). Constitutively active Akt results in the up-regulation of HIF-1α protein in normoxia whereas dominant negative mutants of both PI3K and Akt block HIF-1 dependent gene transcription (Zundel *et al.*, 2000; Zhong *et al.*, 2000).

Several downstream targets of Akt have been implicated in the regulation of HIF-1α activity in normoxia and hypoxia (reviewed by Bardos and Ashcoft, 2005). In particular, the mammalian target of rapamycin (mTOR) has been implicated in the regulation of HIF-1α activity. Treatment of PC-3 cells with rapamycin, an mTOR inhibitor, abrogates the accumulation of HIF-1α, preventing HIF-1 dependent transcription in both hypoxia and normoxia (Hudson *et al.*, 2002). Pore *et al* showed that activation of Akt resulted in an increase in HIF-1α translation under both hypoxic and normoxic conditions and that this response occurred via an mTOR independent pathway (Pore *et al.*, 2006).

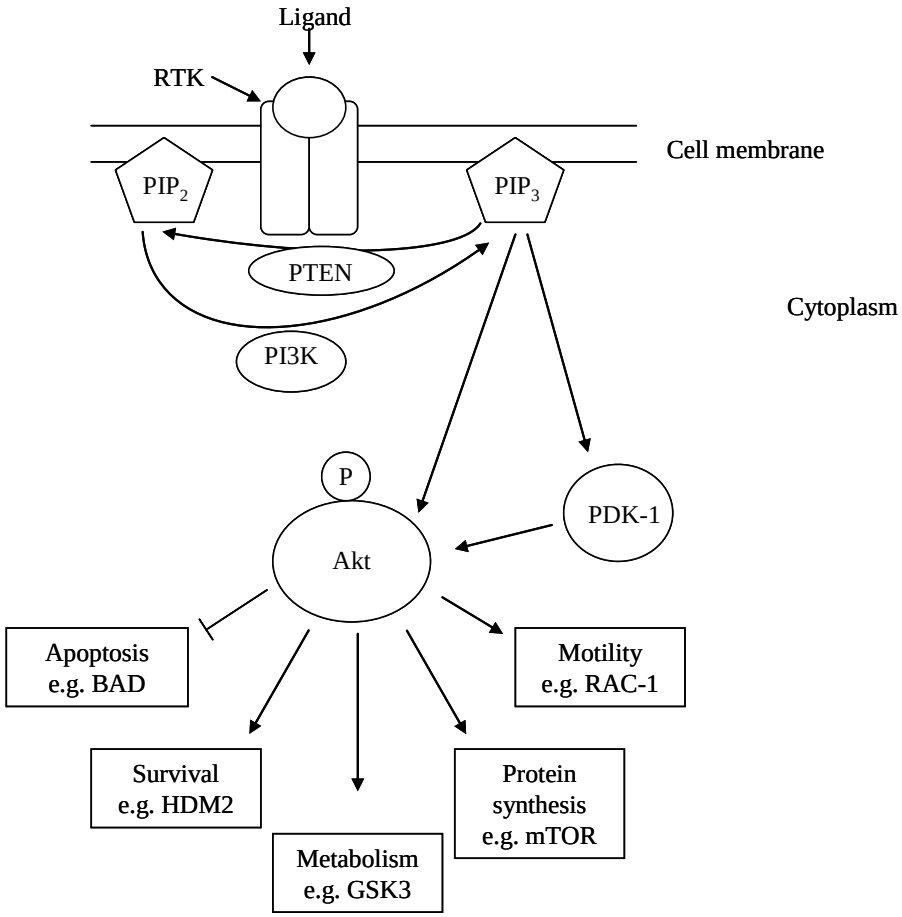


**Figure 1.12 A schematic diagram of the PI3K signalling pathway**

Growth factors such as epidermal growth factor bind to their cognate tyrosine kinase receptor and activate it. This recruits PI3K from the cytoplasm to the cell membrane where phosphorylation of phosphoinositides occurs. This activates PDK-1 which then phosphorylates and activates Akt resulting in downstream Akt signalling. PTEN is a negative regulator of the PI3K pathway and acts by dephosphorylating 3-phosphoinositides.

**Key:** BAD, BCL2 antagonst of cell death; GF, growth factor; GSK3, glycogen synthase kinase 3, HDM2, human double minute 2 homolgue; mTOR, mammalian target of rapamycin; P, phosphate; PDK, phosphoinositide dependent kinase; PI3K, phosphatidylinositol 3 kinase, PTEN, phosphatase and tensin homologue deleted on chromosome 10; 3-PtdIns, 3-phosphorylated phosphatidylinositols.

Therefore, it appears the PI3K signalling pathway regulates HIF-1 activity by increasing HIF-1α mRNA translation via mTOR dependent and independent mechanisms. However, the exact mechanism for either pathway has yet to be elucidated.

### *1.5.2 The regulation of HIF in normoxia via the MAPK pathway.*

Mitogen activated protein kinases (MAPK) belong to a large family of serine-threonine protein kinases that are involved in the regulation of a variety of important cellular processes including gene expression, translation, cell proliferation, cellular differentiation, cell survival, cell death and cell motility (Fang and Richardson, 2005). Classical MAP kinase signalling occurs via cascade pathways where a MAP kinase is activated by a MEK (MAPK kinase /MKK) which is in turn activated by a MEKK (MAPK kinase kinase/MKKK/MEKK). Often MEKK is activated by a GTPase which has itself been activated in response to a stimulus of the MAPK pathway. These stimuli include growth factors, cytokines and neurotransmitters, binding to the appropriate cell membrane receptor (Chang and Karin, 2001; Katsoulidis *et al.,* 2005). In addition, certain viral oncoproteins signal via the MAPK pathway to HIF (Yoo *et al.,* 2003; Sodhi *et al.,* 2000).

Mammals express three major sub-families of MAP kinases; the extracellular signal related kinases (ERK, also known as p42/p44 MAP kinases), the c-JUN amino terminal kinases (JNK, also known as stress activated protein kinases, SAPK) and the p38 proteins (p38α, p38β, p38γ and p38δ). Each group of MAPKs are activated by specific MAPKKs (MEK/MKKs); MEK1 and 2 for ERK 1 and 2, MKK 4 and 7 for the JNK proteins and MKK 3 and 6 for the p38 proteins. Each MAPKK can be activated by more than one MAPKKK and this added complexity is thought to be in response to different stimuli (figure 1.13, Chang and Karin, 2001).

Of the three major MAP kinases, ERK1/2 and p38 have been shown to phosphorylate HIF-1α *in vitro,* with ERK1/2 also phosphorylating HIF-1α and EPAS *in vivo* in hypoxia (Richard *et al.,* 1999; Sodhi *et al.,* 2000; Conrad *et al.,* 1999). These phosphorylation sites have still to be elucidated but several candidate sites have been identified *in vitro.* These residues are serine 641, serine 643 and threonine 796 of HIF-1α and threonine 844 of EPAS (Mylonis *et al.,* 2006; Gradin *et al*, 2002). The JNK MAP kinases have also been identified as playing a role in HIF-1α regulation in normoxia although it has not yet been determined whether phosphorylation contributes to this regulation (Doronzo *et al.,* 2006).

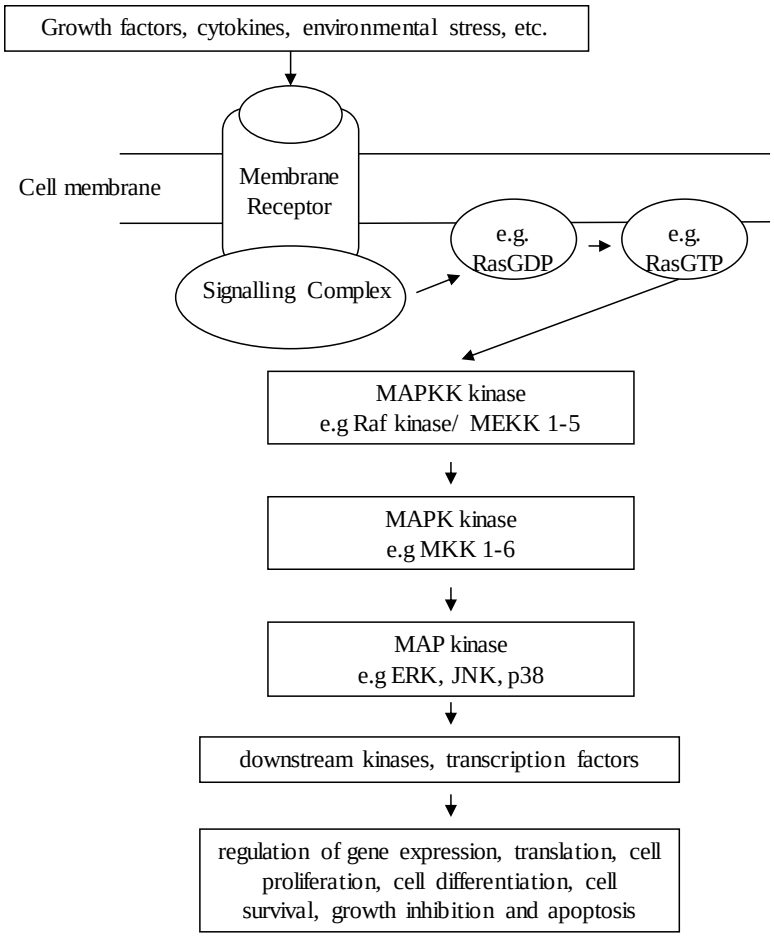


**Figure 1.13 An overview of the MAPK signalling cascade.**

Once a ligand e.g. a growth factor or cytokine has bound to the target membrane receptor, a signalling complex is formed that often results in the activation of a small GTPase e.g. Ras. The small GTPase exchanges the phosphate with MAPKK kinase, thus leading to the activation of MAPKK kinase, which leads to the phosphorylation and activation of a downstream MAPK kinase which, in turn phosphorylates and activates the target MAP kinase of the ligand.. The activated MAP kinase can then signal to other downstream factors, such as transcription factors, which can then elicit a cellular response.

ASK1, apoptosis signal-regulating kinase 1; ERK, extracellular signal related kinases; GDP, guanine diphosphate; GTP, guanine triphosphate; JNK, c-Jun amino terminal kinases; MAP, mitogen activated protein; MAPK, mitogen activated protein kinase; MAPKK/MKK, mitogen activated protein kinase kinase; MAPKKK/MEKK, mitogen activated protein kinase kinase kinase; TAK-1, transforming growth factor-β activating kinase.

IGF1, interleukin1-β, insulin and bacterial lipopolysaccharide, all up-regulate HIF-1α protein expression and the expression of HIF-1 target genes in HCT116 cells, normal human cytotrophoblast cells, human and rat vascular smooth muscle cells and human monocytes, respectively. Pre-treatment of all of these cell lines with

PD98059, a MEK inhibitor, significantly reduced HIF-1α protein up-regulation and expression of a HIF-1 target gene, providing evidence of ERK1/2 involvement in HIF regulation (Fukuda *et al.,* 2002; Qian *et al.,* 2004; Doronzo *et al.,* 2006; Frede *et al.,* 2006). The insulin mediated up-regulation of HIF-1α protein expression was also abrogated by SP600125, a JNK specific inhibitor. This showed that both the ERK1/2 and JNK pathways were involved in HIF regulation in this instance. Cycloheximide abrogated the insulin mediated up-regulation of HIF-1α and expression of a HIF-1 target gene, suggesting the MAP kinases may regulate HIF, in this instance, by increasing protein synthesis (Doronzo *et al.,* 2006).

### *1.5.3 Oncogenic activation of HIF-1 via signalling cascade pathways*

In addition to growth factor, hormonal, cytokine, RNI, ROS and heavy metal induction of HIF-1α in normoxia, HIF-1α expression can also be induced by oncogenic activation or the inactivation of tumour suppressors such as PTEN, succinate dehydrogenase B (SDHB) or pVHL (sections 1.5.1, 4.1.4 and 1.6.5, respectively).

The activated protein products of the oncogenes *ras, Src and Akt* have been shown to induce HIF-1α protein expression in several cell culture systems. Mutations in the *ras* oncogene are present in around 30% of human cancers and can lead to an increase in VEGF expression (reviewed by Adjei, 2004; Bardos and Ashcroft, 2004). Mutations in *Src* are rare and the protein product c-Src is normally overexpressed in human cancers. However, small subsets of colon and endometrial tumours have been found to harbour mutations that cause the C-terminal truncation of c-Src resulting in a constitutively active protein (reviewed by Ishizawar and Parsons, 2004).

Transformation of Rat-1 cells with H-ras led to an increase in *Glut-1* mRNA levels in normoxia that could be further potentiated by hypoxia. The increase in *Glut-1* mRNA levels corresponded with an increase in HIF-1α protein and activity levels in H-Ras transformed Rat-1 cells when compared to un-transformed cells (Chen *et al.,* 2001). The absence of HIF-1α in H-Ras transformed mouse embryonic fibroblasts (mEFs) resulted in a decrease in tumour mass when compared to wild-type H-Ras

transformed mEFs (Ryan *et al.,* 2000). Saos-2 cells overexpressing wild-type and constitutively active c-Src exhibited increased levels of HIF-1α protein in normoxia (Karni *et al.,* 2002).

Overexpression of HIF-1α co-transfected with Ras, v-Src, or Akt in HKO cells (HIF-1α knockout mouse embryonic fibroblasts) resulted in the up-regulation of HIF-1α protein levels in normoxia. HIF-1α induced by co-transfection with Ras and v-Src is not hydroxylated at proline 564. Therefore, Ras and v-Src up-regulated HIF-1α protein levels by inhibiting prolyl hydroxylation and subsequent VHL-mediated ubiquitination and degradation. However, constitutively active Akt does not inhibit prolyl hydroxylation of HIF-1α and must act via an as yet unknown alternative mechanism (Chan *et al.,* 2002).

The protein products of several viral oncogenes also lead to the normoxic up-regulation of HIF-1α via the MAPK pathway. The hepatitis B virus X (HBx) protein has been strongly implicated in angiogenesis and metastasis during hepatocarcinogenesis. HeLa (Chang liver) cells expressing a doxycycline inducible form of the HBx protein showed increased HIF-1α protein stability. HBx also induced phosphorylation of HIF-1α, activation of ERK1/2, and enhanced the transcriptional response of a HIF-1 target reporter gene. This transcriptional response was abrogated by the MEK inhibitor PD98059, suggesting HBx activates HIF-1α through the MAPK pathway (Yoo *et al.,* 2003). A second viral protein product, a constitutively active G protein coupled receptor encoded by the Kaposi's sarcoma-associated herpes virus, enhanced the expression of VEGF through increased HIF-1α activity in NIH 3T3 cells. The enhanced expression of VEGF was associated with an increased phosphorylation of HIF-1α by p38 and ERK MAP kinases (Sodhi *et al.,* 2000). It is probable that the up-regulation of HIF-1α and subsequent up-regulation of HIF-1 target genes by viral oncoproteins, confers a selective advantage to the cell infected with the virus, potentially resulting in tumour development (Ke and Costa, 2006).

### *1.5.4 Normoxic regulation of HIF by nitric oxide (NO)*

Nitric oxide (NO) is produced by nitric oxide synthase (NOS) which converts L-arginine to citrulline and nitric oxide. Three isoenzymes, inducible NOS (iNOS/NOS2), neuronal NOS (nNOS/NOS1) and endothelial NOS (eNOS/NOS3) have been identified and are named after the cell type from which they were first cloned. The major distinction between the three isoenzymes is the manner in which they are regulated. nNOS and eNOS are regulated by cytosolic calcium levels whereas iNOS is regulated by cytokine levels (Zhou and Brune, 2005).

Until a few years ago, the biological effects of NO were unknown however the field has expanded and NO is known to have many biological attributes, including acting as an inflammatory molecule and in the regulation of gene expression. The majority of biological activities attributed to NO signalling are not due to the presence of NO itself, but to reactive nitrogen intermediates (RNI). RNI are oxidation states and adducts of the products of NOS and include NO radical ($^{\bullet}NO$), $NO^-$, $NO^+$ and the adducts of these species such as $NO_2$, $NO_2^-$, $NO_3^-$, $N_2O_3$, $N_2O_4$, peroxynitrite, nitrosyl-metal complexes and S-nitrosothiols such as S-nitroso-glutathione (GSNO), (Zhou and Brune, 2005).

One of the impacts of NO is on the stabilisation and activity of HIF-1. However, this field is somewhat controversial due to the differing results obtained by independent researchers (Bardos and Ashcroft, 2005). For example, some researchers have reported an inhibitory function of NO in hypoxia however, the same response was not observed with the use of a hypoxia mimetic e.g. desferrioxamine (DFO) which was used to chemically induce HIF-1α (Huang *et al.,* 1999). Others have described HIF-1α up-regulation in response to NO in normoxia (Sandau *et al.,* 2001a). The effect of NO on HIF-1α protein levels and on HIF-1 activity has been further complicated by questions about the effects of the type of NO donor, concentration of the NO donor and incubation times of cells with the NO donor. However the drawback of using NO donors has been overcome due to the discovery that overexpression of iNOS in pig tubular LLC-$PK_1$ cells triggered HIF-1 accumulation, as does co-culture with activated macrophages expressing activated iNOS. These results confirmed the positive effect of NO on normoxic HIF-1α and also provided

evidence of a positive feedback loop, as iNOS is a HIF-1 target gene (Sandau *et al.*, 2001; Bardos and Ashcroft, 2005). Further experimentation in HEK 293 cells, with a tetracycline inducible iNOS, have shown that the concentration of NO determines whether there is a positive or negative effect on HIF-1α protein levels. High concentrations of NO (>1 μM) stabilise HIF-1α, regardless of oxygen tension. In contrast to this, low concentrations of NO (< 400nM) result in a decrease of HIF-1α protein levels in hypoxia (Mateo *et al.*, 2003).

Several studies have shown that NO, particularly in the form of GSNO, regulates the level of HIF-1α protein in normoxia by inhibiting the PHD enzymes (Metzen *et al.*, 2003 and Berchner-Pfannschmidt *et al.*, 2007). HIF-1α, PHD2 and PHD3 were induced in human osteosarcoma cells (U2OS) treated with GSNO under normoxic conditions. The accumulation of HIF-1α under these conditions was caused by transient GSNO inhibition of the PHD enzymes (Berchner–Pfannschmidt *et al.*, 2007). Another S-nitrosothiol, S-nitroso –N- acetylpenicillamine, stabilises HIF-1α by inhibiting pVHL recruitment and asparagine hydroxylation by FIH (Park *et al.*, 2008). In addition to up-regulating HIF-1α in normoxia, NO also up-regulates p53 protein levels in MCF 7 cells and causes the transient phosphorylation of ERK in MCF 7 and HEK293 cells (Thomas *et al.*, 2004; Kasuno *et al.*, 2004). The NO mediated up-regulation of normoxic HIF-1α protein levels was inhibited by PI3K and MAPK inhibitors as well as by dominant negative Ras. These results suggest the PI3K and MAPK pathways play a critical role in the NO mediated up-regulation of HIF-1 (Kasuno *et al.*, 2004).

### *1.5.5 Normoxic regulation of HIF by reactive oxygen species (ROS).*

ROS are partially reduced oxygen species that are formed in mammalian cells. ROS are produced in response to exogenous toxic reagents or endogenously as the by-products of $O_2$-utilising enzymes, such as mitochondrial respiratory chain enzymes, NADPH oxidases, cytochrome P450 family members, amino acid oxidases, xanthine oxidase, and glucose oxidases (figure 1.14). Transfer of an electron to $O_2$ gives rise to a superoxide anion radical ($O_2^{\bullet-}$). From the superoxide radical, formation of other ROS can occur including hydrogen peroxide ($H_2O_2$), hydroxyl radicals ($OH^{\bullet}$), peroxynitrite (a RNI, section 1.5.3), singlet oxygen $^1O_2$ and hypochlorous acid (HOCl, reviewed by Sauer *et al.,* 2001; Kietzmann and Görlach, 2005).

In normal physiological conditions the cell has several mechanisms in place that defend against endogenously produced ROS such as superoxide dismutase (SOD), catalase and glutathione peroxidase. The exogenous uptake of vitamins e.g. ascorbate, also helps to combat endogenously produced ROS. However, when ROS production exceeds normal physiological levels, damage to DNA, proteins, polysaccharides and lipids can occur as well as apoptosis and uncontrolled cellular proliferation. In comparison to the damaging effects of excessive ROS, there is increasing evidence that certain stimuli, such as growth factors and metal ions, can cause the generation of lower levels of ROS through enzymatic mechanisms (figure 1.14). Generation of ROS in this way causes them to act as signalling molecules, thus activating certain signalling cascades and regulating the activity of certain transcription factors, including HIF-1$\alpha$ (Kietzmann and Görlach, 2005).

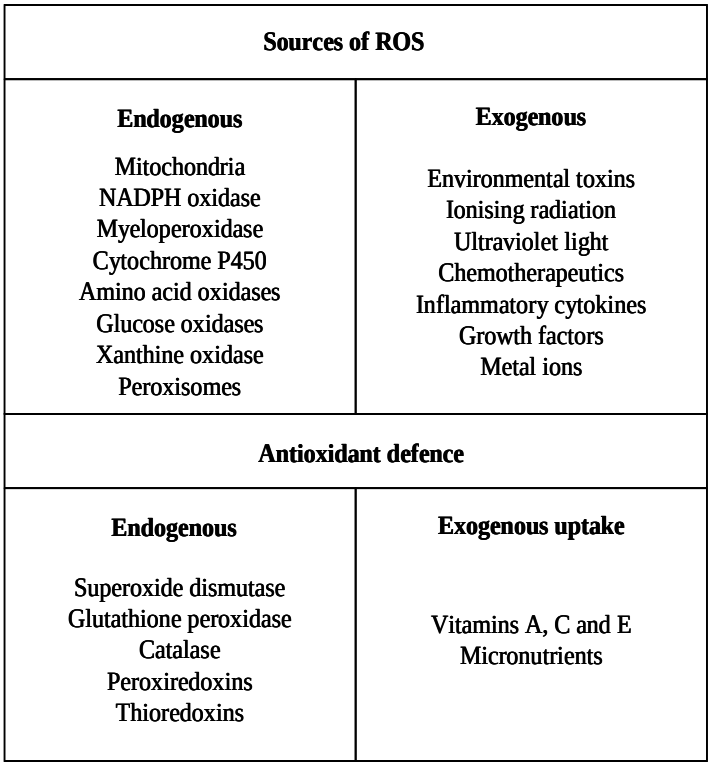


**Figure 1.14 Sources of ROS and intracellular defence mechanisms.**

Reactive oxygen species (ROS) are formed in mammalian cells in response to external stimuli or as by-products of oxygen utilising enzymes. The formation of ROS is counterbalanced by endogenous anti-oxidant defence mechanisms and by the up-take of exogenous components that act as antioxidant scavengers. Based on a figure by Sauer *et al.,* 2001.

Several ROS generating non-hypoxic stimuli have been shown to induce HIF-1α in normoxia. These stimuli include; hydrogen peroxide, vanadate, chromium (VI), radiation, tumour necrosis factor-α (TNF-α), angiotensin II, thrombin, platelet derived growth factor (PDGF) and the overexpression of NADPH oxidase I (Chandel *et al.,* 2000; Gao *et al.,* 2002a; Gao *et al.,* 2002b; Moeller *et al.,* 2004; Haddad and Land, 2001; Richard *et al.,* 2000; Goyal *et al.,* 2004). Many ROS generated by non-hypoxic stimuli act as secondary messengers that can, in some circumstances, activate the MAP kinase and PI3K signalling cascades. For example in vanadate treated DU145 human prostate cells $H_2O_2$ was identified as the major ROS

responsible for the induction of HIF-1α and subsequent expression of VEGF. In this cell type the vanadate mediated expression of HIF-1 and VEGF was dependent upon the PI3K/Akt pathway (Gao *et al.,* 2002a). ROS activation of both the p38 MAP kinase and ERK1/2 pathways has also been observed. p38 signalling mediates the expression of HIF-1 and VEGF in response to chromium (VI) generated ROS in DU145 cells whereas ERK1/2 contributed towards angiotensin II dependent activation of HIF-1 in vascular smooth muscle cells (Gao *et al.,* 2002b; Richard *et al.,* 2000).

## 1.6 HIF and Disease

### *1.6.1 Angiogenesis*

Angiogenesis is the development of new blood vessels from the existing vascular system. During adulthood most blood vessels remain quiescent. However, angiogenesis is an essential process in wound healing and repair. Angiogenesis also plays an important role in several diseases (Bouis *et al.,* 2006). In cancer (see section 1.6.4), rheumatoid arthritis, psoriasis and diabetic eye disease, excessive angiogenesis feeds the diseased tissue, destroying normal tissue in the process. The opposite is true in stroke, heart disease and delayed wound healing where there is insufficient angiogenesis which can lead to poor circulation and tissue death (Carmeliet, 2005).

Angiogenic signalling is stimulated by hypoxia, nutrient deprivation and ROS (North *et al.,* 2005). During angiogenesis proteins belonging to the VEGF family, FGF family, PDGF family and angiopoietins are up-regulated. All of the genes encoding these proteins are targets of HIF signalling.

### *1.6.2 Ischaemia*

Ischaemia is defined as an inadequate blood supply to a local area as a result of blockage in the blood vessels supplying the area and results in hypoxia of the tissue

downstream of the blockage. As a result of ischaemia, there is an increase in angiogenesis in the affected area, often as a result of induced HIF-1 mediated transcription of angiogenic factors. However, in the case of stroke and heart disease the angiogenic response is often not sufficient to overcome the oxygen and glucose deprivation resulting in ischaemic injury of the tissue or in the case of heart disease, a heart attack (section 1.6.1, reviewed by Semenza, 2001; Semenza, 2010).

The induction of HIF-1 as a result of ischaemia is a factor in many types of ischaemia. For example in myocardial ischaemia induction of HIF-1α protein and VEGF protein expression was observed resulting in an angiogenic response (see section 1.6.1, reviewed by Semenza, 2000; 2001). Cerebral ischaemia resulting in either focal ischaemic stroke or transient global ischaemia resulted in elevated levels of HIF-1 and the expression of several HIF-1 target genes including those encoding for iNOS, VEGF and GLUT-1. The up-regulation of these proteins ensures increased blood flow, increased blood vessel formation and increased metabolism, respectively. These responses contribute to the recovery of the injured area (reviewed by Sharp and Bernaudin, 2004). Chronic retinal ischaemia related to diabetes causes HIF-1 dependent VEGF mediated neovascularisation of the retina (Sharp and Bernaudin, 2004).

### *1.6.3 Pulmonary Hypertension*

Pulmonary hypertension is the result of sustained vasoconstriction and pulmonary vascular remodelling. One of the underlying stimuli that can lead to pulmonary hypertension is chronic alveolar hypoxia, a feature of chronic obstructive pulmonary disease. During the early period of hypoxic exposure pulmonary vascular resistance is elevated due to vasoconstriction. However, following sustained hypoxic exposure remodelling of the pulmonary vasculature occurs (reviewed by Hopkins and McLoughlin, 2002). Under sustained hypoxic conditions non-muscular arterioles become muscularised, and partial or completely muscular arterioles undergo medial wall thickening. The effect of medial wall thickening is to reduce the luminal diameter of pulmonary arterioles resulting in the constriction of blood flow and hence increased pulmonary resistance (reviewed by Semenza, 2004). Sustained

hypoxia also causes a reduction in the total number of blood vessels in the vascular bed (reviewed by Hopkins and McLoughlin, 2002).

Studies perfumed in mice have shown the involvement of HIF-1α and HIF-2α in the development of pulmonary hypertension. Mice heterozygous for the *Hif1a* locus (*Hif1a*$^{+/-}$) and exposed to 10% $O_2$ for 1-6 weeks demonstrated a delayed development of polycythemia (increase in red blood cell mass), pulmonary hypertension and pulmonary vascular remodelling when compared to *Hif1a*$^{+/+}$ littermates (Yu *et al*, 1999). Similar experimental studies performed in *Hif2a*$^{+/-}$ mice exposed to 10% $O_2$ for 4 weeks indicated that the mice were not fully protected against pulmonary hypertension and vascular remodelling when compared to *Hif2a*$^{+/+}$ mice. However, *HIF2a*$^{+/-}$ mice did not show impaired development of polycythemia (Brusselmans *et al.*, 2003). The greater impairment of pulmonary hypertension and pulmonary vascular remodelling in HIF-2α partially deficient mice and the delayed development of polycythemia in HIF-1α partially deficient mice suggests distinct roles for both proteins in the development of pulmonary hypertension.

### *1.6.4 HIF and tumourigenesis*

Tumour progression can be associated with both physiological responses to environmental stimuli e.g. hypoxia, or genetic alterations e.g. oncogenic transformation (reviewed by Knowles and Harris, 2001). These alterations have extremely important consequences. For a tumour to proliferate initially there must be adequate oxygen delivery. As tumours proliferate oxygen becomes sparse and tumour cells adapt their metabolism to a reduced oxygen environment via an increase in glucose transport and glycolysis. The lack of oxygen in the proliferating tumour results in tumour vascularisation which occurs after the metabolic switch to glycolysis. This is followed by tumour cells shifting the balance between pro and anti-apoptotic factors, promoting tumour cell survival. HIF-1 controls the expression of genes that are involved in all of these processes.

Typically, when a tumour has a diameter of a few millimetres, tumour hypoxia occurs. Up-regulation of HIF-1 signalling in hypoxic tumour areas results in the up-regulation of proteins involved in glucose transport (e.g. GLUT-1 and GLUT-3) and glycolysis (e.g. aldolase A and C, lactate dehydrogenase and phosphoglycerate kinase 1, Semenza, 2002a). Up-regulation of these proteins allows a tumour to adapt its metabolism to reduced oxygen availability resulting in a switch from the oxidative respiratory pathway to anaerobic glycolysis. This switch ensures the production of ATP and the precursors of anabolic pathways (e.g. amino acids, lipids and nucleic acids) are maintained, which enables tumour cells to grow and proliferate in hypoxia.

In addition to increased glycolysis, tumour hypoxia also stimulates angiogenesis however, when angiogenesis is initiated depends on the type of malignancy and the tumour microenvironment (Blouw *et al.*, 2003). Once a tumour becomes hypoxic there is an increase in transcription of HIF-1 target genes (reviewed by Esteban and Maxwell, 2005). Several HIF-1 target genes encode for pro-angiogenic proteins including VEGF, PDGF and FGF (reviewed by Knowles and Harris, 2001). The up-regulation of these proteins changes the balance of pro and anti-angiogenic factors secreted from the tumour and surrounding cells, resulting in vascularisation of the tumour. However, these vessels are structurally and functionally abnormal resulting in transient vessel occlusion which leads to more areas of transient acute hypoxia within the proliferating tumour (reviewed by Brown, 2002).

The more hypoxic a solid tumour becomes the poorer the prognosis when compared to well oxygenated tumours, mainly due to the difficulties of delivering chemotherapeutic drugs to hypoxic areas with a limited blood supply (reviewed by Shannon *et al.*, 2003). The effectiveness of radiotherapy is also reduced in hypoxic tumours. This is because the ionizing radiation used in radiotherapy causes cell death by producing free radicals that react with DNA. Oxygen rapidly reacts with these free radicals making the DNA damage permanent. Cells with low oxygen levels are more likely to repair the damage, thus evading cell death (Brown, 2002). HIF signalling also plays a part in this process by up-regulating target genes whose protein products are involved in cell survival for example insulin-like growth factor 2 (IGF2, Feldser *et al.*, 1999).

### *1.6.5 von Hippel-Lindau (VHL) Syndrome*

von Hippel-Lindau (VHL) syndrome is a dominantly inherited disease that is characterised by the presence of central nervous system and retinal hemangioblastomas, clear cell renal carcinomas and pheochromocytomas. Hemangioblastomas comprise a mixture of stromal cells and blood vessels, and pheochromocytomas are catecholamine secreting tumours of the sympathetic nervous system (Ivan and Kaelin Jr, 2001; Elder *et al.,* 2005; Maher *et al.,* 2011). The development of *vhl* associated tumours is dependent on the loss or inactivation of both the maternally derived and paternally derived *vhl* alleles. Thus *vhl* acts as a classic tumour suppressor gene that conforms to the two-hit hypothesis of carcinogenesis. Patients with von Hippel-Lindau syndrome normally carry a mutation in one *vhl* allele, tumours arise when the second allele is mutated or deleted in a susceptible cell (Friedrich, 2001).

Families with von Hippel-Lindau syndrome can be sub-divided into categories based on the presence (type 2) or absence (type 1) of pheochromocytomas. Families with type 2 VHL disease can be further sub-categorised based on the risk of developing renal cell carcinoma. Those at low risk suffer from type 2A VHL syndrome and those at high risk suffer from type 2B VHL syndrome. Patients with type 2A or 2B disease often have other VHL associated tumours such as retinal and cerebral hemangioblastomas. Type 2 VHL disease also has a third sub-categorisation, type 2C, patients in this category present with familial pheochromocytoma but no renal cell carcinoma or hemangioblastomas (Maher *et al., 2011*).

The protein product of the *vhl* gene is a component of the ubiquitin ligase complex responsible for targeting HIF-α protein subunits for proteasomal degradation (section 1.3.4 and 1.3.5). Consequentially, tumours associated with VHL syndrome types 1, 2A and 2B are often highly vascularised and overproduce angiogenic factors due to *vhl* inactivation and the resulting de-regulation of HIF-α degradation (Kim and Kaelin Jr, 2004). However, individuals suffering with type 2C VHL syndrome retain the ability to regulate HIF-α degradation suggesting that loss of an additional function of pVHL is responsible for pheochromocytoma development in these patients (Hoffman *et al.,* 2001; Clifford *et al.,* 2001).

## 1.7 Project Aims

Several groups of researchers have carried out proof of principle blockade experiments using peptides (Kung *et al.,* 2000; Li *et al.,* 2000; Williams *et al.*, 2002). The results of these experiments have shown that small molecule blockade of important HIF-1α sequences such as the ODDD or p300 interaction sequences offers the opportunity to develop a small molecule with the potential for use in a therapeutic setting. Therefore, one aim of this project is to develop RNA aptamers, small molecules with high target affinity, towards the ODDD of HIF-1α.

Germ-line and somatic mutations in 3 of the 4 genes (*SDHB, SDHC* and *SDHD*) that encode mitochondrial complex II/succinate ubiquinone oxidoreductase (SQR) predispose affected individuals to head and neck paragangliomas (HNPs) and/or pheochromocytomas, tumours of the autonomic nervous system. These tumours display a high degree of vascularity which is similar in structure to pheochromocytomas harbouring *vhl* mutations (Maher and Eng, 2002). Therefore, a further aim of this project is to determine whether inactivation of SDH results in increased HIF-1α protein levels using another small molecule technology – small interfering RNAs.

# Chapter 2: Materials and Methods.

## 2.1 General materials and methods.

### *2.1.1 Tissue Culture.*

Renal carcinoma 786-O cells (ATCC, Manassas VA, USA), hepatocellular carcinoma Hep G2 cells and cervical adenocarcinoma HeLa cells were grown in RPMI 1640 medium (Invitrogen, Paisley, UK) supplemented with 10% (v/v) foetal calf serum (FCS, Invitrogen), penicillin, streptomycin and glutamine (100 units/ml, 100μg/ml and 2mM, respectively, Invitrogen). Cells were sub-cultured at a ratio of 1:4-1:6 except Hep G2 cells which were sub-cultured at a ratio of 1:3. Rat pheochromocytoma PC12 cells (ATCC) were grown in Dulbeccos modified eagle medium (DMEM, Invitrogen) supplemented with 10% (v/v) foetal calf serum, 5% (v/v) heat inactivated horse serum (Invitrogen) and penicillin, streptomycin and glutamine (100 units/ml, 100μg/ml and 2mM, respectively). PC12 cells were sub-cultured at a ratio of 1:3. All cells were grown at 37°C and 5% $CO_2$ in an Heraeus Hera Cell Incubator (Kendro Laboratory Products Plc, Bishops Stortford, Herts, UK).

### *2.1.2 Plating of Cells.*

Cell numbers were determined before plating at the densities indicated using an improved neubauer haemocytometer (Scientific Laboratory Supplies, Nottingham, UK).

### *2.1.3 SDS-polyacrylamide gel electrophoresis (SDS-PAGE).*

Protein samples were run on 8, 10 or 15% resolving gels based on the method of Laemmli (1970). The chemical compositions of each percentage of resolving gel are shown in the table below.

| Component | 8% resolving gel | 10% resolving gel | 15% resolving gel |
|---|---|---|---|
| dd$H_2O$ | 4.6ml | 4.0ml | 2.3ml |
| 30% Acrylamide/Bis Solution | 2.7ml | 3.3ml | 5.0ml |
| 1.5M Tris-HCl pH8.8 | 2.5ml | 2.5ml | 2.5ml |
| 10%SDS | 0.1ml | 0.1ml | 0.1ml |
| 10% Ammonium Persulfate (APS) | 0.1ml | 0.1ml | 0.1ml |
| TEMED (N,N,N',N' – Tetramethylethylenediamine) | 0.006ml | 0.004ml | 0.004ml |

1 hour after pouring the resolving gel a stacking gel (2.1ml dd$H_2O$, 0.5ml 30% acrylamide/bis solution, 0.38ml 1M Tris-HCl pH6.8, 0.03ml 10% SDS, 0.1ml 10%APS and 0.003ml TEMED, all chemicals were purchased from Sigma, Poole, Dorset, UK except 30% acrylamide/bis solution which was purchased from Bio-Rad Laboratories Ltd., Hemel Hempstead, UK) was poured. A comb was inserted into liquid stacking gel before being left to set for 1 hour. Protein samples were mixed with an equal volume of 2X sample loading buffer (100mM Tris, 4% (w/v) sodium dodecyl sulphate, 20% (v/v) glycerol, 600mM β-mercaptoethanol, and bromophenol blue to colour) and heated at 100 °C for 2 min before loading onto a stacking gel. Samples were separated at a constant current of 40mA per gel in 1X running buffer (25mM Tris, 250mM Glycine and 0.1% (v/v) sodium dodecyl sulphate). Molecular weight markers were Seeblue (Invitrogen) or Precision Plus protein standards (Bio-Rad Laboratories Ltd.) as indicated. Protein samples were either transferred to nitrocellulose or coomassie stained and destained (sections 2.1.4 and 2.1.8, respectively).

### *2.1.4 Western Blotting.*

Protein samples were transferred from the SDS-polyacrylamide gels to a nitrocellulose membrane (Hybond-C, Amersham Biosciences UK Ltd., Little Chalfont, Bucks, UK) at a constant current of 400mA in 1X transfer buffer (0.19M glycine, 0.025M Tris and 20% (v/v) methanol) for 2 hours. Membranes were stained in Ponceau S solution (0.1% (w/v) Ponceau S and 5% (v/v) acetic acid, Sigma,) to detect protein transfer, then washed in 1X Tris buffered saline (TBS, 150mM NaCl and 50mM Tris-HCl pH 7.6) before antigen detection.

Membranes were blocked in 5% (w/v) non-fat milk powder (NFDM, Marvel produced by Premier International Foods (UK) Ltd., Spalding, UK) in TBS-0.1 % (v/v) tween-20 (TBS-T) at room temperature (rt) for 1 hour before incubation in primary antibody (section 2.1.5) at the appropriate dilution in 5% (w/v) NFDM in TBS-T for 1 hour or 1.5 hours at rt or overnight (o/n) at 4°C. Membranes were washed three times for 15 minutes each in TBS-T at rt before incubation with secondary antibody (section 2.1.6) diluted at the appropriate dilution in 5% (w/v) NFDM in TBS-T for 1 hour at rt. Membranes were washed 3 times in TBS-T before detection by enhanced chemical luminescence (ECL, Supersignal West Pico Chemiluminescent Substrate, Perbio Science UK Ltd., Cramlington, UK). 3ml of enhancer solution was combined with 3ml of stable peroxide solution and mixed before addition to the membrane. Membranes were washed in substrate for 1 minute before signal detection using Biomax light film (Kodak Ltd., Hemel Hempstead, UK). Membranes probed with an anti-VHL antibody were subjected to detection using a supersensitive ECL (Supersignal West Dura extended duration substrate, Perbio Science UK Ltd.). 1ml of enhancer solution was combined with 1ml of stable peroxide solution and mixed before addition to the membrane. Membranes were washed in substrate for 45 seconds before signal detection using Biomax film.

### *2.1.5 Primary antibodies.*

| Name of antibody | Antibody Type | Final usage concentration | Incubation Conditions | Supplier |
|---|---|---|---|---|
| ARNT | Mouse monoclonal | 0.25μg/ml | Overnight (o/n) at 4 °C | BD Biosciences (Oxford, UK) |
| ARNT | Mouse monoclonal | 0.93μg/ml | 1.5 hours at room temperature (rt) | NB100-124, Novus Biologicals, Littleton, CO, USA |
| GLUT-1 | Rabbit polyclonal | 10μg/ml | o/n at 4 °C | Calbiochem, San Diego, CA, USA |
| HIF-1α | Mouse monoclonal | 1μg/ml | o/n at 4 °C | BD Biosciences |
| HIF-1α | Mouse monoclonal | 5.9μg/ml | o/n at 4 °C | NB100-105, Novus Biologicals |
| P53 (DO-1) | Mouse monoclonal | 0.4μg/ml | 1 hour at rt | Santa Cruz, Santa Cruz, CA, USA |
| PTEN | Rabbit polyclonal | Diluted 1:1000 | 1 hour at rt | Upstate Biotechnology, Cambridge, UK |
| SDH A | Mouse monoclonal | 0.1μg/ml | 1 hour at rt | Molecular Probes Inc, Eugene, OR, USA |
| SDH B | Mouse monoclonal | 5μg/ml | 1 hour at rt | Molecular Probes Inc |
| VHL | Mouse monoclonal | 1μg/ml | 1 hour at rt | BD Biosciences |

All Novus Biologicals antibodies were incubated in 5% NFDM in 1X western wash (5mM Tris-HCl pH 7.6, 35mM NaCl, 0.1% (v/v) Tween-20).

### *2.1.6 Secondary antibodies.*

| Name of antibody | Final usage concentration | Incubation Conditions | Supplier |
|---|---|---|---|
| HRP linked rabbit anti-mouse IgG | 1.3μg/ml | 1 hour at room temperature (rt) | DAKO, Ely, UK |
| HRP linked swine anti-rabbit IgG | 0.28μg/ml | 1 hour at rt | DAKO |

### *2.1.7 Densitometry.*

Bands from western blots were analysed as indicated using GEL BASE/ GEL BLOT PRO densitometry software (Ultra Violet Products/UVP, Cambridge, UK).

### *2.1.8 Coomassie staining of SDS-PAGE gels.*

SDS-PAGE gels were stained in coomassie blue solution (0.6mM coomassie brilliant blue G250, 0.3M methanol and 0.1M glacial acetic acid, Sigma) for 1 hour before de-staining with de-stain solution (0.3M methanol and 0.1M glacial acetic acid) for 2-4 hours with de-stain changes as required until stained protein bands were of required intensity.

### *2.1.9 Agarose gel electrophoresis.*

Molecular biology grade agarose (Sigma) was dissolved in 100ml 1X TAE (0.04M Tris, 0.02M acetic acid and 1mM EDTA, Sigma) containing 0.2μg /ml ethidium bromide. Linearised DNA was separated on a 0.7% (w/v) agarose gel and DNA inserts were separated on a 3% (w/v) agarose gel. DNA samples were mixed with 6X agarose gel loading buffer (1X TAE, 30% [v/v] glycerol and bromophenol blue to colour) before loading onto the appropriate percentage agarose gel, as indicated

above. Gels were run at a constant 100V in 1X TAE buffer containing 0.2μg/ml ethidium bromide. Double stranded DNA size markers were either a 1 kilobase ladder (1Kb ladder, Invitrogen) or hyperladder V (Bioline Ltd.. London, UK), as indicated.

### *2.1.10 Visualisation of DNA in agarose gels.*

Agarose gels were visualised under high energy UV light in a GDS7600 benchtop transilluminator using GRAB-IT gel capturing software (UVP).

### *2.1.11 DNA purification from agarose gels.*

Using a Qiaex II Gel Extraction Kit (Qiagen Ltd., Crawley, UK) – The DNA was excised in agarose from the gel under low energy UV light using a dual intensity transilluminator (UVP), weighed and re-suspended in buffer QX1 (a high salt containing buffer) at a ratio of 1 volume of gel to 3 volumes of buffer for DNA between 100bp – 4kb. For fragments over 4kb an additional 2 volumes of $H_2O$ were added. 10μl of re-suspended QIAEX II silica particles were added to the sample and incubated at 50 °C for 10 min with vortexing every 2 min. The sample was centrifuged for 30 sec and the supernatant discarded. The pellet was washed with 500μl of QX 1 buffer with vortexing to re-suspend the pellet. The sample was centrifuged for 30 sec and the supernatant discarded. The pellet was washed twice in 500μl of PE buffer (an ethanol containing buffer). The pellet was air dried for ~ 20 min or until the pellet became white. To elute DNA between 100bp and 4kb, 20μl of $H_2O$ was added to the pellet and incubated at rt. For DNA longer than 4kb the pellet and 20μl of $H_2O$ were incubated at 50 °C for 5 min. Samples were centrifuged for 30 sec and the supernatant containing purified DNA retained.

### *2.1.12 HRE dependent transcription of a luciferase reporter gene.*

Hep G2 cells were seeded 100 000 cells/well in 6 well plates as indicated (Triple Red Ltd., Triple Red Ltd., Long Crendon, Bucks, UK). Cells were seeded in triplicate for

each test plasmid and condition. 24 hours after seeding cells were transfected in triplicate with 1μg of either pGL3prevPGK (OBM), pGL3control (Promega) or pCMVluc (OBM). All wells were co-transfected with 0.02μg pRL-SV40 (Promega).

pGL3prevPGK (OB HRE) and pCMVluc were constructed as described by Boast *et al.,* (1999). pGL3prevPGK contains an hypoxia responsive HRE trimer from the gene encoding murine phosphoglycerate kinase (PGK) located upstream of a minimal SV40 promoter. This promoter directs transcription from a cDNA sequence encoding firefly luciferase. pGL3-control contains an SV40 promoter and enhancer that results in the strong expression of firefly luciferase (*Photinus pyralis*). pCMVluc contains an SV40 promoter and enhancer and a CMV immediate early (CMV IE) promoter resulting in the strong expression of firefly luciferase. pRL-SV40 contains an SV40 early enhancer and promoter which provides strong constitutive expression of renilla luciferase (*Renillla reniformis* or sea pansy).

Transcription reporter assays were utilised to investigate the effect of RNA aptamers targeted to the ODDD of HIF-1α, chemical treatment of Hep G2 cells and the effect of SDH B targeting siRNAs in Hep G2 cells on a HIF-responsive luciferase reporter gene encoded by pGL3prevPGK (sections 2.2.18, 2.3.3 and 2.3.4). Each of the three treatments involved a different form of transfection protocol; however cells were seeded in the same manner and the assay to detect luciferase reporter activity remained the same.

### *2.1.13 Analysis of luciferase reporter gene activity.*

Whole cell lysates were centrifuged at 17950g for 5min before the addition of 20μl of each lysate to an opaque ELISA plate. Samples were analysed for luciferase reporter activity using the Dual-luciferase reporter assay system (Promega).

The luciferase assay reagent was prepared by re-suspending lyophilised luciferase assay substrate in 10ml luciferase assay buffer II. The ‘Stop and Glo’ reagent was prepared by adding 200μl of ‘Stop and Glo’ substrate solvent to the ‘Stop and Glo’ substrate making a 50X stock solution. 1 volume of 50X stock solution was added to

50 volumes of 'Stop and Glo' buffer. Reagent injectors of the MRX microtiter plate luminometer (Dynex Technologies Ltd., Worthing, West Sussex, UK) were primed with both luciferase reagents. 100µl of luciferase assay reagent was dispensed into the first well of the ELISA plate. Emitted luminescence from firefly luciferase (*Photinus pyralis)* was measured before the addition of 100µl of 'Stop and Glo' reagent. 'Stop and Glo' reagent quenches the luminescence from the firefly luciferase while providing the substrate for the Renilla (*Renillla reniformis* or sea pansy) luciferase. Emitted luminescence was measured. The above process was carried out for all sample wells and the firefly luciferase to renilla luciferase ratio calculated.

## 2.2 RNA aptamer specific methods.

### *2.2.1 pGEX fusion vectors.*

**pGEX-HIF-1α-ODDD (GHO)** – PCR was used to amplify a 390 base pair region encoding residues 519-647 of the oxygen dependent degradation domain of human HIF-1α from the expression vector pCI-neo-HIF-1a (Oxford Biomedica (OBM), Oxford, UK) using the sense primer HIF1NTADS (5' GGAGGATCCCCATATTGTTTTTATGTGGATAG 3') and antisense primer HIF1NTAD-AS (5' GGACTCGAGGTATGTGGGTAGGAGATGGAG 3'). The amplified product was digested with Bam H I and Xho I, and subcloned into pGEX-4T-3 (Amersham Biosciences UK Ltd.) at the same sites.

**pGEX-EPAS-ODDD (GEO)** – PCR was used to amplify a 390 base pair region encoding residues 488-617 of the oxygen dependent degradation domain of human HIF-2α (based on sequence homology to HIF-1α) from the expression vector pCI EPAS (OBM) using the sense primer EPASNTAD S (5' GGAGGATCCCCATATTACACATCTTTGGATAAC 3') and antisense primer (5' GGACTCGAGGCAGGGATGCTTTGCTTCCGG 3'). The amplified product was digested with Bam H I and Xho I, and subcloned into pGEX-4T-3 at the same sites.

### *2.2.2 PCR amplification of ODDD-encoding cDNA fragments from pCI-neo vectors.*

Each PCR reaction mixture contained 5µl of 10X *Pfu* buffer, 1µl 10mM dNTPs, 1µl *Pfu* polymerase (2.5U/µl, Stratagene Ltd.), 0.1 nmoles of each primer, 1µl of pCI-neo-HIF-1a, pCI EPAS or $H_2O$ and $H_2O$ to a final volume of 50µl. Reactions were carried out in 0.5ml microfuge tubes. Mixes were overlayed with 50µl mineral oil.

The PCR cycle was as follows: -

| Step | Temp °C | Time (in min) |
|---|---|---|
| 1 | 94 | 1 |
| 2 | 94 | 1 |
| 3 | 45 | 2 |
| 4 | 72 | 2 min, cycle to step 2, 30 X |
| 5 | 72 | 5 |
| 6 | 4 | ∞ |

### *2.2.3 Subcloning of ODDD sequences.*

PCR products were sub-cloned into pCR4-TOPO from the 'Zero Blunt TOPO PCR Cloning Kit' (Invitrogen). 1µl PCR product, 1µl of salt solution (1.2M NaCl and 0.06M $MgCl_2$), 1µl of TOPO vector (10ng/µl) and $H_2O$ to a final volume of 5µl were gently mixed and incubated for 5 min at rt then placed on ice. 2µl of the cloning reaction was added to one vial of 'Top10 One Shot Chemically Competent' *E. coli*, gently mixed and incubated on ice for 30 min. Cells were heat pulsed at 42 °C for 30 seconds, then immediately transferred to ice. 250µl of Luria-Bertani media (LB, Sigma) was added to cells, which were then incubated at 37 °C for 1 hour with shaking at 225 – 250 rpm. 25µl of each transformation was spread onto LB-ampicillin (100µg/ml) agar plates. The remaining transformation was micro-centrifuged and the cell pellet re-suspended in LB and plated as before. Plates were

incubated o/n at 37 °C. Colonies were picked and grown o/n in 5ml LB-ampicillin (100μg/ml). DNA was purified using a 'QIAprep Spin Miniprep kit' (Qiagen Ltd.).

### *2.2.4 Plasmid purification.*

A QIAprep Spin Miniprep Kit (Qiagen Ltd.) was used to purify plasmid DNA from bacterial cultures. Single colonies picked from LB-ampicillin (50μg/ml) agar plates were grown in 5ml LB-ampicillin (50μg/ml) o/n at 37 °C with shaking at 225-250 rpm. 3ml of o/n cultures were centrifuged in 1.5ml aliquots and the supernatant discarded. The bacterial pellet was re-suspended in 250μl buffer P1 (resuspension buffer: 50mM Tris-HCl (pH 8.0), 10mM EDTA, 10μg/ml RNase A) followed by the addition of 250μl of buffer P2 (lysis buffer: 200mM NaOH, 1% (w/v) SDS) with mixing. 350μl buffer N3 (neutralisation buffer: 3.0M potassium acetate pH 5.5) was added with mixing then micro-centrifuged for 10 min. Following centrifugation the supernatant was applied to a QIAprep spin column and micro-centrifuged for 60 sec. Flow through was discarded. The column was washed with 0.75ml of PE buffer and micro-centrifuged; the flow through was discarded. The column was micro-centrifuged for a further minute to remove any residual wash buffer. The QIAprep column was placed in a clean micro-centrifuge tube. DNA was eluted by adding 50μl $H_2O$ to the centre of the QIAprep column and incubating at RT for 1 min then micro-centrifuged for 1 min to collect the purified DNA.

### *2.2.5 Restriction digests.*

5μl of DNA was added to 1μl (10U/μl) of restriction enzyme (XhoI or Bam HI, Promega, Southampton, UK), 2μl of 10X reaction buffer, BSA to a final concentration of 0.1μg/μl and water to a final volume of 20 μl. Samples were incubated at 37 °C for 2 hours. 1μl of calf alkaline phosphatase (Promega) was added to linearised vectors giving a final concentration of 0.05u/μl and incubated at 37 °C for a further 30 minutes. 10μl of digested DNA was mixed with 5μl of agarose gel loading buffer and run on an 0.7% (w/v) agarose gel. DNA bands were excised and purified using a Qiaex II Gel Extraction Kit (Qiagen Ltd., section 2.1.11).

### *2.2.6 Ligation.*

For ligation the mass ratio of DNA cloning vector to insert was 1:3. Ligation reactions contained vector DNA, insert DNA, 1µl 10X ligation buffer and 1µl of T4 DNA ligase (New England Biolabs, Hitchin, UK). The final volume was 10µl. Reactions were incubated at 16 °C o/n. To 100µl aliquots of supercompetent XL1-blue *E.coli* cells (Stratagene Ltd. Ltd., Amsterdam, The Netherlands) (thawed on ice) 1.7µl of β-mercaptoethanol was added giving a final concentration of 25mM in each tube. The contents of each tube were swirled gently and incubated on ice for 10 min, swirling gently every 2 min. To each aliquot of cells 5µl of ligation reaction was added. Tubes were incubated on ice for 30 min, heat pulsed at 42 °C for 45 sec then incubated on ice for 2 min. 0.9ml of preheated LB was added to each tube and incubated at 37 °C for 1 hour with shaking (225-250 rpm). 100µl of transformed cells was plated onto LB-ampicillin (50µg/ml) agar. The remaining transformation was micro-centrifuged and the pellet re-suspended in 100µl of LB and plated as before. Plates were incubated at 37 °C o/n. Colonies were picked and grown up in 5ml LB-ampicillin (50µg/ml) o/n at 37 °C with shaking (225-250rpm). Plasmid DNA was purified using a QIAprep Spin Miniprep Kit (Qiagen Ltd.).

### *2.2.7 Transformation of BL21-DE3 E.coli with GST fusion vectors.*

BL21-DE3 *E. coli* cells were cultured in 5ml of LB o/n at 37 °C with shaking.and at 225-250rpm. O/n cultures were added to 100ml LB and incubated for 2.5 hours at 37 °C with shaking and at225-250rpm. The culture was split into two 50ml aliquots and centrifuged for 20 minutes at 1380g and 4 °C in a Beckman GS-6R centrifuge (Beckman Coulter UK Ltd., High Wycombe, Bucks, UK). The supernatants were discarded and bacterial cell pellets were re-suspended in 10ml of cold 0.1M $CaCl_2$ before re-centrifugation for 10 min at 1380g and 4 °C. Supernatants were discarded and bacterial cell pellets were re-suspended in 2ml of cold 0.1M $CaCl_2$ containing 20% (v/v) glycerol. Aliquots were frozen at -80 °C.

Competent BL21-DE3 *E. coli* (Stratagene Ltd.) were transformed with either pGEX-4T-3, GHO or GEO. For each transformation, 1μl of plasmid DNA was added to 30μl of competent bacterial cells and incubated on ice for 1 hour. Transformations were heat pulsed at 42°C for 1.5 min and immediately chilled on ice for 2 min. 1ml of LB was added to each transformation and incubated at 37 °C for 1 hour with shaking at 225-250 rpm. The 1ml recovery cultures were added to 5ml of LB-ampicillin (50μg/ml) and incubated at 37 °C o/n with shaking at 225 – 250 rpm. 1ml of transformed cultures were stored in 20% (v/v) glycerol at –80 °C.

### *2.2.8 GST fusion protein expression and purification.*

BL21-DE3 *E. coli* transformed with pGEX-4T-3, GHO or GEO were cultured o/n in 5ml LB-ampicillin (50μg/ml). 1ml of each o/n culture was sub-cultured into 9ml LB-ampicillin (50μg/ml) and grown for 1 hour at 37 °C with shaking at 225-250 rpm. Isopropyl β-D galactopyranoside (IPTG) was added, to induce fusion protein expression, to each culture, to a final concentration of 1mM and cultures were grown for a further 3 hours. Cells were centrifuged at 1380g, 4 °C for 5 min. Cell pellets were re-suspended in 10 ml of PBS and centrifuged as before. Pellets were frozen o/n at -80 °C.

Pellets (thawed on ice) were re-suspended in PBS – 0.5% (v/v) triton X-100 (PBS-T) containing 100μl of a protease inhibitor cocktail for bacterial cells (18mM AEBSF, 86mM EDTA, 1.7mM bestatin, 0.29mM pepstatin A and 0.22mM E-64, Sigma), where indicated, with rotation at 4 °C for 30 min. Suspensions were sonicated at 7MHz for 30 sec with a probe sonicator and centrifuged at 1380g, 4 °C for 5 min. Supernatants from each tube were added to 20μl of PBS-T washed glutathione sepharose 4B beads (Amersham Biosciences UK Ltd.) and incubated at rt for 1 hour with rotation. Supernatants were discarded and the beads washed 3X in 0.5ml PBS. Beads were re-suspended in 2X SDS-PAGE loading buffer and subjected to SDS-PAGE.

Alternatively, GST fusion proteins were made as above except cultures containing transformed BL21-DE3 cells were grown up in 10ml of LB-ampicillin (50μg/ml) o/n before being sub-cultured into 90ml LB-ampicillin (50μg/ml). Pellets were lysed in 100ml of PBS-T. 250μl of PBS-T washed glutathione sepharose 4B beads were added to the supernatant and incubated at room temp for 2 hours. After washing, beads were re-suspended in 250μl PBS/20% (v/v) glycerol and frozen in 50μl aliquots at –80 °C.

### *2.2.9 pVHL pull down assay.*

Two 50μl aliquots of GST fusion proteins bound to beads were washed 3X in PBS and incubated with either 50μl of rabbit reticulocyte lysate (Promega) or 50μl of NP40 lysis buffer (0.5% (v/v) Nonidet-P40, 10mM Tris and 250mM NaCl pH7.5) at 30 °C for 90 min with gentle agitation every 15 min. Incubations were washed 3X in NP40 lysis buffer. Treated/untreated fusion protein beads were washed 3X in cold lysis buffer and incubated with 200μl of Hela whole cell lysate (section 2.2.10), at 4 °C for 1 hour. Fusion protein beads were washed 3X in NP40 lysis buffer before being subjected to SDS-PAGE and western blotting.

### *2.2.10 Cell lysates for VHL binding assay.*

Hela and 786-O cells were seeded into T75 flasks (Orange Scientific, Braine-l'Alleud, Belgium), grown to ~80% confluent, washed three times in cold PBS and lysed for 20 minutes in 2ml of NP40 lysis buffer (0.5% (v/v) Nonidet-P40, 10mM Tris and 250mM NaCl pH 7.5) at 4 °C. Lysates were micro-centrifuged at 604 g, 4 °C for 5 min and supernatants stored on ice.

### *2.2.11 Thrombin protease cleavage of GST fusion proteins.*

GST bound to glutathione beads was diluted at a ratio of 1:3 with fresh glutathione sepharose beads to standardise the amount of protein relative to fusion proteins purified on beads in parallel. Two 50μl aliquots of both GST bound to beads and

GST-HIF-1α-ODDD (GHO) bound to beads, were rotated at rt for 1 hour in 300µl binding buffer containing BSA (BB-BSA; 50mM Tris-HCl pH 7.6, 120mM NaCl, 2mM EDTA, 0.5% (v/v) Nonidet P-40, 10mg/ml BSA) to reduce non-specific binding. Aliquots were washed 3X in PBS. Thrombin protease (Amersham Biosciences UK Ltd.) was supplied as 500 units of a lyopholised powder which was reconstituted in PBS to a final concentration of 1unit/µl before use in the cleavage assay. Thrombin protease was prepared for the cleavage assay by adding 5% (v/v) thrombin protease to PBS. One aliquot of either GST bound to beads or GHO bound to beads was incubated with rotation with 25µl of either PBS or thrombin protease in PBS (giving a final thrombin protease concentration of 0.05U/µl) at rt for 16 hours unless indicated otherwise. Thrombin protease in PBS was also incubated. Reactions were centrifuged (Gentofuge 16M, 8163g, 5min) and supernatants transferred to separate tubes. 50µl of 2X SDS-PAGE loading buffer was added to all samples before incubating for 5 min at 100 °C. Samples were stored at -20°C.

### *2.2.12 PCR amplification of DNA oligonucleotide pool to produce aptamer library.*

DNA oligonucleotide pool sequence 5' GGGCGCTAAGTCCTCGCTCA-N40-ACGCGCGACTCGGATCCT 3' was PCR amplified using the sense primer FOR POOL 5' TCTAATACGACTCACTATAGGGCGCTAAGTCCTCGCTCA 3' and antisense primer REV POOL 5'GTAGGATCCGAGTCGCGCGT 3'.

10 PCR reactions were performed containing 5µl of 10X Taq polymerase buffer, 2µl of 50mM $MgCl_2$, 1µl 10mM dNTP's, 0.5µl Taq polymerase (5U/µl, Invitrogen), 0.8 nmoles of sense primer and 1.5 nmoles of antisense primer, 30ng DNA oligonucleotide pool and $H_2O$ to a final volume of 50µl. Reactions were carried out in 0.5ml microfuge tubes. Mixes were overlayed with 50µl mineral oil. To control for amplification, reactions containing all reagents, primers and no DNA oligonucleotide, all reagents, DNA oligonucleotide and no primers or DNA oligonucleotide, primers and all reagents except Taq DNA polymerase were prepared. This gave a pool of double stranded DNA oligonucleotides with approximate starting complexity of $7.455 \times 10^{12}$ oligonucleotides. The PCR cycle was as follows: -

| Step | Temp °C | Time (in min) |
|---|---|---|
| 1 | 94 | 4 |
| 2 | 42 | 7 |
| 3 | 72 | 7 min, cycle to step 1 six times |
| 4 | 4 | ∞ |

### *2.2.13 Purification of PCR products.*

PCR products were purified using a MinElute PCR purification kit (Qiagen Ltd.).Up to three 50µl PCR reactions (not including oil) were mixed with five times the volume of buffer PB, applied to a MinElute column and micro-centrifuged for 1 minute. Flow through was discarded. The column was washed in 750µl of PE buffer and micro-centrifuged for 1 minute, flow through was discarded. The column was centrifuged for a further minute to remove any residual wash buffer. DNA was eluted by adding 10µl of $H_2O$ to the centre of the MinElute column and incubating at rt for 1 minute before micro centrifuging for 1 minute to collect purified DNA.

### *2.2.14 T7 RNA polymerase transcription from DNA oligonucleotide pool.*

Each transcription reaction contained 20µl 5X transcription optimised buffer (200mM Tris pH 7.9, 30mM $MgCl_2$, 10mM spermidine and 50mM NaCl), 10µl 100mM DTT, 20µl 2.5mM rNTPs (Promega), 5µg DNA template, 2.5µl RNasin ribonuclease inhibitor (40U/µl, Promega), 2.7µl T7 RNA polymerase (20U/µl, Promega) and nuclease free $H_2O$ to a final volume of 100µl. Reactions were carried out in 0.5ml micro-centrifuge tubes. To control for transcription reactions containing all reagents and $H_2O$ instead of DNA template were prepared. Reactions were incubated at 37 °C for 2 hours. 5µl of RQ1 RNase free DNase (1U/µl, Promega) was added to each reaction and incubated at 37 °C for 15 mins. RNA aptamers synthesised in transcription reactions were purified using a QIAquick nucleotide removal kit.

### *2.2.15 Purification of RNA aptamers.*

RNA aptamers were purified using a QIAquick Nucleotide Removal Kit (Qiagen Ltd.). 10 volumes of buffer PN was added to 1 volume of T7 RNA polymerase transcription reaction and mixed. The sample was applied to a QIAquick spin column and micro-centrifuged at 2939g for 1 min to bind DNA. The flow through was discarded and the Qiaquick column was washed in 750µl of buffer PE. The column was micro-centrifuged at 2939g for 1 min. The flow through was discarded and the column was centrifuged for a further minute at 8163g. 100µl of HPLC purified $H_2O$ was added to the column and incubated at rt for 1 min before centrifugation to elute the DNA.

### *2.2.16 RNA aptamer selection.*

50µl of GST bound to beads (see sections 2.2.8) were washed in 100µl of PBS micro-centrifuged for 1 min at 8163g and the supernatant discarded. This wash step was performed three times. 60µl of purified RNA aptamer pool (see sections 2.2.12 – 2.2.15) was incubated with GST bound to beads for 1 hour at rt with rotation. The RNA aptamer:GST bound to beads incubation mixture was micro-centrifuged as above and the supernatant transferred to a 50µl aliquot of GST-HIF-1α-ODDD (GHO) bound to beads, prepared in the same way as for GST bound to beads. The RNA aptamer pool was incubated with GHO bound to beads at rt for 1 hour with rotation before micro-centrifugation as described previously. The supernatant was discarded and aptamers bound to GHO beads were subjected to thrombin protease cleavage as described in section 2.2.11 for 4 hours at rt. The thrombin protease cleavage incubation was micro-centrifuged as above and supernatant retained for one step RT-PCR of the selected RNA aptamer pool.

### *2.2.17 One step RT-PCR of selected RNA aptamer pool.*

Selected RNA aptamers were subjected to one step RT-PCR (Roche, Lewes, UK). Six reactions were performed in total with each reaction being performed in RNase and DNase free 0.5ml micro-centrifuge tubes (Sarstedt Ltd., Leicester, UK). Each reaction contained 10µl 5X RT-PCR buffer, 0.8µl 25mM dNTPs, 2.5µl 100% DMSO, 2.5µl 100mM DTT, 1.6µl RNasin ribonuclease inhibitors (40U/µl, Promega), 0.1 nmoles of both sense and anti-sense primers (described in section 2.1.12), 2µl of a mixture of *Carboxydothermus hydrogenoformans* and Taq DNA polymerase ('*C. therm* polymerase'), 1µl selected RNA aptamer pool and HPLC purified RNase and DNase free $H_2O$ to a final volume of 50µl. To control for reverse-transcriptase dependent amplification '*C. therm* polymerase' was replaced with $H_2O$.

The aptamer pool was reverse transcribed and then PCR amplified as a one-step reaction. Reactions were incubated at 72 °C for 30 min before PCR using the same cycle conditions as in section 2.1.9 except the PCR cycle was performed 10 times. PCR reactions were purified using a MinElute PCR purification kit (Qiagen Ltd., section 2.2.13).

### *2.2.18 RNA aptamer mediated HIF responsive HRE driven transcription of a luciferase reporter gene.*

Hep G2 cells were seeded 100 000 cells/well in 4ml/well of SFQ supplemented with 10% FCS in six well plates. 24 hours after seeding the media from each well was replaced with 1ml SFQ supplemented with 10% FCS. Cells were transfected using Lipofectamine 2000 (Invitrogen). 4µl/well of Lipofectamine 2000 was diluted in 96µl/well Opti-MEM I (Invitrogen) and incubated at RT for 5 min. 100µl/well of diluted Lipofectamine 2000 was added to six pre-prepared reaction mixtures containing 1µg/well test plasmid (pGL3prevPGK/pGL3-control/pCMVluc, described in section 2.1.12), 0.02µg/well pRL-SV40 (described in section 2.1.12), 0.2µg/well RNA aptamers (r0 starting pool of aptamers or r4 aptamer pool after four rounds of selection) and Opti-MEM to a final volume of 100µl/well. Lipofectamine

2000:DNA:RNA mixtures were incubated at RT for 20 min. Hep G2 cells were transfected in triplicate for each test plasmid with 200µl/well of appropriate Lipofectamine 2000:DNA:RNA complexes. 4 hours after transfection, media was replaced on all wells with 2ml warm SFQ supplemented with 10% FCS. 48 hours after transfection cells were washed twice in PBS and lysed in 200µl/well of cold 1X passive lysis buffer (Promega). Lysates were stored at -80°C before assaying for luciferase reporter activity (described in section 2.1.13).

## 2.3 RNA interference specific materials and methods.

### *2.3.1 Preparation of siRNAs and FITC labelled DNA oligonucleotide.*

Small interfering RNAs (siRNAs) were designed to a human SDH B mRNA sequence. The sequences were designed following the recommendations of Elbashir *et al.,* (2001). Each strand contained two 3' deoxythymidines.

The sequences of the SDH B sense and anti-sense strands were 5' UAAAUGUGGCCCCAUGGUA dTdT 3' and 5' UACCAUGGGGCCACAUUUA dTdT 3' respectively. The control sequence used in this experiment was the inverse of the SDH B sense strand. The sequences of the control siRNA sense and anti-sense strands were 5' AUGGUACCCCGGUGUAAAU dTdT 3' and 5' AUUUACACCGGGGUACCAU dTdT 3' respectively (Dharmacon, Chicago, IL, USA).

Cy3-luciferase GL2 duplex (Dharmacon) was used as a control for the optimization of transfection. The sense sequence was modified with Cy3 at the 5' end and two 3' deoxythymidines and had the following sequence; - 5'CGTACGCGGAATACTTCGA3'.

SDH B, SDH B control and Cy3-luciferase pre-annealed siRNA duplexes were reconstituted in 1ml de-ionised and distilled $H_2O$ ($ddH_2O$) to give a concentration of 20µM.

A fluorescein labelled DNA oligonucleotide (FITC-DNA) with sequence 5'Fluo-TCGAAGTATTCCGCGTACG3' (a gift from M. Pohlschmidt) was also used as a control for transfection optimization.

### *2.3.2 Transfection of cells with small interfering RNAs (siRNA).*

Cells were seeded 100 000 cells/well in 6 well plates (Triple Red). 24 hours after seeding each well was washed three times in RPMI 1640 medium (Invitrogen) supplemented with 2mM glutamine (SFQ, Sigma) then covered in 0.4ml of SFQ. 3μl/well of Oligofectamine (Invitrogen) was incubated with 7μl/well of SFQ for 10 minutes. 6μl/well (1μl/well FITC-DNA) of annealed siRNAs were diluted in 84μl/well (89μl/well for FITC-DNA) of SFQ. Diluted Oligofectamine was added to diluted siRNAs and incubated at rt for 20 minutes. 100μl/well of either Oligofectamine-test siRNA complex, Oligofectamine-control siRNA complex, Oligofectamine-FITC-DNA complex, Oligofectamine-Cy3-siRNA complex, Oligofectamine only or FITC-DNA/Cy3-siRNA only, as indicated, was then added to cells and left for four hours before the addition of 250μl/well of RPMI 1640 medium supplemented with 30% FCS (Invitrogen) and 2ml/well of RPMI 1640 medium supplemented with 10% FCS and 2mM glutamine. 24 hours after the first siRNA transfection a second transfection was carried out in the same way as described above unless otherwise indicated.

Triplicate wells were counted for transfected cells and control cells on the day of the first transfection then 24 hours after the first transfection and at 24 and 48 hours after the second transfection. Duplicate wells were lysed for test cells and control cells 24 and 48 hours after the second transfection. Cells were lysed in 200μl of boiling 2X SDS-PAGE loading buffer. Lysates were analysed by SDS-PAGE and western blotting.

### *2.3.3 Fluorescent cell photography.*

Cells transfected with FITC-DNA or Cy3-siRNA were visualised 24 hours after transfection using a Leica DM1RB inverted fluorescence microscope. Cells were photographed with a TS100 inverted colour cool view CCD camera using Photolite Image acquisition software (Photonic Science, Robertsbridge, EastSussex, UK).

### *2.3.4 siRNA mediated HIF responsive HRE driven transcription of a luciferase reporter gene.*

Hep G2 were seeded 100 000 cells/well in 2ml/well of SFQ supplemented with 10% FCS in six well plates. Cells were transfected 24 hours after seeding using Lipofectamine 2000 (Invitrogen). 4μl/well of Lipofectamine 2000 was diluted in 96μl/well Opti-MEM I (Invitrogen) and incubated at RT for 5 min. 100μl/well of diluted Lipofectamine 2000 was added to reaction mixtures containing 1μg/well test plasmid, 0.02μg pRL-SV40, 240nmol siRNA as indicated and Opti-MEM I to a final volume of 100μl/well. 48 hours after seeding media was replaced on cells with 1ml SFQ supplemented with 10% FCS. 4μl/well of Lipofectamine 2000 was diluted in 96μl/well Opti-MEM I and incubated at rt for 5 min. 100μl/well of diluted Lipofectamine 2000 was added to 240nmol/well siRNA as indicated, diluted to a final volume of 100μl/well in Opti-MEM I and incubated at RT for 20 mins. 200μl/well of Lipofectamine 2000:siRNA complexes were added to appropriate wells. Media was changed 4 hours after transfection for 2ml SFQ supplemented with 10% FCS. 24 hours after the second transfection cells were washed twice in PBS and lysed in 200μl/well of cold 1X passive lysis buffer.

### *2.3.5 Total RNA extraction from cultured cells.*

Total RNA was extracted from cells using an RNeasy kit (Qiagen Ltd.). Cells seeded in 6 well plates were washed twice in PBS before the addition of 350μl/well of buffer RLT containing β-mercaptoethanol (10μl (v/v) 14.5M β-mercaptoethanol per 1ml buffer RLT). Cells lysates were passed 10 times through a 21G needle fitted

onto a 1ml syringe. 350µl 70% ethanol was added to each homogenised sample and mixed. Each sample was applied to an RNeasy mini spin column and micro-centrifuged at 8163g for 15 sec. Flow through was discarded before the addition of 700µl buffer RW1 to the spin column. The spin column was centrifuged as described previously. The RNeasy column was transferred to a clean collection tube before the addition of 500µl of buffer RPE. The RNeasy column was centrifuged as before and the flow through discarded. This step was repeated and the RNeasy column micro-centrifuged for 2 min at maximum speed. The flow through was discarded and the RNeasy column was centrifuged for a further 1 min at maximum speed. RNA was eluted into a clean 1.5ml micro-centrifuge tube by the addition of 30µl RNase free $H_2O$ onto the RNeasy membrane and micro-centrifugation for 1 min at 8163g.

### *2.3.6 DNase digestion of total cellular DNA.*

To remove any cellular DNA present in the samples a DNAse digestion was performed. For each µg of RNA in the sample the following volumes of components were added, 1µl 10X reaction buffer, 1µl DNase I (1U/µl, Invitrogen) and RNase and DNase free $H_2O$ to a final volume of 10µl. Reactions were incubated for 15 min at rt before the addition of 1µl 25mM EDTA. Reactions were incubated for 10 min at 65 °C. RNA was purified using an RNeasy kit (Qiagen Ltd., section 2.1.14).

### *2.3.7 Purification of cellular RNA from DNase digestion reactions.*

RNA was purified following the protocol for RNA cleanup using an RNeasy kit (Qiagen Ltd.). Each RNA sample was adjusted to 100µl with RNase free $H_2O$ before the addition of 350µl buffer RLT containing β-mercaptoethanol (10µl (v/v) β-mercaptoethanol per 1ml buffer RLT). Each sample was mixed thoroughly before the addition of 250µl 100% ethanol. Lysates were mixed by pipetting and each sample was applied to an RNeasy spin column and micro-centrifuged at 8163g for 15 sec. Flow through was discarded and each column was transferred to a clean collection tube. 500µl buffer RPE was added to each column before centrifugation as described. Flow through was discarded and the wash step repeated. RNeasy columns were

micro-centrifuged for 2 min at maximum speed. RNeasy columns were placed in clean 1.5ml micro-centrifuge tubes before the addition of 50µl RNase free $H_2O$ to the RNeasy membrane. RNeasy columns were micro-centrifuged for 1 min at 8163g to elute RNA.

### *2.3.8 Reverse transcription of cellular RNA.*

Each reaction contained 1µg total RNA, 1µl RNaseOUT RNase inhibitor (40U/µl, Invitrogen), 1µl random primers (3µg/µl, Invitrogen) and RNase and DNase free $H_2O$ to a final volume of 10µl. Reactions were prepared in duplicate for each RNA. Reactions were pulse centrifuged, incubated for 10 min at 70 °C and then chilled on ice. Reactions were pulse centrifuged before addition of 10µl per reaction of reverse transcriptase (RT) positive (RT+ve) or negative (RT-ve) master mix consisting of 2µl of RNase and DNase free $H_2O$, 4µl 5X first strand buffer, 1µl 10mM dNTPs, 2µl 0.1M DTT and 1µl Superscript II RT (Invitrogen) for RT+ve reactions and 1µl RNase and DNase free $H_2O$ for RT-ve reactions. RT+ve and RT-ve reactions were incubated for 1 hour at 42 °C followed by 10 min at 70 °C. Reactions were chilled on ice and pulse centrifuged. cDNA was amplified as described in section 2.1.16.

### *2.3.9 PCR amplification of cDNA.*

Each PCR reaction containing 5µl 10X reaction buffer, 1.5µl 50mM $MgCl_2$, 1µl 10mM dNTPs, 1µl sense primer (40pmol/µl), 1µl anti-sense primer (40pmol/µl), 0.5µl Taq DNA polymerase (5U/µl, Invitrogen), 2µl cDNA and RNase and DNase free $H_2O$ to a final volume of 50µl was covered in 20µl of mineral oil and performed in a 0.5ml RNase and DNase free micro-centrifuge tube using the following PCR cycle: -

| Step | Temperature °C | Time (min) |
|---|---|---|
| 1 | 94 | 3 |
| 2 | 94 | 1 |
| 3 | 55 | 1 |
| 4 | 72 | 1.5<br>cycle to step 2 30X |
| 5 | 72 | 10 |
| 6 | 4 | ∞ |

# Chapter 3: The development of HIF targeted RNA aptamers.

## 3.1 Introduction

Experiments performed by several groups have demonstrated blockade experiments are a viable option in the search for therapeutic strategies capable of modulating HIF function. For instance proof of principle experiments showed, the p300/HIF-1 interaction was disrupted by the overexpression of a polypeptide encoding the HIF-1α C-TAD domain (Kung *et al*., 2000, section 1.7.1). Peptide blockade experiments showed peptide overexpression prevented proteasomal degradation of ubiquitinated HIF-1α. Peptide blockade experiments carried out by a second group showed overexpression of prolyl hydroxylated peptides, based on the HIF-1α ODDD, saturated the proteasomal degradation process resulting in upregulation of endogenous HIF-1α and consequently the upregulation of HIF target genes (described in section 1.7.2, Li *et al.*, 2000; Williams *et al.*, 2002).

RNA aptamers are another type of small molecule that could be utilised in blockade experiments. They offer an advantage over short peptides because they have higher affinity and specificity for their targets (reviewed by Gold *et al.*, 1995).

### *3.1.1 RNA aptamers and SELEX (the systematic evolution of ligands by exponential enrichment).*

RNA aptamers have emerged as an oligonucleotide technology that can exploit the abilities of RNA to form three-dimensional structures and interact with other molecules e.g. proteins. RNA aptamers themselves are random pieces of folded single stranded RNA that are selected from large combinatorial pools of sequences, based on their capacity to bind a specific target, for example, a protein domain (Famulok, 1994). The RNA aptamer selection method requires a sequence of steps and has been named the systematic evolution of ligands by exponential enrichment (SELEX, figure 3.1). The first step in the SELEX procedure is the chemical synthesis of a random pool of single stranded DNA oligonucleotides. Each oligonucleotide has two fixed sequences at the 5’ and 3’ end, with a randomly synthesised set of nucleotides in the middle. The single stranded RNA aptamer pool is synthesised by PCR amplification of the single stranded DNA oligonucleotide into a double

stranded DNA library followed by *in vitro* transcription into the RNA aptamer pool. The starting pool typically has a complexity of $10^{14}$ or $10^{15}$ oligonucleotides. Once the RNA aptamer pool has been synthesised, the aptamers are incubated with the target molecule. Unbound aptamers are removed and discarded while bound aptamers are recovered from the target. The recovered (previously bound) RNA aptamers then undergo RT-PCR followed by *in vitro* transcription before undergoing further rounds of the selection process. Typically the selected pool will undergo between 4 and 20 rounds of selection. During these selection rounds, RNA aptamers will evolve towards those that are best able to withstand the selection criteria. The final step in the SELEX procedure is the cloning, sequencing and testing of the aptamers (Gold *et al.*, 1995).

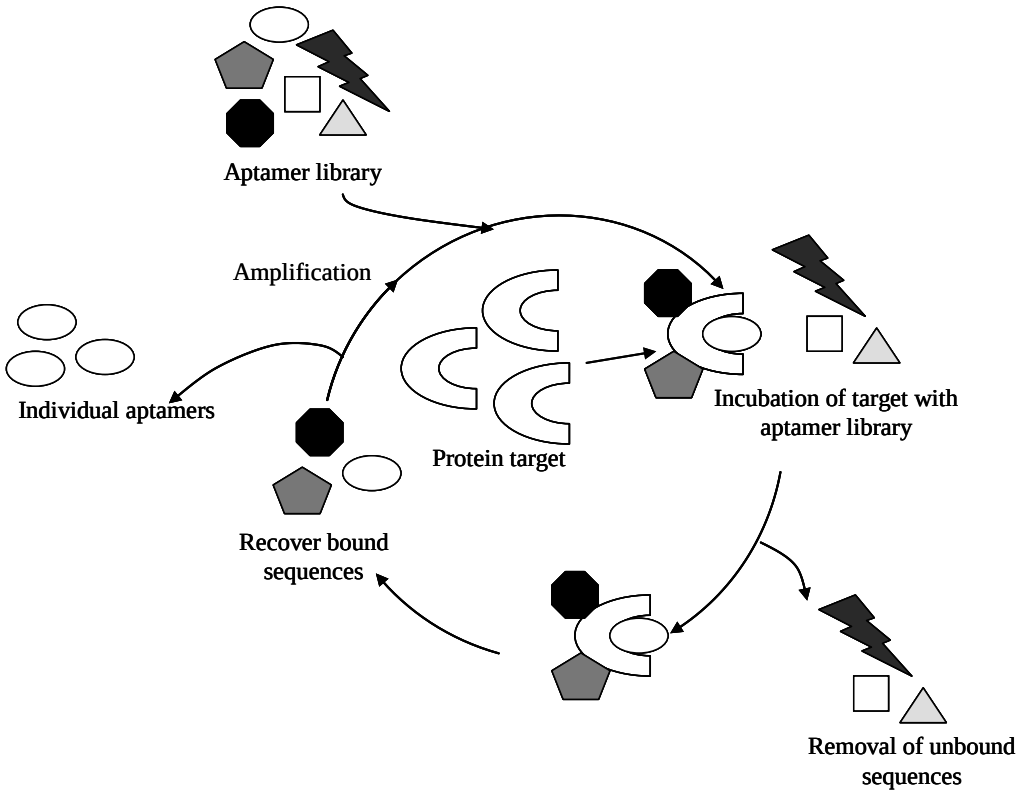


**Figure 3.1 The general principle of SELEX.**

A random pool of RNA oligonucleotides is synthesised to form an aptamer library. The aptamer library is then incubated with the protein target. Unbound aptamers and bound aptamers are partitioned. Bound aptamers are eluted from the target and amplified by RT-PCR. The selected aptamer pool can then undergo a new round of selection. Throughout the following rounds of selection the aptamer population evolves towards the sequences that are best able to withstand the selection process. Once the desired number of selection rounds have been carried out individual aptamers are cloned sequenced and tested.

RNA aptamers isolated from SELEX have a high efficiency of binding to their target sequences, typically in the low nanomolar to high picomolar range. This range is similar to the affinities of monoclonal antibodies for their targets. However, aptamers are advantageous when compared to monoclonal antibodies because they can be chemically synthesised in large quantities for *in vivo* applications. They can also be chemically modified to protect against nucleases or extend blood circulation time and appear to have low toxicity and immunogenicity, all properties that are invaluable *in vivo.* In certain circumstances RNA aptamers can be modified and injected directly into the area where treatment is required. An example of this is an RNA aptamer targeted to VEGF-165 which is injected in to the vitreous humour of the eye and is used for the treatment of age-related macular degeneration (Sullenger and Gilboa, 2002). However, it is anticipated that most RNA aptamer related therapeutics will be incorporated into gene delivery vectors in order to reach the treatment area. One such gene delivery technology that could be utilised in this study is LentiVector®, a lentiviral gene delivery system developed by our collaborators OBM.

### *3.1.2 Hypothesis.*

It is hypothesised that the development of RNA aptamers towards the ODDD of non-proline hydroxylated HIF-1α and EPAS-1 could prevent the action of the PHDs on these proteins. This favourable outcome is hypothesised to result in the stabilisation of HIF-1α and EPAS-1 and a subsequent upregulation in transcription which would be measured by a transcription reporter assay. Therefore the aims of this project are to develop RNA aptamers targeted towards the ODDD of non-proline hydroxylated HIF-1α and EPAS-1 and to determine whether selected targeted apatamers can up-regulate a HIF responsive transcription reporter assay.

## 3.2 Experimental strategy

The aim of this study was to develop RNA aptamers using SELEX towards known sequences of both the HIF-1α and EPAS ODDD. These sequences represented the

minimal motif of amino acids required to elucidate an oxygen dependent response and for the purposes of this study were not subjected to prolyl hydroxylation.

Before the development of the RNA aptamers could begin it was necessary to synthesise the target peptide sequences and develop a method in which RNA aptamers bound to the target protein sequence could be released (Section 3.3). DNA sequences encoding for HIF-1α-ODDD or EPAS ODDD were incorporated into expression vectors that introduced a GST moiety. The GST fusion vectors were expressed in bacteria and the resulting GST fusion proteins were purified using affinity chromatography, in this instance glutathione Sepharose 4B beads. A thrombin protease cleavage assay was developed which would be used to release RNA aptamers bound to the target protein sequence from GST. GST remained bound to the affinity chromatography column. Once these initial experimental steps had been undertaken the development, enrichment and testing of the RNA aptamers was carried out (section 3.4).

## 3.3 Target protein synthesis and purification

### *3.3.1 GST fusion protein vector development*

Experiments carried out by Huang *et al* (1998) and O'Rourke *et al* (1999) identified the sequences of amino acids within HIF-1α and EPAS that were responsible for elucidating oxygen dependent degradation of HIF-1α and EPAS, respectively. Pugh *et* al (1997) identified that the minimal sequence of amino acids that could result in independent oxygen regulated activity of HIF-1α was 549 -582. Based upon Huang *et al* (1998) and Pugh *et al's* (1997) findings sequence determined upon for HIF-1α encompassed amino acid residues 519 -647 of HIF-1α. Based upon findings by O'Rourke *et al* (1999) and sequence similarity analysis between HIF-1α and EPAS using BLAST the EPAS sequence spanned amino acid residues 488-617. These sequences also encompassed the prolyl hydroxylation sites $P^{564}$ of HIF-1α and $P^{572}$ of EPAS.

XL1-blue competent *E. coli* cells were transformed with pCI-neo-HIF-1a and pCI-EPAS using the same method as described for BL21-DE3 *E. coli* cells (sections 2.2.7 and 2.2.1). DNA plasmids were purified and sequences encoding amino acid residues 519 – 647 of HIF-1α and 488 – 617 of EPAS 1 were amplified by PCR (sections 2.2.4 and 2.2.2, respectively). PCR products were resolved by agarose gel electrophoresis. DNA was excised and purified then sub-cloned into the TOPO vector (sections, 2.1.9, 2.1.11 and 2.2.3). TOPO vectors containing the appropriate PCR-generated inserts were sequenced to confirm their identity, restriction digested and the resulting inserts ligated into the p-GEX-4T-3 vector to produce the vectors p-GEX-HIF-1α-ODDD or p-GEX-EPAS-ODDD (sections 2.2.5, 2.2.6 and 2.2.1).

### *3.3.2 Expression of GST fusion proteins*

BL21-DE3 competent *E.coli* cells were either transformed with p-GEX–4T-3, p-GEX-HIF-1α-ODDD or p-GEX-EPAS-ODDD (section 2.2.7.) GST fusion protein expression was induced by the addition of IPTG to a final concentration of 1mM.

Bacterial cell lysates were prepared 3 hours after the addition of IPTG and resolved by SDS-PAGE (section 2.1.8 and 2.1.3). The SDS-PAGE gel was coomassie stained and destained to visualise the proteins (section 2.1.8, figure 3.2).

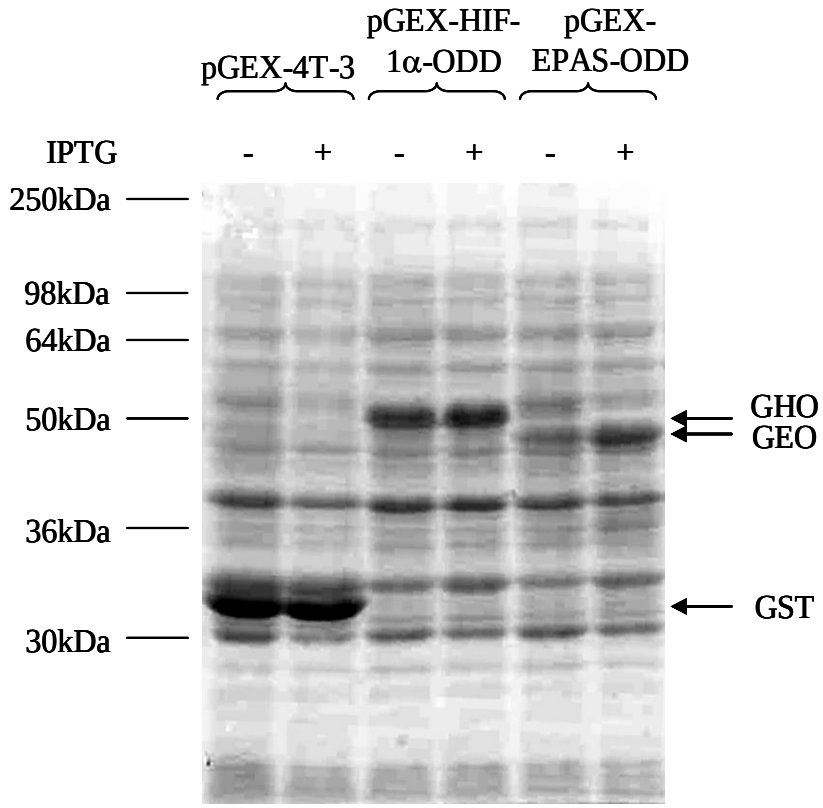


**Figure 3.2 Expression of GST fusion proteins in *E. coli***

BL21-DE3 cells transformed with p-GEX-4T-3, p-GEX-HIF-1α-ODD or p-GEX-EPAS-ODD were incubated with or without IPTG to a final concentration 1mM, as indicated to induce GST fusion protein expression Bacterial cell lysates, prepared 3 hours after IPTG inoculation, were resolved by SDS-PAGE. The SDS-PAGE gel was coomassie stained and destained to visualise proteins (N=2; sections 2.2.7, 2.1.8 and 2.1.3). Mobilities of standard proteins are indicated (Seeblue, Invitrogen,)

**Key:** EPAS, endothelial PAS protein; GEO, GST-EPAS-ODD; GHO, GST-HIF-1α-ODD; GST, glutathione-s-transferase; HIF, hypoxia inducible factor; IPTG, isopropyl β-D galactopyranoside; kDa, Kilodaltons

The glutathione-s-transferase (GST) and GST-HIF-1α-ODDD (GHO) fusion proteins were both expressed in the absence of IPTG. However, the addition of IPTG resulted in a higher fold induction of both the GST and GHO fusion proteins. The GST-EPAS-ODDD fusion protein was only modestly expressed in the absence of IPTG. A much higher fold induction of the GEO protein was observed following the addition of IPTG. These results showed that addition of IPTG resulted in a greater expression of all three fusion proteins than when IPTG was not added. Therefore in all subsequent cultures GST fusion protein expression was induced using IPTG.

### *3.3.3 Purification of GST fusion proteins*

Theoretically, development of GST fusion proteins allows for their purification using glutathione Sepharose 4B beads or a glutathione Sepharose 4B column. To ensure the GHO and GEO fusion proteins could be purified, a batch purification procedure using glutathione Sepharose 4B beads (henceforth referred to as beads) was performed. BL21-DE3 cells either untransformed, or transformed with pGEX-4T-3, pGEX-HIF-1α-ODDD or pGEX-EPAS-ODDD, were grown in culture as before and bacterial cell lysates were prepared (section 2.2.8). Lysates were sonicated before micro-centrifugation. The insoluble protein pellets (I) were retained for analysis, while the supernatants, containing soluble proteins, were mixed with a slurry of beads. 10% of each supernatant was retained for analysis (S-soluble protein). After incubation with beads the mixtures were micro-centrifuged. Supernatants from this step contained soluble proteins that did not bind to the beads (NB). The glutathione Sepharose bead pellet from this step contained proteins bound to beads (B). Equivalent proportions of all the fractions (I, S, NB and B) were analysed by SDS-PAGE. The SDS-PAGE gel was coomassie stained and de-stained to visualise the proteins (figure 3.3). Proteins of the approximate expected mobilities of GST, GHO and GEO, bound to beads (figure 3.3, lower panel). However, there appeared to be some degradation of the GST fusion proteins, in particular GEO, possibly caused by proteases in the BL21-DE3 cells (figure 3.3, lower panel).

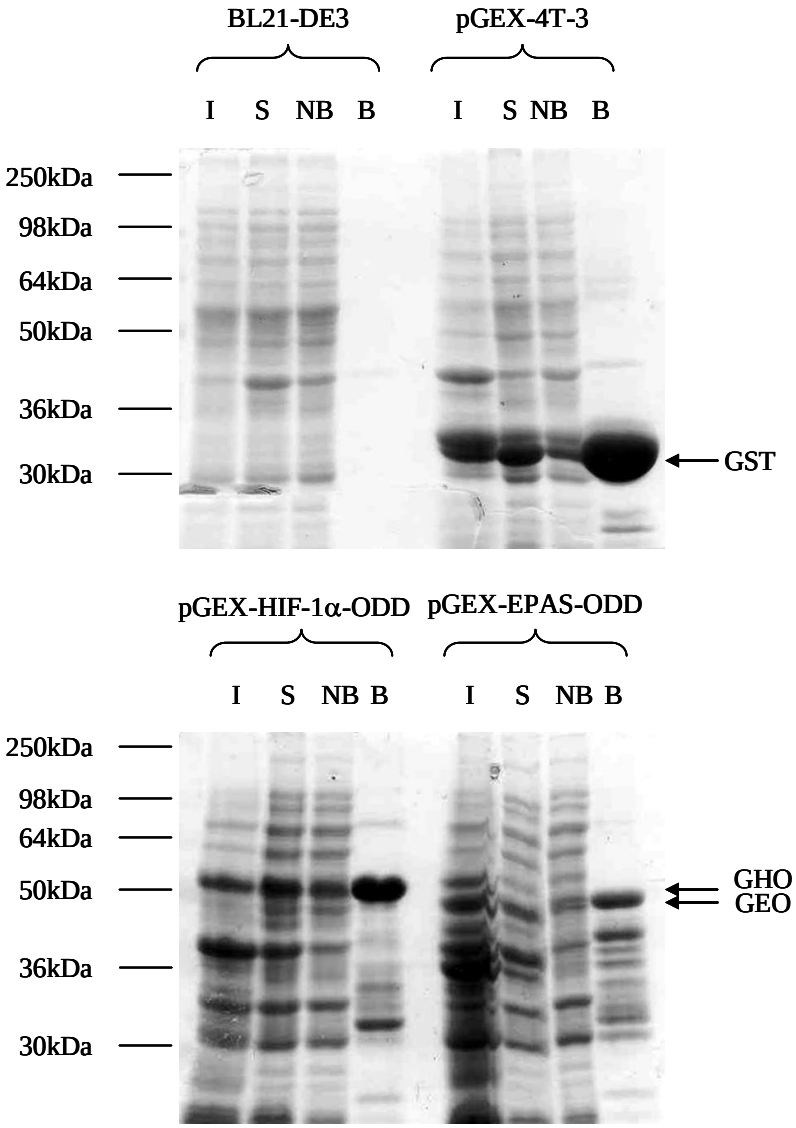


**Figure 3.3 Purification of GST fusion proteins**

BL21-DE3 cells and BL21-DE3 cells transformed with p-GEX-4T-3, p-GEX-HIF-1α-ODD or p-GEX-EPAS-ODD were incubated with 1mM IPTG to induce GST fusion protein expression (GST, GHO and GEO, respectively). Cell lysates were prepared and the supernatant incubated with glutathione sepharose 4B beads. Insoluble protein (I), soluble protein (S), proteins not bound to beads (NB) and proteins bound to beads (B) were resolved using SDS-PAGE and coomassie stained (N=1; section 2.2.8).. Mobilities of standard proteins are indicated (Seeblue, Invitrogen).

**Key:** B, Proteins bound to beads; EPAS, endothelial PAS protein; GEO, GST-EPAS-ODD; GHO, GST-HIF-1α-ODD; GST, glutathione-s-transferase; HIF, hypoxia inducible factor; I, insoluble protein; IPTG, isopropyl β-D galactopyranoside; NB, proteins not bound to beads; S, soluble protein.

To determine whether this apparent degradation of the GST fusion proteins could be prevented, BL21-DE3 cells transformed with p-GEX-4T-3, pGEX-HIF-1α-ODDD or p-GEX-EPAS-ODDD were cultured as before.

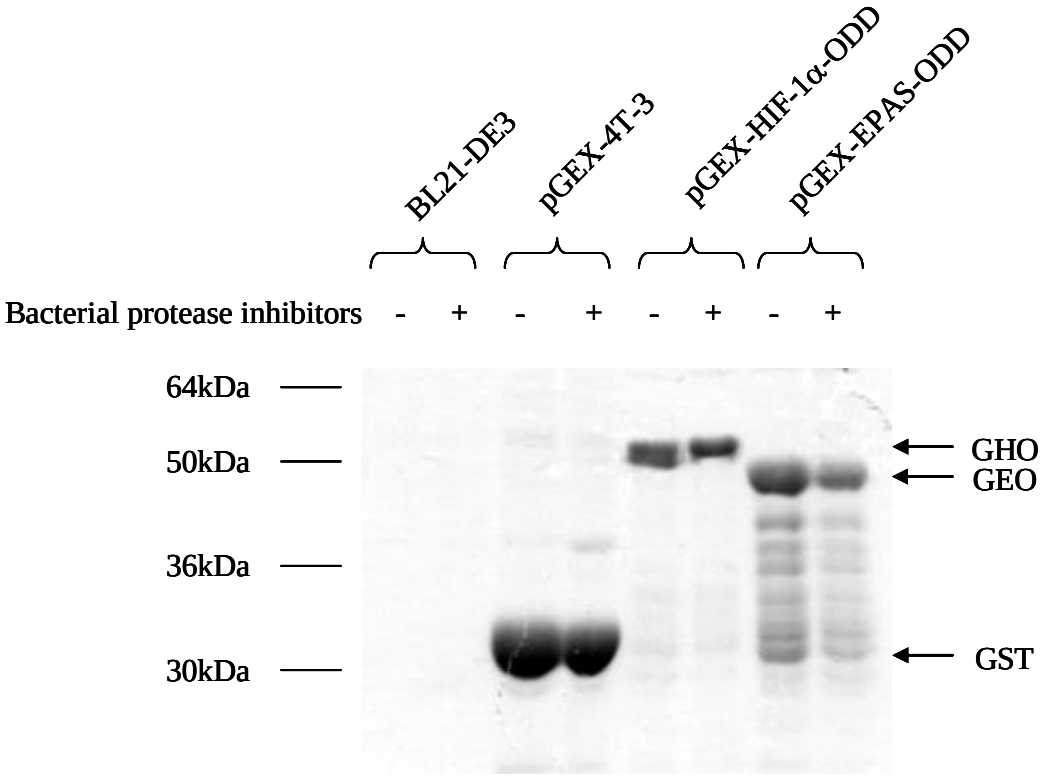


**Figure 3.4 The effect of bacterial protease inhibitors on GST fusion protein purification.**

BL21-DE3 cells and BL21-DE3 cells transformed with p-GEX-4T-3, p-GEX-HIF-1α-ODD or p-GEX-EPAS-ODD were incubated with or without IPTG to a final concentration of 1mM. Bacterial cell lysates were prepared 3 hours after IPTG inoculation in lysis buffer with (+) or without (-) bacterial protease inhibitors, as indicated. Soluble proteins were bound to glutathione sepharose 4B beads. Proteins bound to beads were resolved using SDS-PAGE. The SDA-PAGE gel was coomassie stained and destained to visualise proteins (N=2; sections 2.2.7, 2.2.8, 2.1.3 and 2.1.8). Mobilities of standard proteins are indicated (Seeblue, Invitroge).

**Key:** EPAS, endothelial PAS protein;; GEO, GST-EPAS-ODD; GHO, GST-HIF-1α-ODD; GST, glutathione-s-transferase; HIF, hypoxia inducible factor; IPTG, isopropyl β-D galactopyranoside; kDa, kilodalton

A bacterial protease inhibitor cocktail containing serine protease, metalloprotease, aminopeptidase, acid protease and cysteine protease inhibitors was added to the lysis buffer before proteins were extracted. Bacterial cell lysates were resolved by SDS-PAGE. The SDS-PAGE gel was coomassie stained and destained in order to visualise the proteins (figure 3.4).

Bacterial protease inhibitors appeared to have very little effect on the apparent degradation products of GST and GHO (figure 3.4). The weaker staining of GEO and GEO related fusion protein products in the bacterial protease treated sample appears to be due to protein loading error. The apparent failure of the bacterial protease inhibitors to prevent the breakdown of the GST, GHO and GEO fusion proteins could be because the bacterial protease inhibitor cocktail is not comprehensive. Due to the higher proportion of GEO related fusion protein products compared to GHO related fusion protein products and growing evidence in the published literature that HIF-1α was the more globally expressed protein, it was decided to perform all further experiments only using the GHO fusion protein (section 1.2.2). GST continued to be used as the control. Bacterial protease inhibitors were also omitted from subsequent experiments because they appeared to have no effect on GHO related fusion protein products (figure 3.4).

### *3.3.4 Optimisation of thrombin protease cleavage of recombinant HIF-1α-ODDD from the GST fusion protein.*

RNA aptamers were to be bound to GST fusion proteins. Before the amplification of the specifically bound aptamers could be undertaken they had to be released from the fusion proteins. The pGEX-4T-3 vector encoded a thrombin protease cleavage site between the GST and fusion partner encoding regions. Therefore, the cleavage of the HIF-1α-ODDD from GST using thrombin protease was attempted. It was hypothesised that this would allow aptamers only binding to HIF-1α-ODDD to be released, preventing a mixed pool of aptamers that would require a further purification step to isolate those that could only bind to HIF-1α-ODDD. BL21-DE3 cells transformed with either pGEX-4T-3 or pGEX-HIF-1α-ODDD were grown in culture, lysed and fusion proteins were bound to glutathione transferase 4B beads, as

previously described. GST proteins bound to beads were equalised for loading. Aliquots of GST and GHO bound to beads were incubated with binding buffer containing BSA (BB-BSA) then washed in PBS. Fusion proteins were incubated with or without thrombin protease for 16 hours. Thrombin protease was incubated alone as a control. Samples were resolved by SDS-PAGE before the gel was coomasie stained and destained in order to visualise the proteins (section 2.2.11, figure 3.5).

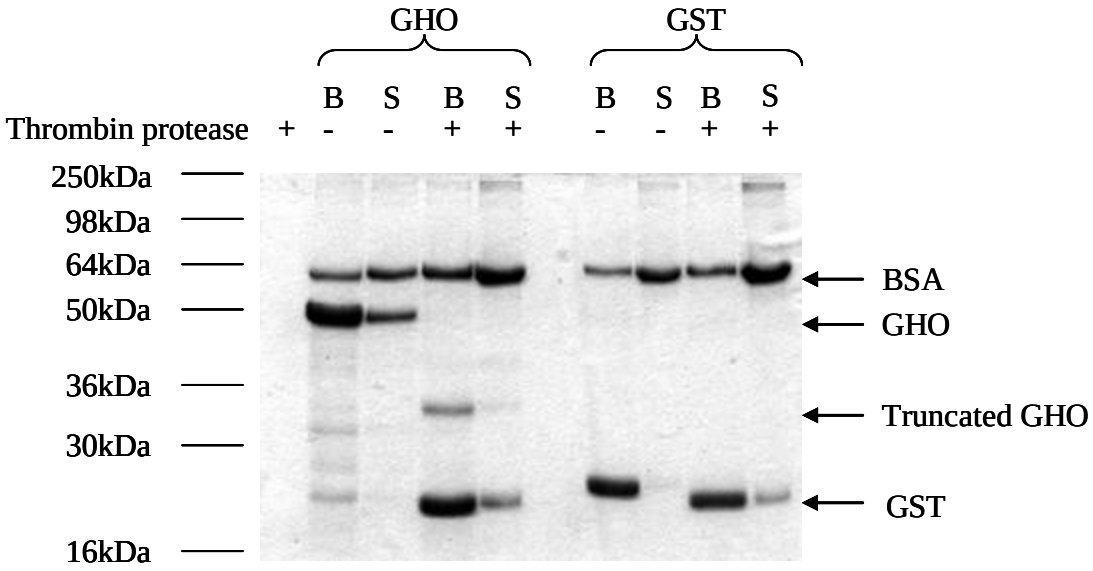


**Figure 3.5 Thrombin protease cleavage of HIF-1α-ODD from GST.**

BL21-DE3 cells transformed with either pGEX-4T-3 or pGEX-HIF-1α-ODD were grown in culture inoculated with IPTG to a final concentration of 1mM to induce GST fusion protein expression. 3 hours after IPTG inoculation bacterial cells were lysed and fusion proteins were bound to glutathione transferase 4B beads. GST and GHO fusion proteins bound to beads were incubated with binding buffer containing BSA and washed in PBS before incubation with (+) or without (-) thrombin protease, as indicated. Samples were incubated at room temperature for 16 hours. Beads (B) and supernatants (S) from beads were separated. Proteins were resolved by SDS-PAGE. The SDS-PAGE gel was coomassie stained and destained to visualise proteins (N=1; sections 2.2.7, 2.2.8, 2.2.11, 2.1.8 and 2.1.3). Mobilities of standard proteins are indicated (Seeblue, Invitrogen).

**Key:** B, beads; BSA, bovine serum albumin; GHO, GST-HIF-1α-ODD; GST, glutathione-s-transferase; HIF, hypoxia inducible factor; IPTG, isopropyl β-D galactopyranoside; kDa, kilodalton; PBS, phosphate buffered saline; S, supernatants from beads.

The GST moiety is approximately 26kDa therefore any HIF-1α-ODDD that had been cleaved from bead bound GST would have a predicted weight of 24kDa. However, although cleavage of the HIF-1α-ODDD from GST was the only cleavage process observed there appeared to be no protein band that corresponded solely to the HIF-1α-ODDD in the thrombin protease treated GHO supernatant (S) sample. It is possible that the presence of the HIF-1α-ODDD protein band had been masked by GST wash off, due to the similarity in molecular weight.

Another explanation for the lack of a HIF-1α-ODDD specific band could be due to the processes that resulted in truncated GHO, as seen in the thrombin protease treated GHO bead (B) sample. Truncated GHO had an approximate molecular weight of 33kDa and was still connected to GST as the larger proportion remained bead associated. The truncation was the result of non-specific enzymatic cleavage because truncation was not present in protease free GHO samples. The cleavage was non-specific because the HIF-1α-ODDD sequence does not have a specific thrombin protease cleavage site. However, the non-specific cleavage of GHO and cleavage of the remaining HIF-1α-ODDD from bead associated GST would result in two small peptide fragments. These fragments may have been so small that they ran off of the SDS-PAGE gel or be of so low an abundance that they do not readily stain with coomassie.

RNA aptamer enrichment begins with the selection of aptamers towards bead bound GST. This is a negative selection process which removes aptamers that bind to beads, GST or GST and beads. The positive selection of RNA aptamers towards GHO bound to beads follows the negative selection process. The thrombin protease cleavage assay resulted in three possible HIF-1α-ODDD derived species; - full length HIF-1α-ODDD and two smaller fragments as a result of truncated GHO. The cleavage of full length HIF-1α-ODDD from GST or the truncated HIF-1α-ODDD protein from GST would select two types of RNA aptamer species, those that specifically bound HIF-1α-ODDD and those that bound GST-HIF-1α-ODDD. Future enrichment of the RNA aptamers would result in the removal of GST-HIF-1α-ODDD associated aptamers through the negative selection process. Aptamers released from truncation of GHO, where the larger proportion of the GHO protein

remained bead associated, would only bind the HIF-1α-ODDD moiety. Therefore although thrombin protease non-specifically cleaved GHO it was hypothesised that the RNA aptamer selection protocol was stringent enough to remove any aptamers that did not specifically target HIF-1α-ODDD. As a result of this the thrombin protease cleavage assay was optimised. A time course of the incubation was performed as for the 16 hour experiment, except aliquots of the reactions were taken at 2, 4, 6 and 8 hour intervals (figure 3.6). The majority of the cleavage reaction was completed within eight hours, based on the disappearance of the GHO band with an apparent molecular weight of 50kDa (figure 3.6D)

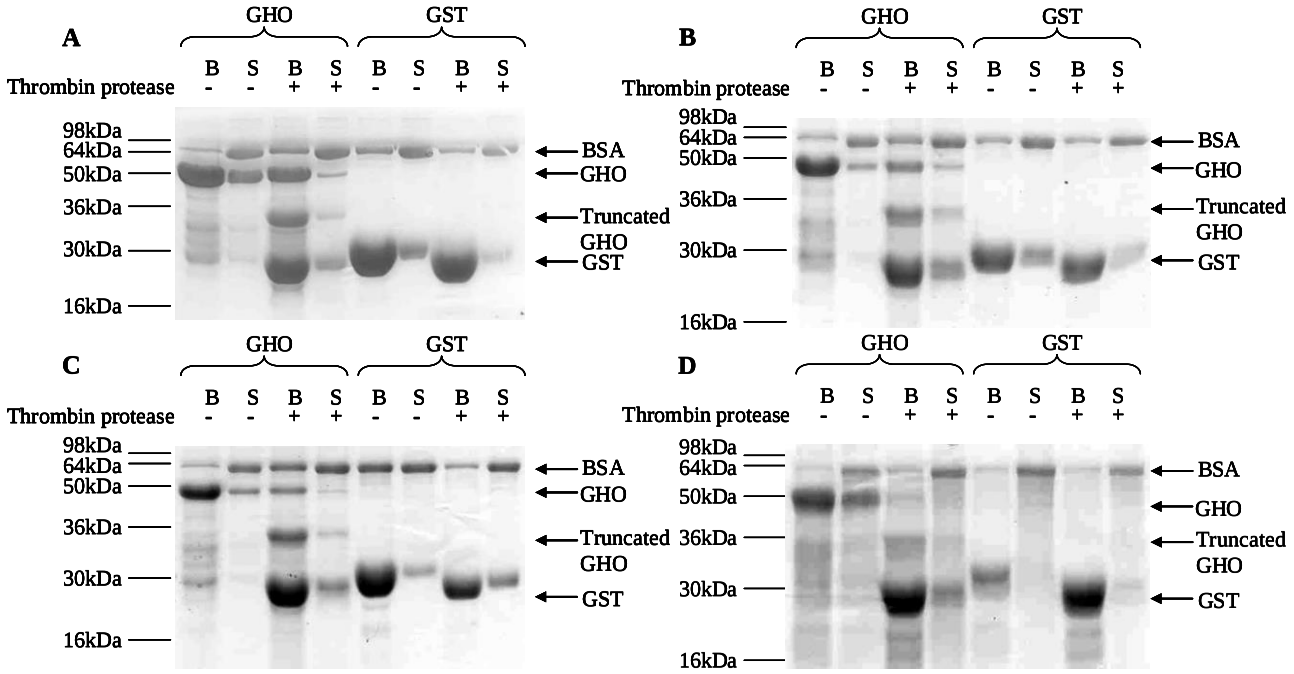


**Figure 3.6 A time course of thrombin protease cleavage of HIF-1α-ODD from GST.**

BL21-DE3 cells transformed with either pGEX-4T-3 or pGEX-HIF-1α-ODD were grown in culture inoculated with IPTG to a final concentration of 1mM to induce GST fusion protein expression. 3 hours after IPTG inoculation bacterial cells were lysed and fusion proteins were bound to glutathione transferase 4B beads. GST and GHO fusion proteins bound to beads were incubated with binding buffer containing BSA and washed in PBS before incubation with (+) or without (-) thrombin protease, as indicated. Samples were incubated at room temperature for 2,4,6 and 8 hours. Beads (B) and supernatants (S) from beads were separated. Proteins were resolved by SDS-PAGE. The SDS-PAGE gel was coomassie stained and destained to visualise proteins (N=1; sections 2.2.7, 2.2.8, 2.2.11, 2.1.8 and 2.1.3). Mobilities of standard proteins are indicated (Seeblue, Invitrogen).

**Key:** B, beads; BSA, bovine serum albumin; GHO, GST-HIF-1α-ODD; GST, glutathione-s-transferase; HIF, hypoxia inducible factor; IPTG, isopropyl β-D galactopyranoside; kDa, kilodalton; PBS, phosphate buffered saline; S, supernatants from beads.

### *3.3.5 Binding of recombinant HIF-1α-ODDD to pVHL.*

*In vivo* the oxygen dependent degradation domain of HIF-1α is bound by pVHL causing ubiquitination of the protein and hence its degradation by the 26S proteasome (section 1.3). To assess whether the recombinant HIF-1α-ODDD protein was correctly folded, it was necessary to test whether the protein could associate with pVHL. Aliquots of GST and GHO bound to glutathione 4B Sepharose beads were incubated in reticulocyte lysate or NP40 lysis buffer as a negative control. The reticulocyte lysate was used to ensure post-translational modification of proline 564 to hydroxy-proline in the HIF-1α-ODDD (Maxwell *et al.*, 1999; Masson *et al.*, 2001). Samples were then incubated with Hela whole cell lysates. Hela cells, a cervical adenocarcinoma cell line, have a known wild type pVHL genotype and have been used for similar experiments by other investigators (Yu *et al.*, 2001). 786-O cells, a renal carcinoma cell line, lack one VHL allele while the other allele encodes a non-functional truncated VHL protein.

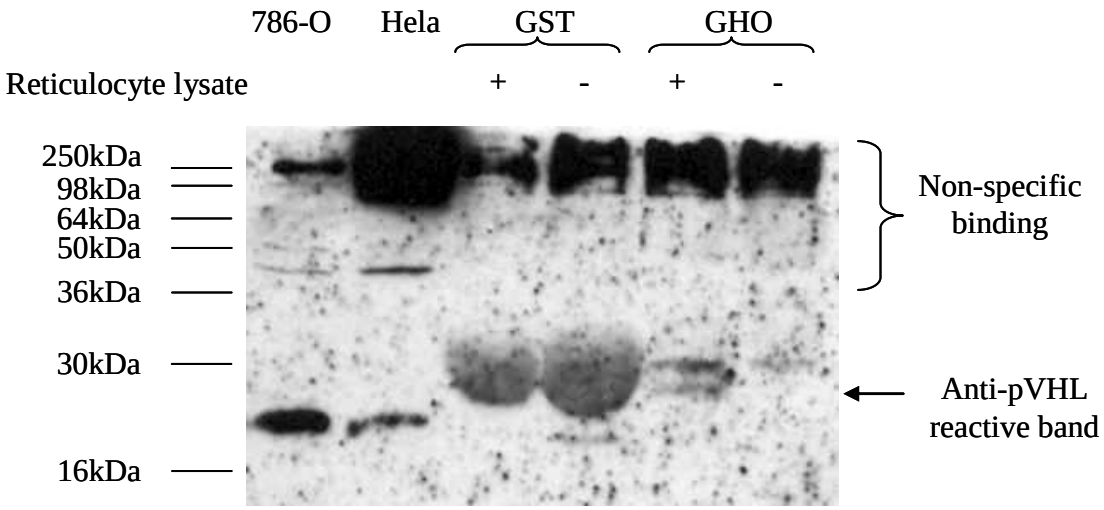


**Figure 3.7 pVHL binding assay**

BL21-DE3 cells transformed with either pGEX-4T-3 or pGEX-HIF-1α-ODD were grown in culture inoculated with IPTG to a final concentration of 1mM to induce GST fusion protein expression. 3 hours after IPTG inoculation bacterial cells were lysed and fusion proteins were bound to glutathione transferase 4B beads. GST and GHO bound to beads were incubated with either reticulocyte lysate (+) or NP40 lysis buffer (-), as indicated for 90 minutes at 30°C. Samples were subsequently incubated with Hela whole cell lysate for 1 hour at 4°C. 786-O whole cell lysate, Hela whole cell lysate and proteins bound to beads were resolved by SDS-PAGE. Proteins were western blotted and probed with an anti-VHL antibody (N=1; sections 2.2.7, 2.2.8, 2.2.9, 2.2.10, 2.1.3 and 2.1.4).. Mobilities of standard proteins are indicated (Seeblue, Invitrogen).

**Key:** GHO, GST-HIF-1α-ODD; GST, glutathione-s-transferase; HIF, hypoxia inducible factor; IPTG, isopropyl β-D galactopyranoside; kDa, kilodalton.

786-O whole cell lysates were used as a negative control for identification of pVHL. Proteins associated with bead bound GST and GHO, Hela whole cell lysate and 786-O whole cell lysate were resolved by SDS-PAGE, western blotted and probed with an anti-pVHL antibody (figure 3.7).

GHO treated with reticulocyte lysate (GHO+) retained two anti-VHL reactive protein bands, the lower of which was not present in the GHO- sample (GHO not treated with reticulocyte lysate). This could have been pVHL however failure to detect the endogenous pVHL in Hela whole cell lysate precluded an assignment based on gel mobility. GST also runs at the same mobility as the band in the GHO + lane. If a similar band was present in the GST +/- lane it would be masked by the non-specific

GST signal. Further experiments to eradicate the non-specific binding of the anti-pVHL antibody to GST were performed (data not shown). However, the above data (figure 3.7) could not be replicated due to a large amount of non-specific binding and high background levels on western blots which masked the presence of any results and made interpretation impossible. This precluded any further controls due to the unreliability of the anti-pVHL antibody. Despite this set-back it was decided to use the GHO protein in subsequent experiments.

## 3.4 RNA aptamer development and their effect on a HIF responsive transcriptional reporter assay.

### *3.4.1 DNA oligonucleotide pool synthesis and purification*

A double stranded DNA pool was synthesised by a specific 6 cycle PCR of a DNA oligonucleotide template shown below.

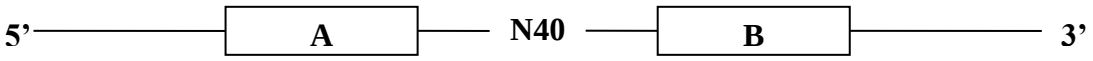


The DNA oligonucleotide template consisted of two known primer site sequences at the 5' and 3' ends represented by boxes A and B, respectively. These known sequences were either side of a random sequence of 40 nucleotides represented above by N40 (section 2.2.12). The 5' primer for this PCR introduced an *in vitro* T7 polymerase promotor sequence for T7 RNA polymerase transcription of the DNA. oligonucleotide pool into an RNA aptamer pool (section 3.3.2). The starting sequence complexity of the DNA pool was estimated to be $7.16\times10^{12}$ oligonucleotides. This was determined as shown below:

$$\frac{\text{Moles of DNA oligonucleotide template X Avogadro's number } (6.022 \times 10^{23})}{3.348} = \text{Total number of oligonucleotides in 1mg of single stranded DNA pool}$$

*Total Number of oligonucleotides X amount of DNA pool per PCR reaction (in mg) X number of PCR reaction = Estimated starting pool complexity*

The PCR products were resolved by agarose gel electrophoresis and visualised under ultra violet light to confirm synthesis had occurred (section 2.1.9, figure 3.8). A PCR

product of a size consistent with the predicted 78 base pair length of the double stranded transcription template was detected in the test reaction. No PCR products were detected in the negative control lanes.

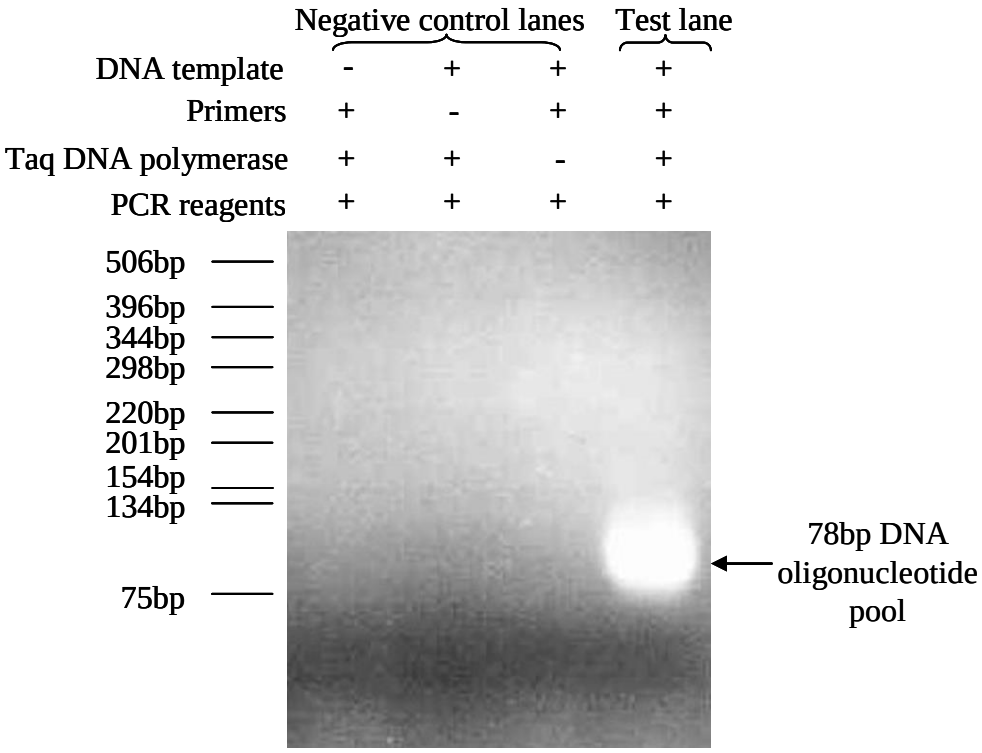


**Figure 3.8 PCR synthesis of DNA oligonucleotide pool transcription template.**

A DNA oligonucleotide pool was synthesised by PCR using specific primers from a DNA oligonucleotide template consisting of 40 random nucleotides with a known primer site sequence at the 5' and 3' ends. The 5' primer site introduced a T7 polymerase promotor sequence. Negative control PCR reactions were undertaken, as indicated. PCR products were resolved by agarose gel electrophoresis and visualised under ultra violet light (N=2; sections 2.2.12 and 2.1.9). Molecular weight markers are indicated.

**Key:** bp, base pairs; DNA, deoxyribonucleic acid; PCR, polymerase chain reaction.

In order to prevent any PCR reagents or primers from interfering with subsequent T7 transcription of the amplified DNA oligonucleotide pool, it was necessary to purify the PCR product. This was accomplished by size exclusion purification through a silica gel membrane. A buffer with a high salt concentration was mixed with the PCR

reaction. This enabled DNA to adsorb to the silica gel membrane while contaminants passed through. The DNA was then washed and eluted from the silica gel membrane (section 2.2.13). Synthesis of the DNA oligonucleotide pool required 10 individual PCR reactions in order to provide the appropriate degree of complexity, the PCR products were pooled before purification. Purified and unpurified PCR products were analysed by agarose gel electrophoresis and visualised under ultraviolet light, to determine the success of the purification (figure 3.9).

No primers were detectable in either the purified or unpurified PCR product indicating that all primers were consumed in the PCR reaction. However, the purification of the amplified DNA oligonucleotide pool is still necessary in order to remove any remaining PCR reagents that may interfere with subsequent transcription. Following purification, the concentration of DNA present in the transcription template was determined to be 0.75ng/μl.

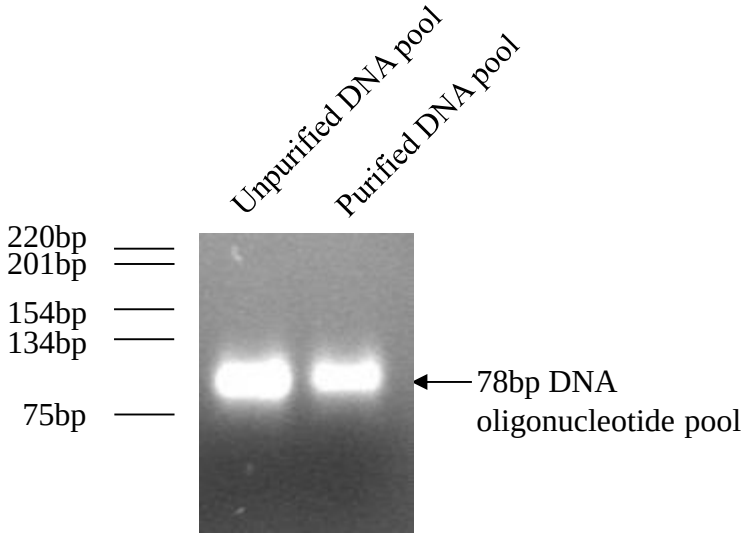


**Figure 3.9 Purification of DNA oligonucleotide pool PCR product.**

A DNA oligonucleotide pool was synthesised by PCR from a DNA oligonucleotide pool template consisting of 40 random nucleotides using sense and antisense primers to known primer site sequences at the 5' and 3' ends of the template. The 5' primer introduced a T7 polymerase promotor sequence. The DNA oligonucleotide pool PCR product was purified using a Qiagen Minelute PCR purification kit. Unpurified and purified DNA oligonucleotide pool PCR products were subjected to agarose gel electrophoresis and visualised under ultra violet light (N=1; sections 2.2.13, 2.2.14 and2.1.9). Molecular weight markers are indicated.

**Key:** bp, base pairs; DNA, deoxyribonucleic acid; DNA pool, DNA oligonucleotide pool; PCR, polymerase chain reaction.

### *3.4.2 RNA aptamer pool synthesis and purification.*

RNA aptamers were synthesised by transcribing purified DNA oligonucleotide pool using T7 RNA polymerase. The transcription reaction was then subjected to DNase digestion and purified using a nucleotide removal kit (sections 2.2.14 and 2.2.15). Samples from each step of the T7 RNA polymerase transcription, DNase digestion and purification were analysed by agarose gel electrophoresis and visualised under ultraviolet light (figure 3.10).

The same volume of both the negative control and test transcription reactions was visualised on the agarose gel (T7 RNA polymerase – and T7 RNA polymerase +,

respectively). As expected a band was present in the negative control transcription reaction. This band represented the DNA oligo pool template and was completely removed by DNase digestion (figure 3.10, lane 3). Purification of the negative control transcription reaction after DNase digestion resulted in no visible DNA on the agarose gel (figure 3.10, lane 5). The test transcription reaction (figure 3.10, lane 2) had a higher intensity band than the negative control transcription reaction which suggested T7 dependent RNA transcription had taken place. The band shift visible in this reaction was due to the T7 RNA polymerase transcription complexes. DNase digestion of the test transcription reaction resulted in a low intensity band representing the RNA aptamer pool (figure 3.10, lane 4). Purification of the RNA aptamer pool resulted in the visualisation of a very low intensity band, representing the RNA aptamer pool, on the agarose gel (figure 3.10, lane 6). The results from this experiment showed the transcription and purification steps were successful. The low intensity of the RNA aptamer pool visualised on the agarose gel represents a small portion of the overall starting pool. However, the purification procedure does appear to result in some loss of RNA aptamers which represents a loss of complexity from the starting RNA aptamer pool. However, due to the high level of estimated RNA aptamer starting pool complexity ($7.16 \times 10^{12}$ aptamers) a small loss of RNA aptamers in the purification procedure was deemed acceptable.

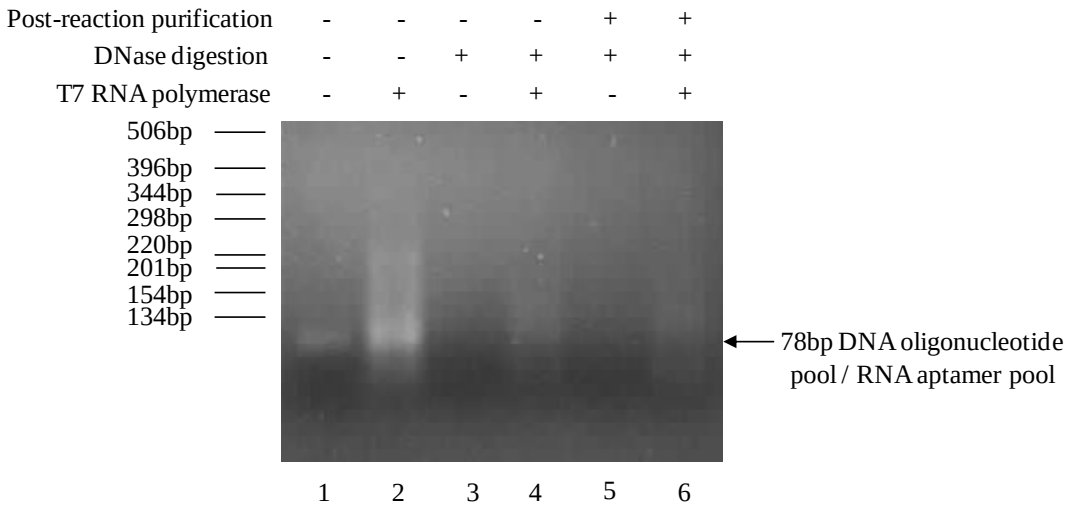


**Figure 3.10 Transcription and purification of the RNA aptamer pool**

A DNA oligonucleotide pool was synthesised via PCR. The PCR products were purified using a Qiagen Minelute PCR purification kit. The purified DNA oligonucleotide pool was then transcribed using T7 RNA polymerase, as indicated to produce the RNA aptamer starting pool. Transcribed and untranscribed reactions were subjected to DNase digestion (lanes 3-6) before purification using a Qiaquick nucleotide removal kit (lanes 5 and 6). Samples from each stage of the transcription and purification process were subjected to agarose gel electrophoresis and visualised under ultra violet light (N=2; sections 2.2.12, 2.2.13, 2.2.14, and 2.1.9). Molecular weight markers are indicated.

**Key:** bp, base pairs; DNA, deoxyribonucleic acid; RNA, ribonucleic acid; PCR, polymerase chain reaction.

### *3.4.3 Optimisation of one-step RT-PCR.*

Once the RNA aptamer pool had been transcribed, DNase digested and purified it was subjected to the selection procedure. The original experimental design of the selection procedure entailed the negative selection of RNA aptamers against GST bound to beads. This removed any aptamers that only bound to the beads, GST or a combination of the beads and GST, respectively. Unbound RNA aptamers were then incubated with GHO. Aptamers bound to GHO were released from the beads by thrombin protease cleavage. A further experimental step would then be required to remove the aptamers from GHO before RT-PCR could take place. The need for this additional step was negated by the use of a one-step RT-PCR procedure using *C. therm* polymerase. *C. therm* polymerase is comprised of the Klenow fragment of

DNA polymerase from *Carboxydohermus hydrogenoformans* and Taq DNA polymerase. This mix allows reverse transcription to occur between 60°C and 70°C, a higher temperature than conventional reverse transcription which is performed at 42°C. The higher temperature reverse transcription reaction is beneficial to the RNA aptamer selection procedure because it was hypothesised that this would cause the RNA and protein to dissociate due to conformational changes in the secondary and tertiary structure of the protein, therefore replacing the need for an additional purification procedure to separate the aptamers from GHO. Before embarking on the RNA selection procedure the one-step RT-PCR reaction was optimised using the starting RNA aptamer pool $r_0$. This pool was subjected to one step-RT-PCR with either 10 or 20 PCR cycles (section 2.2.17). Samples were analysed by agarose gel electrophoresis and visualised under UV light (figure 3.11).

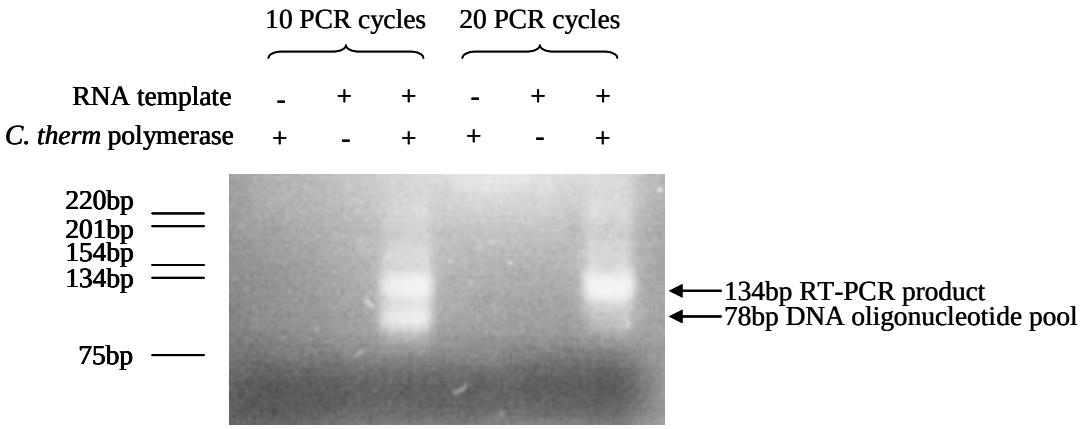


**Figure 3.11 Optimisation of one step RT-PCR – part 1.**

The starting RNA aptamer pool (RNA template) was subjected to one-step RT-PCR with or without *C. therm* polymerase, as indicated. The PCR step of the reaction was performed for either 10 or 20 cycles, as indicated. Negative control RT-PCR reactions were undertaken for the 10 and 20 cycle reactions. RT-PCR products were resolved by agarose gel electrophoresis and visualised under ultra violet light (N=1; sections 2.2.12 - 2.2.15, 2.2.17 and 2.1.9). Molecular weight markers are indicated.

**Key:** bp, base pairs; DNA, deoxyribonucleic acid; PCR, polymerase chain reaction; RNA, ribonucleic acid; RT-PCR, reverse transcription polymerase chain reaction.

RNA and *C. therm* dependent products were seen in both the 10 cycle RT-PCR and 20 cycle RT-PCR reactions. However, unexpectedly a doublet was seen in the 10

cycle RT-PCR with the lower band of the doublet corresponding to the expected 78bp product. The higher band of the doublet corresponded to approximately 134bp. The 134bp product was seen again in the 20 cycle RT-PCR. However in this RT-PCR reaction no 78bp product was visualised. The 134bp product in either cycle reaction could not have been caused by contamination as indicated by the negative control lanes. It is possible that the 134bp product could be artifactual concatamers caused by high levels of substrate and non-specific hybridisation (Crompton M, personal communication).

To try and eliminate the 134bp product, one-step RT-PCR of $r_0$ was carried out with primer concentrations of 0.1nmoles and 0.2nmoles and a 10 cycle PCR (section 2.2.17). Reactions were separated by agarose gel electrophoresis and visualised under UV light (figure 3.12).

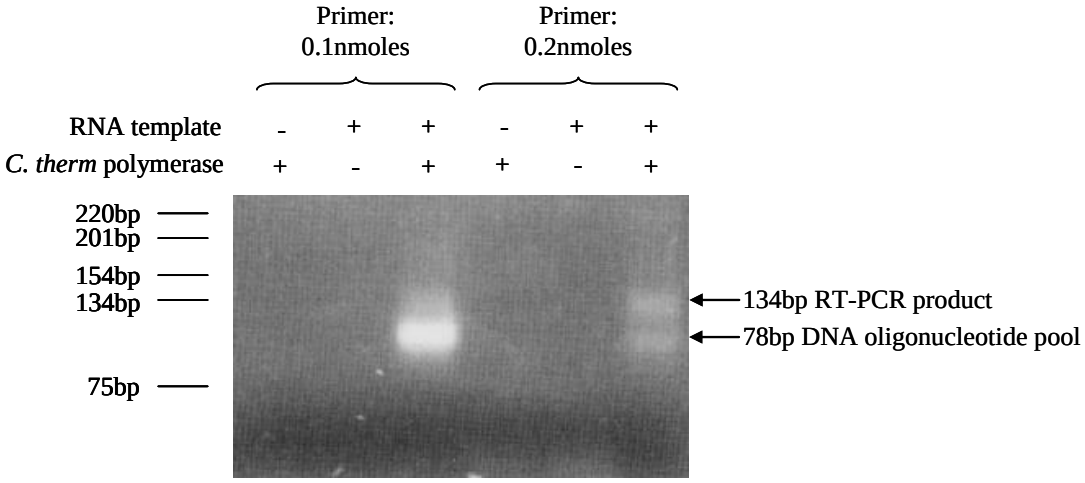


**Figure 3.12 Optimisation of one-step RT-PCR – part 2.**

The starting RNA aptamer pool (RNA template) was subjected to one-step RT-PCR with or without *C. therm* polymerase, as indicated. . The PCR step of the reaction was performed with either 0.1 nmoles or 0.2nmoles of primers, as indicated. Negative control RT-PCR reactions were undertaken for both primer concentrations. RT-PCR products were resolved by agarose gel electrophoresis and visualised under ultra violet light (N=1; sections 2.2.12 - 2.2.15, 2.2.17 and 2.1.9). Molecular weight markers are indicated.

bp, base pairs; DNA, deoxyribonucleic acid; PCR, polymerase chain reaction; RNA, ribonucleic acid; RT-PCR, reverse transcription polymerase chain reaction.

As expected all negative control lanes were devoid of any DNA for both primer concentrations. Reverse transcription and amplification with 0.1nmoles of primer resulted in only one visible band at approximately 78bp. However, reverse transcription and amplification of $r_0$ with 0.2nmols of primer resulted in the appearance of a doublet with the lower band corresponding to approximately 78bp and the higher band corresponding to approximately 134bp. Therefore from the results in figures 3.11 and 3.12 the conditions used for subsequent one-step RT-PCR are 0.1nmoles of primers combined with a 10 cycle PCR.

### *3.4.4 RNA aptamer selection and enrichment.*

A starting pool of RNA aptamers ($r_0$) was transcribed, DNase digested and purified as previously described. $r_0$ was then incubated with GST bound to beads, in the presence of an RNase inhibitor, for 1hr. The supernatant was removed and incubated with GHO bound to beads. The GHO and aptamer incubation was microcentrifuged and the supernatant discarded. Aptamers and GHO were released from the glutathione Sepharose 4B beads by thrombin protease cleavage before being subjected to one-step RT-PCR (sections 2.2.16 and 2.2.17). Samples from the RT-PCR were analysed by agarose gel electrophoresis and visualised under UV light (figure 3.13).

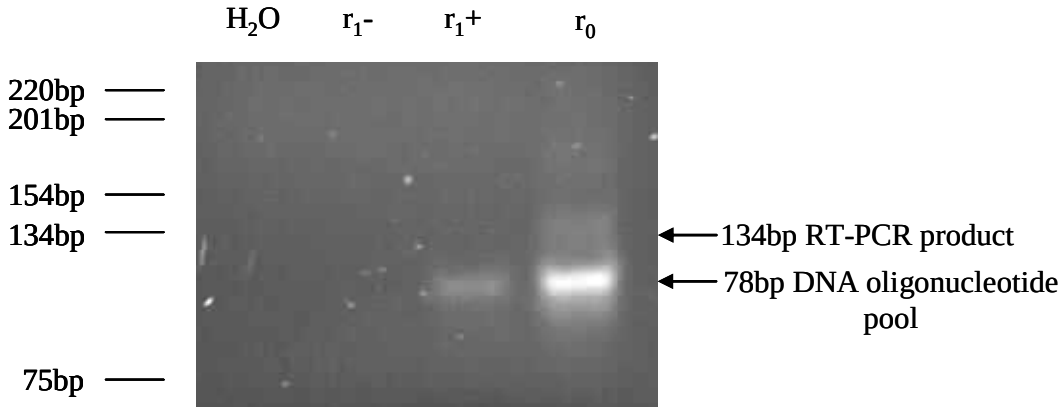


**Figure 3.13 First round of RNA aptamer selection.**

A starting pool of RNA aptamers was negatively selected against GST bound to beads. RNA aptamers were then positively selected against GHO bound to beads (section 2.2.16). Bound aptamers and GHO were released from glutathione sepharose 4B beads via thrombin protease cleavage (section 2.2.11). This first round of selected RNA aptamers ($r_1$) was then subjected to one-step RT-PCR either with or without *C. therm* polymerase ($r_1$+ or $r_1$-, as indicated; section 2.2.17). A negative ($H_2O$) control reaction was undertaken. RT-PCR products were analysed by agarose gel electrophoresis and visualised under ultra violet light. A reverse transcribed sample of the starting aptamer pool ($r_0$) was visualised on the gel for positive identification of the $r_1$+ product. Molecular weight markers are indicated (N=1; section 2.1.9)

**Key:** bp, base pairs; DNA, deoxyribonucleic acid; GST, glutathione-s-transferase; GHO, GST-HIF-1α-ODD; $H_2O$, water; PCR, polymerase chain reaction; $r_0$, starting RNA aptamer pool; $r_1$, 1st round of selected RNA aptamers; RNA, ribonucleic acid; RT-PCR, reverse transcription polymerase chain reaction.

As expected both negative control lanes were devoid of any visible band. However, a band of approximately 78bp was observed in the reverse transcribed and amplified 1st selection lane ($r_1$+). $r_0$ was run next to $r_1$ in order to positively identify the $r_1$ pool. The same proportions of both the r1 and r0 RT-PCR reactions were run on the agarose gel. When compared together the 78bp band representing $r_1$ is of a much lower intensity than $r_0$ suggesting a lower amount of DNA in the $r_1$ sample. Therefore, an additional PCR was incorporated into the selection process using the same reaction criteria as the PCR stage of the one-step RT-PCR (section 2.1.9). Following the additional PCR, The $r_1$ DNA oligonucleotide pool was purified using a MinElute PCR purification kit.

The second round of aptamer selection had some additional control incubations introduced as a proof of principle of the chosen selection criteria. $r_1$ DNA oligonucleotides were T7 RNA polymerase transcribed with or without T7 RNA polymerase (T7+ or T7-, respectively) to form the $r_1$ RNA aptamer pool. The $r_1$ pool was subjected to DNase digestion and purified using a QiaQuick nucleotide removal column. The T7+ and T7- $r_1$ pools were then negatively selected against GST bound to glutathione sepharose beads before half of each pool was positively selected against GHO bound to beads. The remaining halves of the T7+ and T7- $r_1$ pools were incubated with separate aliquots of glutathione sepharose 4B beads. The T7+GHO, T7-GHO, T7+beads and T7-beads incubations were microcentrifuged and the supernatants discarded before undergoing thrombin protease cleavage. The second round of selected RNA aptamers ($r_2$) from the four incubation reactions underwent one-step RT-PCR either with or without RT (+RT and -RT, respectively).

Samples from the one-step RT-PCR were analysed by agarose gel electrophoresis and visualised under UV light before the subsequent PCR and purification steps (figure 3.14).

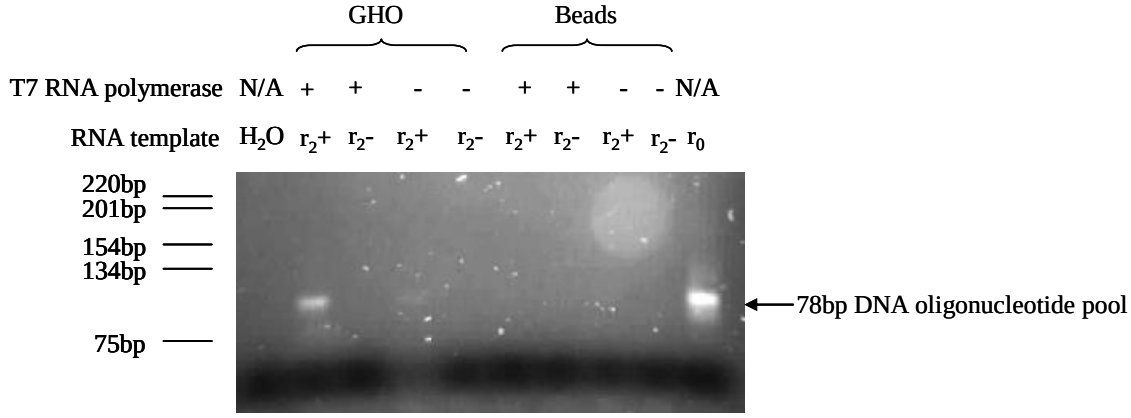


**Figure 3.14 RT-PCR of RNA aptamers from the second round of selection.**

DNA oligonucleotides from the first round of selection were subjected to a transcription reaction either with or without T7 RNA polymerase, as indicated, to create the $r_1$ RNA aptamer pool (sections 2.2.13 - 2.2.15). Each transcription reaction was negatively selected against GST bound to beads. Half of each transcription reaction was incubated with GHO bound to beads while the other half was incubated with beads only, as indicated (section 2.2.16). RNA aptamers were released from each incubation condition through thrombin protease cleavage (section 2.2.12). The second round selected RNA aptamers ($r_2$) were then subjected to one-step RT-PCR either with or without *C. therm* polymerase ($r_2$+ or $r_2$-, as indicated). A negative ($H_2O$) control reaction was undertaken (section 2.2.17). RT-PCR products were analysed by agarose gel electrophoresis and visualised under ultra violet light. A reverse transcribed sample of the starting aptamer pool ($r_0$) was visualised on the gel for positive identification of the $r_2$+ product (section 2.1.9). Molecular weight markers are indicated. (N=1)

**Key:** bp, base pairs; DNA, deoxyribonucleic acid; GST, glutathione-s-transferase; GHO, GST-HIF-1α-ODD; $H_2O$, water; PCR, polymerase chain reaction; $r_0$, starting RNA aptamer pool; $r_1$, 1st round of selected RNA aptamers; $r_2$, 2nd round of selected RNA aptamers; RNA, ribonucleic acid; RT-PCR, reverse transcription polymerase chain reaction.

No contamination was present in any of the reagents used for the RT-PCR reaction as can be seen in the $H_2O$ lane. It was anticipated that only the GHOT7+$r_2$+ lane would have had a visible product. However, upon visualisation of the gel both the GHOT7+$r_2$+ and GHOT7-$r_2$+ lanes had a visible product. However, when compared together the intensity of the GHOT7-$r_2$+ product was very minor when compared to the GHOT7+$r_2$+ lane. In the case of the GHOT7+$r_2$+ lane, the product was RT dependent as can be seen by comparing lanes GHOT7+$r_2$+ and GHOT7+$r_2$- together. Positive identification of this product was made by comparing it to the original $r_0$

pool. The GHOT7-$r_2$+ lane should not have contained any template because the $r_1$ DNA oligonucleotide pool was not transcribed in this lane and all reactions were subjected to DNase digestion. The intensity of this product is very low when compared to GHOT7+$r_2$+ and is therefore probably due to an incomplete DNase digestion of the $r_1$ DNA oligonucleotide pool. A positive result in the GHOT7-$r_2$+ lane suggested the possibility that a mixed RNA and DNA aptamer pool was occuring. However, all other lanes were devoid of any RT-PCR product suggesting that DNase digestion had been successful in those lanes. This indicated a low probability of a mixed RNA and DNA aptamer pool occurring.

The lack of an RT-PCR product in the beadT7+$r_2$+ lane indicated there were no bead associated aptamers. This suggested the negative selection criteria being used in the RNA aptamer enrichment process was removing aptamers that had a preference for glutathione Sepharose 4B beads before positive aptamer selection against GHO. However, some aptamers that bound only to GST may be incorporated into the positive selection process because there is some wash off of GST from beads (figure 3.6A, B and C).

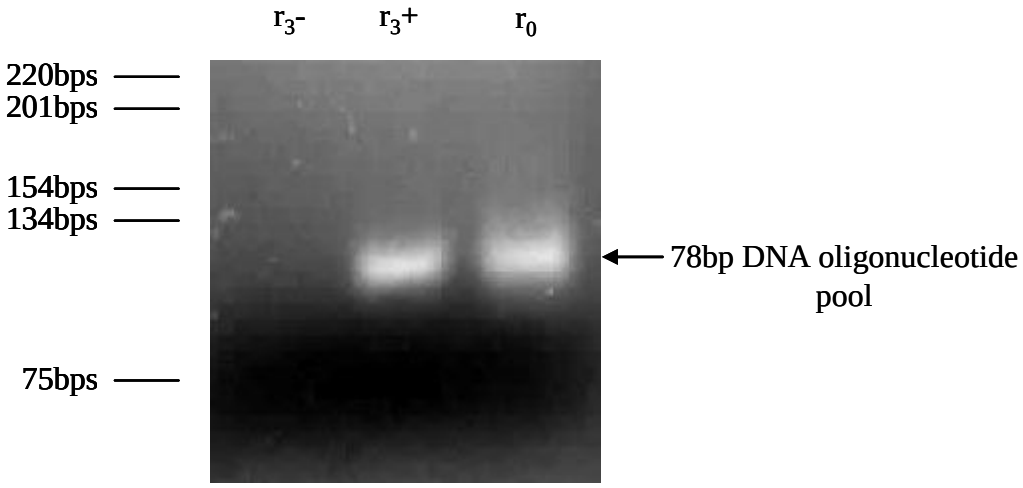


**Figure 3.15 RT-PCR of RNA aptamers from the third round selection.**

RNA aptamers from the second round of selection were negatively selected against GST bound to beads. Unbound RNA aptamers were then positively selected against GHO bound to beads (section 2.2.16). Bound aptamers and GHO were released from glutathione sepharose 4B beads via thrombin protease cleavage giving the third round of selected RNA aptamers ($r_3$) (section 2.2.12).The $r_3$ pool was then subjected to one-step RT-PCR either with or without *C. therm* polymerase ($r_3$+ or $r_3$-, as indicated; section 2.2.17). RT-PCR products were analysed by agarose gel electrophoresis and visualised under ultra violet light. A reverse transcribed sample of the starting aptamer pool ($r_0$) was visualised on the gel for positive identification of the $r_3$+ product (section 2.1.9). Molecular weight markers are indicated. (N=1)

**Key:** bp, base pairs; DNA, deoxyribonucleic acid; GST, glutathione-s-transferase; GHO, GST-HIF-1α-ODD; $H_2O$, water; PCR, polymerase chain reaction; $r_0$, starting RNA aptamer pool; $r_3$, 3rd round of selected RNA aptamers; RNA, ribonucleic acid; RT-PCR, reverse transcription polymerase chain reaction.

Once this proof of principle experiment had proven the RNA aptamer selection process was adequate, rounds 3 and 4 of the selection process were undertaken as described for round 1 of the selection process. Samples from the one-step RT-PCR were taken after each round of selection, analysed by agarose gel electrophoresis and visualised under UV light (figures 3.15 and 3.16, respectively).

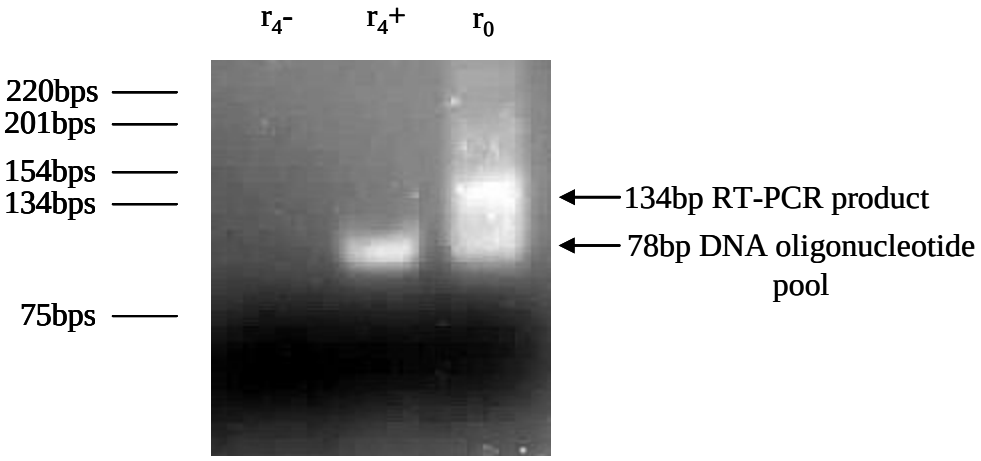


**Figure 3.16 RT-PCR of RNA aptamers from the fourth round selection.**

RNA aptamers from the third round of selection were negatively selected against GST bound to beads. Unbound RNA aptamers were then positively selected against GHO bound to beads (section 2.2.16). Bound aptamers and GHO were released from glutathione sepharose 4B beads via thrombin protease cleavage giving the third round of selected RNA aptamers ($r_4$; section 2.2.12).The $r_4$ pool was then subjected to one-step RT-PCR either with or without *C. therm* polymerase ($r_4$+ or $r_4$-, as indicated; section 2.2.17). RT-PCR products were analysed by agarose gel electrophoresis and visualised under ultra violet light. A reverse transcribed sample of the starting aptamer pool ($r_0$) was visualised on the gel for positive identification of the $r_4$+ product (section 2.1.9). Molecular weight markers are indicated (N=1).

**Key:** bp, base pairs; DNA, deoxyribonucleic acid; GST, glutathione-s-transferase; GHO, GST-HIF-1α-ODD; $H_2O$, water; PCR, polymerase chain reaction; $r_0$, starting RNA aptamer pool; $r_4$, 4th round of selected RNA aptamers; RNA, ribonucleic acid;

Both round 3 and round 4 of aptamer selection produced reverse transcriptase dependent products. These products were approximately 78bp in size and were positively identified as such by comparison with the original $r_0$ pool.

### *3.4.5 The effect of RNA aptamer enrichment on the transcriptional activity of an HRE driven transcription reporter gene.*

The most effective RNA aptamers are produced on average between 4 and 10 rounds of aptamer pool selection (Marshall and Ellington, 2000). Therefore after the fourth round of aptamer selection a transcription reporter assay was performed to determine the effectiveness of the RNA aptamers produced so far. If no difference in the results between $r_0$ and $r_4$ aptamers was observed the selection process could be repeated to further enrich the RNA aptamers.

Hep G2 cells were used in the transcription reporter assay because they were readily available and had a known hypoxia response and the ability to respond to desferrioxamine (DFO) a hypoxia mimetic (data not shown). The transcription reporter assay was based on a method that involved co-transfecting cells with reporter plasmids and small interfering RNAs using lipofectamine (Elbashir *et al*., 2001).

Hep G2 cells seeded at low density (100 000 cells/well) were transfected in triplicate 24 hours after seeding with either the $r_0$ aptamer pool or the $r_4$ aptamer pool. Cells were co-transfected with an SV40 control plasmid, a CMV control plasmid or a test plasmid (pGL3 control, pCMVluc or pGL3prevPGK, respectively). All wells were also co-transfected with a plasmid expressing *Renilla* luciferase (pRL-SV40), as an internal control to normalise transfection efficiencies. The test plasmid (pGL3prevPGK/ OB HRE) and CMV control plasmid (pCMVluc ) were constructed as described by Boast *et al.*, (1999). The test plasmid contains an hypoxia responsive HRE trimer from the gene encoding murine phosphoglycerate kinase (PGK) located upstream of a minimal SV40 promoter. This promoter directs transcription from a cDNA sequence encoding firefly luciferase. The SV40 control plasmid (pGL3-control) contains an SV40 promoter and enhancer that results in the strong expression of firefly luciferase (*Photinus pyralis*). CMV control contains an SV40 promoter and enhancer and a CMV immediate early (CMV IE) promoter resulting in the strong expression of firefly luciferase. SV40 control contains an SV40 early enhancer and promoter which provides strong constitutive expression of renilla luciferase (*Renilla reniformis* or sea pansy, section 2.1.12).

48 hours after transfection cells were lysed. Cell lysates were analysed for firefly luciferase activity and corrected against *Renilla* luciferase activity (sections 2.1.12, 2.1.13 and 2.2.18). Figure 3.17 shows the results of two independent experiments. The smaller inset panels of the upper and lower panels show the test plasmid results on a larger scale. Two control plasmids with different promotor sequences were used in this assay because previous experimentation performed by Oxford Biomedica had revealed the SV40 control plasmid was not always significantly expressed in all cell types (Binley K, personal communication), therefore the CMV control plasmid was utilised in these experiments.

The test plasmid results from two independent experiments indicated cells with $r_4$ aptamers had a reduced level of luciferase expression compared with those transfected with $r_0$ aptamers (fig. 3.17, inset panels). However, although these results when taken on their own appear significant, this significance is lost when compared with the control plasmid results.

The CMV and SV40 control plasmid results vary when the two independent experiments are compared to each other. For example results in the upper panel of figure 3.17 indicate the $r_4$ aptamer pool increases the level of luciferase expression from cells transfected with the CMV or SV40 control plasmids when compared to the $r_0$ aptamer pool. However, in the lower panel although the results from cells transfected with the CMV control plasmid are the same as the upper panel, the result is not nearly as pronounced. Another difference between the two experiments is that in the lower panel the $r_4$ aptamer pool reduces the level of luciferase expression in cells transfected with the SV40 control plasmid when compared to the $r_0$ pool. This is the reverse of the results obtained in the first experiment (fig 3.17 upper panel).

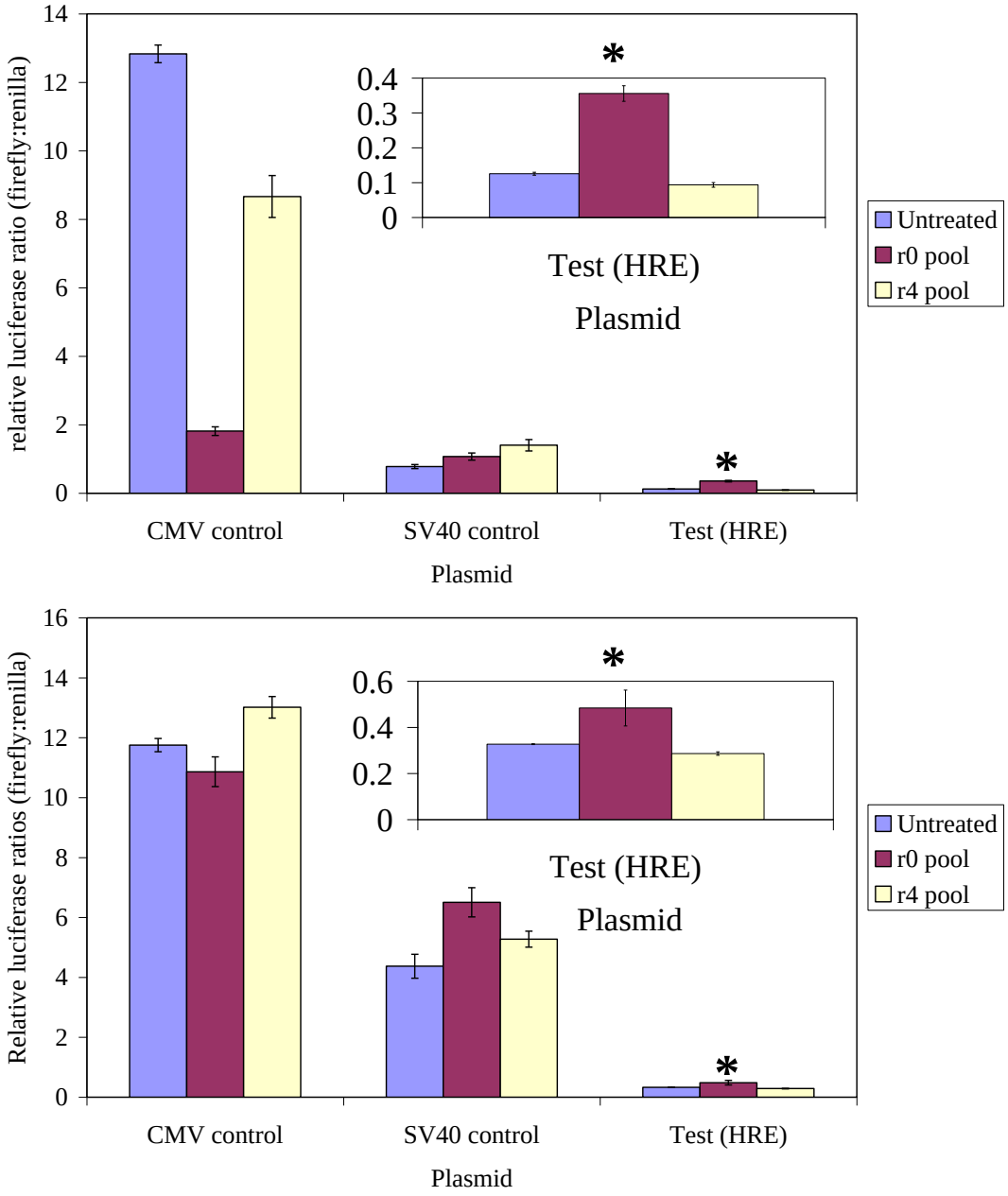


**Figure 3.17 The effect of starting and enriched RNA aptamer pools on HIF responsive HRE dependent transcriptional reporter assays.**

Hep G2 cells seeded at low density (100 000 cells/well) were either left untreated or transfected in triplicate 24 hours after seeding with $r_0$ pool or $r_4$ pool. All cells were co-transfected with either CMV control, SV40 control or test (HRE) plasmid. All wells were co-transfected with pRL-SV40. 72 hours after seeding whole cell lysates were prepared. Lysates were assayed for firefly luciferase activity and corrected against *Renilla* luciferase activity to normalize transfection efficiencies. Inset panels (*) represent Test (HRE) plasmid results on a larger scale. N=2 - Results shown are from two independent experiments. Error bars are ± S.D.

**Key:** CMV, cytomegalovirus: HIF, hypoxia inducible factor; HRE, hypoxia responsive element; $r_0$, starting RNA aptamer pool; $r_4$, 4$^{th}$ round of selected RNA aptamers

In all instances the level of luciferase expression in cells transfected with an RNA aptamer pool and a control plasmid are greater then those achieved in the test plasmid.

The variability of the interdependent results make any conclusions difficult to discern. More repetitions of each stage of the selection process, the luciferase reporter assay and further optimisation of the luciferase reporter assay or investigation into other assays that can determine the effectiveness of the selected RNA aptamers would be necessary in order to further this work. However, as no phenotypic response was observed from a challenging transcription reporter assay, careful consideration was given to the time and resources that would be required to undertake further experimentation to try and determine the cause of the variability and also the cloning of the RNA aptamer pool. As a consequence of these considerations it was decided that further experimentation including the cloning of the RNA aptamer pool was not the best use of the time and resource remaining.

## 3.5 Discussion

The hypothesis outlined in section 3.1.2 stated that RNA aptamers would be designed with affinity to the HIF-1α ODDD thus preventing the action of the PHDs and preventing pVHL mediated ubiquitin dependent degradation of HIF-1α. This would result in an HIF dependent increase in transcription. Aptamers that achieved this result could be therapeutically useful in ischaemia and pulmonary hypertension (sections 1.6.2 and 1.6.3).

### *3.5.1 The function of an enriched RNA aptamer pool was undeterminable.*

The enrichment of the RNA aptamer pool appeared to be successful with optimisation of the selection process occurring as any problems arose, for example the appearance of the 134bp non-specific RT-PCR product (section 3.3.3). However, verifying whether the selected aptamers were functional and conformed to the

proposed hypothesis (section 3.1.2) was very difficult due to the variable results obtained in the transcription reporter assay (section 3.3.5, figure 3.17). One possible explanation of the variable results seen in the transcription reporter assay is the culture conditions of the Hep G2 cells. Although all controllable culture conditions (with the exception of cell passage number, see below) were the same for both reporter assay experiments, it is possible an unknown variable in the culture conditions affected the results.

Another explanation for the experimental variation observed in the transcription reporter assay, is the passage number of the cells. The Hep G2 cells used for both of these experiments were of unknown passage number and each experiment was performed on Hep G2 cells of different passage numbers. Although no evidence has been published that shows variation in experimental results with regard to the use of Hep G2 cells, data is accumulating in other cell types that shows the same experiments performed in higher passage number cells give different results from those carried out in lower passage cells. Many of these experiments have focussed on the Caco-2 colon cancer cell line and cell line specific characteristics. However experiments have also been performed in MCF7 human breast cancer cells and LNCaP prostatic adenocarcinoma cells (reviewed by Hughes *et al.*, 2007).

High passage number cells can exhibit differences in cell morphology, growth rate, protein expression and cell signalling when compared to low passage number cells of the same type (reviewed by Hughes *et al.*, 2007; ATCC technical bulletin no.7). Two ways of determining whether Hep G2 passage number was responsible for the experimental variation observed in figure 3.17 are to monitor cell morphology and undertake a growth curve analysis (ATCC technical bulletin no.7). Hep G2 cell morphology was regularly observed and compared with examples shown on the ATCC website (data not shown). However, regular growth curve analysis was not undertaken. Further experimentation to determine whether passage number was a factor in the transcription reporter assay results could involve performing a growth curve analysis on existing Hep G2 cells or purchasing new Hep G2 cells and repeating the transcription reporter assays.

Although the experimental results of the transcription reporter assay may have been affected by the passage number of Hep G2 cells, there is also the possibility that no conclusive results were gained due to enzymatic attack of the RNA aptamer pool once it had been transfected e.g. by nucleases and it is known that un-modified RNA oligonucleotides are extremely unstable in biological fluids and have a half life of less than one minute (de Smidt *et al.,* 1991). However, by chemically modifying components of RNA aptamers this can increase their biological stability. For instance, incorporating 2'-O-methyl nucleotides into RNA aptamers resulted in their nuclease resistance (Green *et al.,* 1995). This kind of modification can now be easily incorporated due to the discovery of T7 RNA polymerase variants capable of utilising modified nucleotides as substrates (Chelliserrykattil and Ellington, 2004). Incorporation of this form of modification in future RNA aptamer selection rounds could achieve a more beneficial outcome from the transcription reporter assay if coupled with the use of new Hep G2 cells. In contrast to this hypothesis is RNA interference (RNAi) which is a highly successful technology, utilising unmodified small interfering RNAs, which is used for target validation and gene function analysis including determining the differential roles of HIF-1α and HIF-2α in colon cancer (Imamura *et al.,* 2009). The success of an un-modified RNA technology suggests that the methods used in order to carry out the RNA aptamer transcription reporter assay may also play a part in affecting the experimental results.

It is possible that the use of the transcription reporter assay could be negated completely by optimising the pVHL binding assay (section 3.5.2) or following the methods of other researchers in the aptamer field. Typically, other investigators clone the aptamer pool and then sequence the resulting aptamer clones. Representative aptamers are then used in binding assays to determine binding affinity to the target molecule, characterise their binding features and determine any specialised features the aptamer may have. Truncation and mutation experiments can then be performed in order to determine the smallest functional region of the aptamer before any post-translational modifications, such as the incorporation of modified nucleotides to increase aptamer stability, are performed. These modifications are often carried out before the use of the individual aptamers in assays which determine the usefulness of the selected aptamer as a future therapeutic agent, in the case of

medical/pharmaceutical research (reviewed by Stoltenburg *et al.*, 2007; Marshall and Ellington, 2000; Gold *et al.*, 1995).

### *3.5.2 Further experimentation.*

Although enrichment of the RNA aptamer pool appeared to be successful, some additional experimentation could have been carried out to confirm certain steps in the selection process were performing the functions they had been designed for. However, it is unlikely that these experiments would affect the overall interpretation of results (section 3.5.1). For instance, an experiment that was overlooked during the RNA aptamer selection process was testing whether the negative selection of RNA aptamers against GST bound to beads was successful. This process was employed in order to remove RNA sequences that preferentially bound to GST, GST:beads or beads from the RNA aptamer pool. Testing of the negative selection step would simply have involved thrombin protease cleavage of GST from beads after a negative selection of the RNA aptamer pool, followed by one-step RT-PCR; the same process was also employed for aptamer recovery from GHO (section 3.4.4). Although the negative selection process was never properly assessed, experiments were conducted that showed RNA aptamers were not binding to beads alone (figure 3.14). However, use of a negative selection method has been corroborated in the experiments of other researchers who have also removed unwanted RNA aptamers by employing negative selection steps using GST bound to a matrix before selecting against a GST tagged target protein (Jeong *et al.*, 2010; Kimoto *et al.*, 1998).

As an alternative to the transcription reporter assay in the first instance, further optimisation of the pVHL binding assay, could be used to assess the functionality of the RNA aptamer pool (section 3.3.5). RNA aptamers that prevented pVHL binding and hence inhibit HIF-1 ubiquitin mediated degradation could be achieved by incubating GHO bound to beads with reticulocyte lysate. Reticulocyte lysate contains PHDs which hydroxylate $Pro^{564}$ of HIF-1α ODDD. Hydroxylated GHO could then be purified and either incubated with or without RNA aptamers that had already undergone a negative selection process with non-hydroxylated GHO bound to beads. This negative selection step would remove RNA aptamers with a higher affinity for

non-hydroxylated GHO. By incubating the hydroxylated GHO:RNA aptamer complexes in Hela cell lysate containing tagged and overexpressed pVHL, it would then be possible to determine whether RNA aptamers could inhibit pVHL binding. If the assay were successful, the predicted outcome would be pVHL bound to hydroxylated GHO in samples that were not treated with RNA aptamers and little to no pVHL presence in samples treated with RNA aptamers. In order to optimise this binding assay it would be necessary to introduce a tag to pVHL, possibly by His or Biotin labelling. This would result in a completely identifiable protein and remove the protein identification problems associated with the previous pVHL binding assay (figure 3.7). Chemical modification of the 2'OH group of ribose in RNA aptamers during the selection process would confer nuclease resistance and could help to achieve a successful outcome from this assay (section 3.5.1). Alternatively, RNA aptamers could be developed that inhibited the hydroxylating action of the PHDs. This could be achieved developing a similar type of binding assay. GHO bound to beads would be incubated either with or without RNA aptamers. The GHO: RNA aptamer/ GHO complexes would then be incubated with reticulocyte lysate, followed by Hela cell lysate containing tagged and overexpressed pVHL, it would then be possible to determine whether RNA aptamers could inhibit pVHL binding. If the assay were successful, the predicted outcome would be pVHL bound to GHO in samples that were not treated with RNA aptamers and little to no pVHL presence in samples treated with RNA aptamers.

If functionality of the RNA aptamer pool using a pVHL binding assay could be achieved, cloning and sequencing of the aptamers would be the next logical step. Sequences can then be assessed for consensus sequence binding and predictive secondary structure assessment using a computer modelling program such as the MULFOLD program (Zuker, 2003).

### *3.5.3 The future of RNA aptamer technology*

Experiments carried out since SELEX was first developed in the early 1990s have resulted in several methodological improvements to RNA aptamer synthesis. Most aptamers are purified via nitrocellulose filtration however, other methods have also

included gel affinity chromatography and immunoprecipitation (author). Other methods of SELEX have also been developed such as cell-SELEX. However, the majority of recent aptamers have been developed using automated or microarray based SELEX. Automated of microarray SELEX allow for the selection and characterisation of RNA aptamers to multiple targets within a few days rather than the weeks or months that were previously required (Zhou *et al.,* 2010).

Further improvements to the stability of RNA aptamers have also been essential due to the fact that unmodified therapeutic RNA aptamers, when delivered via the most common means i.e. intravenous, subcutaneous or intravitreous delivery, are metabolically unstable, subject to rapid renal filtration due to their small size and rapid biodistribution from plasma compartments into tissues. Several modifications have been developed which increase the structural stability of the RNA aptamer and also the half-life of the molecule against renal clearance. The most common of these modifications are to the ribose of the RNA and include 2' Fluoro, 2' O- Methyl, linked nucleic acids and spiegelmers (aptamers targeted to the mirror image of the target peptide). Aptamers can be conjugated to cholesterol or polyethylene glycol which reduces the level of renal filtration of the aptamer (Burnett and Rossi, 2012).

Several RNA aptamers have now reached clinical trials including Pegatanib, an RNA aptamer targeted towards VEGF, the REG1 anticoagulation system, consisting of an aptamer – antidote pair to factor IXa and AS1411 and RNA apatamer targeted to nucleolin, a protein often overexpressed on the surface of cancer cells (Table 3.1).

**Table 3.1 Aptamer Therapeutics in Clinical Trials**

| **Aptamer Therapeutic** | **Target** | **Disease** | **Current Status** |
|---|---|---|---|
| Pegaptanib (Macugen) | VEGF | Age related macular degeneration | Approved |
| ARC1905 | Complement component 5 | Neovascular age related macular degeneration | Phase I |
| E10030 | PDGF | Neovascular age related macular degeneration | Awaiting phase III |
| REG 1 (RB006 and RB007 apatamers) | Factor IXa | Coronary artery disease | Awaiting phase III trials |
| NU172 | α - thrombin | Coronary artery disease | Phase II |

| Aptamer Therapeutic | Target | Disease | Current Status |
|---|---|---|---|
| ARC19499 | Tissue factor pathway inhibitor | Hemophilia | Uncertain status (Phase I/II) |
| AS1411 | nucleolin | Renal cell carcinoma / non-small cell lung cancer | Awaiting phase III trials |
| NOX-A12 | Stroma cell-derived factor-1 | Tumour | Phase II recruitment |
| ARC1779 | Activated von Willebrand Factor | Von Willebrands Disease | Awaiting phase III |
| NOX-E36 | Monocyte chemoattractant protein 1 | Type II diabetes. Renal impairment/ neuropathy. Lupus nephritis | Phase IIa |

Sundaram *et al.*, 2013 and Burnett and Ross, 2012.

**Key:** PDGF, platelet derived growth factor; VEGF, vascular endothelial growth factor;

Pegaptanib sodium also known commercially as Macugen, is an anti-VEGF RNA aptamer which is used for the treatment of all types of neovasular age related macular degeneration. It is the first aptamer to be approved for clinical use (Ng *et al.*, 2006). Other RNA aptamers have also reached the clinical trial phase. Of particular importance for cancer therapy is AS1411, the first RNA aptamer to enter oncology clinical trials. AS1411 is an RNA aptamer that specifically targets nucleolin, a protein that is found on the surface of many cancer cells, including cancer cells associated with acute myeloid leukaemia and renal cell carcinoma. AS1411 is systemically administered and its internalisation results in a decrease in several cancer related mRNAs which results in reduced cell proliferation (Soundararajan *et al*, 2009 and Reyes-Reyes *et al.*, 2010).

The REG 1 anticoagulation system is also in clinical trials and represents an aptamer-antidote pair to coagulation factor IXa (FIXa). RB006 is the active aptamer drug that binds FIXa and RB007 is the antidote which is an oligonucleotide controlling agent that is complementary to a portion of RB006 and when bound neutralises the anti-FIXa activity of RB006. This drug is particularly useful in the treatment of thrombotic disease and represents a highly specific and controllable drug (Povsic *et al.*, 2010).

Further developments in the RNA aptamer field have resulted in a fusion of technologies such as RNA aptamer delivery by siRNAs and RNA aptamer delivery by nanobiotechnology particles (reviewed by Guo *et al.*, 2008). However, given that only one RNA aptamer has been approved for use in a clinical setting it seems this promising technology has still to fulfil its full potential.

# Chapter 4: The impact of succinate dehydrogenase (SDH) inhibition on HIF

## 4.1 Introduction

It has recently been discovered that germ-line and somatic mutations in 3 of the 4 genes (*SDHB*, *SDHC* and *SDHD*) that encode mitochondrial complex II/succinate ubiquinone oxidoreductase (SQR) predispose affected individuals to head and neck paragangliomas (HNPs) and/or pheochromocytomas, tumours of the autonomic nervous system. The most common sites for these tumours are in the carotid body (CB) and adrenal medulla, respectively. HNPs and pheochromocytomas harbouring *SDH* mutations show a high degree of vascularity that is similar to the vasculature observed in sporadic carotid body (CB) tumours caused by chronic hypoxic exposure (reviewed by Maher and Eng, 2002) and pheochromocytomas harbouring *VHL* mutations (section 1.6.5), suggesting a link with the oxygen sensing pathway (Baysal *et al.*, 2000).

### *4.1.1 SQR structure and function.*

SQR straddles the inner mitochondrial membrane in a manner that allows complex participation in the citric acid/Kreb's/tricarboxylic acid cycle (TCA) and the electron transport chain (ETC). The two largest subunits, SDH A (Fp, 70kDa) and SDH B (Ip, 30kDa), form succinate dehydrogenase (SDH), the enzymatic portion of the complex. SDH A has a covalently bound FAD molecule while SDH B contains three distinct iron-sulphur centres. SDH C (15kDa) and D (12.5kDa), anchor SQR to the inner mitochondrial membrane, they share a heme b prosthetic group and the ubiquinone (UQ) binding site (figure 4.1).

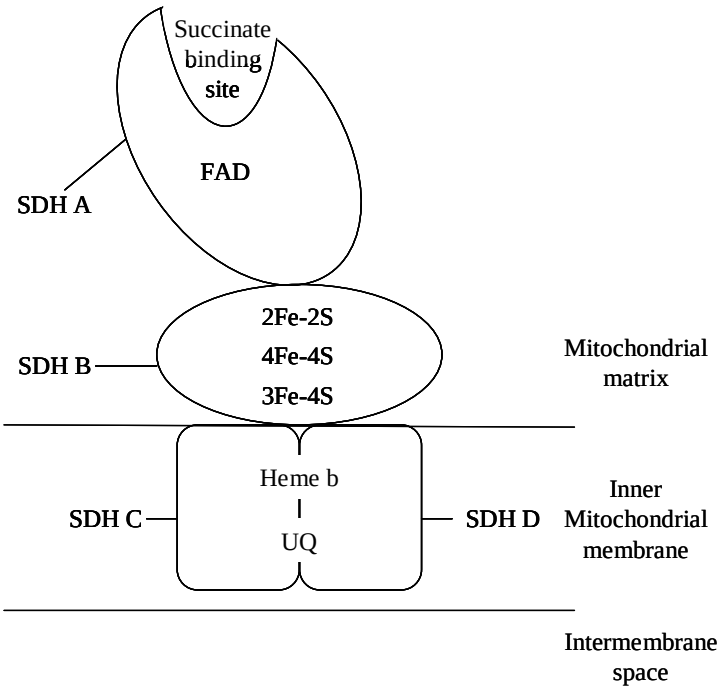


**Figure 4.1 Succinate ubiquinone:oxidoreductase (SQR).**

SQR straddles the inner mitochondrial membrane and is comprised of four subunits SDH A-D. SDH A and B form the catalytic portion of the complex, succinate dehydrogenase (SDH). SDH A contains a covalently bound FAD moiety and SDH B contains three iron-sulphur centres. SDH C and D are the anchoring subunits and share a heme b group and the ubiquinone (UQ) binding site.

**Key:** FAD, flavine adenine dinucleotide; FE-S, Iron-sulphur centres; SDH A-D, succinate dehydrogenase subunits A-D; SQR, succinate ubiquinone:oxidoreductase; UQ, ubiquinone

Based on a figure by Ackrell, 2000.

The TCA cycle oxidises an acetyl CoA group derived from glycolysis to $CO_2$ via a series of reactions that occur in the mitochondrial matrix (figure 4.2). The seventh reaction in this series is the oxidation of succinate to fumarate which is catalysed by succinate dehydrogenase (SDH). The oxidation of succinate occurs after succinate has bound to the active site of SDH A, which is located between the covalently bound FAD molecule and the capping domain (Leger *et al.*, 2001). After succinate has bound the capping domain is thought to move towards the binding site (reviewed by Ackrell, 2000).

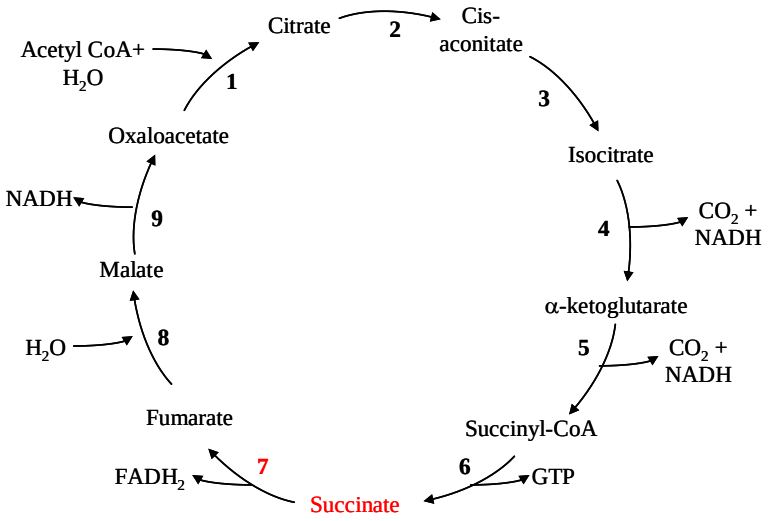


**Figure 4.2 An overview of the tricarboxylic acid (TCA) cycle.**

The reactions of the tricarboxylic acid cycle are shown above. The reactions are catalysed by a series of enzymes, shown below as numbered in the diagram; -

1.Citrate Synthase
2.Aconitase
3.Aconitase
4.Isocitrate dehydrogenase
5.a-ketoglutarate dehydrogenase
6.Succinyl CoA synthetase
7.Succinate dehydrogenase
8.Fumarase
9. Malate Dehydrogenase

**Key:** $CO_2$, Carbon Dioxide; FADH, flavin adenine dinucleotide; GTP, Guanine triphosphate; $H_2O$, water; NADH, nicotinamide adenine dinucleotide

Based on a figure by Raimundo *et al.*, 2012.

A hydrogen ion is then transferred from one methyl group of succinate to the N5 position of FAD. Another hydrogen ion is then transferred from the second methyl group of succinate to a conserved arginine residue of the capping domain. Fumarate is thought to be released by movement of the capping domain away from the dicarboxylate binding site (Lancaster, 2003). The method by which FADH is reduced to $FADH_2$ remains unclear.

The proposed mechanism of succinate oxidation is thought to be the reverse of fumarate reduction because SQRs and fumarate reductases (QFRs, quinol: fumarate oxidoreductases) are closely related. Evidence that supported the proposed mechanism was found in *E. coli* where SQRs and QFRs were found to be functionally able to replace each other (Lancaster, 2003). Comparison of the crystal structures for *E. coli* and *W. succinogenes* QFRs with the crystal structure of *E. coli* SQR showed a close similarity between the SDH A and SDH B subunits of *E. coli* SQR and the flavoprotein and iron sulphur proteins of *E. coli* and *W. succinogenes* QFRs (Yankovskaya *et al.,* 2003). It is also known that the residues implicated in substrate binding and catalysis are conserved throughout the SQR and QFR superfamily suggesting the function of each complex could be reversible if necessary.

The FAD molecule reduced during the oxidation of succinate to fumarate is covalently bound to the SDH A subunit of complex II, also known as succinate:ubiquinone oxidoreductase (SQR). Therefore, electrons from $FADH_2$ must enter the mitochondrial respiratory chain (section 4.1.2) at this point. The pair of electrons are passed from $FADH_2$ through three linearly aligned Fe-S clusters located in the SDH B subunit before being transferred to a bound ubiquinone at one of the two ubiquinone binding sites which are comprised of residues from both SDH C and SDH D, the membrane anchoring subunits of SQR (Yankovskaya *et al.,* 2003). Electrons from the first bound ubiquinone are passed to a second bound ubiquinone which, when reduced to ubiquinol, is released into the membrane soluble ubiquinol pool (figure 4.4). Residues from SDH C and SDH D also form a cytochrome *b* containing a heme b group (reviewed by van den Heuval and Smeitink, 2001). The function of the heme *b* is not clearly understood as it does not appear to participate in any redox reactions associated with succinate oxidation however it is thought to play a structural role within SQR (Kim *et al.,* 2012). The transfer of electrons through SQR is not linked with proton translocation and this is the only complex in the mitochondrial respiratory chain that does not act as a proton pump.

### *4.1.2 An overview of the mitochondrial respiratory chain.*

The mitochondrial respiratory chain is a series of four protein complexes that function in a specific order (figure 4.3). The passage of electrons through these four complexes releases energy that is stored as a proton gradient across the inner mitochondrial membrane. This proton gradient is used to drive the formation of ATP by the fifth complex found in the inner mitochondrial membrane, ATP synthase/ $F_1F_0$ ATPase (van den Heuval and Smeitink, 2001).

Electrons enter the mitochondrial respiratory chain when NADH or $FADH_2$ produced in the TCA cycle are oxidised by Complexes I or II (see section 4.1.3), respectively. Complex I, also referred to as NADH:ubiquinone oxidoreductase / NADH:quinone oxidoreductase, is an L shaped complex consisting of a hydrophilic / promontory domain that protrudes into the mitochondrial matrix and a hydrophobic domain that is embedded in the inner mitochondrial membrane (Yano, 2002). The promontory domain is comprised of two subunits, a flavoprotein (Fp) subunit containing non-covalently bound flavin mononucleotide (FMN) and two of the 8 or 9 Fe-S clusters, and an iron sulphur protein which contains the remaining Fe-S clusters. Once NADH has bound to the Fp subunit, it is reduced by FMN. The two electrons are then passed through the Fe-S clusters to bound ubiquinone whose binding site is located in the hydrophobic subunit of complex I. The transfer of two electrons from the terminal Fe-S cluster in the Ip subunit reduces ubiquinone to ubiquinol. It is at this point that electron transfer is coupled to the translocation of four protons across the inner mitochondrial membrane into the intermembrane space (Yano, 2002 and Hirst *et al.*, 2003).

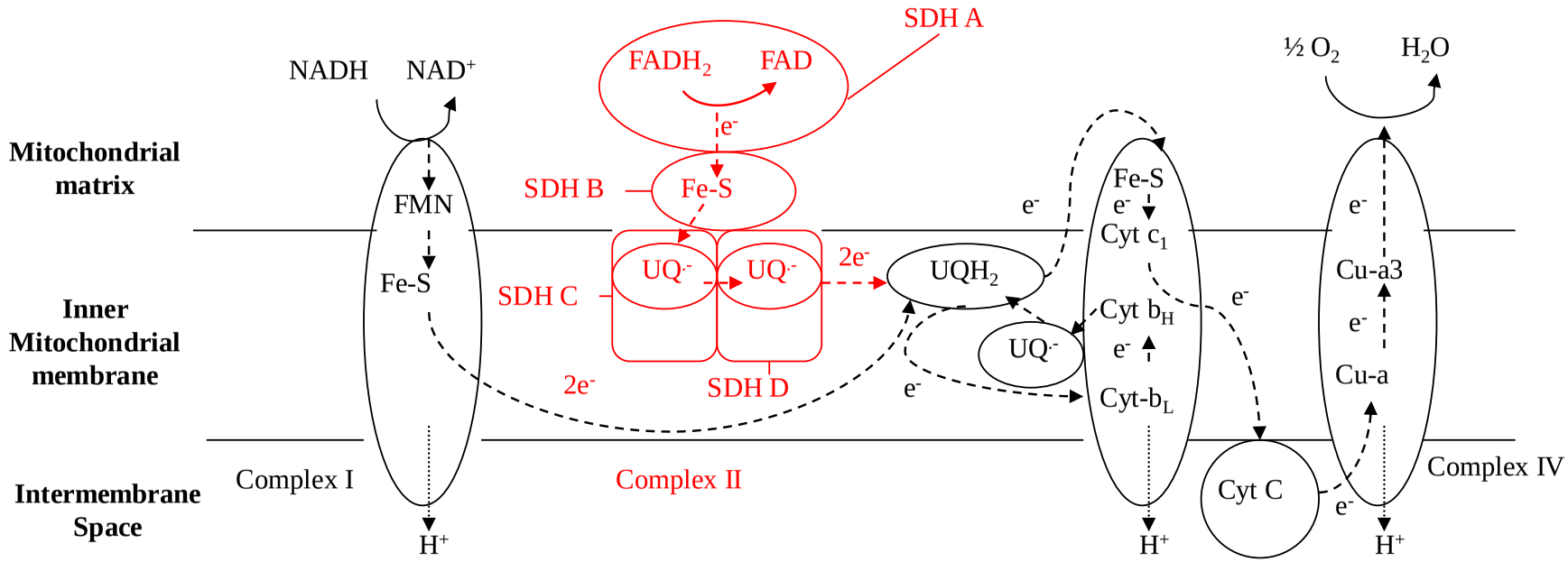


**Figure 4.3 The Electron Transport Chain.**

A diagram of the mitochondrial electron transport chain indicating the pathway of electron ($e^-$) transfer (dashed arrows) and proton ($H^+$) pumping (dotted arrows). Electrons are transferred between complexes I and III and II and III by ubiquinone. Electrons are transferred from complex III to IV by the peripheral membrane protein Cytochrome *C* (Cyt C). Once electrons have passed through complex IV, oxygen is reduced to $H_2O$ in the mitochondrial matrix.

**Key:** SDH A-D – Succinate dehydrogenase sub-units A-D, FMN – flavin mononucleotide, Fe-S – Iron-sulphur centres, Cyt – Cytochrome, UQ – ubiquinone, $UQH_2$ – ubiquinol, $UQ^{\cdot-}$ - semiquinol.

Based on a figure by Cecchini, 2003.

Electron transfer from ubiquinol that has been reduced by complexes I and II is catalysed by the third complex in the mitochondrial respiratory chain, decylubiquinol:cytochrome *c* oxidase/ cytochrome $bc_1$ complex. Cytochrome $bc_1$ is a homodimeric complex where three out of the eleven subunits that comprise each monomer carry prosthetic groups. Cytochrome $c_1$ contains heme $c_1$, cytochrome *b* contains heme $b_H$ and $b_L$ and the Rieske protein contains an iron-sulphur cluster. The $bc_1$ complex links the oxidation of a membrane bound ubiquinol and reduction of a water soluble cytochrome *c* with the translocation of protons across the inner mitochondrial membrane in a process known as the protonmotive Q cycle (van den Heuval and Smeitink, 2001).

The Q cycle (figure 4.4) involves both ubiquinol oxidation and ubiquinone reduction. These reactions occur at two separate centres known as $Q_p$ (which is located near the electropositive side of the inner mitochondrial membrane) and $Q_N$ (located near the electronegative side of the membrane). The oxidation of the first ubiquinol molecule at $Q_p$ releases two electrons. The first electron is recycled through cyt *b* to a ubiquinone molecule located at $Q_N$ producing a semi-quinone anion while the second electron is passed through the iron sulphur cluster in the Rieske protein and cyt $c_1$ to cyt *c*. The oxidation of the second ubiquinol results in the reduction of the semi-quinone at $Q_N$ by the first electron coupled with the uptake of two protons from the mitochondrial matrix. The second electron is channelled through the redox centres of the Rieske and cyt $c_1$ proteins to a cyt *c* molecule. The oxidisation of each ubiquinol results in the pumping of two protons into the inter-membrane space (Hunte *et al.*, 2003).

Electrons are transferred from the cytochrome $bc_1$ complex via cytochrome *c* which acts as an electron shuttle, to the terminal complex in the mitochondrial respiratory chain, cytochrome *c* oxidase (COX). The mammalian COX complex is functional as a dimer, with each monomer being comprised of 13 subunits, the largest of which, subunits I-III, are encoded by the mitochondrial genome with the remaining 10 subunits encoded by the nuclear genome (Richter and Ludwig, 2003). Subunits I and II contain the four redox centres of the COX complex. The $Cu_A$ centre is located in subunit II and the heme *a* centre and the binuclear centre comprised of heme $a_3$ and $Cu_B$ are located in subunit I. Electrons enter the COX complex when cytochrome *c*,

bound to subunit II, transfers electrons to the $Cu_A$ centre then to heme *a* and finally to the binuclear heme $a_3$:$Cu_B$ centre where dioxygen is reduced to water by the incoming four electrons together with four protons from the matrix. The reduction of dioxygen to two water molecules releases enough energy for the translocation of four protons across the inner mitochondrial membrane (Pecina *et al.*, 2004; Richter and Ludwig, 2003).

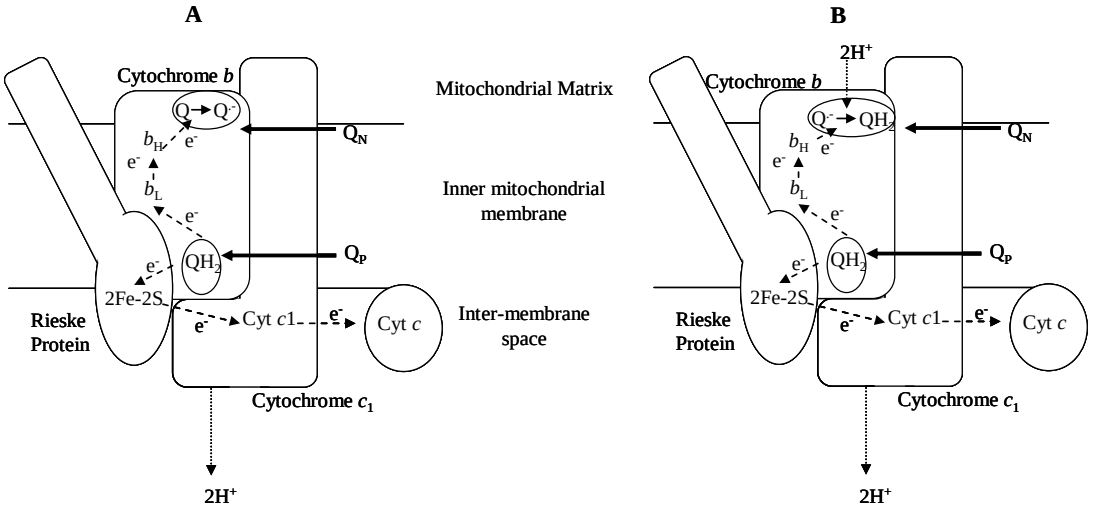


**Figure 4.4 The Q Cycle**

A diagrammatic representation of the pathway of electron transfer through complex III is indicated above. The three sub-units containing redox centres are indicated, other sub-units have not been shown. Electron transfer is indicated by dashed arrows and direction of proton ($H^+$) movement by dotted arrows.
**A**) Ubiquinol ($QH_2$) is oxidised at centre P (Qp) in a reaction that transfers one electron ($e^-$) to the iron-sulphur cluster (2Fe-2S) located in the Rieske protein and the second electron to heme $b_L$ in the cytochrome *b* sub-unit resulting in the release of ubiquinone (Q). The electron from the Rieske protein is transferred to cytochrome $c_1$ in the cytochrome $c_1$ sub-unit and then to cytochrome *c*. The oxidisation of the Rieske protein is accompanied by the translocation of an $H^+$ across the inner mitochondrial membrane. The second electron is transferred to heme $b_H$ located in the cytochrome *b* sub-unit and then to a bound ubiquinone at centre N ($Q_N$) which is reduced to semiquinone ($Q^{-}$). **B**) A second $QH_2$ is oxidised at $Q_P$ electrons are transferred in the same manner as for A. Transfer of the electron from heme $b_H$ results in the reduction of $Q^{-}$ to $QH_2$ accompanied by the uptake of $2H^+$ at $Q_N$. Based on a figure by Hunte *et al.*, 2003.

**Key:** $e^-$, electron; FE-S, Iron – sulphur cluster; H, hydrogen; Q, ubiquinone; $QH_2$, ubiquinol

The final step in oxidative phosphorylation is the synthesis of ATP from ADP and Pi, a process catalysed by complex V, more commonly known as ATP synthase or the $F_1F_0$ ATPase. The simplest $F_1F_0$ ATPases are found in prokaryotes e.g.. *E. coli*. They are bipartite proteins that are comprised of 8 subunits which form an $F_0$ portion and an $F_1$ portion linked by two stalks (figure 4.5).

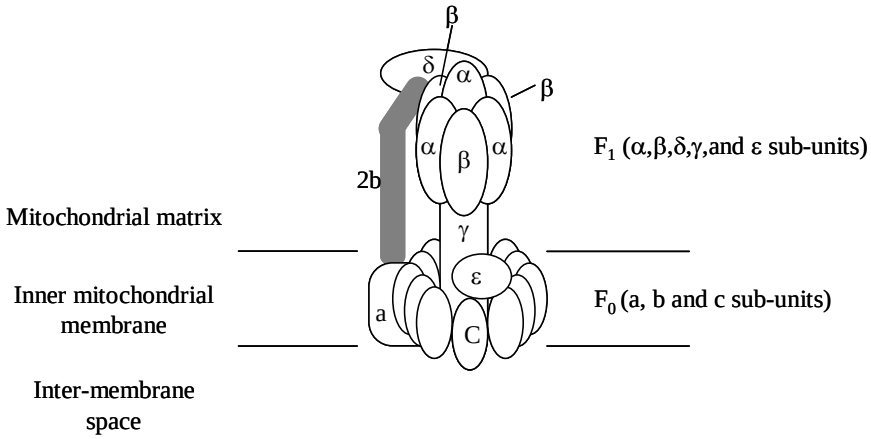


**Figure 4.5 The *E. coli* $F_1F_0$ ATPase.**

A diagrammatic representation of the 8 sub-units that comprise the *E. coli* $F_1F_0$ ATPase. The $F_0$ portion of the complex is embedded in the inner mitochondrial membrane and is responsible for proton translocation. The $F_1$ portion of the complex acts as the ATPase . The $F_1$ and $F_0$ portions of the complex are linked via two stalks comprised of the δ and β subunits and the γ and ε subunits, respectively. Based on figures by Weber and Senior, 2003 and Capaldi and Aggeler, 2002.

The $F_0$ portion of the complex is responsible for proton translocation. It is embedded in the inner mitochondrial membrane and consists of 1 a, 2 b and 10-12 c subunits. The $F_1$ portion of the complex acts as the ATPase. It resides in the mitochondrial matrix and is comprised of 3 α, 3 β, δ γ and ε subunits (Capaldi and Aggeler, 2002). The two stalks that link the $F_1$ and $F_0$ portions of the complex are comprised of the δ and β subunits and the γ and ε subunits, respectively (figure 4.5). The mammalian $F_1F_0$ ATPase is comprised of between 16-18 subunits the additional subunits do not, as yet, have an assigned role or location within the mitochondrial complex.

ATP is synthesised when the $F_0$ portion of the ATPase translocates protons that were pumped into the inter-membrane space by complexes I, III and IV. The movement of these protons drives rotation of the rotor, which is comprised of the γ, ε and c subunits, leading to the synthesis of ATP by one of the three catalytic sites located in the $\alpha_3\beta_3$ hexagon. The δ and b subunits prevent the rotation of the $\alpha_3\beta_3$ hexagon with the rotor.

### *4.1.3 Hereditary paraganglioma (PGL).*

PGL is a rare autosomal dominant disease characterised by tumours of the paraganglionic system, a range of organs and cell clusters derived from neural crest cells (Baysal., 2003; Heutink *et al.,* 1992). The most common locations for PGL associated tumours are in the adrenal medulla and the head and neck paraganglia. Two types of tumours are associated with PGL; pheochromocytomas which are catecholamine secreting tumours that can lead to hypertensive crises, and head and neck paragangliomas (HNPs), hormonally silent tumours clinically recognised because of the pressure effects exerted by them in the head and neck (Maher *et al.,* 2002; Baysal., 2003).

Four loci have been identified that pre-dispose affected individuals to PGL. The responsible genes at the PGL1, PGL3 and PGL4 loci have been identified as *SDHD*, *SDHC,* and *SDHB*, respectively. These genes encode for three of the four proteins that comprise Succinate:Ubiquinone oxidoreductase (SQR, section 4.1.3). The first locus to be identified, PGL1, was genetically mapped in a five generation Dutch pedigree to chromosome band 11q23 (Heutink *et al.,* 1992) and was later identified as *SDHD*, the gene that encodes SDH D (Baysal *et al.,* 2000). The putative PGL2 locus was mapped to 11q13 in a single large Dutch family suffering from paragangliomas, and the gene responsible has been identified as *SDHAF2*, which encodes for SDH assembly factor 2 (SDHAF2), which is essential for SDH – dependent respiration and SDH A flavination (reviewed by Maher and Eng, 2002; Hao *et al.,* 2009). Following the identification of *SDHD* as the PGL1 locus other components of the SQR complex were analysed for mutations in individuals with paraganglioma and/or pheochromocytoma. This led to the discovery of PGL3 as the

*SDHC* locus in a single German family with PGL (Niemann and Muller, 2000) and PGL4 the *SDHB* locus in several families suffering from familial pheochromocytoma with or without HNPs (Astuti *et al.*, 2001, Table 4.1).

**Table 4.1 Summary of PGL disease type and affected gene.**

| PGL Type | Locus | Affected Gene | Associated Tumour Types | References |
|---|---|---|---|---|
| PGL1 | 11q22-23 | *SDHD* | Paraganglioma; Pheochromocytoma | Heutink *et al.*, 1992; Baysal *et al.*, 2000 |
| PGL2 | 11q13 | *SDHAF2* | Paraganglioma | Hao *et al.*, 2009 |
| PGL3 | 1q21-23 | *SDHC* | Paraganglioma | Niemann and Muller., 2000 |
| PGL4 | 1p36 | *SDHB* | Paraganglioma; Pheochromocytoma | Astuti *et al.*, 2001 |

**Key:** PGL, hereditary paraganglioma; *SDHB-D, succinate dehydrogenaseB-D genes; SDHAF2, succinate dehydrogenase assembly factor 2 gene.*

### *4.1.4 Maternal Imprinting of PGL1.*

The PGL1 phenotype is only observed when transmitted through the father, whereas no phenotype is observed when transmitted maternally. This clinical observation was believed to show that PGL1 was maternally imprinted i.e. the maternally derived gene is transcriptionally inactivated by methylation of the promoter during female oogenesis. Reactivation of the gene can only be achieved during spermatogenesis when methylation of the promoter is removed (van der Mey *et al.*, 1989).

The precise mechanism of PGL1 imprinted inheritance has still to be determined because evidence of *SDH D* biallelic expression has been shown in lymphoblastoids and leukocytes from affected and imprinted carrier individuals (Baysal *et al.*, 2000; Badenhop *et al.*, 2001) and in unaffected adult brain, foetal brain and foetal kidney tissue (Baysal *et al.*, 2000). Analysis of paraganglioma and pheochromocytoma tissue from affected PGL1 individuals showed monoallelic expression of the mutated paternal allele combined with a loss of heterozygosity (LOH) of the wild-type

maternal allele at the PGL1 loci (Baysal *et al.*, 2000; Taschner *et al.*, 2001; Gimenez-Roqueplo *et al.*, 2001). Retention of the mutated paternal allele and loss of the wild-type maternal allele suggests *SDH D* acts as a classical tumour suppressor requiring two mutational occurrences for tumourigenesis to occur. However the transmittance of the disease through the paternal line only suggests *SDH D* acts as tumour suppressor gene subject to maternal imprinting. All other PGL loci are not subject to maternal imprinting.

### *4.1.5 Mutational effects on the structure and function of Succinate Ubiquinone Oxidoreductase (SQR).*

Many mutations in the four genes that comprise SQR have now been identified, they lead to either severe encephalomyopathy in the case of *SDH A* mutations or tumour formation if subunits *SDH B-D* are affected. To date no mutations in *SDH A* have been identified that cause a pre-disposition in individuals to PGL, HNPs or apparently sporadic pheochromocytomas (ASPs, Table 4.2).

Individuals carrying the homozygous arg554trp or the heterozygous ala524val mutation of *SDH A* all present with Leigh syndrome, a progressively neurodegenerative disease whose symptoms include neural lesions dystonia, ataxia, myopathy and breathing difficulties (Bourgeron *et al.*, 1995; Parfait *et al*, 2000). The R554W and A524V mutations, located in the C-terminal domain of SDH A, are thought to be located near the catalytic site of SDH because they allow substrate binding but cause loss of activity of the SQR complex (reviewed by Ackrell, 2002).

Individuals carrying the heterozygous R451C mutation have a non-covalently bound FAD moiety which prevents the oxidisation of succinate from occurring. Individuals survive because the second *SDH A* allele is unaffected (Ackrell, 2000).

Analysis of SQR activity in pheochromocytoma tumour tissue harbouring the A43P, R46G, R46Q, 725 deleted c and IVS 4+1 g→a (IVS- intervening sequence) mutations in *SDH B*, demonstrated a complete loss of function of the SQR complex (Gimenez-Roqueplo *et al.*, 2002, 2003; Douwes-Dekker *et al.*, 2003). Tumour tissue from individuals with the above mutations as well as tumour tissue from individuals

with the R27X, H132P and 713-718 deleted tctc mutations in *SDH B* was found to have a loss of the wild-type allele at the *SDH B* locus (Gimenez-Roqueplo *et al.*, 2003; Neumann *et al.*, 2002; Maier-Woelfle *et al.*, 2004; Vanharanta *et al.*, 2004, respectively). This demonstrated that *SDH B* acts as a classical tumour suppressor gene.

**Table 4.2 A Summary of *SDH* mutations**

| SQR gene | Nucleotide change | Amino acid change | Disease phenotype | Reference |
|---|---|---|---|---|
| *SDH A* | 1a→c | M1L | Leigh syndrome | Parfait *et al.*, 2000 |
| *SDH A* | 1351c→t | R451C | Neurodegenerative disease, optic atrophy,ataxia and myopathy | Reviewed by Rustin and Rotig, 2002 |
| *SDH A* | 1571c→t | A524V | Leigh syndrome | Parfait *et al.*, 2000 |
| *SDH A* | 1660c→t | R554W | Leigh syndrome | Bourgeron *et al.*, 1995 |
| *SDH B* | 79c→t | R27X | ASP PGL4,RCC | Neumann *et al.*, 2002, Vanharanta *et al.*, 2004 |
| *SDH B* | 86-87 ins cag | ins Q after A29 | ASP | Neumann *et al.*, 2002 |
| *SDH B* | 127g→c | A43P | ASP | Gimenez-Roqueplo *et al.*, 2003 |
| *SDH B* | 136c→g | R46G | ASP | Neumann *et al.*, 2002, Gimenez-Roqueplo *et al.*, 2003 |
| *SDH B* | 137g→a | R46Q | ASP | Gimenez-Roqueplo *et al.*, 2002 |
| *SDH B* | 174-175gc→tt | Q59X | HNPs | Baysal *et al.*, 2002 |
| *SDH B* | 207-210 ins c | Frameshift after M70 | PGL4 | Baysal *et al.*, 2002 |
| *SDH B* | 260t→c | L87S | ASP | Astuti *et al.*, 2001a |
| *SDH B* | 268c→t | R91X | Hereditary pheochromocytoma and HNPs | Astuti *et al.*, 2001a |
| *SDH B* | 302g→a | C101Y | ASP | Neumann *et al.*, 2002 |
| *SDH B* | 392c→g | P131R | PGL4 | Baysal *et al.*, 2002 |
| *SDH B* | 395a→t | H132P | PGL4 | Maier-Woelfe *et al., 2004* |
| *SDH B* | 574t→c | C192R | ASP | Neumann *et al.*, 2002 |
| *SDH B* | 587g→a | C196Y | ASP | Neumann *et al.*, 2002 |
| *SDH B* | 590c→g | P197R | Hereditary pheochromocytoma | Astuti *et al.*, 2001a |
| *SDH B* | 591del c | Frameshift after P197 | ASP | Astuti *et al.*, 2001a and Gimenez-Roqueplo *et al.*, 2003 |
| *SDH B* | 620-621 del tg | Frameshift after Y206 | ASP | Gimenez-Roqueplo *et al.*, 2003 |
| *SDH B* | 688c→t | R230C | ASP | Gimenez-Roqueplo *et al.*, 2003 |
| *SDH B* | 713-718 del tctc | Frameshift after L240 | ASP PGL4 and RCC | Neumann *et al.*, 2002, Vanharanta *et al.*, 2004 |

| SQR gene | Nucleotide change | Amino acid change | Disease phenotype | Reference |
|---|---|---|---|---|
| *SDH B* | 725 del c | Frameshift after Y241 | ASP | Astuti *et al.*, 2001a |
| *SDH B* | 747c→a | C249X | ASP | Neumann *et al.*, 2002 |
| *SDH B* | IVS 4+1 g→a | Splice defect | HNPs | Douwes Dekker *et al.*, 2003 |
| *SDH C* | 3g→a | M1V abolishes start codon | PGL3 | Niemann and Muller, 2000 |
| *SDH D* | 1g→c | M1I | PGL1 | Badenhop *et al.*, 2001 |
| *SDH D* | 14g→a | W5X | ASP | Neumann *et al.*, 2002 |
| *SDH D* | 33c→a | C11X | ASP | Neumann *et al.*, 2002 |
| *SDH D* | IVS1 +2 t→g | Splice defect | Paraganglioma and pheochromocytoma | Gimm *et al.*, 2000 |
| *SDH D* | 34g→a | G12S | PGL1,ASP, Polymorphism | Gimm *et al.*, 2000, Taschner *et al.*, 2001 |
| *SDH D* | 36-37 del tg | Frameshift after A13 | ASP | Neumann *et al.*, 2002 |
| *SDH D* | 54 ins c | Frameshift after A18 | PGL1 | Taschner *et al.*, 2001 |
| *SDH D* | 64c→t | R22X | PGL1 | Taschner *et al.*, 2001 |
| *SDH D* | 95c→t | S32X | PGL1 | Milunsky *et al.*, 2001 |
| *SDH D* | 94-97 del ct | Frameshift after S32 | Hereditary Pheochromocytoma | Astuti *et al.*, 2001b |
| *SDH D* | 106c→t | Q36X | PGL1 | Baysal *et al.*, 2000 |
| *SDH D* | 112c→t | R38X | ASP | Baysal *et al.*, 2000, Gimm *et al.*, 2000 |
| *SDH D* | 120 ins c | Frameshift after P41 | PGL1 | Taschner *et al.*, 2001 |
| *SDH D* | 191-192 del tc | Frameshift after L64 | PGL1 | Badenhop *et al.*, 2001 |
| *SDH D* | | Frameshift after W66 | Hereditary pheochromocytoma | Astuti *et al.*, 2001b |
| *SDH D* | 208a→g | R70G | PGL1 | Taschner *et al.*, 2001 |
| *SDH D* | 242c→t | P81L | ASP | Baysal *et al.*, 2000, Gimm *et al.*, 2000 |
| *SDH D* | 274g→t | D92Y | PGL1 | Baysal *et al.*, 2000 |
| *SDH D* | 276-278 del cta | del Y93 | PGL1 | Badenhop *et al.*, 2001 |
| *SDH D* | 284t→c | L95P | PGL1 | Taschner *et al.*, 2001 |
| *SDH D* | 305a→t | H102L | PGL1 | Baysal *et al.*, 2000 |
| *SDH D* | 325c→t | Q109X | PGL1 | Baysal *et al.*, 2002 |
| *SDH D* | 336-337 ins t | D113X | PGL1 | Milunsky *et al.*, 2001 |
| *SDH D* | 341a→g | Y114C | PGL1 | Milunsky *et al.*, 2001 |
| *SDH D* | 361c→t | Q121X | ASP | Neumann *et al.*, 2002 |
| *SDH D* | 381-383 del g | Frameshift after L128 | PGL1 | Baysal *et al.*, 2002 |
| *SDH D* | 416t→c | L139P | PGL1 | Taschner *et al.*, 2001 |
| *SDH D* | 441-443 del c | Frameshift after G148 | PGL1 | Milunsky *et al.*, 2001 |
| *SDH D* | IVS3 -32 t→c | Splice defect | PGL1 | Taschner *et al.*, 2001 |

Nucleotide mutations and the corresponding amino acid change are indicated for each *SDH* gene along with the disease phenotype(s) the mutation has been associated with.

**Key:** ASP, Apparently sporadic pheochromocytoma: HNPs, Head and neck paragangliomas; RCC, Renal cell carcinoma; PGL 1-4, Hereditary Paraganglioma Type 1-4 IVS, Intervening sequence

The only mutation to have been identified in *SDH C* to date abolishes the atg start codon causing the replacement of methionine 1 with valine. Tumour tissue from affected individuals was found to have loss of the unaffected *SDH C* allele while retaining the affected allele, demonstrating *SDH C* acts as a tumour suppressor (Niemann and Muller, 2000). Presumably, because both SDH C and SDH D are required for membrane association of SDH A and SDH B, tumours from individuals with the met1val mutation and loss of the wild type allele would only have SDH D present in the mitochondrial membrane (Ackrell, 2002).

PGL1 tumours exhibiting LOH of the *SDH D* locus affecting the maternal allele have been found to harbour the mutations R22X, Q36X, R38X, P81L, D92Y, H102L and L139P (Gimenez-Roqueplo *et al.,* 2001; Baysal *et al.,* 2000; Taschner *et al.,* 2001). These mutations cause a complete loss of function of the SQR complex (Gimenez-Roqueplo *et al.,* 2001; Douwes-Dekker *et al.,* 2003). Preferential expression of the mutated paternal allele in tumour tissue from PGL1 individuals harbouring the M1I mutation has also been demonstrated (Badenhop *et al.,* 2001). Pheochromocytoma tumour tissue that is not associated with PGL1 has also been found to exhibit LOH of the wild type-allele, the remaining mutated allele encodes for the P81L protein mutation (Gimm *et al.,* 2000). Other mutations are predicted to produce truncated proteins or mutations that alter the structure of SDH D and these include R38X, P81L, Q109X and 381-383 deleted g (Baysal *et al.,* 2002).

### *4.1.6 Other TCA cycle associated tumour syndromes*

As well as germ-line mutations being identified in *SDH A-D,* they have also been identified in the fumarase gene (fumarate hydratase, *FH*) which encodes for fumarase, another enzyme of the TCA cycle. Fumarase (FH) catalyzes the conversion of fumarate to malate, which is the subsequent reaction after the catalysis of succinate to fumarate by SDH.

Germ-line homozygous mutations of the *FH* gene cause fumarase deficiency, an autosomal recessive condition that is not associated with a tumour syndrome. This is similar to homozygous mutations in the *SDH A* gene which also cause a non-tumour

associated condition. Heterozygous mutation of *FH* causes an autosomal dominant syndrome known as multiple cutaneous and uterine leiomyomatosis (MCUL). Male individuals with MCUL suffer from multiple leiomyomatas (benign smooth muscle tumours) of the skin while female sufferers present with skin and uterine leiomyomatas. MCUL is associated with an increased risk of type II papillary renal cell cancer and leiomyosarcoma and this form of the disease is called hereditary leiomyomatosis and renal cell cancer (HLRCC, Alam *et al.*, 2003). In both MCUL and HLRCC the fumarase has been found to act as a classical tumour suppressor, as preferential loss of the wild-type allele and retention of the mutated allele is often seen in leiomyomata and renal cell carcinomas (Tomlinson *et al.*, 2002). Loss of FH activity in cutaneous leiomyomatas relative to overlaying normal skin has also been demonstrated (Tomlinson *et al.*, 2002).

Renal cell cancer is also known to be a feature of VHL syndrome (section 1.6.5). The finding that mutation of another enzyme of the TCA cycle predisposes individuals to a form of cancer known to be related to VHL syndrome perhaps suggests an involvement of FH in oxygen sensing (Tomlinson *et al.*, 2002).

### *4.1.7 Approaches to inhibiting SDH*

Germ-line and sporadic mutations in, *SDH B, SDH C* and *SDH D* are known to pre-dispose affected individuals to paraganglioma and/or pheochromocytoma (Astuti *et al.*, 2001; Niemann and Muller, 2000 and Baysal *et al.*, 2000, respectively). Pheochromocytoma also occurs in VHL syndrome, an autosomal dominant condition causing a pre-disposition of affected individuals to pheochromocytoma, renal cell carcinoma and central nervous system (CNS) hemangioblastomas (reviewed by Kondo and Kaelin Jr, 2001).

One of the functions of pVHL, the protein product of *VHL*, is the regulation of hypoxia inducible factor-1α (HIF-1α, Maxwell *et al.*, 1999). HIF-1α dimerises with ARNT/HIF-1β to form hypoxia inducible factor 1 (HIF-1), a transcription factor that regulates a variety of genes that are involved angiogenesis, oxygen transport, glucose uptake, glycolysis and growth factor signalling. All of these processes are involved

in tumour cell survival and proliferation (reviewed by Bardos and Ashcroft, 2004; section 1.3.4). Inactivating mutations in *VHL* when combined with loss of expression or mutational inactivation of the remaining *VHL* allele prevent the regulation of HIF-1α, leading to a phenotype that resembles adaptation to hypoxia occurring under normoxic conditions (reviewed by Safran and Kaelin Jr, 2003).

Vascularisation is a feature of the tumours involved in VHL disease because of the transcriptional activation by HIF-1 of genes encoding proteins involved in angiogenesis, oxygen transport, glucose transport, glycolysis and growth factor signalling. A high degree of vascularisation was observed in paraganglionic tumours harbouring germ-line *SDH D* mutations (Baysal *et al.*, 2000). The similarities in tumour types and tumour pathology in individuals with VHL disease and in individuals with tumours caused by *SDH B* or *SDH D* mutations (*SDH C* mutations have yet to be identified in pheochromocytoma) suggested an involvement of the hypoxic response pathway. This led to the hypothesis that inactivation of SDH would lead to an up-regulation of HIF-1α subsequently followed by an increase in HIF-1 transcriptional activation of target genes.

#### *4.1.7.1 The chemical inhibition of succinate dehydrogenase (SDH).*

Before embarking on expensive highly specific methods of disrupting succinate dehydrogenase (SDH) (e.g.. RNA interference) a less expensive model was sought after in the form of chemical inhibition.

Preliminary experiments were performed with 3-nitropropionic acid/3-nitropropionate (3-NPA) before testing whether malonate could produce the same effect. Both 3-NPA and malonate are analogues of succinate. The chemical structures of succinate, 3-NPA and malonate are shown in figure 4.7.

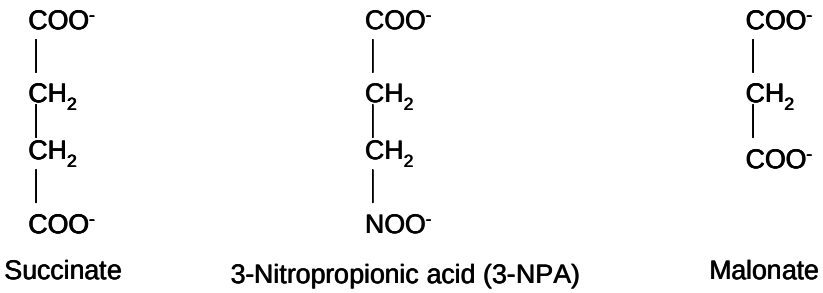


**Figure 4.6 Structural similarities between succinate and inhibitors of succinate dehydrogenase.**

3-nitropropionic acid (3-NPA) is a toxin from the *Indigofera endecaphylla* plant. 3-NPA is an isoelectric analogue of succinate that once bound to SDH A acts by progressively and irreversibly inactivating the enzyme and as such is defined as a suicide inhibitor (Alston *et al.,* 1977). It is thought inactivation occurs by the slow oxidisation of 3-NPA into 3-nitroacrylate via the reduction of FAD to $FADH_2$. An -SH group located in the binding site of SDH A is thought to combine with the double bond in 3-nitroacrylate to form an irreversible covalent adduct (Coles *et al.,* 1979).

Malonate is a reversible competitive inhibitor of SDH (O'Donnell *et al.,* 1995). Both 3-NPA and malonate were employed to model the inactivation of SDH. Unfortunately this model has some limitations. Mutations associated with pheochromocytoma are usually found in SDH B or D not in SDH A which is the subunit targeted for inactivation by 3-NPA and malonate. Another limitation of this model is the specificity of action of both inhibitors as they may have other targets as well as SDH A.

*4.1.7.2 The inhibition of succinate dehydrogenase (SDH) by RNA interference (RNAi).*

An alternative approach to inhibiting SDH function is to use a specific targeted approach such as RNA interference (RNAi). RNAi is an evolutionary conserved pathway, first identified in plants, that was initially identified as a cellular defence mechanism against viral invasion and transposon expansion. However, RNAi also

has a more general role whereby specific genes in plants and mammals are regulated by post-transcriptional gene silencing. Following the discovery of RNA interference it has quickly become a valuable gene function analysis tool. In nature RNAi occurs when the host cell encounters a long piece of double stranded RNA (dsRNA). In *Homo sapiens* dsRNAs are processed by an RNase-III like enzyme called Dicer into small interfering RNA (siRNAs) duplexes of between 21 and 23 nucleotides. The duplexed siRNAs are subsequently incorporated into an RNA induced silencing complex (RISC) which unwinds the siRNA duplex. RISC complexes that incorporate the anti-sense strand of the unwound siRNA duplex guide the sequence specific cleavage of complementary or near complementary target mRNAs (reviewed by Meister and Tuschl, 2004).

siRNAs have been commercially developed and utilised for target validation and gene function analysis e.g.. validation of Brk as a therapeutic target in breast cancer and more recently in determining the differing roles of HIF-1α and HIF2α in colon cancer (Harvey and Crompton 2003; Imamura *et al.*, 2009). Several RNAi-based therapeutics have now reached clinical trials; these include RNAi-based therapeutics for the treatment of age related macular degeneration, hepatitis B and solid tumours (reviewed by Castanotto and Rossi, 2009)

More SDH B mutations are associated with pheochromocytoma than SDH D or SDH C mutations (table 4.2). Therefore, inhibition of SDH B is a better model for studying the effect of tumour associated mutations. An antibody for SDH B was also commercially available thereby providing an important experimental tool for sample analysis.

### *4.1.8 Hypothesis*

The aim of this work is to determine whether chemical inhibition of SDH by 3-NPA or malonate (chemical inhibitors of SDH A analogous to succinate) results in up-regulation of HIF-1α. A further aim of this study is to determine whether inhibition of the SDH B subunit by RNA interference results in up-regulation of HIF-1α and subsequent up-regulation of HIF target genes.

## 4.2 Development of a chemical inhibition model to determine the effects of SDH mutation in pheochromocytoma.

### *4.2.1 The optimisation of 3-NPA treatment of Hep G2 and T-47D cells.*

Previous studies performed using 3-NPA, have used varying concentrations to inhibit succinate dehydrogenase in cultured cells. These concentrations ranged from 4-8mM in PC12 cells and from 1-20mM in experiments designed to assess whether estradiol could attenuate the 3-NPA induced modulation of ATP production, mitochondrial membrane potential, reactive oxygen species (ROS) production and cell viability observed in SK-N-SH neuroblastoma cells (Mandavelli *et al.,* 2005 and Wang *et al.,* 2001, respectively). Wang *et al*, (2001). Based on the experiments of Wang *et al.,* the concentration of 3-NPA used in initial optimisation experiments designed to determine whether 3-NPA had any effect on HIF-1α protein levels was 12.5mM.

At the time of performing these preliminary experiments it had been shown that p53 could inhibit HIF-1 dependent transcription (Blagosklonny *et al.,* 1998 ) by promoting Mdm2 mediated proteasomal degradation of HIF-1α (Ravi *et al.,* 2000). Therefore it was of interest to see if any apparent effects on HIF-1α protein levels caused by cell incubation with 3-NPA were also dependent on the presence of wild-type p53. With this aim in mind Hep G2 cells expressing wild-type p53 (Ho *et al.,* 1999) and T-47D cells, which express p53 containing a C-T mis-sense mutation in exon 6 resulting in a truncated protein, were used in preliminary experiments.

Hep G2 and T-47D cells were treated 24 hours after seeding with 12.5mM 3-NPA or a carrier control (sterile $H_2O$). Whole cell lysates prepared 3 and 6 hours after treatment were resolved by SDS-PAGE, western blotted and probed with an anti-HIF-1α antibody (figure 4.7). Equal protein loading of the membranes was determined by Ponceau S staining (data not shown).

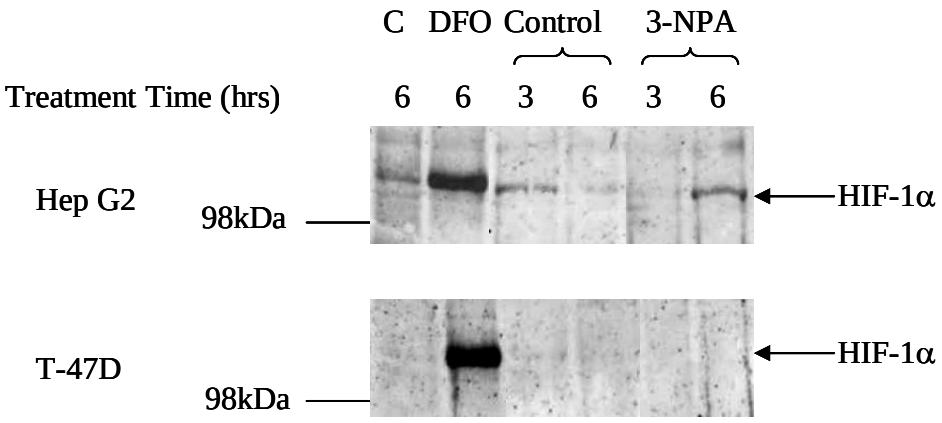


**Figure 4.7 The effect of 3-NPA treatment on HIF-1α protein levels in Hep G2 and T-47D cells.**

Hep G2 and T-47D cells were incubated 24 hours after seeding with either a carrier control or 3-NPA to a final concentration of 12.5mM, as indicated. Whole cell lysates were prepared 3 and 6 hours after treatment. As a positive control to identify for HIF-1α protein, cells were incubated for 6 hours with either a carrier control (C) or DFO to a final concentration of 100μM before whole cell lysates were prepared. Whole cell lysates were resolved by SDS-PAGE, western blotted and probed with an anti-HIF-1α antibody (Novus Biologicals). Equal protein loading of the membranes was determined by Ponceau S staining. The mobility of a standard protein is indicated (sections 2.1.1 - .2.16;). Figure represents n=1.

**Key:** 3-NPA, 3-nitropropionic acid; C, carrier control; DFO, Desferrioxamine; HIF-1α, hypoxia inducible factor 1α; hrs, hours; kDa, kilodaltons.

In Hep G2 cells, 3-NPA appeared to induce HIF-1α protein at the 6 hour time-point when compared to carrier control however the converse appeared to be the case at the 3 hour time-point, where more HIF-1α protein was detected in the carrier control sample than in the 3-NPA treated sample. 3-NPA did not induce any detectable HIF-1α protein in T-47D cells at either time-point. A low level of HIF-1α protein can be detected in the control treated lysates of T-47D cells at both time-points. DFO, an iron chelator that induces HIF-1α protein levels in cells not subjected to hypoxia, was used to treat Hep G2 and T-47D lysates. These lysates were used as positive controls for the detection of HIF-1α protein.

Due to the low level of HIF-1α protein induced by 3-NPA in Hep G2 cells and the absence of induction in T-47D cells, the incubation time of cells with 3-NPA was increased. Hep G2 and T-47D cells were treated 24 hours after seeding with either

12.5mM 3-NPA or carrier control. Whole cell lysates were prepared 16 and 24 hours after treatment, resolved by SDS-PAGE, western blotted and probed with an anti-HIF-1α antibody (figure 4.8).

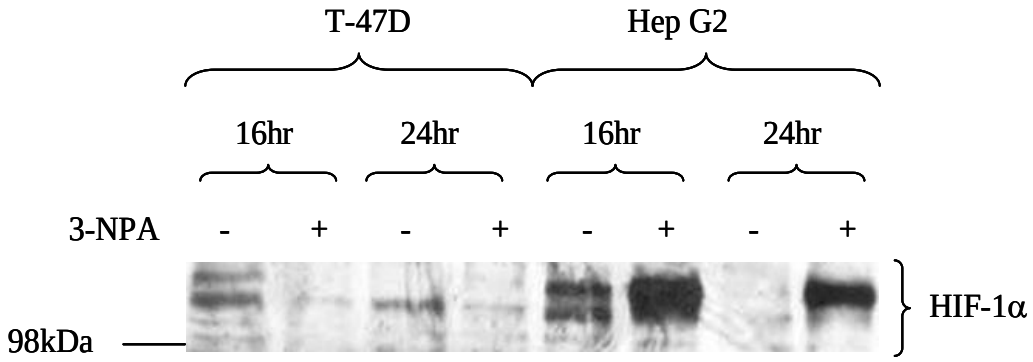


**Figure 4.8 The effect of 3-NPA treatment on HIF-1α protein levels in Hep G2 and T-47D cells.**

Hep G2 and T-47D Cells were incubated 24 hours after seeding with either carrier control (-) or 3-NPA to a final concentration of 12.5mM (+). Whole cell lysates were prepared 16 and 24 hours after treatment, were resolved by SDS-PAGE, western blotted and probed with an anti-HIF-1α antibody (Novus Biologicals). Equal protein loading was determined by Ponceau S staining of the membrane. The mobility of a standard protein is indicated. (sections 2.1.1 – 2.1.6;). Figure represents one experiment (n=1).

**Key:** 3-NPA, 3-nitropropionic acid; C, carrier control; DFO, Desferrioxamine; HIF-1α, hypoxia inducible factor 1α; hrs, hours; kDa, kilodaltons.

A low level of HIF-1α protein was detectable in T-47D samples treated with 3-NPA, however the corresponding control lanes contain more HIF-1α protein than is detectable in test lanes. In Hep G2 cells elevated levels of HIF-1α protein were detected in samples treated with 3-NPA when compared to control treated samples at both 16 and 24 hours. The multiple anti-HIF-1α bands detected in all samples could be due to post-translational modifications including the conjugation of a mono or poly-ubiquitin tail and/or phosphorylation.

To confirm the results observed in figure 4.8 the experiment was repeated (figure 4.9). DFO treated Hep G2 and T-47D cells were used as a positive control for the detection of HIF-1α protein.

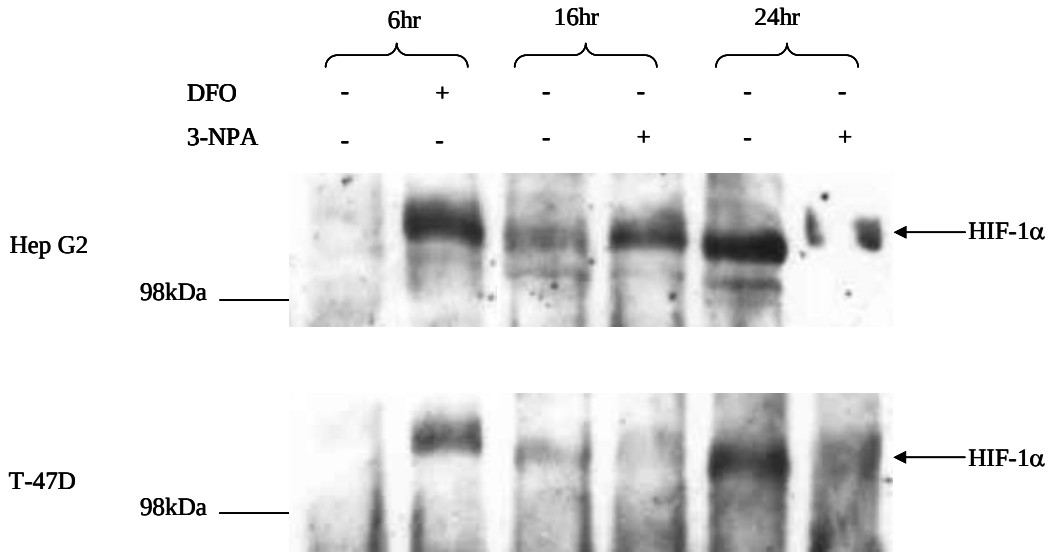


**Figure 4.9 The effect on HIF-1α protein levels in Hep G2 and T-47D cells incubated with 3-NPA.**

Hep G2 and T-47D cells were incubated 24 hours after seeding with either a carrier control (3-NPA -) or 3-NPA to a final concentration of 12.5mM (3-NPA +), as indicated. Whole cell lysates prepared 16 and 24 hours after treatment. As a positive control for detection of HIF-1α protein, Hep G2 and T-47D whole cell lysates were prepared 6 hours after treatment with either carrier control (DFO -) or DFO (DFO +) to a final concentration of 100μM as indicated. Whole cell lysates were resolved by SDS-PAGE, western blotted and probed with an anti-HIF-1α antibody (Novus Biologicals). Equal protein loading of the membranes was determined by Ponceau S stainings. The mobility of a standard protein is indicated (sections 2.1.1 – 2.1.6). Figure represents one experiment (n=1).

**Key:** 3-NPA, 3-nitropropionic acid; DFO, Desferrioxamine; HIF-1α, hypoxia inducible factor 1α; hrs, hours; kDa, kilodaltons.

A higher level of HIF-1α protein was detected in Hep G2 cells treated with 3-NPA when compared to carrier control treated cells at 16 hours however, at 24 hours the converse appeared to be the case. Multiple bands representing anti-HIF-1α cross-reactive species were observed in Hep G2 carrier control treated samples at 16 and

24 hours and in the 16hr 3-NPA treated sample. The mobility of detectable HIF-1α protein in carrier control and 3-NPA treated samples was higher than in Hep G2 cells treated with DFO. However there was also some variability in HIF-1α protein mobility between samples treated with carrier control, which exhibited a higher mobility, and samples treated with 3-NPA which exhibited a lower mobility.

Treatment of T-47D cells with 3-NPA appeared to cause a suppression of HIF-1α protein levels at both 16 and 24 hours when compared to HIF-1α protein expressing carrier control samples. The same shift in HIF-1α protein mobility as was observed in Hep G2 cells could also be seen in T-47D cells. Carrier control treated samples contained a higher mobility HIF-1α protein than DFO treated sample. Multiple HIF-1α reactive species could not be observed in T-47D cells.

Figures 4.8 and 4.9 highlighted the variability of HIF-1α protein levels in control samples for both cell types. There was also a large variability in results between two experiments conducted in the same manner. The variability of HIF-1α protein expression in both cell types made the results difficult to interpret.

### *4.2.2 The effect of low pH on cells incubated with 3-NPA.*

The optimisation experiments performed previously (section 4.2.1), involved the dissolution of 3-NPA in sterile $H_2O$ before addition to a final concentration of 12.5mM to either Hep G2 or T-47D cells. This addition of 3-NPA caused the cells to be incubated in acidic conditions before lysis. Cells incubated with carrier control were not subjected to acidic conditions because the carrier control was sterile $H_2O$ which did not affect pH.

To determine whether low pH was the cause of variable induction of HIF-1α in 3-NPA treated cells, Hep G2 and T-47D cells were treated 24 hours after seeding with either 3-NPA pH 7.6 (buffered with NaOH) or a carrier control (sterile $H_2O$ containing the same amount of $Na^+$ ions in the form of NaCl as used to buffer 3-NPA). Whole cell lysates prepared 16 and 24 hours after treatment, were resolved by SDS-PAGE, western blotted and probed with an anti-HIF-1α antibody (figure 4.10).

DFO treated HepG2 or T-47D cells were used as positive controls for the detection of HIF-1α.

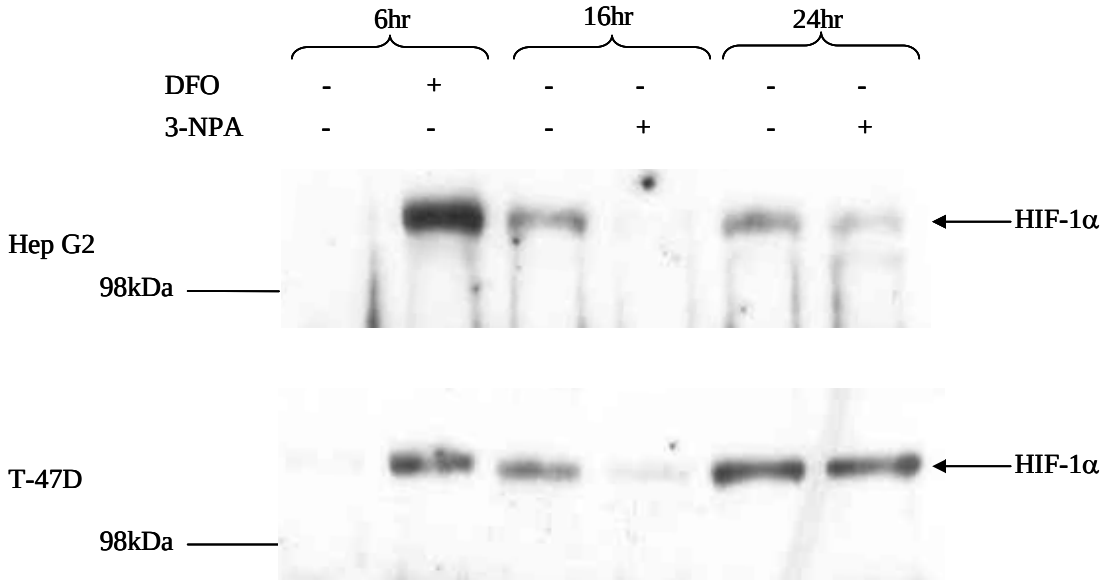


**Figure 4.10 The effect of 3-NPA pH 7.6 on HIF-1α protein levels in Hep G2 and T-47 D cells.**

Hep G2 and T-47D cells were incubated 24 hours after seeding with either carrier control (sterile $H_2O$ containing the same amount of $Na^+$ ions in the form of NaCl as used to buffer 3-NPA, -) or 3-NPA pH 7.6 (buffered with NaOH, +), to a final concentration of 12.5mM, as indicated. Whole cell lysates prepared 16 and 24 hours after treatment. As a positive control for the detection of HIF-1α protein Hep G2 and T-47D whole cell lysates were prepared six hours after treatment of cells with either or carrier control (-) or DFO to a final concentration of 100μM (-) as indicated. Whole cell lysates were resolved by SDS-PAGE, western blotted and probed with an anti-HIF-1α antibody (Novus Biologicals). Equal protein loading of the membranes was determined by Ponceau S staining. The mobility of a standard protein is indicated (sections 2.1.1 – 2.1.6). Figure represents one experiment (n=1).

**Key:** 3-NPA, 3-nitropropionic acid; DFO, Desferrioxamine; HIF-1α, hypoxia inducible factor 1α; hrs, hours; kDa, kilodaltons.

At 16 and 24 hours after 3-NPA treatment a low level of HIF-1α could be detected in treated Hep G2 cells however corresponding control samples contained a greater amount of HIF-1α protein (figure 4.10). T-47D samples at 16 hours contained a greater level of detectable HIF-1α protein in the control sample when compared to

the 3-NPA treated sample (figure 4.10). At 24 hours there was no discernable difference in HIF-1α protein levels between the control and 3-NPA treated samples in T-47D cells.

The experiments performed to optimise the use of 3-NPA in both Hep G2 and T-47D cells showed a large degree of variability in the results obtained. Figures 4.8, 4.9 and 4.10 showed a differing amount of HIF-1α protein present in Hep G2 control samples at 16 hours. At 24 hours the presence of detectable HIF-1α in control treated samples was variable. Figures 4.9 and 4.10 clearly indicated that HIF-1α protein could be detected in control treated samples at 24 hours yet in figure 4.8 HIF-1α protein was not detected. In T-47D cells HIF-1α protein was detected in control treated samples at both time-points as shown in figures 4.8, 4.9 and 4.10.

The effect of 3-NPA on HIF-1α protein levels was also variable. Figure 4.10 clearly showed 3-NPA caused an increase in HIF-1α protein levels at both time-points when compared to carrier control treated samples in Hep G2 cells. However, these results were not clearly reproduced in figures 4.9 and 4.10. The effect of 3-NPA treatment of T-47D cells was even more erratic. In figure 4.8, 3-NPA appeared to suppress the level of HIF-1α protein detected when compared to carrier control treated samples at both 16 and 24 hours. Figure 4.9 showed 3-NPA had no effect on HIF-1α protein levels and figure 4.10 showed 3-NPA treated samples contained less HIF-1α protein than carrier control treated samples at 16 hours but at 24 hours 3-NPA had no effect on HIF-1α protein levels when compared to carrier control treated samples.

The results obtained seemed to indicate that low pH is not necessarily the cause of the variable HIF-1α protein levels observed in the preceding experiments. This can be shown more clearly if figures 4.9 and 4.10 are compared. Figure 4.9 showed a slight increase in HIF-1α protein levels at 16 hours, in response to 3-NPA, when compared to control in Hep G2 cells. At 24 hours the converse appeared to be the case. Figure 4.10 showed an apparent suppression of HIF-1α protein in 3-NPA treated cells when compared to controls at both time-points. T-47D cells treated with 3-NPA showed a suppression in the level of HIF-1α protein when compared to controls at both time-points (figures 4.9 and 4.10).

### *4.2.3 The effect of cell confluence on HIF-1α protein levels.*

The variability in results observed in figures 4.8, 4.9 and 4.10 manifested themselves more often than not at the 24 hour time-point where there appeared to be more HIF-1α protein present in control samples. This was not due to a difference in protein loading as determined by Ponceau S staining of the membranes prior to western blotting.

During the course of the optimisation experiments it was observed that cells were becoming confluent after plating. Cultures of Hep G2 cells grown at a high density in an air-5% $CO_2$ environment have been shown to utilise more $O_2$ than can diffuse from the gas environment into the pericellular environment, indicating that confluent Hep G2 cells manifest a pseudo-hypoxic response (Metzen *et al.,* 1995). High cell density has also been shown to induce nuclear HIF-1α protein expression and the activity of an HRE (hypoxia responsive element) reporter construct in LNCap (human prostate) cells cultured in normoxic conditions (Sheta *et al.,* 2001). Figures 4.9 and 4.10 showed HIF-1α protein expression in control treated Hep G2 cells cultured in normoxic conditions at 24 hours yet in figure 4.8 no detectable HIF-1α protein was detected in the equivalent cell lysate. The variability in these results could be due to differences in cell density between experiments. Therefore, Hep G2 cells were seeded at varying densities and cell confluence was judged by eye 48 hours after seeding. A 200 000 cell starting population gave a good dispersal of cells in a monolayer across a well at the end of this time-period. The starting number of this cell population was approximately 50% less than used in previous experiments.

### *4.2.4 The effect of 3-NPA on HIF-1α protein levels.*

Previous studies performed using 3-NPA, have used varying concentrations to inhibit succinate dehydrogenase in cultured cells and tissues. These concentrations ranged from 10-100μM in rat hippocampal slice cultures, 25-100μM in rat striatal and corticostriatal slice cultures, 4-8mM in PC12 cells and from 1-20mM in SK-N-SH neuroblastoma cells (Wei *et al.,* 2004, Storgaard *et al.,* 2000, Mandavelli *et al.,* 2005 and Wang *et al.,* 2001, respectively). To determine whether a different dose of 3-NPA could produce an effect on HIF-1α protein levels Hep G2 cells were seeded 200 000 cells/well. 24 hours after seeding cells were treated with concentrations of 3-NPA ranging between 25mM and 12.2μM 3-NPA pH 7.6 (buffered with NaOH) or carrier control (medium containing the same amount of $Na^+$ ions in the form of NaCl as used to buffer 3-NPA). 24 hours after treatment whole cell lysates were prepared. Whole cell lysates were resolved by SDS-PAGE, western blotted and probed with anti HIF-1α, anti-ARNT as a loading control additional to protein staining and anti-p53 antibodies (figure 4.11). Both ARNT and p53 were chosen as loading controls; -ARNT because it has a similar protein structure to HIF-1α and therefore if any differences in protein level was observed in one protein and not the other it was likely that this was a specific result rather than a generalised one. ARNT has also been documented to be a constitutively expressed protein in all cells except ARNT null tumour cells (Griffiths *et al.,* 2002). p53 is a protein that undergoes ubiquitin mediated degradation by the proteasome and it was for this reason that it was chosen as a control as it would be possible to establish whether any changes in HIF-1α protein levels were specific to HIF rather than due to generalised protein turnover. A more general protein such as actin was not considered as a control protein as it was felt ARNT and p53 protein levels were sufficient to determine whether anychanges in HIF-1α protein levels were specific to HIF-1α or due to a generalised effect as a result of the chemical treatment of Hep G2 cells.

HIF-1α protein could not be detected in any samples and therefore no change in protein levels between 3-NPA treated samples and corresponding carrier control samples could be detected. ARNT protein detection was performed as a protein loading control in addition to Ponceau S staining of the membrane. ARNT was

thought to be a suitable control as it has been reported to be a constitutively expressed protein in all cells except ARNT null tumour cells (Griffiths *et al.*, 2002). Therefore, it was somewhat surprising to discover that ARNT protein levels were reduced in 3-NPA treated samples when compared to corresponding carrier controls between 25mM and 0.78mM and at 12.2µM. Very little variation in ARNT protein levels was visible between 3-NPA treated samples and corresponding carrier controls at all other concentrations.

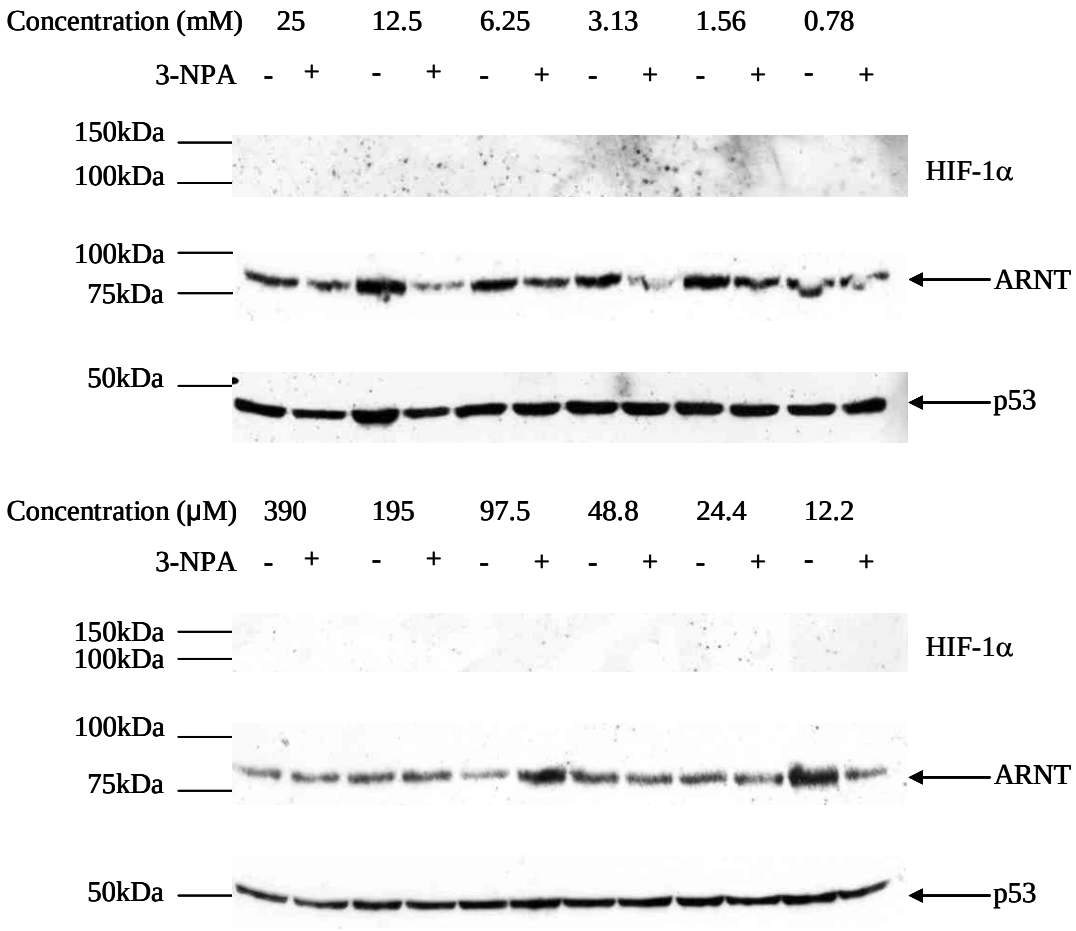


**Figure 4.11 The effect of different doses of 3-NPA on protein levels.**

Hep G2 cells seeded at low density (200 000 cells per well) were treated 24 hours after seeding with 3-NPA pH 7.6 (+, buffered with NaOH) to final concentrations ranging between 12.2μM and 25mM or a corresponding carrier control. Whole cell lysates prepared 24 hours after treatment were resolved by SDS-PAGE, western blotted and probed with anti HIF-1α (Novus Biologicals), anti-ARNT (Novus Biologicals) and anti-p53 antibodies, as indicated. Equal protein loading of membranes was determined by Ponceau S staining (data not shown). Mobilities of standard proteins are indicated (sections 2.1.1. – 2.1.6). Figure represents one experiment (n=1).

**Key:** 3-NPA, 3-nitropropionic acid; ARNT, Aryl hydrocarbon nuclear translocater; DFO, Desferrioxamine; HIF-1α, hypoxia inducible factor 1α; kDa, kilodaltons; mM, millimolar; μM, micromolar

Due to the variability in ARNT protein levels between 3-NPA treated and carrier control treated samples another loading control had to be found. p53 was chosen as a loading control because of similarities shared with HIF-1α. Both HIF-1α and p53 are

predominantly localised in the nucleus of a cell and both proteins are subject to ubiquitin mediated proteasomal degradation. p53 protein levels were not affected by 3-NPA treatment when compared to carrier control treated samples between 25mM and 0.78mM. At 12.5mM there appeared to be slightly more p53 protein in the carrier control treated sample when compared to the 3-NPA treated sample. This difference in protein levels was mirrored in the corresponding ARNT protein levels however the fold decrease of ARNT protein between carrier control and 12.5mM 3-NPA treated samples appeared larger when compared to the fold decrease in p53 protein levels. Any differences in ARNT protein levels between samples treated with concentrations of 3-NPA from 390μM downwards, with the exception of 12.2μM, and the respective carrier controls were mirrored in the p53 protein levels suggesting these variations were dependent on protein content rather than caused by 3-NPA treatment. Ponceau S staining of the membranes also confirmed a slight difference in protein loading between the samples in question.

The absence of any detectable HIF-1α protein in any of the cell lysates probed appeared to indicate that the variability in HIF-1α protein levels observed in previous experiments could be due to cell density. However, it is worth noting that less protein was loaded on the gel in this experiment than in previous experiments. Therefore, it is possible there was too little HIF-1α to be detected by Western blotting.

The results shown in figure 4.11 indicate that the dose of 3-NPA that has the greatest knockdown effect on ARNT was 12.5mM. This was the dosage used in previous optimisation experiments and mM dosages had also been used by other researchers (Wang *et al.,* 2001; Peng and Geddes, 1997).

### *4.2.5 The effect of 3-NPA and malonate on HIF-1α, ARNT, and SDH B protein levels.*

The change in ARNT protein levels discovered in the dose response experiment (section 4.2.4) was an extremely unexpected finding due to all published literature showing ARNT to be a constitutively expressed protein except in ARNT null cells (Griffiths *et al.,* 2002). The results from the dose response experiment (section 4.2.4)

also appeared to confirm the hypothesis that changes in HIF-1α protein levels observed in previous may have been influenced by cell density, and thus subject to inter-experimental variability due to differences in oxygen diffusion through the media, an increase in growth factors in the incubation media or depletion of nutrients from the media.

To confirm the observations from figure 4.11 cells were treated with 12.5mM 3-NPA. Cells were also treated with another inhibitor of SDH, malonate, to determine whether the change in ARNT protein levels would be observed with a different inhibitor. Hep G2 and T-47D cells were seeded at low density (200 000 cells/well). 24 hours after seeding cells were treated with either, 12.5mM 3-NPA pH7.6 (buffered with NaOH), carrier control as previously described, sterile $H_2O$, 12.5 mM malonate pH7.4 or carrier control for malonate (media). Whole cell lysates were prepared 24 hours after treatment. Lysates were resolved by SDS-PAGE, western blotted and probed with anti-HIF-1α, anti-ARNT and anti-p53 antibodies as indicated (figure 4.12).

HIF-1α protein was detected in 3-NPA and $H_2O$ treated Hep G2 cells. No HIF-1α protein could be detected in T-47D cells treated with 3-NPA. None of the control treated samples in either cell type contained any detectable HIF-1α protein. Malonate did not appear to induce any up-regulation of HIF-1α protein in either cell type. Again, 3-NPA caused a decrease in ARNT protein levels in both Hep G2 and T-47D cell types. All other samples from both cell types contained detectable ARNT protein. In Hep G2 cells the detectable ARNT protein was seen as multiple bands but this was not observed in T-47D cells. These could be due to post-translational modifications or antibody recognition of related proteins such as ARNT 2 or ARNT 3. Whole cell lysates were probed with an anti-p53 antibody to confirm protein loading. In cells incubated with media less p53 protein was detected in both cell types. The lower amount of protein present was reflected in the ARNT western blot. Slightly less p53 was observed in Hep G2 cells incubated with 3-NPA when compared to NaCl. This difference was also observed in the ARNT western blot but to a much greater extent. T-47D cells treated with 3-NPA had multiple p53 reactive bands which were of a lower molecular weight than in control samples. These

smaller p53 bands may be due to p53 protein that has not undergone post-translational modification for example by ubiquitin.

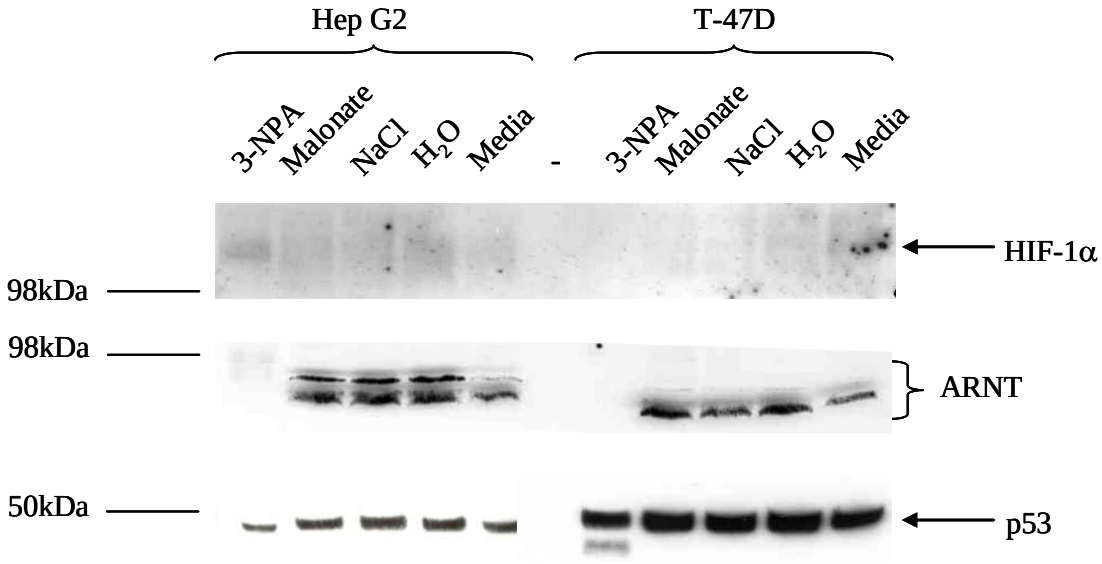


**Figure 4.12 Treatment of low density Hep G2 and T-47D cells with 3-NPA and Malonate.**

Hep G2 and T-47D cells seeded at low density (200 000 cells/well) were treated 24 hours after seeding with either 3-NPA pH7.6 (buffered with NaOH,) to a final concentration of 12.5mM, carrier control (NaCl), sterile $H_2O$, malonate pH7.4 to a final concentration of 12.5.mM or carrier control for malonate (media). Whole cell lysates prepared 24 hours after treatment were resolved by SDS-PAGE, western blotted and probed with anti-HIF-1α (Novus Biologicals), anti-ARNT (Novus Biologicals) and anti-p53 antibodies, as indicated. A blank lane was introduced between the two different cell lysates (-).Equal protein loading of the membranes was determined by Ponceau S staining (data not shown). Mobilities of standard proteins are indicated (sections 2.1.1 – 2.1.6). Figure represents one experiment (n=1).

**Key:** 3-NPA, 3-nitropropionic acid; ARNT, aryl hydrocarbon receptor nuclear translocator; $H_2O$, water; HIF-1α, hypoxia inducible factor 1α; kDa, kilodaltons; NaCl, sodium chloride; NaOH, sodium hydroxide.

Following this experiment it was decided to concentrate research in Hep G2 cells because of the differences in HIF-1α and ARNT protein levels and also because of the wild-type p53 content. Pheochromocytoma tumours expressing mutated SDH B have so far, not been associated with any mutations in p53 therefore Hep G2 and not

T-47D cells may offer a better model for chemical SDH B inhibition due to their wild-type p53 status.

To confirm the Hep G2 results observed in figure 4.12 the above experiment was repeated solely in Hep G2 cells. Whole cell lysates, prepared 24 hours after treatment were resolved by SDS-PAGE, western blotted and probed with anti HIF-1α, anti ARNT and anti-p53 antibodies (figure 4.13). To confirm that the HIF-1α and ARNT results were not due to some form of protein modification at the site of antibody binding, alternative antibodies were employed that recognised distinct epitopes on the two proteins. Figures 4.7 -4 .12 utilised antibodies from Novus Biologicals that recognised HIF-1α amino acid residues 432-528 and ARNT amino acid residues 496-789. The BD Biosciences antibodies used in figure 4.13 recognised HIF-1α amino acid residues 610-727 and ARNT amino acid residues 461-574. DFO treated Hep G2 cell lysate was used as a positive control for HIF-1α identification (figure 4.13).

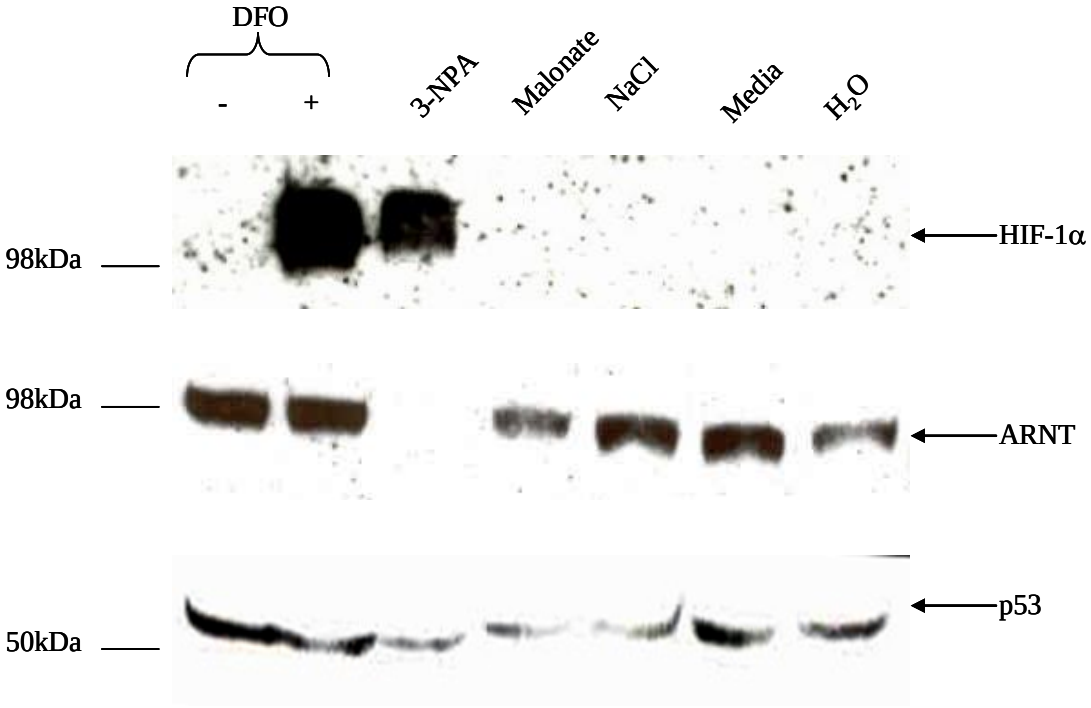


**Figure 4.13 The effect of 3-NPA and malonate treatment on low density Hep G2 cells.**

Hep G2 cells seeded at low density (200 000 cells/well) were treated 24 hours after seeding with either 3-NPA pH7.6 (buffered with NaOH,) to a final concentration of 12.5mM, carrier control (NaCl), sterile $H_2O$, malonate pH7.4 to a final concentration of 12.5.mM or carrier control for malonate (media). Whole cell lysates prepared 24 hours after treatment. As a positive control for HIF-1-α protein detection Hep G2 whole cell lysates were prepared six hours after treatment with either DFO (+) to a final concentration of 100μM or carrier control (-) as indicated. Whole cell lysates were resolved by SDS-PAGE, western blotted and probed with anti-HIF-1α (BD Biosciences), anti-ARNT (BD Biosciences) and anti-p53 antibodies as indicated.. Protein loading of the membranes was determined by Ponceau S staining (data not shown). Mobilities of standard proteins are indicated (sections 2.1.1 – 2.1.6). Figure represents one experiment (n=1)

**Key:** 3-NPA, 3-nitropropionic acid; ARNT, aryl hydrocarbon receptor nuclear translocator; DFO, desferrioxamine; $H_2O$, water; HIF-1α, hypoxia inducible factor 1α; kDa, kilodaltons; NaCl, sodium chloride; NaOH, sodium hydroxide.

Cells treated with 3-NPA showed an increase in HIF-1α protein when compared to NaCl. Malonate did not induce any detectable HIF-1α protein. No HIF-1α protein was detected in either $H_2O$ or media treated samples. ARNT protein was detectable in all samples except cells treated with 3-NPA where no ARNT protein was detected

(fig. 4.13). Protein loading was confirmed by probing samples with an anti-p53 antibody (figure 4.13).

Independent experiments using antibodies with distinct epitopes confirmed the reduction of ARNT protein levels in cells treated with 3-NPA. No constitutive HIF-1α expression was detected in multiple samples in repeated experiments on low density Hep G2 cultures except if treated with 3-NPA. This confirmed the possibility that high cell density was capable of inducing HIF-1α accumulation. 3-NPA treatment of Hep G2 cells induced a clear accumulation of HIF-1α protein, relative to p53 protein. Malonate treatment resulted in no appreciable difference in protein levels.

### *4.2.6 Time course of the effect of 3-NPA treatment on HIF-1α and ARNT protein levels.*

The increase in HIF-1α protein and the decrease in ARNT protein observed in previous experiments could have been due to two distinct pathways. To determine whether the two phenomena were coincident, or one happened before the other and therefore might be causal of the other a time-course of 3-NPA treatment of Hep G2 cells was performed. 24 hours after seeding at low density (200 000 cells/well) a whole cell lysate of untreated cells was prepared. Remaining cells were treated 24 hours after seeding with either 12.5mM 3-NPA pH 7.6, DFO to a final concentration of 100μM or respective carrier controls for each chemical. Whole cell lysates were prepared at 1, 3, 8 and 24 hours after treatment. Lysates were resolved by SDS-PAGE, western blotted and probed with anti-HIF-1α, anti ARNT and anti-p53 antibodies (figure 4.14). A repeat of the above experiment was performed to confirm the results obtained (figure 4.15).

No HIF-1α protein could be detected in any sample at 0 or 1 hours in either experiment (figures 4.14 and 4.15). At 3 hours no HIF-1α could be detected in any sample in figure 4.14. This observation was confirmed in figure 4.15 except for DFO treated cells. At 8 hours HIF-1α protein could only be detected in cells treated with DFO in figure 4.14 however, figure 4.15 showed elevated levels of HIF-1α protein in

3-NPA and DFO treated cells when compared to the relevant controls. Both figures showed elevated levels of HIF-1α protein in 3-NPA and DFO treated cells when compared to relevant controls at 24 hours. ARNT protein could be detected in all samples at 0, 1 and 3 hours for both experiments. At 8 and 24 hours, in both experiments there was a noticeable reduction in ARNT protein in cells treated with 3-NPA when compared to NaCl treated cells. The elevated HIF-1α and reduced ARNT protein levels were not due to a difference in protein loading between samples as indicated by the level of p53 protein present in each sample. Even protein loading was also confirmed by Ponceau S staining of the membranes.

The chemical treatment of Hep G2 cells with an SDH inhibitor was intended to create a model for succinate dehydrogenase mutations in pheochromocytoma tumours. The published literature so far has only identified mutations in *SDH B* or *SDH D* that pre-dispose an individual to pheochromocytoma tumour development. It was therefore of interest to determine whether chemical inhibitors of SDH had any effect on SDH B protein levels. The effect on SDH D protein levels could not be investigated due to the lack of a commercially available antibody. Samples from figure 4.15 were additionally probed with an anti-SDH B antibody. No change in SDH B protein levels was observed in any sample at any time-point therefore SDH B seemed to be a suitable as a second loading control.

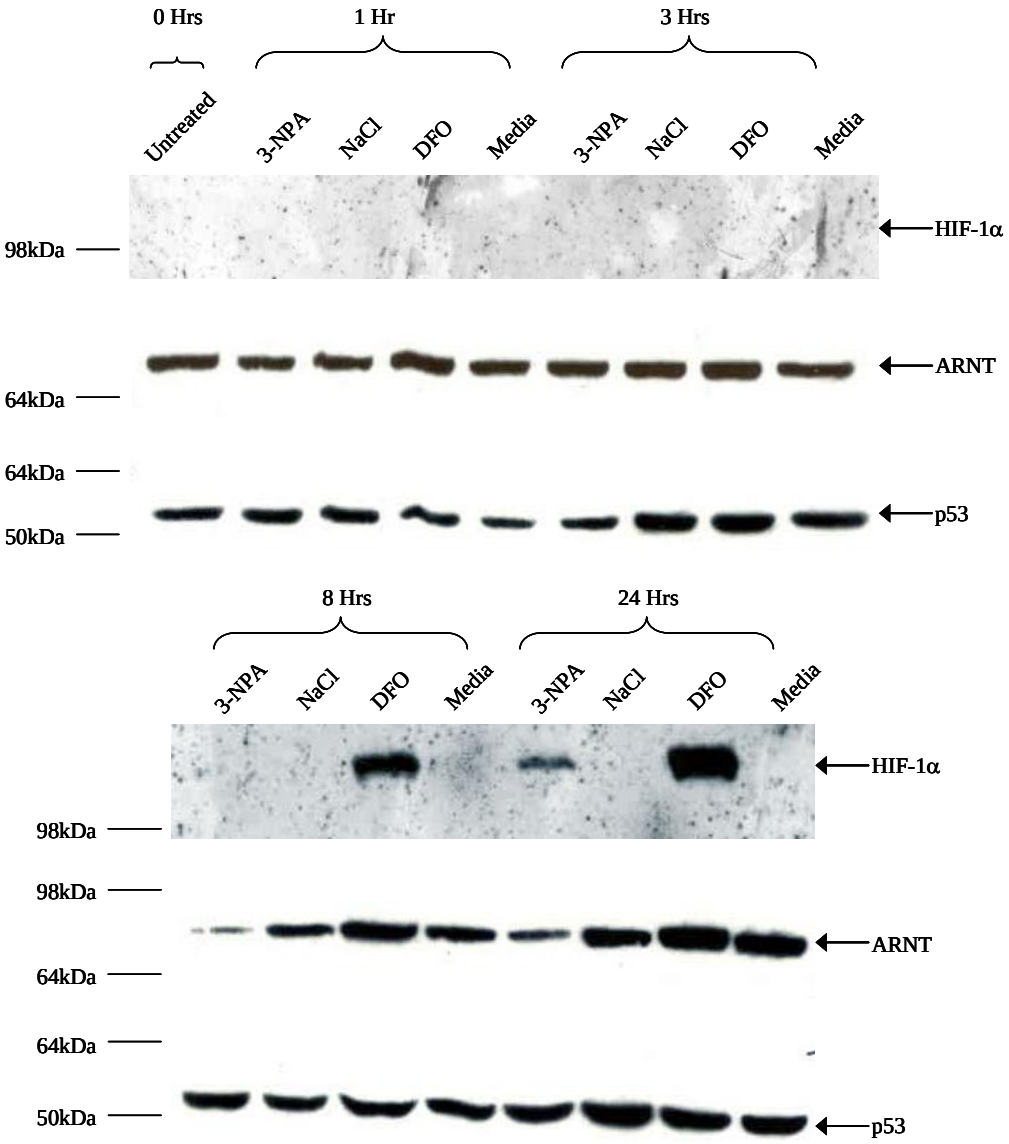


**Figure 4.14 The effect of 3-NPA treatment of Hep G2 cells on HIF-1α and ARNT protein levels at different time points.**

Hep G2 cells were seeded at low density (200 000 cells/well). 24 hours after seeding cells were either left untreated and lysed (0hr) or treated with 12.5mM 3-NPA pH7.6 (buffered with NaOH, 3-NPA), 100μM DFO (DFO) or their respective carrier controls (NaCl or media). Whole cell lysates for each treatment were prepared at the time points indicated above. Lysates were resolved by SDS-PAGE, western blotted and probed with anti HIF-1α (BD Biosciences), anti ARNT (BD Biosciences) and anti-p53 antibodies. Membranes were Ponceau S stained to determine protein loading (data not shown). Mobilities of standard proteins are indicated (sections 2.1.1 -2.1.6). Figure represents one expermiment (n=1).

**Key:** 3-NPA, 3-nitropropionic acid; ARNT, aryl hydrocarbon receptor nuclear translocator; DFO, desferrioxamine; $H_2O$, water; HIF-1α, hypoxia inducible factor 1α; hrs, hours; kDa, kilodaltons; NaCl, sodium chloride; NaOH, sodium hydroxide.

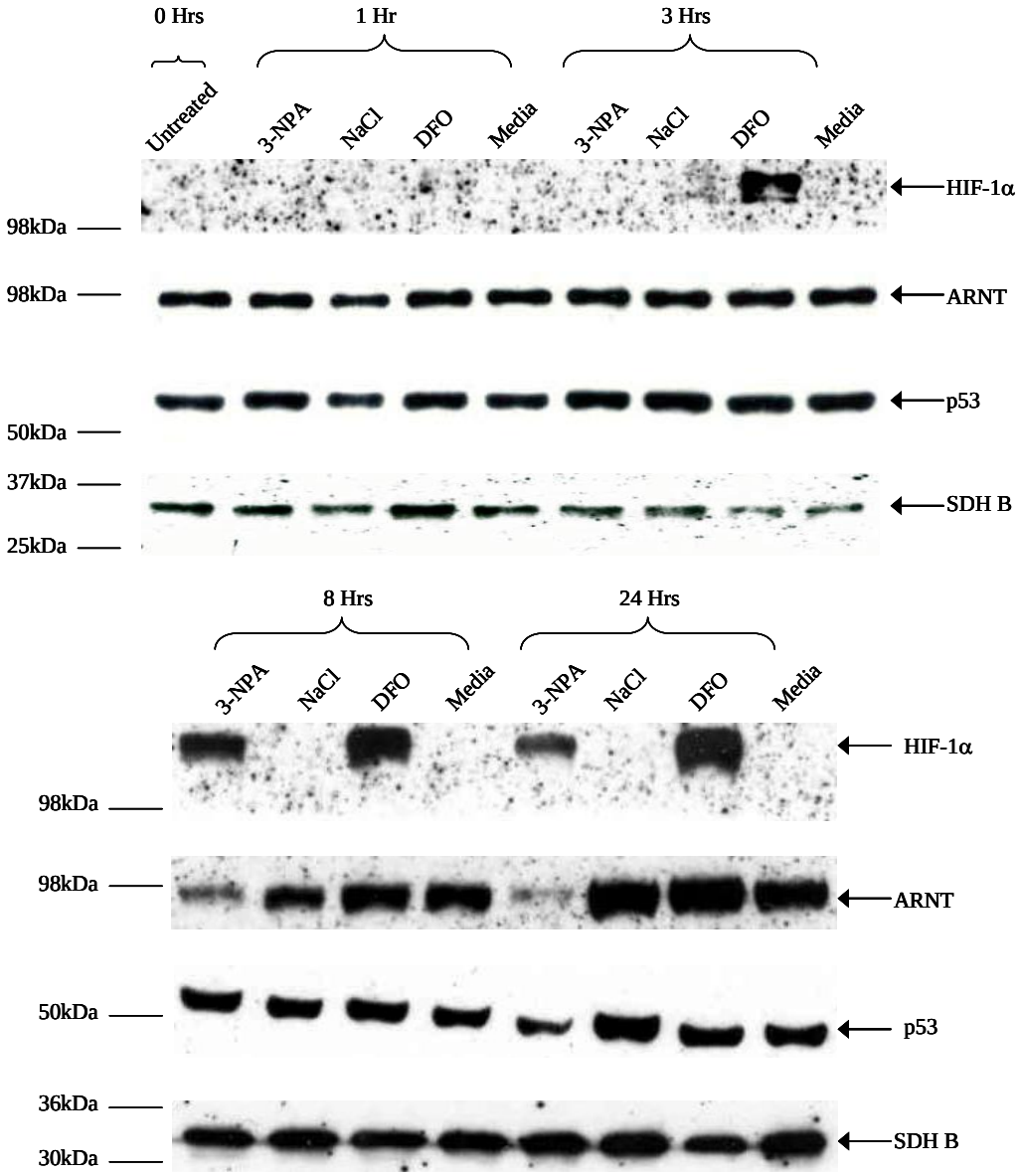


**Figure 4.15 Repeated time-course of the effect of 3-NPA treatment of Hep G2 cells on HIF-1α and ARNT protein levels**

Hep G2 cells were seeded at low density (200 000 cells/well). 24 hours after seeding cells were either left untreated and lysed (0hr) or treated with 12.5mM 3-NPA pH7.6 (buffered with NaOH, 3-NPA), 100μM DFO (DFO) or their respective carrier controls (NaCl or media). Whole cell lysates for each treatment were prepared at the time points indicated above. Lysates were resolved by SDS-PAGE, western blotted and probed with anti HIF-1α (BD Biosciences), anti ARNT (BD Biosciences) and anti-p53 antibodies. Membranes were Ponceau S stained to determine protein loading (data not shown). Mobilities of standard proteins are indicated (sections 2.1.1 -2.1.6). Figure represents one experiment (n=1).

**Key:** 3-NPA, 3-nitropropionic acid; ARNT, aryl hydrocarbon receptor nuclear translocator; DFO, desferrioxamine; $H_2O$, water; HIF-1α, hypoxia inducible factor 1α; hrs, hours; kDa, kilodaltons; NaCl, sodium chloride; NaOH, sodium hydroxide; SDH B, succinate dehydrogenase B.

Figures 4.14 and 4.15 indicated that p53 protein levels remained relatively constant at each time-point irrespective of the imposed treatment conditions. SDH B protein levels also remained unchanged at each time-point irrespective of the treatment cells were subjected to. ARNT protein levels remained constant in all samples between 0 and 3 hours however at 8 and 24 hours protein levels fell in cells subjected to 3-NPA treatment but remained constant in control and DFO treated samples (figures 4.14 and 4.15). HIF-1α protein levels were more un-predictable, in figure 4.14, HIF-1α protein could be detected in samples treated with DFO at 8 hours yet in figure 4.15, HIF-1α was clearly detected in DFO treated cells at 3 hours. HIF-1α was detected in samples treated with 3-NPA at 24 hours in figure 4.14 but at the earlier time-point of 8 hours in figure 4.15. The detection of HIF-1α in samples treated with 3-NPA always happened at the time-point following HIF-1α detection in DFO treated cells (figure 4.14 and 4.15) suggesting that DFO acts more quickly than 3-NPA. Figure 4.15 showed the elevation of HIF-1α protein levels and the disappearance of ARNT protein levels occurring at the same time-point however this was not the case in figure 4.14. The discrepancy between the time-courses with regard to the time at which HIF-1α protein levels became elevated and ARNT protein levels reduced made interpretation of any putative relations between the respective pathways involved difficult to determine.

### *4.2.7 The effect of 3-NPA treatment of Hep G2 cells on the transcriptional activity of an HRE driven transcription reporter gene.*

HIF-1, a heterodimer comprised of the subunits HIF-1α and ARNT, is known to drive the hypoxia responsive transcription of genes containing an HRE promoter, only when both subunits are present. To determine whether the increase in HIF-1α protein levels and decrease in ARNT protein levels caused by the treatment of Hep G2 cells with 3-NPA could affect the transcription of hypoxia responsive genes, a transcription reporter assay was utilised. Hep G2 cells, seeded at low density (100 000 cells/well), were transfected in triplicate 24 hours after seeding with either test plasmid, SV40 control plasmid or CMV control plasmid (pGL3prevPGK, pGL3control or pCMVluc, respectively, as described in sections 2.1.12 and 3.3.5). All wells were also co-transfected with a plasmid expressing *Renilla* luciferase (pRL-

SV40), as an internal control to normalise transfection efficiencies. 48 hours after seeding cells were treated with 12.5mM 3-NPA pH 7.6, 3-NPA carrier control (NaCl), 100μM DFO or DFO carrier control (media). Cells were lysed 72 hours after seeding/24 hours after chemical treatment. Cell lysates were assayed for firefly luciferase activity and corrected against *Renilla* luciferase activity (figure 4.16).

Figure 4.16 shows the results from two independent experiments. The treatment of cells with DFO was used as a positive control for HRE dependent transcription of a luciferase reporter gene. In both experiments DFO treated cells (yellow) exhibited a strong HRE dependent expression of the luciferase reporter gene when compared to control treated cells (green). The experiment represented in the upper panel of figure 4.16 showed a 42 fold-induction of HRE dependent luciferase expression in cells treated with DFO when compared to control treated cells. The second experiment (figure 4.16, lower panel) showed a 19 fold induction for the same treatments. Very little fold induction of HRE dependent luciferase expression was observed in the upper panel of figure 4.16 when 3-NPA treated cells (blue) were compared to NaCl treated cells (purple) however a 3 fold induction was seen in the lower panel.

There was no significant difference in relative luciferase ratios between treatments in cells transfected with SV40 control in one experiment (figure 4.16, upper panel). The repeat experiment (lower panel) showed an increase in the relative luciferase ratio value for cells treated with 3-NPA when compared to NaCl and in cells treated with DFO when compared to media however the fold inductions of these increase were negligible.

CMV promoter driven luciferase reporter gene transcription (CMV control) was elevated in DFO treated cells when compared to carrier control in both experiments although the fold induction was less than two in both cases. This mimicked the results observed in DFO cells transfected with the test plasmid. Cells treated with 3-NPA demonstrated an almost 2 fold reduction of the transcription of the luciferase reporter gene under control of the CMV promoter when compared to carrier control in both experiments.

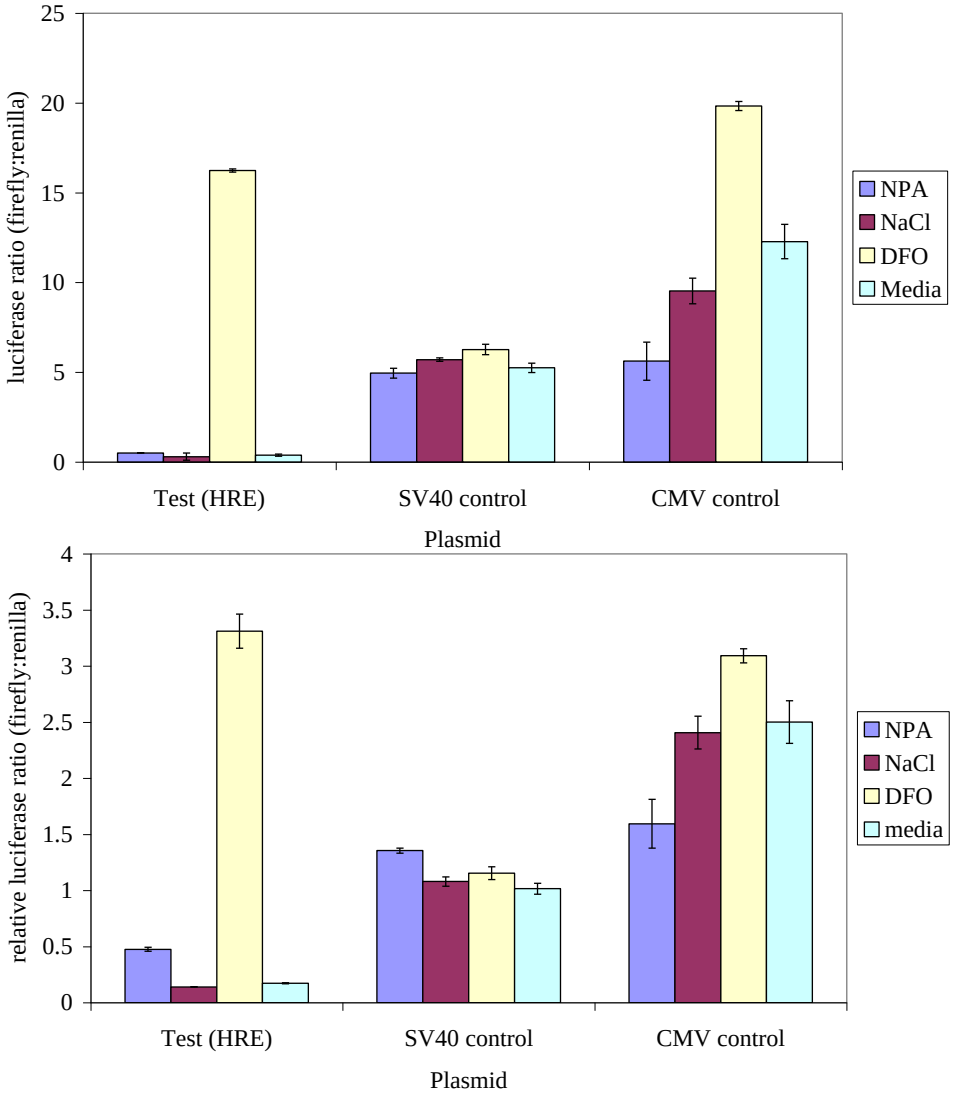


**Figure 4.16 HIF responsive transcriptional reporter assays of 3-NPA treated Hep G2 cells.**

Hep G2 cells seeded at low density (100 000 cells/well) were transfected in triplicate 24 hours after seeding with test (HRE) , SV40 control or CMV control plasmids (sections 2.1.12 and 3.3.5). All wells were also co-transfected with a plasmid expressing *Renilla* luciferase (pRL-SV40). 24 hours after transfection cells were treated with 12.5mM 3-NPA pH 7.6 (buffered with NaOH, blue), carrier control for 3-NPA (NaCl, purple), 100μM DFO (yellow) or DFO carrier control (media, green). Whole cell lysates were prepared 24 hours after chemical treatment (72 hours after seeding). Lysates were assayed for firefly luciferase activity and corrected against *Renilla* luciferase activity to normalise for transfection efficiencies using the Dual-luciferase reporter assay system (Promega, section 2.1.13). Results shown are from two independent experiments (n=2). Error bars are ± S.D.

**Key:** 3-NPA, 3-nitropropionic acid; CMV, cytomegalovirus; DFO, desferrioxamine; HIF, hypoxia inducible factor; HRE, hypoxia responsive element; NaCl, sodium chloride; NaOH, sodium hydroxide; S.D., Standard Deviation

ARNT and HIF-1α are subunits that comprise HIF-1 and both must be present for transcriptional activation. The depletion of ARNT protein levels by 3-NPA treatment of cells, as previously demonstrated (figures 4.10 - 4.15, inclusive), was expected to abrogate the transcriptional activation of a HRE dependent luciferase reporter gene. However, the three fold induction of an HRE dependent luciferase reporter gene in cells treated with 3-NPA when compared to NaCl contradicts this hypothesis (figure 4.16, lower panel). One possibility for this contradiction is the observation in 3-NPA time-course studies that 3-NPA induced HIF-1α protein levels before ARNT protein levels were fully depleted (figures 4.14 and 4.15). Therefore, if 3-NPA induced HIF-1α protein levels before ARNT protein levels were depleted in cells transfected with an HRE dependent luciferase reporter gene, then a low level of transcription would occur as shown in figure 4.16.

### *4.2.8 The effect of 3-NPA on DFO treated Hep G2 cells.*

In order to further explore the outcome of ARNT depletion by 3-NPA, experiments were carried out to assess whether 3-NPA depletes ARNT in DFO-induced Hep G2 cells. Hep G2 cells were seeded at low density (200 000 cells/well). 24 hours after seeding cells were left untreated or treated with; carrier controls for 3-NPA (NaCl) and DFO (media), 100μM DFO and 3-NPA carrier control, 12.5mM 3-NPA pH 7.6 and DFO carrier control or 12.5mM 3-NPA pH 7.6 and 100μM DFO. Whole cell lysates were prepared 24 hours after treatment. Lysates were resolved by SDS-PAGE, western blotted and probed with anti-HIF-1α, anti-ARNT, anti-p53, anti SDH-B and anti-PTEN antibodies (figure 4.17).

No detectable HIF-1α protein was present in untreated cells or cells treated with carrier controls only in either experiment. Cells treated with 3-NPA and media contained a small amount of detectable HIF-1α protein when compared to cells treated with DFO and NaCl or cells treated with 3-NPA and DFO. The largest amount of detectable HIF-1α was observed in cells treated with DFO and NaCl. The effect of 3-NPA on the induction of HIF-1α by DFO appeared to be one of suppression, because visibly less HIF-1α protein was detectable in cells treated with 3-NPA and DFO than those treated with NaCl and DFO (figure 4.17). ARNT protein

was detectable in all cells except those treated with 3-NPA. Equal protein loading was confirmed by Ponceau S staining and as an additional control by probing western blots with anti-p53. Equal protein loading of the membranes was obtained in the second experiment (figure 4.17, right hand panel) however less protein was present in samples treated with 3-NPA and media in the first experiment (figure 4.17 left hand panel). This reduction in protein was not observed in western blots probed with an anti-SDH B antibody as an additional loading control. In both experiments the levels of protein detected using an anti-SDH B antibody is lower in cells treated with chemicals i.e. 3-NPA and DFO when compared to untreated cells or cells treated with controls (media and NaCl).

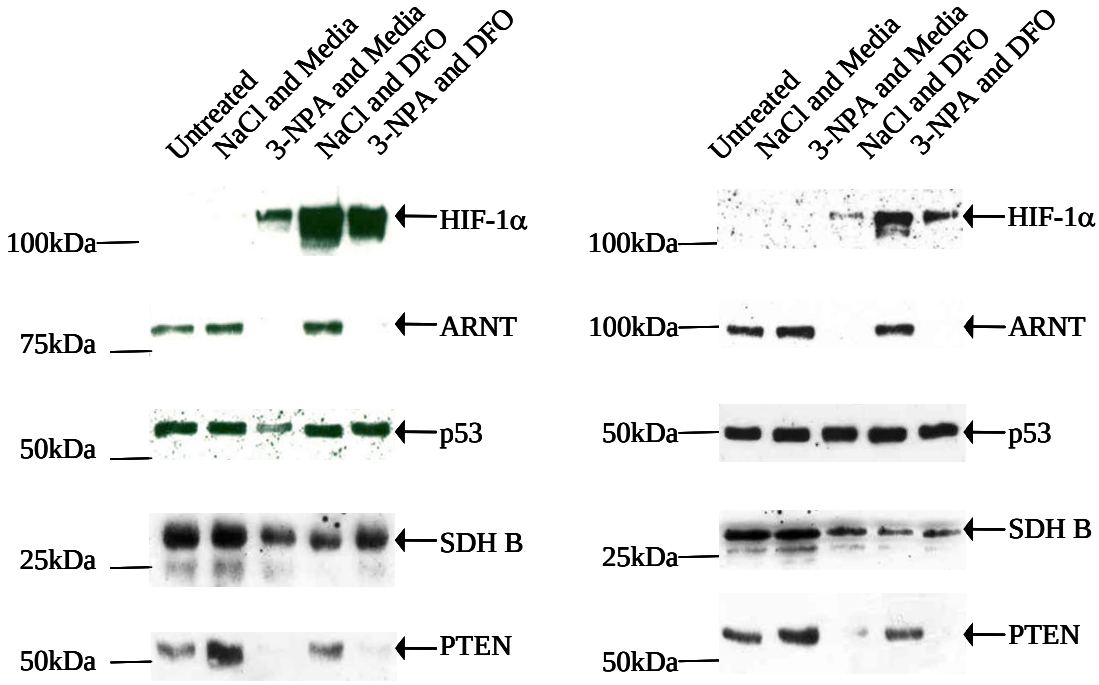


**Figure 4.17 The effect of 3-NPA on protein levels in DFO treated Hep G2 cells.**

Hep G2 cells seeded at low density (200 000 cells/well) were either left untreated 24 hours after seeding or were treated with carrier controls (NaCl and media), 12.5 mM 3-NPA pH7.6 and DFO carrier control (3-NPA and media), 100μM DFO and 3-NPA carrier control (DFO and NaCl) or 12.5mM 3-NPA pH7.6 and 100μM DFO (3-NPA and DFO). Whole cell lysates were prepared 24 hours after treatment, resolved by SDS-PAGE, western blotted and probed with anti HIF-1α (BD Biosciences), anti-ARNT (BD Biosciences), anti-p53, anti-SDH B and anti-PTEN antibodies. Membranes were Ponceau S stained to determine protein loading. Mobilities of standard proteins are indicated. Each panel of western blots represents an independent experiment (n=2).

**Key:** 3-NPA, 3-nitropropionic acid; ARNT, aryl hydrocarbon receptor nuclear translocator; DFO, desferrioxamine; HIF-1α, hypoxia inducible factor 1α; kDa, kilodaltons; NaCl, sodium chloride; NaOH, sodium hydroxide; PTEN, phosphatase and tensin homologue deleted on chromosome ten; SDH B, succinate dehydrogenase B.

To determine whether the reduction in ARNT protein levels resulting from 3-NPA treatment was solely restricted to the nucleus whole cell lysates were resolved by SDS-PAGE, western blotted and probed with an anti-PTEN antibody (figure 4.17). The cellular localisation of PTEN is cell type dependent, for instance in epithelial cells such as those of skin, colon and breast the majority of PTEN is localised in the

cytoplasm. In contrast, neurons and fibroblasts have a high proportion of PTEN localised in the nucleus. No published literature was available about the cellular localisation of PTEN in hepatoma cells. However, PTEN is involved in the PI3K/AKT pathway which occurs at the plasma membrane. This involves at least a small proportion of PTEN protein being localised to the plasma membrane (Reviewed by Sulis and Parsons. 2003). PTEN protein was detected in control samples and in cells treated with DFO and NaCl but no protein was detected in cells treated with 3-NPA and media or with 3-NPA and DFO. This finding paralleled the results observed for ARNT protein levels.

A transcription reporter assay was utilised to determine whether the apparent differences in HIF-1α and ARNT protein levels observed between control samples and samples treated with DFO and 3-NPA (figure 4.17) could result in a change in the transcriptional response of a firefly luciferase reporter gene under the control of an HRE containing promoter. Hep G2 cells were seeded at low density (100 000 cells/well). 24 hours after seeding cells were transfected in triplicate with test plasmid, SV40 control plasmid or CMV control plasmid (pGL3prevPGK, pGL3control or pCMVluc, respectively, section 2.1.12). All wells were co-transfected with a plasmid expressing *Renilla* luciferase (pRL-SV40), as an internal control to normalise transfection effieciencies. 48 hours after seeding (24 hours after transfection) cells were either left untreated or treated with NaCl (3-NPA carrier control) and media (DFO carrier control), 12.5mM 3-NPA pH 7.6 (buffered with NaOH) and media, 100μM DFO and NaCl or 12.5mM 3-NPA pH 7.6 and 100μM DFO. Whole cell lysates were prepared 24 hours after treatment (72 hours after seeding) and assayed for firefly luciferase activity before correction against *Renilla* luciferase activity (figure 4.18 which shows the results of two independent experiments).

Hep G2 cells were treated with DFO and NaCl as a positive control for HRE responsive luciferase expression (yellow). In both experiments, Hep G2 cells treated with DFO and NaCl induced luciferase expression compared with carrier controls (blue). The experiment represented in the upper panel if figure 4.18 showed a 37 fold induction of HRE dependent luciferase expression in cells treated with DFO and NaCl when compared to control treated cells (media and NaCl). The second

experiment showed a 33 fold induction for the same treatments (figure 4.18, lower panel). However, cells treated with DFO and 3-NPA (green) exhibited a twofold reduction and a 19 fold reduction in the level of luciferase expression when compared with the DFO and NaCl treated cells, indicating 3-NPA was affecting the DFO response in Hep G2 cells treated with both chemicals (figure 4.18 upper and lower panels, respectively). In both experiments cells treated with DFO and NPA exhibited a higher level of expression of a HRE dependent luciferase reporter gene than when compared to 3-NPA and media (burgundy).

Cells transfected with SV40 control did not exhibit any significant difference in luciferase reporter gene transcription between samples, in the first experiment (figure 4.18, upper panel). The repeat experiment showed a reduction in the relative luciferase ratio value for cells treated with DFO and 3-NPA when compared to media and NaCl, media and NPA and NaCl and DFO. However, in all cases this fold reduction was less than two.

The CMV control plasmid results exhibited the same luciferase expression pattern to those of the test plasmid samples (figure 4.18) except for the NaCl: DFO sample in the second experiment (figure 4.18, lower panel). The difference in results between the independent experiments with regard to cells treated with NaCl and DFO in the CMV control sample is difficult to account for.

However, results from these experiments indicated that NPA appears to have the ability to reduce HRE dependent luciferase expression, which if HIF related, could indicate that SDH inhibition via depletion of ARNT inhibits HIF function.

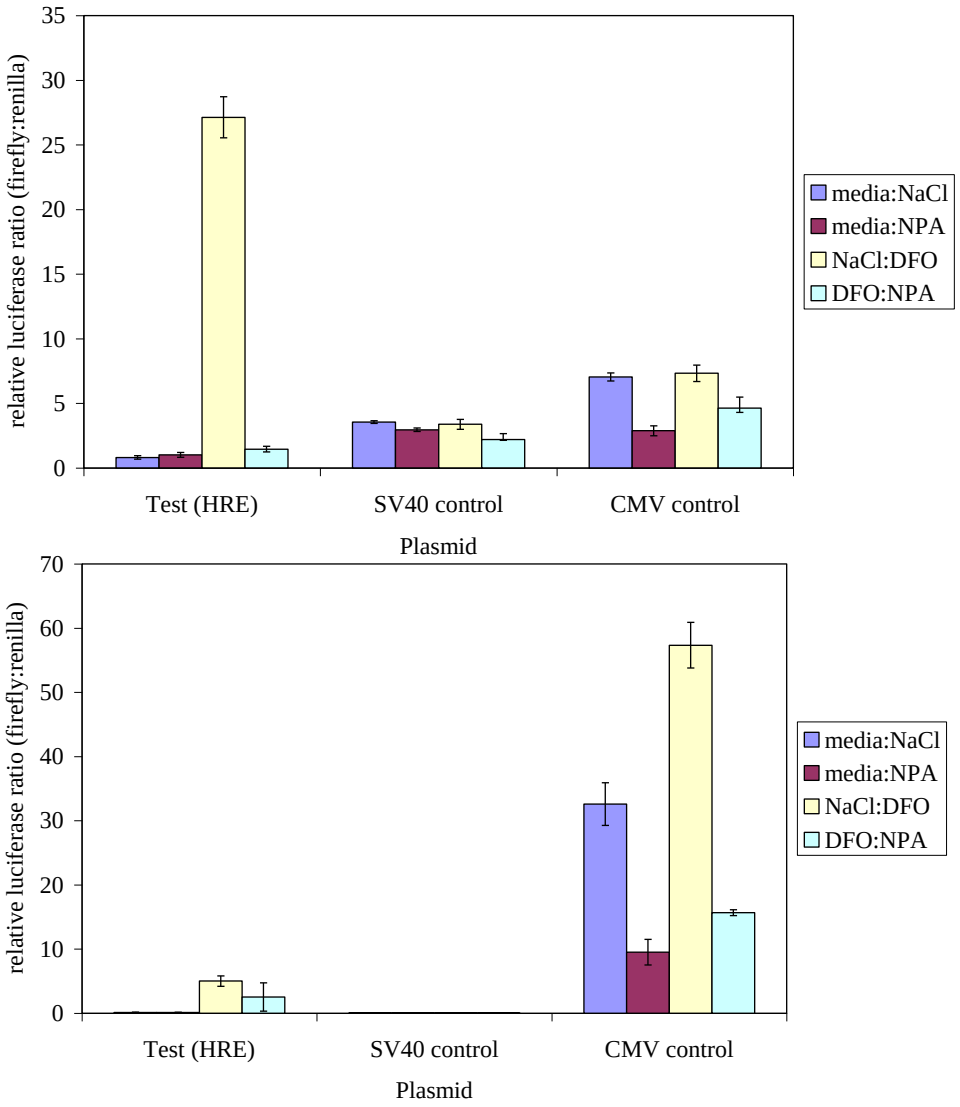


**Figure 4.18 The effect of 3-NPA on the DFO induced transcriptional response of a firefly luciferase reporter gene.**

Hep G2 cells seeded at low density (100 000 cells/well) were transfected in triplicate 24 hours after seeding with a test (HRE), SV40 control or CMV control plasmid. All wells were co-transfected with a plasmid expressing *Renilla* luciferase (pRL-SV40). 24 hours after transfection cells were treated with media and NaCl (carrier controls for DFO and 3-NPA respectively, blue bars), 12.5mM 3-NPA pH7.6 and media (purple bars), 100μM DFO and NaCl (yellow bars) or 12.5mM 3-NPA pH 7.6 and 100μM DFO (green bars). Whole cell lysates were prepared 24 hours after chemical treatment. Lysates were assayed for firefly luciferase activity and corrected against *Renilla* luciferase activity to normalise for transfection efficiencies using the Dual-luciferase reporter assay system (Promega, section 2.1.13). Results shown are from two independent experiments (n=2). Error bars are ± S.D.

**Key:** 3-NPA, 3-nitropropionic acid; CMV, cytomegalovirus; DFO, desferrioxamine; HIF, hypoxia inducible factor; HRE, hypoxia responsive element; NaCl, sodium chloride; NaOH, sodium hydroxide; S.D., Standard Deviation

### *4.2.9 The effect of 3-NPA treatment on membrane permeability.*

3-NPA treatment of Hep G2 cells caused a reduction in the detectable level of ARNT and PTEN. To determine whether the selective loss of these proteins was due to the cell membrane becoming compromised, cells were incubated with trypan blue, a dye used to distinguish the permeability of cell membranes. Non-permeable cell membranes result in non-stained cells and permeable membranes result in stained cells. Hep G2 cells were treated 24 hours after seeding at low density (200 000 cells/well) with either 12.5mM 3-NPA pH7.6 or carrier control (NaCl). Adherent and non-adherent cells were stained in trypan blue and counted in triplicate at 0 hours (untreated cells) and 1, 3, 8 and 24 hours after treatment (figure 4.19).

There was a progressive difference in total cell counts (i.e. adherent, non-adherent, non-permeable and permeable cell counts combined) between control (light blue) and 3-NPA (burgundy) treated cells after 3 hours. At 24 hours there was a greater than 2 fold difference in total cell count between carrier control treated cells and 3-NPA treated cells. This difference was paralleled in adherent non-permeable cells where there was a greater than 2 fold difference between control and 3-NPA treated cells (figure 4.19, light yellow and light green bars, respectively). The proportion of adherent permeable cells was very low whatever the treatment. Very little difference in cell number was observed between control treated adherent permeable cells (purple bars) and 3-NPA treated adherent permeable cells (salmon bars) at any time-point (figure 4.19). The amount of non-adherent cells was less than 1% of the total cell count under all circumstances. There were no statistically significant differences between permeable adherent or non-adherent cell counts whatever the treatment.

These results indicated that 3-NPA did not appear to have an effect on cell membrane permeability when compared to control treated cells. 3-NPA appeared to arrest Hep G2 proliferation when compared to control treated cells. This arrest of proliferation by 3-NPA coupled with depleted ARNT and PTEN protein levels may indicate a novel 3-NPA mode of action.

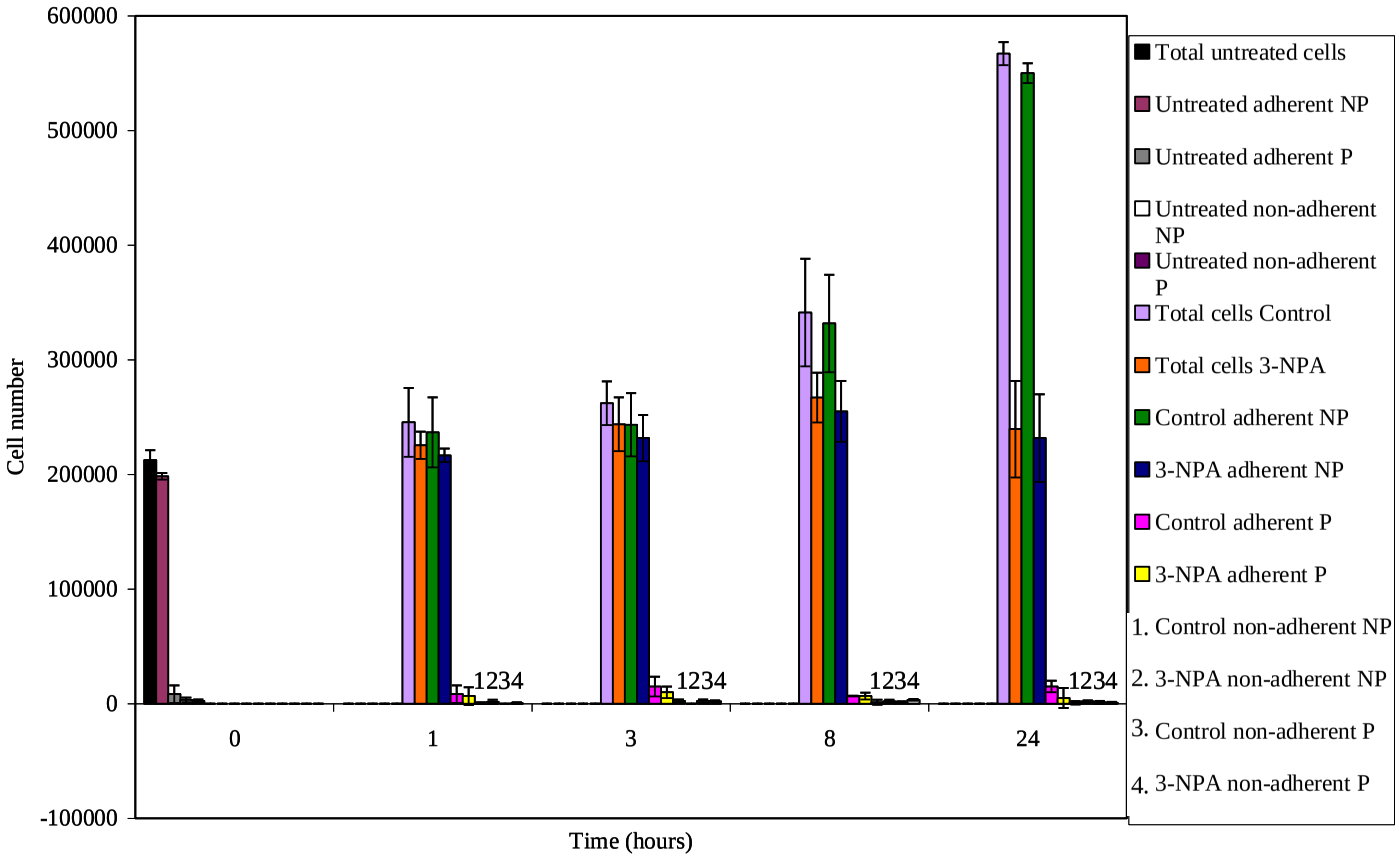


**Figure 4.19 The effect of 3-NPA on Hep G2 cell membrane permeability.**

Hep G2 cells seeded at low density (200 000 cells/well) were treated 24 hours after seeding with either 12.5mM 3-NPA pH 7.6 (buffered with NaOH) or carrier control (NaCl). In triplicate adherent and non-adherent cells were incubated with trypan blue and counted at 0 (untreated cells) 1, 3, 8 and 24 hour time-points for control and 3-NPA as indicated. Unstained cells were considered non-permeable (P) and stained cells considered permeable (P). Total cells (black, lilac and orange bars) encompass all adherent and non-adherent counts for each treatment.

### *4.2.10 The effect of lactacystin, a proteasomal inhibitor, on the 3-NPA induced disappearance of detectable ARNT protein levels.*

The discovery that 3-NPA did not affect cell membrane permeability appeared to infer that the selective loss of ARNT and PTEN was occurring via some other process. Due to the involvement of proteasomal degradation in the HIF pathway, an experiment was performed to determine whether 3-NPA induced ARNT suppression was due to a similar process. Lactacystin, a proteasomal inhibitor was used at a concentration of 20μM based on experiments performed by Salceda and Caro (1997). Hep G2 cells were treated 24 hours after seeding at low density (200 000 cells/well) with either 12.5mM 3-NPA pH 7.6 (buffered with NaOH) or carrier control (NaCl). Treated cells were co-incubated with either 20μM lactacystin or lactacystin carrier control (SF media). Whole cell lysates were prepared 8 hours after incubation (the earliest time-point of ARNT disappearance observed). Whole cell lysates were resolved by SDS-PAGE, western blotted and probed with anti-HIF-1α, anti-ARNT, anti-p53 and anti SDH B antibodies (figure 4.20).

If lactacystin was successfully inhibiting proteasomal degradation, HIF-1α protein levels would have been expected to increase when cells were treated with lactacystin however, this did not occur in cells treated with NaCl and lactacystin. Hep G2 cells treated with 3-NPA and lactacystin showed elevated levels of detectable HIF-1α protein compared to 3-NPA treated cells without lactacystin or NaCl treated cells with or without lactacystin (figure 4.20). 3-NPA has been shown to increase detectable HIF-1α protein levels in previous experiments, this was not the case in cells treated with 3-NPA without lactacystin. The increase in HIF-1α protein levels observed between cells treated with 3-NPA with or without lactacystin could solely be due to the action of lactacystin or, the combined effect of 3-NPA and lactacystin.

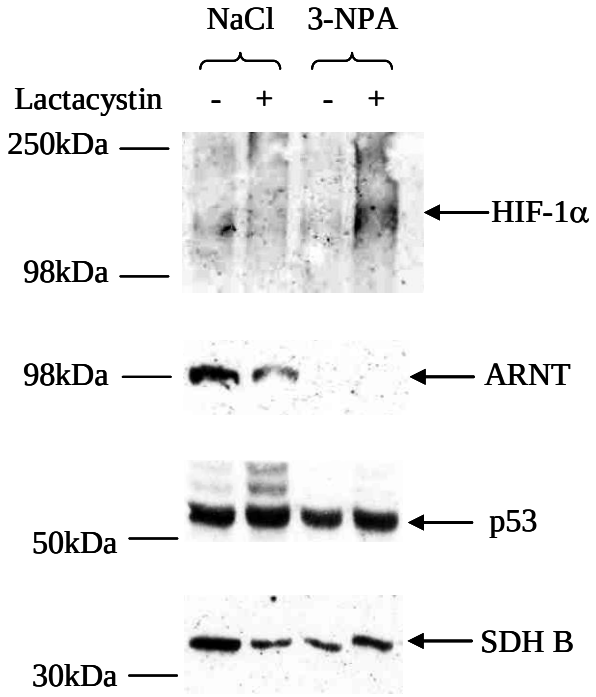


**Figure 4.20 The effect of the proteasomal inhibitor lacatcystin on 3-NPA induced ARNT disappearance.**

Hep G2 cells were treated 24 hours after seeding at low density (200 000 cells/well) with 12.5mM 3-NPA pH 7.6 (buffered with NaOH) or carrier control (NaCl). Treated cells were co-incubated with either 20μM lactacystin (+) or carrier control (-) as indicated. Whole cell lysates prepared after 8 hours were resolved by SDS-PAGE, western blotted and probed with anti-HIF-1α (BD Biosciences), anti-ARNT (BD Biosciences), anti-p53 and anti-SDH B antibodies, as indicated. Membranes were Ponceau S stained to confirm protein loading. Mobilities of standard proteins are indicated. Figure represents an independent experiment (n=1).

**Key:** 3-NPA, 3-nitropropionic acid; ARNT, aryl hydrocarbon receptor nuclear translocator; HIF-1α, hypoxia inducible factor-1α kDa, kilodaltons; NaCl, sodium chloride; NaOH, sodium hydroxide; SDH B, succinate dehydrogenase B.

Whole cell lysates were also probed with an anti-p53 antibody to determine whether lactacystin was active under these conditions. p53 is targeted for ubiquitin mediated proteasomal degradation by the binding of Hdm2 (Giaccia and Kastan., 1998). The effect of a proteasomal inhibitor would be to prevent p53 degradation. In cells treated with NaCl without lactacystin higher molecular weight protein species, possibly

representing ubiquitin modified p53, could be observed above the 50kDa standard protein marker. In cells treated with NaCl and lactacystin these species were more prominent. p53 was detectable in cells treated with 3-NPA, however higher molecular weight p53 species were only detected in cells not treated with 3-NPA, which suggests that the action of 3-NPA was affecting p53 ubiquitination in some way (figure 4.20).

No appreciable change in ARNT protein levels in response to lactacystin could be detected relative to SDHB and overall protein levels which were detected by Ponceau S staining (figure 4.20). Treatment of Hep G2 cells with 3-NPA caused the complete disappearance of detectable ARNT protein levels and lactacystin had no effect on this disappearance. This data suggested the selective loss of ARNT was not due to proteasomal degradation of the protein.

### *4.2.11 The effect of 3-NPA treatment on ARNT, PTEN and SDH B protein levels in PC12 cells.*

The chemical inhibition model used to determine the effects of SDH mutation in pheochromocytoma was developed in Hep G2 cells (sections 4.2.2 – 4.2.10). The Hep G2 cell line is derived from a hepatoma, therefore results observed in previous experiments may be specific to this cell type. To determine whether the results observed in Hep G2 cells were representative, experiments were performed in PC12 cells, a rat pheochromocytoma cell line. PC12 pheochromocytoma cells were not used in the development of the chemical inhibition model due to the lack of a commercially available HIF-1 antibody that could recognise rat protein.

PC12 cells were either left untreated or treated with 12.5mM 3-NPA pH 7.6 (buffered with NaOH), NaCl (carrier control for 3-NPA), 100μM DFO or media (DFO carrier control) 24 hours after seeding (200 000 cells/well). 24 hours after treatment whole cell lysates were prepared and resolved by SDS-PAGE, western blotted and probed with anti-ARNT, anti-PTEN and anti-SDH B antibodies (figure 4.21).

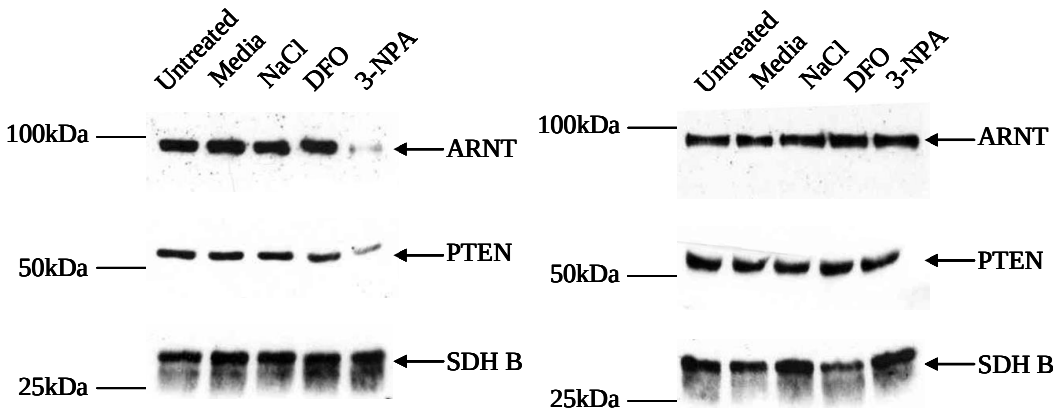


**Figure 4.21 The effect of 3-NPA treatment on PC12 cells.**

PC12 cells were seeded at low density (200 000 cells/well). 24 hours after seeding cells were left untreated or were treated with 12.5mM 3-NPA pH 7.6 (buffered with NaOH), NaCl (3-NPA carrier control), 100μM DFO or media (DFO carrier control). Whole cell lysates prepared 24 hours after treatment were resolved by SDS-PAGE, western blotted and probed with anti-ARNT (BD Biosciences), anti-PTEN and anti-SDH B antibodies, as indicated. Membranes were Ponceau S stained to confirm protein loading. Mobilities of standard proteins are indicated. Left and right-hand panels represent two independent experiments (n=2; sections 2.1.1 -2.1.6).

**Key:** 3-NPA, 3-nitropropionic acid; ARNT, aryl hydrocarbon receptor nuclear translocator; DFO, desferrioxamine; kDa, kilodaltons; NaCl, sodium chloride; NaOH, sodium hydroxide; PTEN, phosphatase and tensin homologue deleted on chromosome 10; SDH B, succinate dehydrogenase B.

Anti-HIF-1α and anti-p53 antibodies were not reactive with rat proteins and therefore were not used. 3-NPA treatment of PC12 cells resulted in a noticeable reduction of ARNT and PTEN protein levels in the first experiment (figure 4.21, left hand panel) but in the repeat experiment (right hand panel) no reduction was observed when compared to all other treatments. Equal protein loading of the membranes was confirmed by probing samples with an anti-SDH B antibody and by Ponceau S staining of the membranes (figure 4.21).

The lack of consistency from PC12 experiments made the results difficult to interpret. The first experiment seemed to suggest that 3-NPA mediated ARNT and PTEN loss was not Hep G2 specific but this was contradicted by the second experiment, due to an unknown variable of cell culture. From previous experiments it

was known 3-NPA mediated ARNT loss was not Hep G2 specific as ARNT loss was also observed in T-47D cells (figure 4.12).

## 4.3 The effect of RNAi inhibition of SDH B on HIF-1α protein function

### *4.3.1 siRNA design*

To determine whether the 3-NPA mediated up-regulation of HIF-1α and down-regulation of ARNT reflects the regulatory effects in tumours, a specific means of targeting SDH was employed in the form of RNA interference. The best cell system in which to study a model of SDH B inhibition would have been a well characterised pheochromocytoma cell line. The only cell line available that fitted this criterion was the rat pheochromocytoma cell line, PC12. At the time of designing the SDH B targeting siRNAs no SDH B mRNA or cDNA sequences for rat were available and the only commercial SDH B and HIF-1α antibodies had no specificity for rat protein. Therefore RNA interference experiments were performed in Hep G2 cells. This also provided continuity between the chemical inhibition model of SDH, where the majority of experiments were performed in Hep G2 cells, and the more specific RNA interference model which targeted SDH B.

An SDH B siRNA sequence was designed following the recommendations of Elbashir *et al* (2002) to target a 19 nucleotide sequence in human SDH B mRNA. This sequence corresponded to base pairs 362-384 of the human mRNA sequence (accession number gi22043306). The SDH B sense and anti-sense and control sense and anti-sense siRNAs were analysed using the Basic Local Alignment Search Tool (BLAST) at the National Center for Biotechnology Information (NCBI). The non-redundant (nr) and human expressed sequence tags (EST) databases were searched using blastn for nucleotide sequences that were a similar or exact match to the control and SDH B siRNA sequences. The SDH B targeting siRNA was only homologous to *Homo sapiens* SDH B mRNA. There was no similarity to any other *Homo sapiens* mRNA. The control siRNA did not show 100% identity to any other human mRNA.

### *4.3.2. Oligofectamine mediated transfection of Hep G2 cells*

Hep G2 cells were utilised in all experiments in this section for continuity purposes (section 4.2.5, paragraph 4 explains the reasons behind the original decision to use Hep G2 cells).

To determine whether Hep G2 cells could be transfected using Oligofectamine, cells were seeded at low density (100 000 cells/well). 24 hours after seeding, cells were transfected with oligofectamine only, FITC labelled DNA oligonucleotide (FITC-DNA) or FITC-DNA and oligofectamine. Cells were photographed by light microscopy, in a random field of view, 24 hours after transfection (figure 4.22 panels A, C and E).The same field of view was subjected to fluorescence microscopy and images were constructed after 400 integrations (figure 4.22 panels B, D and F). No fluorescence could be detected in Hep G2 cells transfected with oligofectamine only or FITC-DNA only. Almost 100% of Hep G2 cells, transfected with oligofectamine and FITC-DNA retained fluorescence, showing the protocol for siRNA transfection already in existence was likely to be suitable for Hep G2 siRNA transfection.

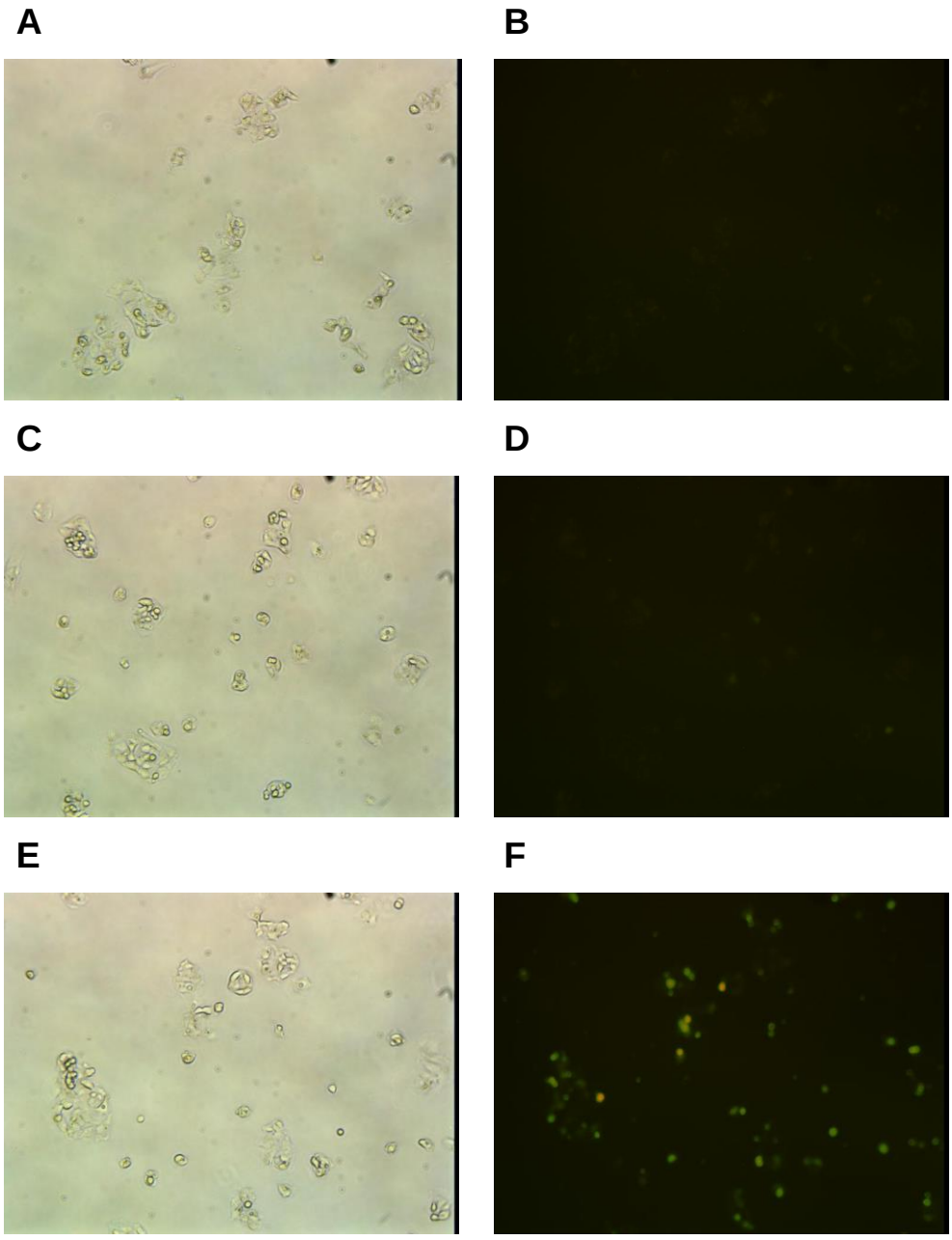


**Figure 4.22. Oligofectamine mediated transfection of Hep G2 cells with a FITC labelled DNA oligonucleotide.**

Hep G2 cells were seeded 100 000 cells/well. 24 hours after seeding cells were transfected with oligofectamine only (A and B), FITC labelled DNA oligonucleotide only (C and D) or FITC DNA oligonucleotide and oligofectamine (E and F). Cells were visualised 24 hours after transfection by light microscopy in a random field of view and photographed (A, C and E). This field of view was then subjected to fluorescence microscopy. Images were constructed after 400 integrations (B, D and F). Magnification ×100. Figure represents one experiment.

To determine whether Hep G2 cells could be transfected with duplexed siRNA, Hep G2 cells were seeded at low density (100 000 cells/well). 24 hours after seeding cells were transfected with oligofectamine only, a Cy3 labelled siRNA duplex (Cy3-siRNA) only or oligofectamine and Cy3-siRNA. 24 hours after transfection cells were visualised in a random field of view by light microscopy and photographed (figure 4.23 panels A, C and E). The same field of view was subjected to fluorescence microscopy and photographed after 200 integrations of the image at 100X magnification (figure 4.23 panels B, D and F).No fluorescence could be detected in cells transfected with oligofectamine only (figure 4.23 panel B). Fluorescence was observed in Hep G2 cells transfected with Cy3-siRNA only and Hep G2 cells transfected with oligofectamine and Cy3 (figure 4.23 panels D and F, respectively). Cy3-siRNA appears to have a level of background fluorescence that is exhibited in Hep G2 cells transfected with Cy3-siRNA only (figure 4.23 D). This could be due to the Cy3-siRNA being internalised by Hep G2 cells without the presence of transfection reagent. It is also possible that the Cy3-siRNA was sticking to the cell membrane. However, the intensity of fluorescence, as observed by the naked eye, is more intense in Hep G2 cells transfected with Cy3-siRNA and oligofectamine (figure 4.23 F).

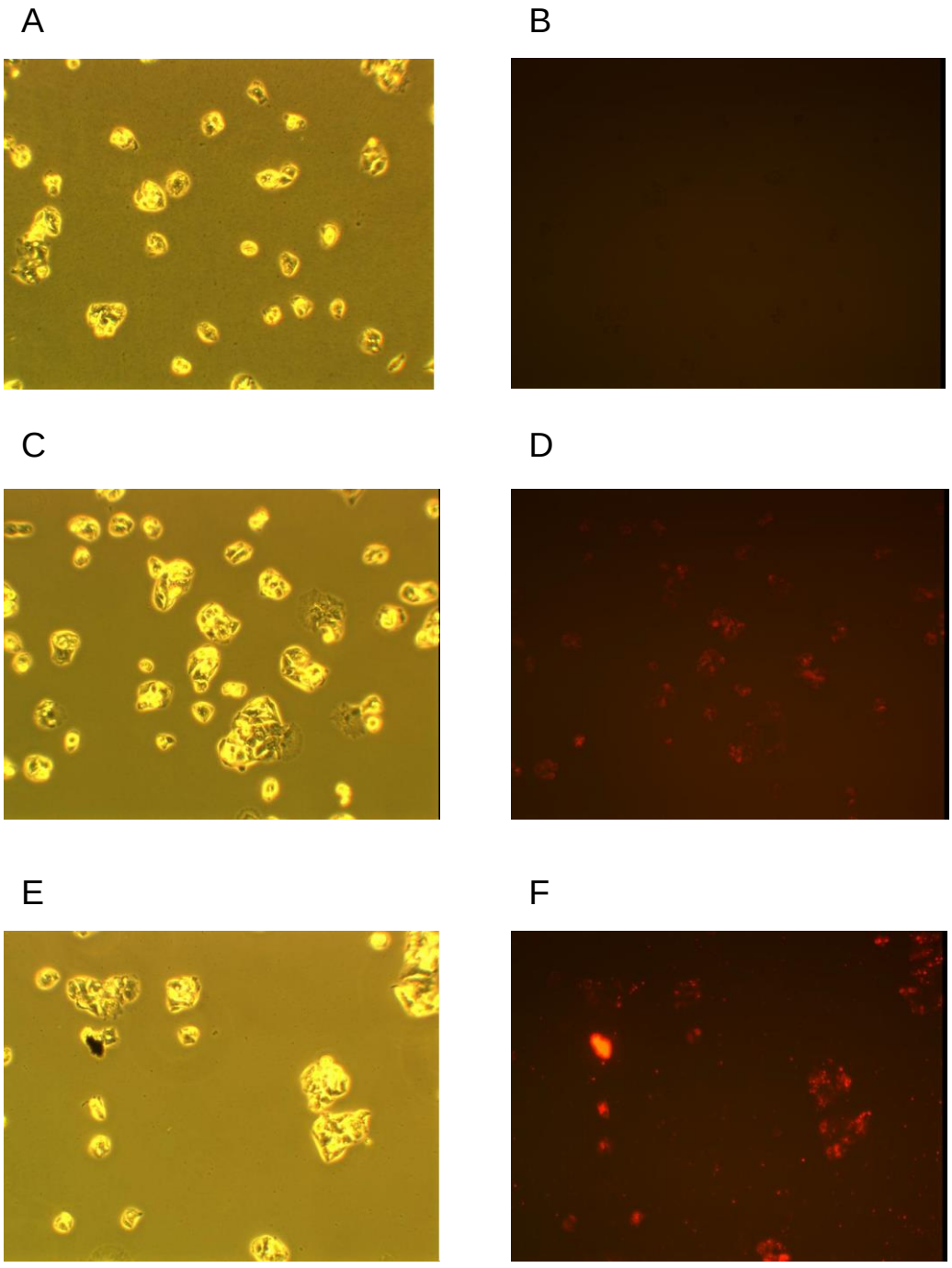


**Figure 4.23 Oligofectamine mediated transfection of Hep G2 cells with a Cy3 labelled siRNA duplex.**

Hep G2 cells were seeded 100 000 cells/well. 24 hours after seeding cells were transfected with oligofectamine only (A and B), Cy3 labelled siRNA duplex only (C and D) or Cy3 labelled siRNA duplex and oligofectamine (E and F). 24 hours after transfection cells were visualised by light microscopy in a random field of view and photographed (A, C and E). This field of view was then subjected to fluorescence microscopy and images were compiled after 200 integrations (B, D and F). Magnification X100. Figure represents one experiment.

### *4.3.3 Optimisation of RNA interference targeted towards SDH B.*

To determine the amount of siRNA that would give the best knockdown of SDH B protein, several optimisation experiments were carried out in a similar manner. Hep G2 cells were seeded at low density (100 000 cells/well). 24 hours after seeding each well was transfected with either control or SDH B siRNA in the amounts indicated in figure 4.24. 24 hours after the first transfection cells were either re-transfected with the same concentrations of appropriate siRNA or lysed in 2X SDS-PAGE loading buffer. Cells were also lysed 24 and 48 hours after the second transfection. Whole cell lysates were resolved by SDS PAGE, western blotted and probed with an anti-SDH B antibody (figure 4.24).

The preliminary optimisation experiment showed all four amounts of SDH B siRNA reduced the detectable amount of SDH B protein 24 hours after the first transfection, and 24 and 48 hours after the second transfection when compared to the relevant control lanes (figure 4.24 panels A-C, respectively). Densitometry of these results indicated that in all cases SDH B protein levels were reduced in cells treated with SDH B targeting siRNA. The maximum percentage reduction in SDH B protein levels was 62.2% and this was achieved 24 hours after the second transfection in cells targeted with 120nmol SDH B siRNA when compared to control targeted cells. Cells targeted with 240nmol SDH B siRNA at the same time point showed a similar level of SDH B protein reduction – 61.8% when compared to cells targeted with control siRNA. At 48 hours after the second transfection cells targeted with 120nmol or 240nmol SDH B siRNA still exhibited the highest percentage knockdown of SDH B protein when compared to control targeted cells, 46.1% and 50.7%, respectively, but percentage knockdown achieved 48 hours after the second transfection of siRNAs was not to the same level as observed at 24 hours post second transfection. 48 hours after the second transfection, samples from cells targeted with 120nmol, 240nmol or 360nmol SDH B siRNA appeared to produce a similar suppression of SDH B protein when compared to relevant control samples (figure 4.24, panel C). Densitometry of these results indicated that the maximum level of reduction in SDH B protein was achieved at each time point by cells targeted with 120nmol or

240nmol of SDH B siRNA. The maximum knockdown of SDH B protein was 62.2% in cells targeted with 120nmol of occurred 24 hours after the second transfection of SDH B siRNA. A second experiment was carried out to confirm SDH B protein suppression in Hep G2 cells using 120nmol SDH B siRNA (figure 4.24 panel D). However, SDH B protein suppression in this experiment was not as pronounced as in the preliminary optimisation experiment (figure 4.24 panels A-C). Densitometry of the results showed the maximum knockdown of SDH B protein 24 hours after the second transfection was 26.3% and at 48 hours the maximum knockdown was 59.5%. However, at 48 hours after the second transfection this level of knockdown was not consistent in both SDH B targeted samples. This could be due to the combined effects of transfection efficiency and the transient nature of RNA interference. Therefore, a final optimisation experiment was carried out to determine which of either 120nmol or 240nmol SDH B siRNA provided the largest suppression of SDH B protein. p53 was used a protein loading control for this experiment (figure 4.24 panels E to J).This experiment clearly indicated that both amounts of SDH B targeting siRNA were capable of suppressing SDH B protein levels when compared to their respective controls. However, 48 hours after the second transfection, the level of SDH B protein suppression was more pronounced in samples treated with 240nmol SDH B siRNA. Densitometry of the results showed 48 hours after the second transfection of SDH B siRNA that the percentage knockdown of SDH B protein was 44% for 120nmol and 46.9% for 240nmol. Based on these experiments 240nmol SDH B siRNA was utilised in further experiments.

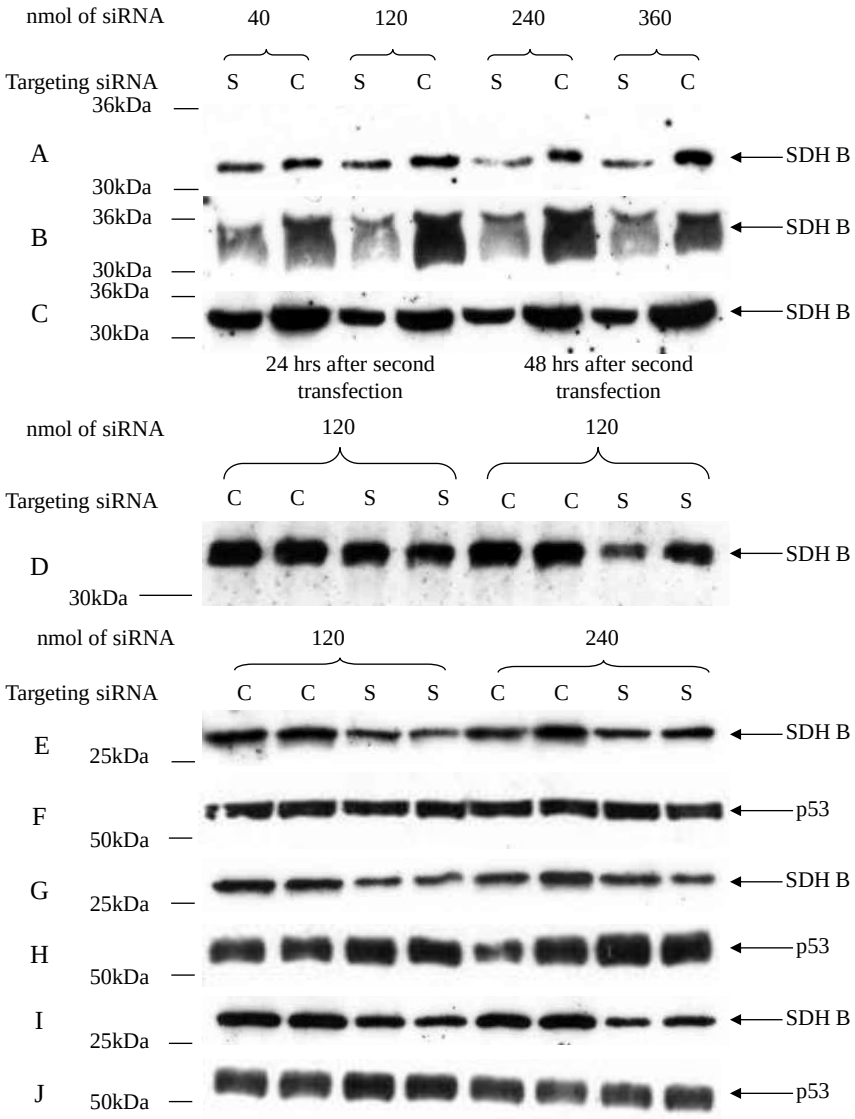


**Figure 4.24 Optimisation of SDH B targeted RNA interference.**

Hep G2 cells seeded at low density (100 000 cells/well) were transfected consecutively, 24 hours (all panels) and 48 hours (B-E, Fand H-K) after seeding with control or SDH B siRNA in the amounts indicated (control –C, SDH B - S). Whole cell lysates were prepared 24 hours after the first transfection (A, E and F) and 24 hours (B, D, and G-J) and 48 hours after the second transfection (C, D, I and J) were resolved by SDS-PAGE, western blotted and probed with an anti-SDH B antibody or anti-p53 antibody as indicated. Mobilities of standard proteins are indicated. Detection of p53 was as a loading control but equal protein loading was also determined by Ponceau S staining of the membranes. Figure shows all data from three independent experiments (A-C (n=1); D (n=1) and E-J (n=1).

**Key:** C, control siRNA targeted; kDa, kilodaltons; nmol, nanomoles; S, SDH B siRNA targeted; SDH B, succinate dehydrogenase; siRNA, small interfering siRNA.

### *4.3.4 The effect of siRNA targeted SDH B suppression on HIF-1α, ARNT and p53.*

To determine the effect of SDH B suppression on HIF-1α, ARNT and p53 protein levels, Hep G2 cells were seeded at low density (100 000 cells/well). In consecutive transfections 24 and 48 hours after seeding, cells were transfected with either control or SDH B targeting siRNA. Whole cell lysates prepared 24 hours and 48 hours after the second transfection of siRNAs were resolved by SDS-PAGE, western blotted and probed with anti-SDH B, anti-p53, anti-ARNT and anti-HIF-1α antibodies. Equal protein loading of the membrane was determined by Ponceau staining (figure 4.25).

Probing samples with an anti-SDH B antibody confirmed SDH B targeting siRNAs knocked down the level of SDH B protein 24 and 48 hours after the second transfection when compared with relevant controls (figure 4.25 as indicated). Ponceau staining of the membrane confirmed the decrease in SDH B protein levels 24 and 48 hours after the second transfection were not due to un-equal protein loading or transfer. Probing with an anti-ARNT antibody (figure 4.25 as indicated) showed no change in ARNT protein levels between samples treated with control or SDH B targeting siRNA at either time-point. At both the 24 hour and 48 hour after second transfection time-points, HIF-1α protein could be detected in control samples although the level of HIF-1α detection was variable. No HIF-1α protein could be detected in corresponding SDH B targeted samples. DFO treated Hep G2 cells were used as a positive control for detection of HIF-1α protein levels. No change in p53 protein levels could be detected between SDH B targeted or control targeted samples at either 24 or 48 hours after the second transfection.

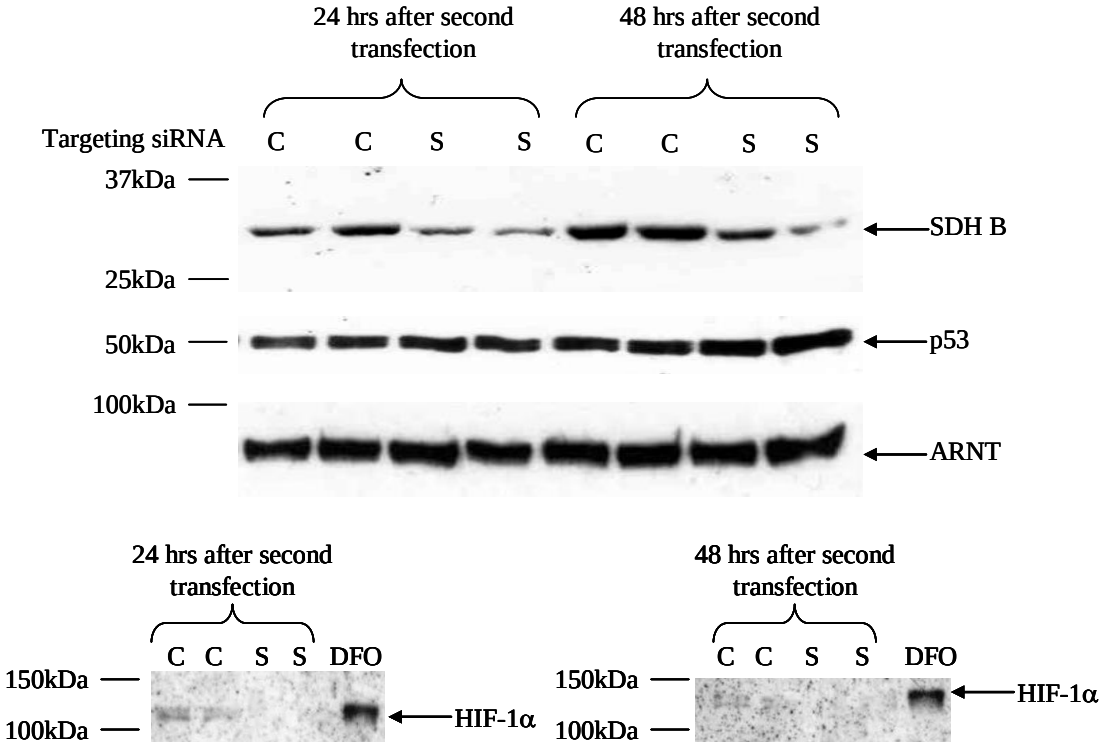


**Figure 4.25 The effect of SDH B suppression on ARNT and HIF-1α protein levels.**

Hep G2 cells seeded at low density (100 000 cells/well) were transfected consecutively, 24 and 48 hours after seeding with 120nmol of either control (C) or SDH B (S) targeting siRNA. Whole cell lysates, prepared 24 and 48 hours after the second siRNA transfection were resolved by SDS-PAGE, western blotted and probed with anti-SDH B anti-p53, anti-ARNT (BD Biosciences) and anti-HIF-1α (BD Biosciences) antibodies as indicated. Mobilities of standard proteins are indicated.
As a positive control for the identification for HIF-1α protein Hep G2 cells were treated with DFO to a final concentration of 100μM. 6 hours after treatment whole cell lysates were prepared. Figure representative of two independent experiments (n=2; repeat data shown in figure 4.26).

**Key:** ARNT**,** Aryl hydrocarbon nuclear translocator; C, Control; DFO, desferrioxamine; HIF-1α, hypoxia inducible factor 1α; kDa, kilodaltons; S, cells transfected with SDH B siRNA; SDH B, succinate dehydrogenase B.

Repetition of the experiment confirmed the results observed in figure 4.25 (figure 4.26). Densitometry of these results indicated that SDH B protein was reduced by 49.9% in SDH B targeted cells when compared to control targeted cells 24 hours after the second transfection. 48 hours after the second transfection SDH B protein

was reduced by 78.9% in cells targeted with SDH B siRNA when compared to cells targeted with control siRNA (figure 4.26). To determine that apparent SDH B knockdown was not due to a difference in protein loading, membranes were Ponceau stained. As in the previous experiment (figure 4.25) western blotting whole cell lysates and probing with either an anti-p53 antibody or an anti-ARNT antibody (figure 4.26 as indicated) showed no difference in protein levels between SDH B targeted or control targeted cells. HIF-1α protein can be clearly detected in control samples at 24 and 48 hours after the second transfection, however in SDH B targeted cells little or no HIF-1α protein could be detected (figure 4.26 as indicated).

Figures 4.25 and 4.26 conclusively indicated the effectiveness of the SDH B targeting siRNA at knocking down SDH B protein levels. Probing samples with an anti-p53 antibody confirmed the observed SDH B protein knockdown was not due to unequal protein loading of the membranes. The knockdown of SDH B protein did not affect ARNT protein levels, in clear contrast to the result of 3-NPA treatment. The apparent decrease of HIF-1α protein levels in SDH B targeted samples also contrasted with the result of 3-NPA treatment.

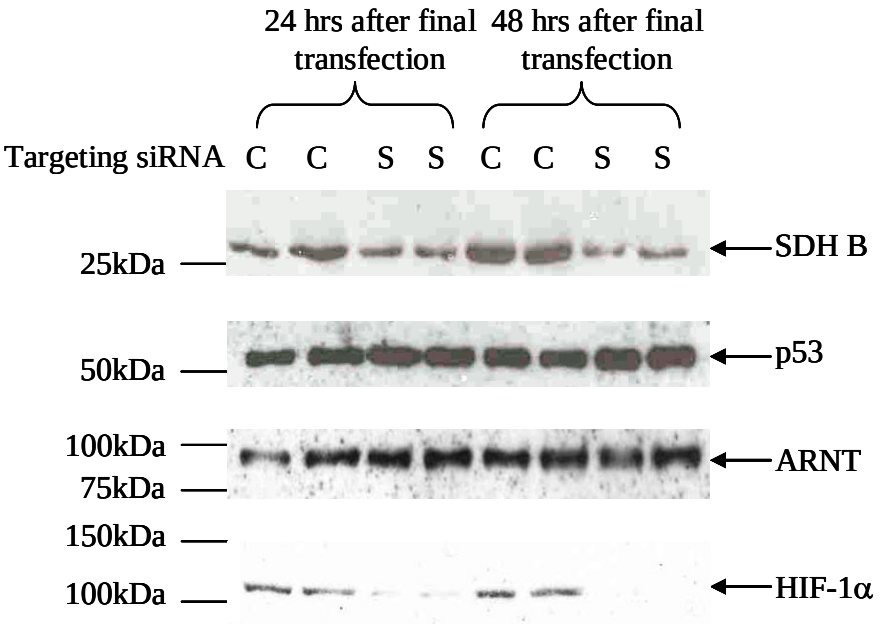


**Figure 4.26 A repeat experiment to determine the effect of SDH B suppression on ARNT and HIF-1α protein levels.**

Hep G2 cells seeded at low density (100 000 cells/well) were transfected consecutively, 24 and 48 hours after seeding with either control (C) or SDH B (S) targeting siRNA. Whole cell lysates, prepared 24 and 48 hours after the second siRNA transfection were resolved by SDS-PAGE, western blotted and probed with anti-SDH B anti-p53, anti-ARNT (BD Biosciences) and anti-HIF-1α (BD Biosciences) antibodies as indicated. Mobilities of standard proteins are indicated. Figure represents two indenpent experiments (n=2; repeat data shown in figure 4.25)

**Key:** ARNT**,** Aryl hydrocarbon nuclear translocator; C, Control; HIF-1α, hypoxia inducible factor 1α; kDa, kilodaltons; S, cells transfected with SDH B siRNA; SDH B, succinate dehydrogenase B.

### *4.3.5 The effect of siRNA transfection on Hep G2 growth rate*

HIF-1α protein levels are affected by increasing cell density (Sheta *et al.*, 2001). To determine whether the apparent down-regulation of HIF-1α protein levels in SDH B targeted cells was due to a difference in growth rate between control and SDH B. siRNA targeted cells, Hep G2 cells were seeded at low density and transfected as previously described. Three wells for each test condition were counted at 24, 48, 72 and 96 hours after seeding. These time-points correspond to consecutive transfections 24 and 48 hours after seeding. 72 hours corresponds to 24 hours after the second transfection in western blot figures and 96 hours corresponds to 48 hours after the second transfection in western blot figures. The average cell number for each condition was plotted and standard deviation determined. Figure 4.27 shows two representative experiments. Both experiments indicated that there was no significant difference in growth rate between control siRNA and SDH B siRNA targeted Hep G2 cells. The results of both experiments were tested for statistical significance at the 96 hour time point using a two-tailed T-test. The p values were 0.26 (figure 4.27, upper panel) and 0.15 (figure 4.27, lower panel). For any differences observed between samples to be generally deemed to be statistically significant $p \leq 0.05$; therefore there was no significant difference between the proliferation in control or SDH B targeted cells. These results indicated that the effect of cell confluence on HIF-1α protein levels was not a contributing factor towards the differences in HIF-1α protein levels observed between control and SDH B targeted cells.

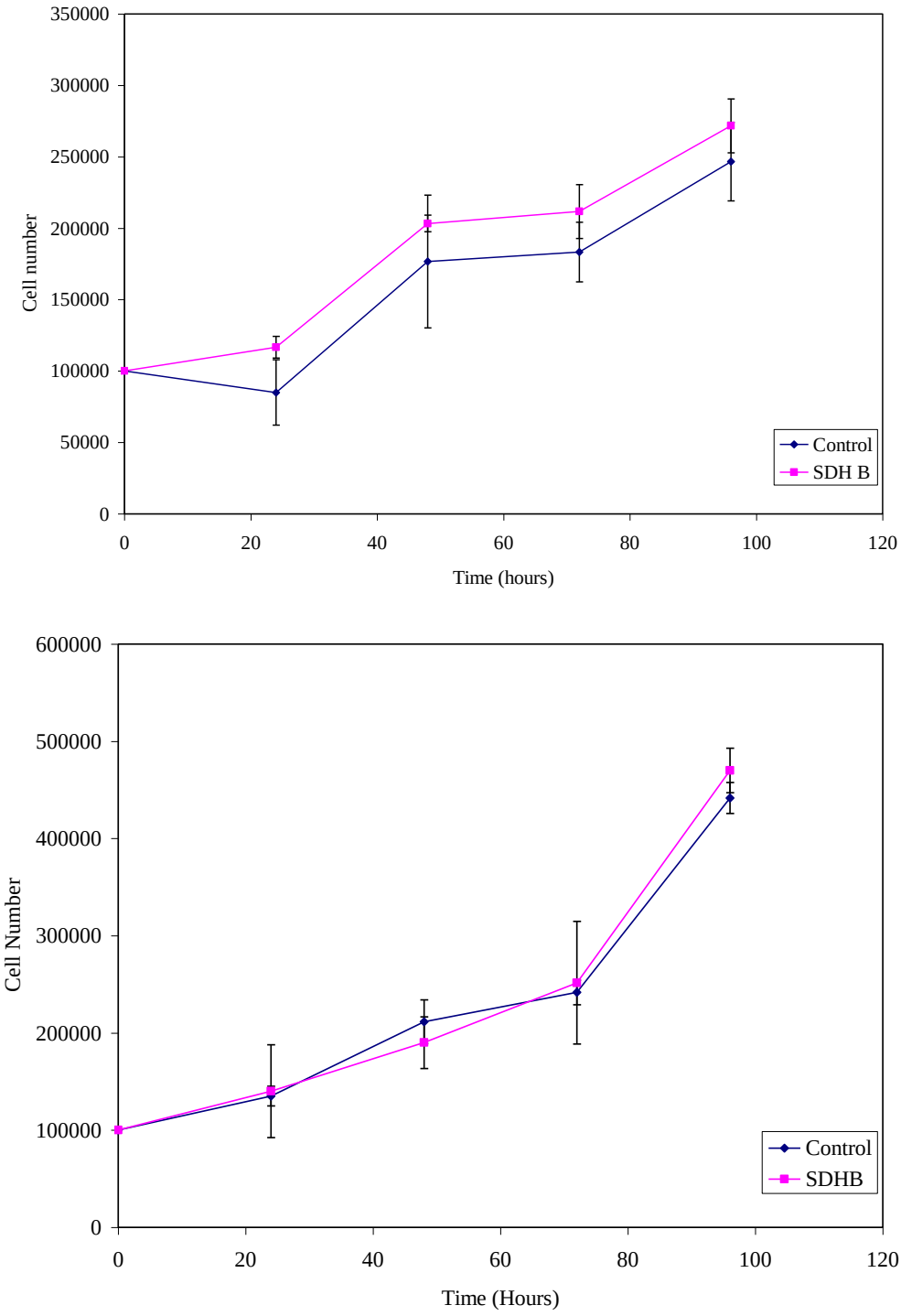


**Figure 4.27 Cell proliferation curves of Hep G2 cells transfected with control or SDH B siRNAs**.

Hep G2 cells seeded at low density (100 000 cells/well) were transfected 24 and 48 hours after seeding with control (blue) or SDH B targeting siRNA (pink). Three wells for each test condition were counted at 24, 48, 72 and 96 hours after seeding. The average cell number for each condition was plotted and standard deviation determined. Data shown is for two independent experiments (n=2).

**Key:** SDH B, Succinate dehydrogenase B

### *4.3.6 The effect of SDH B suppression on the transcriptional activity of an HRE driven transcription reporter gene.*

To determine whether the decrease in HIF-1α protein levels in cells targeted with SDH B siRNA could cause a difference in the transcription of hypoxia responsive genes, a transcription reporter assay was used. Hep G2 cells seeded at low density (100 000 cells/well) were transfected in triplicate 24 hours after seeding with either control or SDH B targeting siRNA. Cells were co-transfected with an SV40 control plasmid, a CMV control plasmid or a test plasmid (pGL3 control, pCMVluc or pGL3prevPGK, respectively). All wells were also co-transfected with a plasmid expressing *Renilla* luciferase (pRL-SV40), as an internal control to normalise transfection efficiencies (These plasmids have been described previously in sections 2.1.12 and 3.4.5). 48 hours after seeding Hep G2 cells were transfected in triplicate with either control or SDH B targeting siRNA. 72 hours after seeding cells were lysed. Cell lysates were analysed for firefly luciferase activity and corrected against *Renilla* luciferase activity to normalise transfection efficiencies. Figure 4.28 shows the results from three independent experiments. In two of the three experiments, Hep G2 cells transfected with a control siRNA induced more HRE dependent transcription of the luciferase reporter gene (test [HRE]) than Hep G2 cells transfected with SDH B targeting siRNA (figures 4.28 inset charts, upper and central panels). These results when taken on their own correspond with the HIF-1α expression data observed in figure 4.26, namely that SDH B targeting siRNA reduces both HIF-1α protein expression and HRE dependent transcription of a luciferase reporter plasmid when compared with the respective controls. However, although the luciferase reporter assay results when taken on their own appear significant, this significance is lost when compared with the control plasmid results. In all three experiments SDH B targeting siRNA suppressed the level of luciferase expression in Hep G2 cells transfected with SV40 control and CMV control when compared with control siRNA samples. In all instances the level of luciferase expression is greater in cells transfected with siRNA and control plasmid when compared to cells transfected with siRNA and test (HRE) plasmid. The observation that the pattern of luciferase expression in cells transfected with control luciferase reporter genes exactly mimics that of the test luciferase reporter gene makes these results difficult to interpret.

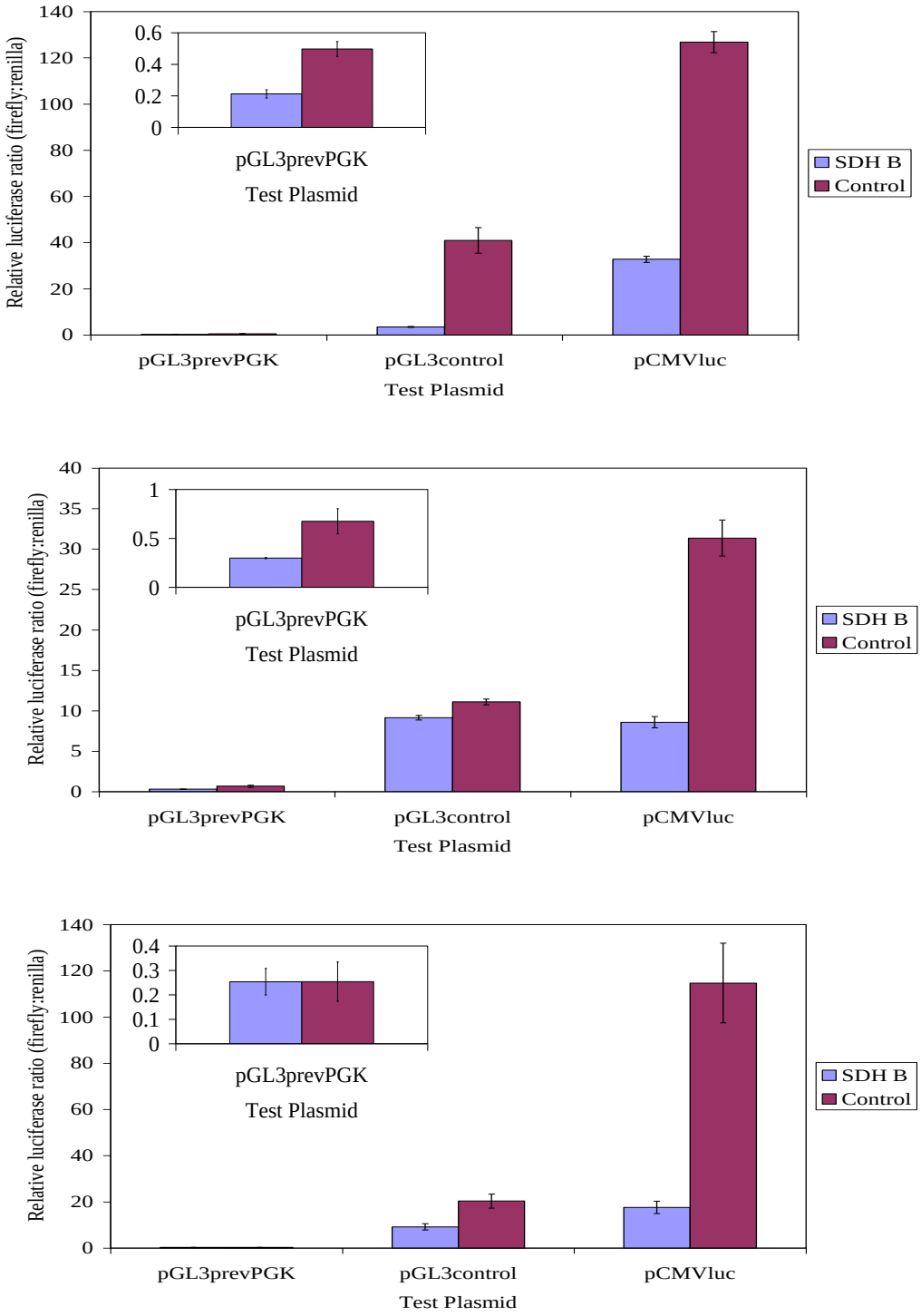


**Figure 4.28 Transcriptional reporter assay of siRNA transfected Hep G2 cells.**

Hep G2 cells seeded at low density (100 000 cells/well) were transfected in triplicate 24 hours after seeding with 240nmol of either control or SDH B targeting siRNA. Hep G2 Cells were co-transfected with 1µg of either pGL3prevPGK, pGL3control or pCMVluc. All wells were co-transfected with 0.02µg pRL-SV40. 48 hours after seeding cells were transfected with 240nmol of control (purple) or SDH B siRNA (blue). 72 hours after seeding whole cell lysates were prepared in passive lysis buffer. Lysates were assayed for firefly luciferase activity and corrected against *Renilla* luciferase activity to normalise transfection efficiencies. Inset panels (*) represent pGL3prevPGK results on a larger scale. Results shown are from three independent experiments (n=3). Error bars are ± S.D.

**Key:** CMV, cytomegalovirus: HRE, hypoxia responsive element; $r_0$, SDH B, succinate dehydrogenase B.

### *4.3.7 The effect of SDH B suppression on GLUT-1 protein levels and HIF-1α mRNA levels.*

Due to the difficulty in interpreting the data from figure 4.28 an alternative means of inferring the transcriptional activity of HIF was to investigate the protein level of a downstream target in the hypoxia pathway. GLUT-1 is a protein up-regulated when there is an increase in active HIF-1 due to the presence of an HRE near the promotor of the gene that encodes for GLUT-1. Hep G2 cells were seeded at low density (100 000 cells/well). 24 hours after seeding cells were transfected with either control or SDH B targeting siRNA. Transfection was repeated 48 hours after seeding. Whole cell lysates prepared 24 hours and 48 hours after the second transfection of siRNA (72 and 96 hours after seeding) were resolved by SDS-PAGE, western blotted and probed with anti-SDH B, anti-p53, anti-HIF-1α and anti-GLUT-1 antibodies (figure 4.29, as indicated).

As observed in previous experiments SDH B targeting knocked down the level of SDH B protein 24 and 48 hours after the second transfection when compared to control targeted samples. Probing membranes with an anti-p53 antibody confirmed equal protein loading. HIF-1α protein was undetectable in cells targeted with SDH B siRNA when compared to control targeted samples at 48 hours after the second transfection. Probing samples with an anti-GLUT-1 antibody revealed no change in GLUT-1 protein levels between samples targeted with SDH B or control siRNAs with the exception of one sample targeted with SDH B siRNAs 48 hours after the second transfection. This apparent decrease in GLUT-1 protein was accompanied by a moderate increase in p53 protein levels that had not been observed in any previous experiments (figure 4.29, as indicated). All samples contained multiple anti-GLUT-1 reactive bands indicating GLUT-1 protein may undergo some form of post-transcriptional modification for example, phosphorylation.

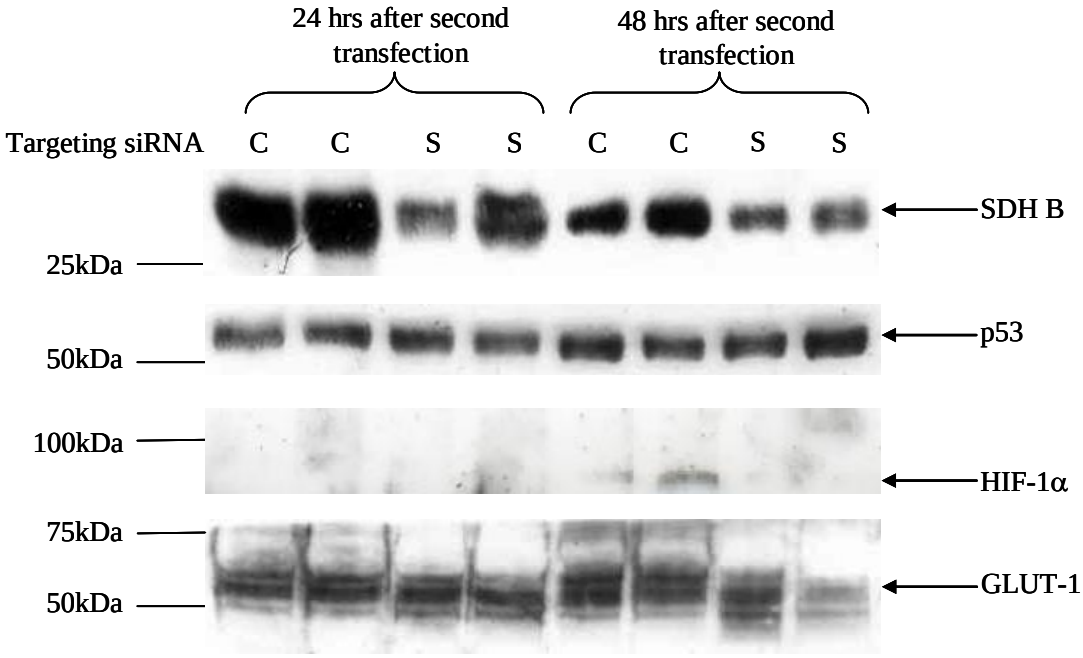


**Figure 4.29 The effect of SDH B suppression on GLUT-1 protein levels.**

Hep G2 cells seeded at low density (100 000 cells/well) were transfected 24 and 48 hours after seeding with 120nmol of either control (C) or SDH B (S) targeting siRNA. Whole cell lysates prepared 24 and 48 hours after the second transfection were resolved by SDS-PAGE, western blotted and probed with anti- SDHB, anti-p53, anti-HIF-1α (BD Biosciences) and anti-GLUT-1 antibodies, as indicated. The mobilities of standard proteins are indicated. Figure represents one experiment (n=1).

**Key:** C, Control; GLUT-1;glucose transporter-1; HIF-1α, hypoxia inducible factor 1α; kDa, kilodaltons; nmol, nanomoles; S, cells transfected with SDH B siRNA; SDH B, succinate dehydrogenase B.

A repeat experiment was performed to determine whether the slight suppression in GLUT-1 protein levels in one SDH B targeted sample could be replicated (figure 4.30). As observed in previous experiments SDH B targeting knocked down the level of SDH B protein 24 and 48 hours after the second transfection when compared to control targeted samples. Probing membranes with anti-p53 and and anti-ARNT antibodies confirmed equal protein loading. HIF-1α protein was undetectable in cells targeted with SDH B siRNA when compared to control targeted samples at both 24 and 48 hours with the greatest level of HIF-1α suppression observed at 48 hours after the second transfection. Due to a lack of HIF-1α protein induction at 24 hours in the

first experiment (figure 4.29), HIF-1α levels were only suppressed in SDH B targeted samples 48 hours after the second transfection. Probing samples with an anti-GLUT-1 antibody revealed there was no apparent difference in GLUT-1 protein levels in SDH B targeted cells when compared to control targeted cells 24 hours after the second transfection (figure 4.30 as indicated). This concurred with the results observed in figure 4.29. GLUT-1 levels were elevated in control targeted cells when compared to SDH B targeted cells 48 hours after the second transfection, and also elevated compared with the control targeted cells 24 hours earlier (figure 4.30).

This result was not in agreement with the result obtained in figure 4.29 where control levels were not elevated. The apparent delay before GLUT-1 protein levels became elevated 48 hours after the second transfection could have been due to a requirement for a certain threshold level of HIF-1 protein, HIF-1α protein modification or simply the time taken for HIF-1 nuclear translocation. If a threshold level of HIF-1α protein were required for induction of GLUT-1 expression, this may explain the absence of elevated GLUT-1 levels in figure 4.29.

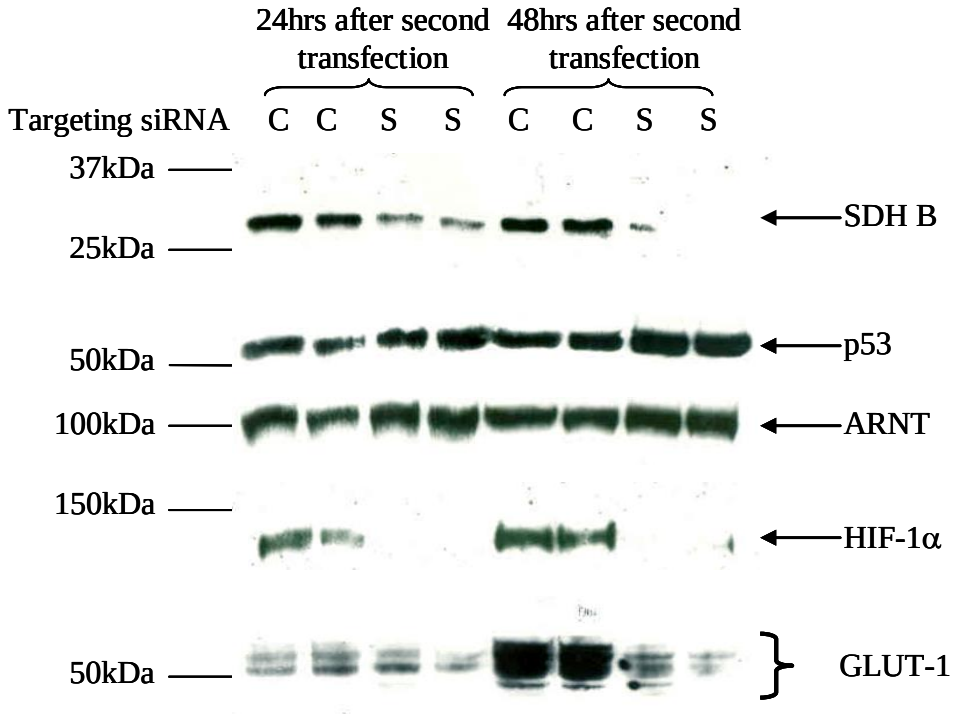


**Figure 4.30 A repeat experiment to determine the effect of SDH B suppression on GLUT-1 protein levels**.

Hep G2 cells seeded at low density (100 000 cells/well) were transfected 24 and 48 hours after seeding with 120nmol of either control (C) or SDH B (S) targeting siRNA. Whole cell lysates prepared 24 and 48 hours after the second transfection were resolved by SDS-PAGE, western blotted and probed with anti-SDHB, anti-p53, anti-HIF-1α (BD Biosciences) and anti-GLUT-1 antibodies, as indicated. The mobilities of standard proteins are indicated. Figure represents one experiment (n=1).

**Key:** C, Control; GLUT-1;glucose transporter-1; HIF-1α, hypoxia inducible factor 1α; kDa, kilodaltons; nmol, nanomoles; S, cells transfected with SDH B siRNA; SDH B, succinate dehydrogenase B.

To determine whether the suppression of HIF-1α protein levels by SDH B targeting siRNA was due to a reduction in HIF-1α mRNA levels an RT-PCR was performed on parallel samples to those analysed in figure 4.30. Total RNA was extracted 24 and 48 hours after the second transfection, DNase digested and subjected to reverse transcription with or without reverse transcriptase. The resulting cDNA was amplified by PCR using exon/intron spanning primers specific for HIF-1α mRNA

and β-actin mRNA that yielded 462 bp and 486bp PCR products, respectively. $H_2O$ was amplified as a control for contamination (figure 4.31).

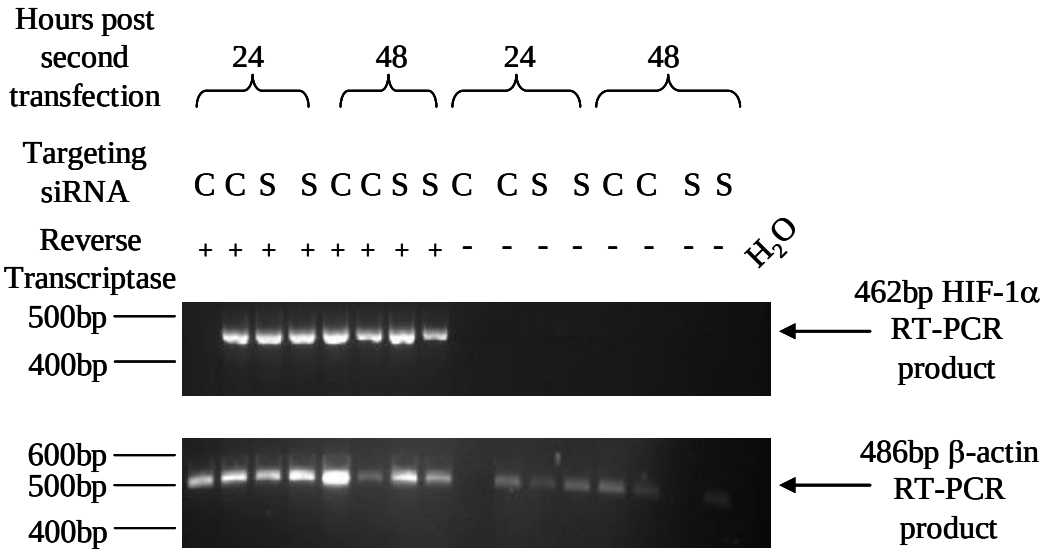


**Figure 4.31 The effect of SDH B suppression on HIF-1α and β-actin mRNA levels.**

Hep G2 cells seeded at low density (100 000) cells per well were transfected 24 and 48 hours after seeding with 120nmol of either control or SDH B targeting siRNA. Cells were lysed 24 and 48 hours after the second siRNA transfection. Cell lysates were DNase digested and RNA was purified using a Qiagen RNeasy kit, as indicated. 1μg of total RNA was transcribed with (+) or without (-) reverse transcriptase and subjected to PCR with HIF-1α or β-actin primers as indicated. A negative control PCR reaction was undertaken for each primer set ($H_2O$). PCR products were resolved by agarose gel electrophoresis and visualised under ultra violet light. Molecular weight markers are indicated. Figure represents one experiment (n=1).

**Key:** bp, base pairs; C, control siRNA; $H_2O$, water; HIF-1α, Hypoxia inducible factor-1α; RT-PCR, reverse transcriptase- polymerase chain reaction; S, SDHB siRNA; SDH B, succinate dehydrogenase B.

HIF-1α product and β-actin product were detected in both control and SDH B targeted cells employing RNA subjected to reverse transcription with reverse transcriptase. RNA extracted from a control targeted sample 24 hours after the second transfection did not amplify with HIF-1α primers. No detectable HIF-1α

product was observed in samples reversed transcribed without reverse transcriptase or in the $H_2O$ control lane. In reverse transcriptase negative samples amplified with β-actin primers a product was visualised in all lanes except a control targeted sample lane 24 hours after the second transfection and an SDH B targeted sample lane 48 hours after the second transfection. These bands were not caused by contamination because no detectable DNA was observed in the $H_2O$ control lane. The β-actin product visible in reverse transcriptase negative lanes could be caused by a pseudogene. Incomplete DNAse digestion of the DNA encoding the pseudogene could allow amplification, revealing the product bands observed in the reverse transcriptase negative β-actin lanes. Alternatively, total RNA in reverse transcriptase negative samples could be reverse transcribed by Taq and then amplified. Reverse transcription by Taq has been reported and reverse transcriptase independent RT-PCR of a subset of RNA sequences has been observed previously (Grabko *et al.,* 1996; M R Crompton pers. commun). The variation observed in HIF-1α mRNA levels between control and SDH B samples 48 hours after the second transfection was also observed in β-actin mRNA indicating the quality of the RNA was the probable cause of the variability. These results confirm that SDH B targeting siRNAs do not have an off target effect resulting in HIF-1α mRNA degradation. The variability in the data was probably due to the small number of cells employed in this experiment. More quantitative analysis of any changes in mRNA levels would require an alternative approach, for instance employing quantitative PCR assays or more cells per assay (for example by the establishment of cell lines with constitutive siRNA expression).

### *4.3.8 The effect of SDH B suppression on SDH A.*

Mutations that prevent the translation of SDH B or mutations that are predicted to alter the folding of SDH B are predicted to destabilise the SDH complex (Yankovskaya *et al.,* 2003). Not only would these mutations abrogate the catalytic activity of SQR but they would also prevent the binding of SDH A, because SDH A itself does not bind to the anchoring subunits SDH C and D. If SDH B binding was essential for SDH A protein stability, then suppression of SDH B could perhaps result in the degradation of SDH A. To test this hypothesis whole cell lysates

prepared in 4.3.7 (figure 4.30) were resolved by SDS-PAGE, western blotted and probed with anti SDH A and anti-ARNT antibodies (figure 4.32, as indicated). To enable the loading control to be on the same blot as SDH A, ARNT was used instead of p53. Figure 4.29 indicates there is no difference in ARNT protein levels between control and SDH B targeted samples. The same figure also shows no difference in protein loading between p53 and ARNT. These observations justify the use of ARNT as a loading control.

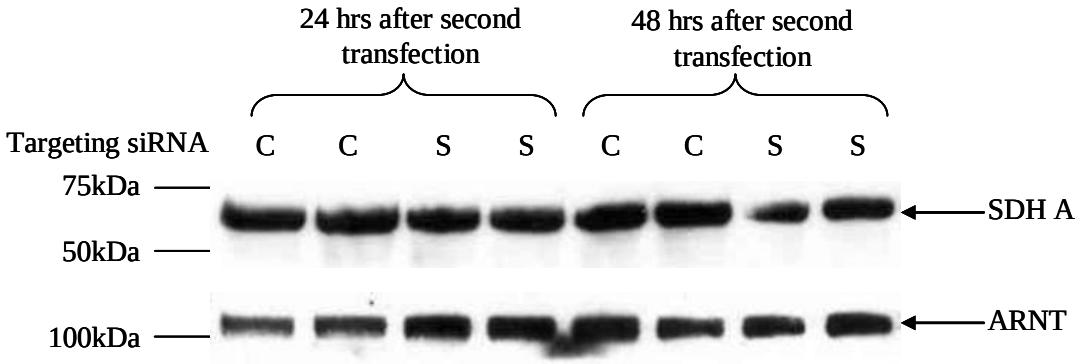


**Figure 4.32 The effect of SDH B suppression on SDH A**.

Hep G2 cells were seeded at low density (100 000) cells/well. 24 and 48 hours after seeding cells were transfected with 240nmol control (C) or SDH B (S) targeting siRNA. Whole cell lysates prepared 24 and 48 hours after the final transfection were resolved by SDS-PAGE, western blotted and probed with anti-SDH A and anti-ARNT (BD Biosciences) antibodies, as indicated. Mobilities of standard proteins are indicated. Data represents on experiment (n=1).

**Key:** ARNT**,** Aryl hydrocarbon nuclear translocator; C, Control; kDa, kilodaltons; S, cells transfected with SDH B siRNA; SDH A, succinate dehydrogenase A; SDH B, succinate dehydrogenase B.

There was no appreciable difference in SDH A protein levels between control targeted and SDH B targeted samples at 24 or 48 hours after the second transfection. Probing samples with an anti-ARNT antibody confirmed equal protein loading of the membrane. These results indicated that SDH A protein was not degraded in samples that had knocked down SDH B protein levels. The nature of RNA interference is to produce a knockdown phenotype rather than a knockout phenotype. In these experiments complete suppression of SDH B was never achieved, therefore, it is possible that the remaining SDH B protein binds the SDH A protein present in

mitochondria and therefore no change in SDH A protein levels is observed. It is also possible that suppression of SDH B results in unbound SDH A that is not subject to targeted degradation in its un-complexed form. This would also explain why no changes in SDH A protein levels were observed between control and SDH B targeted samples.

## 4.4 Discussion

The hypothesis outlined in section 4.1.6 stated that the inhibition of SDH would result in an up-regulation of HIF-1α protein levels followed by an increase in HIF-1 transcriptional activation of target genes. The aim was to determine whether pharamacological inhibition in the form of 3-NPA would support the hypothesis and then to verify the findings using a more targeted approach in the form of RNA interference. Results obtained using 3-NPA mediated inhibition supported the hypothesis (figures 4.12 - 4.15). However, siRNA mediated inhibition of SDH B contradicted the 3-NPA data (figures 4.25 – 4.26 and 4.29 – 4.30).

### *4.4.1 Differences and similarities between pharmacological inhibition and siRNA mediated knockdown.*

One possible explanation for the differing results observed between cells treated with 3-NPA (pharmacological inhibition) and those subjected to RNA interference mediated silencing of SDH B is the method by which inhibition or knockdown is achieved. Although the aim of both strategies is the same – to perturb the function of a target protein, the methodology is not. Pharmacological inhibition abrogates the function of the target protein but the protein itself is still present. This means that the target protein although lacking in activity can potentially still bind to binding partners or be incorporated into complexes. If the target proteins incorporation into a protein complex is also important for its biological activity, this could still take place if only the protein enzymic activity has been perturbed. In contrast, RNA interference mediated knockdown targets the mRNA of the protein of interest resulting in knockdown of mRNA and hence protein level. If enzymic activity and incorporation into a protein complex are important for protein function both will be

abrogated by RNA interference mediated knockdown compared to just enzymic activity by a pharmacological inhibitor (Weiss *et al.*, 2007).

Both inhibition and knockdown can result in off target effects. 3-NPA for example is a relatively simple molecule (figure 4.6) and it is possible that the function of other proteins could be inhibited by 3-NPA treatment of Hep G2 cells. Microarray analysis of RNA interference first identified that siRNAs were capable of silencing unintended targets as well as the original target (Jackson *et al.*, 2003). siRNAs can also result in up-regulation of Type I interferons and cytokines, proteins which can lead to inflammation *in vivo* (Samuel-Abraham and Leonard., 2010). It is possible, given the outdated methodology of siRNA design used in these studies that siRNA mediated interference of SDH B could have resulted in unintended off target effects (discussed in section4.4.5). Taking into account the disparity in results between 3-NPA inhibition of SDH and siRNA mediated suppression of SDH B and the differences between the two methods of inhibition/knockdown, the results obtained are discussed separately.

### *4.4.2 3-NPA suppresses ARNT and PTEN protein levels*

3-NPA mediated the suppression of ARNT and PTEN protein levels in Hep G2 and PC12 cells, indicating this was not a cell type specific response (figures 4.17 and 4.21 left hand panel, respectively). ARNT and PTEN protein levels were also suppressed by 3-NPA in the presence of DFO. Treatment of Hep G2 cells with 3-NPA and lactacystin, a proteasomal inhibitor, confirmed the suppression of ARNT protein levels was not due to ubiquitin mediated proteasomal degradation, suggesting ARNT protein levels were being suppressed by another, as yet unknown, mechanism (figure 4.20). The suppression of ARNT and PTEN proteins at 24 hours was not due to 3-NPA induced permeability of the Hep G2 cell membrane. This was determined by a trypan blue exclusion experiment (figure 4.19). The trypan blue exclusion experiment showed a marked difference in growth rate between control and 3-NPA treated Hep G2 cells. Extending the time course of the trypan blue exclusion experiment would be required to determine if cell growth appeared to be arrested by 3-NPA and if this were the case to determine whether 3-NPA caused cell death in

Hep G2 cells. However, at the time-point of 3-NPA treatment at which marked selective suppressions of the levels of PTEN and ARNT were observed, there was no selective loss of plasma membrane integrity of the cells assayed, and protein loss could not simply be accounted for as being due to cell permeabilisation. Further experimentation to determine whether the suppression of ARNT and PTEN was regulated at the protein or mRNA level, could be determined by quantitative RT-PCR.

One possible explanation for 3-NPA mediated suppression of PTEN and ARNT protein levels is microRNA repression. MicroRNAs (miRNAs) are a class of endogenous non-coding RNAs approximately 18-25 nucleotides in length. They are capable of negatively regulating gene expression by binding to the 3' un-translated region (3'UTR) of target messenger RNAs which causes either translational repression or degradation (Bartel, 2004).

Recently, two different miRNAs have been identified that repress ARNT and PTEN, they are miRNA 107 and miRNA 21, respectively. miRNA 107 is p53 regulated and when the pre-cursor to miRNA-107 is overexpressed, is able to inhibit ARNT expression in the human colon cancer cell line HCT116 (Yamakuchi *et al.*, 2010). miRNA 21 represses PTEN in non-small cell lung cancer tumour tissue (Zhang *et al.*, 2010). The discovery that miRNAs can repress ARNT and PTEN leads to the hypothesis that 3-NPA treatment of Hep G2 cells promotes the increase of one or more miRNAs which either repress *ARNT* and *PTEN* mRNA levels or inhibit *ARNT* and *PTEN* mRNA translation, thus leading to a reduction in ARNT and PTEN protein levels. 3-NPA has been shown to cause apoptosis and autophagy in rat striatum (Zhang *et al.*, 2009). Therefore, it could also be hypothesised that suppression of PTEN and ARNT in 3-NPA treated Hep G2 cells is essential for reducing cell viability and be a pre-cursor to apoptosis. Extension of the trypan blue exclusion experiment could confirm whether cell viability was compromised at a later time-point and western blotting protein samples for a pro-apoptotic marker protein such as caspase 3 could indicate an apoptotic response to 3-NPA in Hep G2 cells. However, in order to prove the involvement of miRNAs a microarray approach would be required.

### *4.4.3 The effect of 3-NPA on HIF-1α protein levels in Hep G2 cells.*

Following optimisation of the 3-NPA treatment protocol (sections 4.2.1 - 4.2.5), subsequent experiments showed 3-NPA treatment of Hep G2 cells resulted in the induction of HIF-1α protein levels when compared to control treated samples (figures 4.13 - 4.15). 3-NPA suppressed the HIF-1α protein response to DFO in Hep G2 cells when compared to cells treated with DFO and carrier control. However, the protein levels of HIF-1α in cells treated with 3-NPA and DFO were higher than in cells treated with 3-NPA and carrier control (figure 4.17). The effect of 3-NPA on HIF-1α protein levels in PC12 cells could not be assessed due to the lack of an anti-HIF-1α antibody that would recognise the rat protein. The induction of HIF-1α protein in Hep G2 cells could have been caused by reactive oxygen species (ROS), particularly hydrogen peroxide, $H_2O_2$. 3-NPA has been shown to induce ROS production in HM06 human microglia cells (Ryu *et al.*, 2003) and induce the production of $H_2O_2$ in PC12 cells (Mandavilli *et al*., 2005). These results indicated that 3-NPA mediated ROS production was not cell type specific and it was predicted that ROS/$H_2O_2$ production was occurring in Hep G2 cells. $H_2O_2$ has been shown to elevate HIF-1α protein levels in normoxic Hep 3B and HEK 293 cells (Chandel *et al*., 2000). If $H_2O_2$ was being produced in Hep G2 cells after 3-NPA treatment, this may have been the cause of the elevated HIF-1α protein levels observed in figures 4.13 – 4.15 and figure 4.17. This hypothesis could be tested by pre-treating cells with catalase, a scavenger of $H_2O_2$, before treating cells with 3-NPA. Similar experiments have been performed by Zhou *et al.*, who treated PC-3 cells with catalase before treating with insulin in order to determine whether insulin mediated up-regulation of $H_2O_2$ resulted in increased VEGF and HIF-1α expression (Zhou *et al., 2007).*

One hypothesis that links both PTEN suppression and HIF-1α up-regulation is that 3-NPA induces the production of $H_2O_2$. As described in 4.4.1, 3-NPA has been shown to induce $H_2O_2$ in PC12 cells (Mandavilli *et al*., 2005) and $H_2O_2$ has been shown to inactivate purified PTEN *in vitro* (Lee *et al.*, 2002). The loss of, or suppression of PTEN protein levels (as shown in figure 4.17 and 4.21) would be predicted to cause the constitutive activation of the phosphatidylinositol 3-kinase (PI3K) signalling

pathways mediated by Tec family tyrosine kinases, AKT/PKB and Rac/Rho GTPases (figure 4.33).

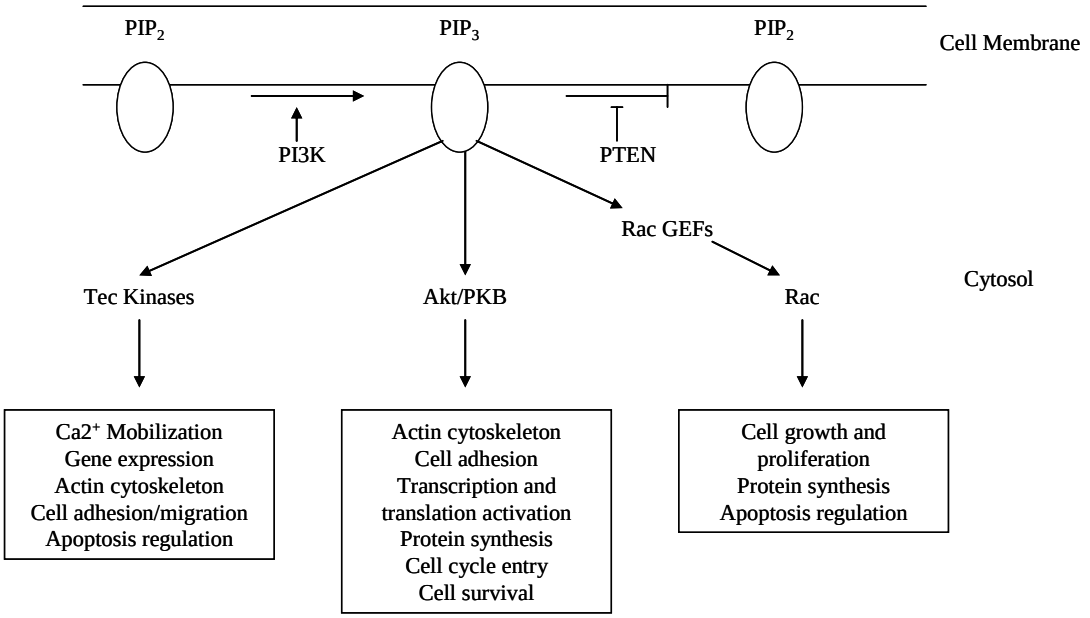


**Figure 4.33 PI (3, 4, 5) $P_3$ dependent pathways constitutively activated through the loss of PTEN.**

Loss of PTEN prevents the dephosphorylation of the second messenger phosphatidylinositol - (3, 4, 5) – trisphosphate, PI (3, 4, 5) $P_3$, back to phosphatidylinositol – (4, 5) diphosphate, PI (4, 5) $P_2$. This causes the constitutive, PI3K (phosphatidylinositol 3 kinase) dependent activation of Tec family kinases, Akt/PKB (protein kinase B) and Rac/Rho family GTPases, which are involved in the regulation of the pathways indicated in the figure (Fruman D., 2004, Takesono *et al.,* 2002, Welch *et al.,* 2003 and Cantrell D., 2001).

The mammalian target of rapamycin (mTOR) is a downstream target of Akt/PKB, which has been implicated in the upregulation of HIF-1α protein levels in normoxia and hypoxia (Hudson *et al.,* 2002). Suppression of PTEN protein levels in Hep G2 cells due to the increase in $H_2O_2$ would be predicted to constitutively activate the Akt/PKB pathway resulting in the mTOR mediated up-regulation of HIF-1α protein levels. This combined with the hypothesised $H_2O_2$ up-regulation of HIF-1α protein levels (section 4.4.1) could explain the 3-NPA mediated increase in HIF-1α protein levels observed in figures 4.13 – 4.15 and figure 4.17. One way of testing this hypothesis would be to probe samples with a phospho-Akt antibody. Activated Akt is phosphorylated, therefore if 3-NPA samples contained more phosphorylated Akt

than control samples, this could support the hypothesis described above (Vara *et al.*, 2004).

### *4.4.4 The effect of 3-NPA on transcription.*

The discovery that 3-NPA suppressed the levels of ARNT protein in Hep G2 cells resulted in the expectation that Hep G2 cells treated with 3-NPA would not exhibit a transcriptional response from an HRE driven luciferase reporter construct. However, figure 4.16 showed that 3-NPA induced a small transcriptional response of an HRE dependent luciferase reporter construct when compared to carrier control samples, this was particularly apparent in the second independent experiment (figure 4.16 lower panel). The low level of response was probably caused by incomplete 3-NPA mediated ARNT disappearance, which is illustrated in figures 4.14 and 4.15. 3-NPA suppressed the DFO response of an HRE driven luciferase reporter gene when compared to DFO. However, DFO and 3-NPA induced a higher level of expression when compared to 3-NPA alone (figure 4.18). In the 3-NPA time course experiments, DFO induced HIF-1α protein before 3-NPA which could explain why DFO and 3-NPA induced a higher level of expression of an HRE driven reporter gene than 3-NPA alone (figures 4.14 and 4.15). However, although the above results can be explained in terms of the HRE data alone, it is by no means conclusive because, as seen in previous luciferase assays (figure 3.17), the controls for these assays were variable. The most pronounced variability was seen in the CMV control data (figures 4.16 and 4.18). One explanation for this variability is the effect of cell passage number on protein expression, cell signalling and growth rate as described in section 3.5.1.

Another possible explanation could be that the cell culture, transfection or chemical treatment conditions that Hep G2 cells were subjected to in this experiment, resulted in the CMV driven transcription of luciferase as a result of a stress response. For example, in FR cells (rat skin cells), Hep G2 cells and human prostate cancer cell lines, exposure to chemotherapeutic stimuli resulted in an increase in CMV promoter driven transcription of exogenous gene expression (Kinoshita *et al.*, 2008 and Svensson *et al.*, 2007). In the FR cells this upregulation was accompanied by

increased mRNA levels of *c-fos* and *c-jun* (Kinoshita *et al.,* 2008). These genes encode for proteins that are members of the Fos and Jun family of proteins which are important in regulation of the cell cycle and stress responses. Fos and Jun proteins dimerise to form the inducible transcription factor activator protein -1 (AP-1) and there is an AP-1 binding site in the CMV enhancer (Sambucetti *et al.,* 1989). The CMV enhancer also has an ATF (activating transcription factor) binding site and ATF is a known downstream target of the p38 MAPK pathway which when activated is thought to have up-regulated CMV promoter activity in human prostate cells (Sambucetti *et al.,* 1989 and Svensson *et al.,* 2007). Consistent with these findings Bruening *et al.,* had previously shown that p38 MAPK pathway inhibitors were able to block arsenite induced CMV promoter driven transcription (Bruening *et al.,* 1998). It is therefore feasible that one or both of these pathways could have been up-regulated in Hep G2 cells transfected with CMV control and each treatment condition potentiated a different level of CMV promoter driven response; DFO being the most potent initiator and 3-NPA the least. This may be explained by the findings that RNA extracted from the liver of rats treated with 3-NPA contained increased levels of *c-fos* mRNA when compared to control samples. However *junb* mRNA levels were reduced when compared to control samples (Przybyla-Zawislak *et al.,* 2005). If the induction of CMV promoter driven transcription observed in Hep G2 cells treated with DFO or carrier controls were due to AP1 mediated transcription, it could be hypothesised that reduced levels of Jun proteins as a result of the 3-NPA mediated decrease in *junb* mRNA levels, may result in the low level of CMV control luciferase expression in 3-NPA samples when compared to carrier control and DFO samples (figure 4.16 and figure 4.18). Both p38 MAPK and JNK (c-Jun N-terminal Kinase) are known inducers of Fos and Jun proteins, therefore the use of a p38 MAPK or JNK inhibitor in the transcription reporter assay could determine whether transcription of CMV control could be due to AP1 or ATF binding.

It is also possible that a *trans* effect between the promotors of the reporter plasmids used in the luciferase reporter assay may have affected the expression levels observed in figure 4.16 (Farr and Roman. 1992). It is possible that a *trans* effect can be observed due to incorrect ratios between co-transfected plasmids or the effect can be cell type specific (Promega Technical Bulletin – pRL *Renilla* luciferase reporter vectors). One way to assess whether a *trans* effect is responsible for the variability if

results observed in figure 4.16 would be to carry out a luciferase reporter assay in an alternative cell type of low passage number. If no variability in the controls were observed in an alternative cell type this would indicate the results seen in figure 4.16 were cell type specific.

### *4.4.4 The effects of siRNA mediated SDH B suppression.*

Initially it was predicted that loss of SDH B expression would cause an increase in HIF-1α protein levels (section 4.1.6). However, inhibition of SDH B protein levels using RNA interference reproducibly suppressed HIF-1α protein levels, a finding that opposed our initial predictions (figures 4.25 and 4.26 and 4.29 and 4.30). Hep G2 cells appeared to have a basal level of GLUT-1 protein expression (the protein product of a a HIF-1 target gene) when cultured under the conditions used in these experiments. In SDH B targeted cells where HIF-1α protein levels were suppressed, GLUT-1 protein levels also showed a substantial reduction (figure 4.30). However this reduction only occurred when GLUT-1 levels were substantially elevated and was not reproducible suggesting that there was a threshold level of HIF-1α suppression required for down regulation of GLUT-1 (figure 4.29). The suppression of HIF-1α protein level was not due to an off target effect of the SDH B targeting RNAi as HIF-1α mRNA levels were not substantially altered by SDHB targeting RNAi (figure 4.31).

Confirmation of HIF-1α protein suppression mediated by SDHB targeting RNAi was sought by using an HRE driven transcription reporter assay. However, once again there were intra and inter experimental variability in the SV40 and CMV controls which prevented any meaningful discussion of the Test (HRE) results achieved. As previously described, this variability may have been due to cell passage number or expression of the SV40 and CMV driven luciferase reporter genes in a cell type dependent manner, possibly due to transcription factor binding to consensus sequences present in the promoter region of CMV (section 3.5.1 and 4.4.3).

The level of cell density/confluency in cultured cells has been reported to affect HIF-1α stabilisation in 293T, RCC, PC3 and LNCaP cells (Paltoglou and Roberts, 2005;

Sheta *et al.,* 2001). However, SDH B targeting in Hep G2 cells had no effect on cell proliferation when compared to control targeted Hep G2 cells (figure 4.27). Therefore the suppression of HIF-1α and GLUT-1 protein levels mediated by SDH B targeting could not be attributed to differential cell densities. Hep G2 cells have been reported to be hypoxic in confluent cultures (Metzen *et al.,* 1995), however all RNAi targeted cells were harvested when sub-confluent. Therefore, the detection of HIF-1α protein in control targeted Hep G2 cells is probably not due to pericellular hypoxia induced by high cell density but due to non-oxygen dependent pathways that can up-regulate HIF-1α protein levels in normoxic conditions. Two signalling pathways that have been identified in the non-oxygen dependent regulation of HIF-1α are those involving PI-3-kinases, and mitogen-activated protein kinases (MAP kinases, reviewed by Bardos and Ashcroft, 2004 and Semenza G., 2002). Although it is difficult to ascertain the exact nature by which one of these pathways may be affecting HIF-1α in Hep G2 cells, treating Hep G2 cells, cultured in the same conditions as for SDHB targeting RNAi experiments, with PI3K or MAPK inhibitors, such as LY294002 or PD 98059, respectively may indicate which pathway is involved.

The presence of HIF-1α in control targeted Hep G2 cells could also be explained by the presence of glucose in the culture media. Hep G2 cells can produce lactose in a glucose dependent manner. This would generate glycolytic ATP and therefore reduce the dependency of Hep G2 cells on the TCA cycle and electron transport for ATP production (Weber *et al.,* 2002). The ability of Hep G2 cells to produce lactose in this manner is probably due to a phenomenon known as the Warburg effect, where cancer and cultured cells display high levels of aerobic glycolysis. The end products of glycolysis, lactate and pyruvate, have been shown to activate HIF-1α in normoxia (Lu *et al.,* 2002). SDH B mutations mainly predispose individuals to extra-adrenal pheochromocytomas and most tumours associated with SDH B mutations have a high malignant potential. It is thought that the ability of these tumours to proliferate is manifested via the Warburg effect although this has not yet been conclusively proven (reviewed by Kantorovich *et al.,* 2010). In support of this are the findings that a Chinese hamster cell line harbouring a mutation in one of the SDH membrane

anchoring sub units grows normally in cell culture when glucose is provided (Oostveen *et al.,* 1995).

In contrast to the results in this study where SDH B inhibition resulted in HIF-1α suppression (figures 4.25 and 4.26 and 4.29 and 4.30), other researchers have shown that mutation of *SDH B* and *SDH D* results in increased HIF activity (Gimenez-Roqueplo *et al.,* 2001; Selak *et al.,* 2005; Lee *et al.,* 2005; Pollard *et al.,* 2005; Guzy *et al.,* 2008). Of particular interest are the results of Selak *et al.,* who carried out experiments using RNA interference to knockdown *SDHD.* They identified that knockdown of *SDHD* mRNA levels resulted in the increased activity of an HRE dependent luciferase reporter gene and increased HIF-1α protein levels. *SDHD* knockdown by RNA interference also resulted in the accumulation of *VEGF* mRNA and *VEGF* target gene of HIF-1.

*SDHD* knockdown by RNA interference results in an accumulation of succinate and loss of SDH B in is also known to result in an accumulation of succinate (Selak *et al.,* 2005; Pollard *et al.,* 2005). This accumulation inhibits PHD activity, resulting in increased HIF stabilisation and increased transcription of HIF target genes, thus providing a direct link between SDH B-D mutation and tumourigenesis (Selak *et al*., 2005; Lee *et al.,* 2005; Pollard *et al.,* 2005; Koivunen *et al.,* 2007).

One possibility as to why HIF-1α protein levels do not accumulate when SDH B protein levels are suppressed, is that succinate oxidation may still occur, possibly due to the limited levels of suppression observed (figures 4.25 and 4.26 and 4.29 and 4.30). In support of this theory is the finding that suppression of SDH B did not affect SDH A protein levels in Hep G2 cells, a finding that has also been observed in tumours harbouring either SDH B or SDH D mutations (Douwes Dekker *et al*., 2003).

Continued succinate oxidation does not explain the reduction in HIF-1α protein levels as a result of SDH B RNAi targeting. One possibility for this suppression could be a disruption to the homeostasis of the TCA cycle. Limited succinate oxidation would be predicted to not only result in a build up of succinate but also

other TCA cycle intermediates that occur prior to succinate, such as α-ketoglutarate. A fall in TCA cycle intermediates may also occur after succinate oxidation, for example fumarate levels. The levels of both α-ketoglutarate and fumarate can directly affect the activity of the PHDs. α-ketoglutarate (2-oxoglutarate) is a substrate of the PHDs that is required as well as molecular oxygen for their ability to hydroxylate HIF-α subunits (Epstein *et al.,* 2001). Conversely, fumarate inhibits the activity of the PHDs and is a more potent inhibitor than succinate (Pollard *et al.,* 2005). Therefore, it could be hypothesised that SDH B suppression results in increased α-ketoglutarate levels and decreased fumarate levels, as a result of this, PHD activity increases and HIF-1α protein levels fall. In support of this hypothesis is the finding that derivatives of α-ketoglutarate can alleviate pseudohypoxia in succinate dehydrogenase deficient cells (MacKenzie *et al.,* 2007). Fumarate inhibition can also be alleviated by elevated α-ketoglutarate (2 oxoglutarate) levels (Isaacs *et al.,* 2005). It is also interesting to note that α-ketoglutarate levels are 'topped' up by glutaminolysis, the process by which glutamine, a component added to cell culture media, is converted first to glutamate and then α-ketoglutarate (Mates *et al.,* 2009). This presents the possibility that glutaminolysis may also be a contributory factor to increased PHD activity. One way of assessing this hypothesis in vitro would be to treat Hep G2 cells targeted with control or SDH B RNAi with α-ketoglutarate or fumarate and assess the effect on HIF-1α protein levels.

The complexity in determining the effect of *SDH B-D* mutations on HIF can be further increased by the findings that mutations in *SDH B-D* can be accompanied by increased levels of ROS in some circumstances but not in others, suggesting there may be two pathways responsible for the regulation of HIF protein levels. For instance, Selak *et al.* did not detect any ROS in cells where SDH D expression was suppressed. Similarly, Pollard *et al.* did not detect any ROS in paraganglioma tissue harbouring *SDH* B mutations. However, in contrast to these findings elevated levels of ROS were found in *C. elegans* carrying a mis-sense mutation in *SDHC (*Senoo-Matsuda *et al.,* 2001*).* The corresponding mutation in mammals also resulted in elevated ROS levels (Ishii *et al.,* 2005). Stably suppressed SDH B has also been shown to cause elevated ROS levels, leading to the activation of hypoxia inducible factor (Guzy *et al.,* 2008).

In addition to *SDH* mutations identifying *SDH B-D* as tumour suppressor genes, mutations in the genes encoding for fumarate hydratase (FH) and isocitrate dehydrogenase 1 (IDH1) have identified them as tumour suppressors. Interestingly deficiencies in each of these metabolic enzymes present with distinct tumour types but a similar mode of tumourigenesis. For instance, biallelic *FH* mutations result in the inherited cancer syndrome hereditary leiomyomatosis and renal cell cancer (HLRCC, Tomlinson *et al.,* 2002). HLRCC kidney tumours show increased levels of HIF-1α when compared to normal kidney tissue, which results in increased expression of HIF target genes (Pollard *et al.,* 2005). The exact mechanism by which pseudohypoxic drive (the aberrant stabilisation of HIF under normoxic conditions) occurs as a result of *FH* mutation is not completely clear. However, it is possible that tumourigenesis due to *FH* mutation occurs in a similar manner as proposed for *SDH* mutation i.e. loss of fumarate hydratase activity results in increased fumarate levels which inhibit PHD activity, resulting in up-regulation of HIF-1α and subsequently HIF target genes. However, experiments performed in an HLRCC derived cell line showed HIF stabilisation occurred as a result of increased ROS levels, thus adding another level of complexity to the manner in which *FH* mutations result in up-regulation of the HIF pathway (Sudarshan *et al.,* 2009). Mutations in the gene encoding for IDH1 are mainly found in gliomas although one *IDH1* mutation has been identified in a sporadic paraganglioma (Zhao *et al.,* 2009; Kang *et al.,* 2009 and Gaal *et al.,* 2010). Inactivation of isocitrate dehydrogenase in human glioblastoma cells resulted in decreased levels of α-ketoglutarate, leading to decreased PHD activity and an increase in HIF-1α activity, thus resulting in tumourigenesis as a result of HIF pathway activation (Zhao *et al.,* 2009*).* Therefore it is clear that the mode of tumourigenesis for the majority of *SDH, FH,* and *IDH1* mutations involves loss of function of the proteins these genes encode for, resulting in up-regulation of the HIF pathway which is a known contributor to tumourigenesis. The fact that the abnormal de-regulation of HIF in so many forms of cancers including tumour cells harbouring TCA cycle mutations indicates the importance of HIFs role in tumourigenesis.

The finding that SDH B targeting results in the suppression of HIF-1α protein levels is difficult to fit into a model of how *SDHB* acts as a tumour suppressor gene. This is because HIF-1α accumulation caused by loss of pVHL has been proposed as an important mechanism for tumourigenesis and several other signalling pathways implicated in oncogenesis result in the up-regulation of HIF-1α (reviewed in Semenza G., 2002 and Bardos and Ashcroft. 2004). However, it should be noted that *VHL* mutations that result in type 2C VHL disease only pre-dispose carrier individuals to pheochromocytoma. These tumours retain the ability to regulate HIF-1α protein levels (Hoffman *et al.,* 2001 and Clifford *et al.,* 2001). This would suggest that the de-regulation of other pVHL functions is responsible for the development of pheochromocytoma in pre-disposed individuals and that the accumulation of HIF-1α may not be required in all cases of pheochromocytoma development. Therefore, pheochromocytoma tumours harbouring *SDHB* mutations may develop due to the de-regulation of other, as yet, unknown pathways and not, as hypothesised in this study, by accumulation of HIF-1α. It is also interesting to note that suppression of another TCA cycle enzyme also results in reduction of HIF-1α protein levels. IDH2 is an NADP+ dependent mitochondrial isocitrate dehydrogenase, which catalyses the conversion of isocitrate to α-ketoglutarate. The conversion of isocitrate to α-ketoglutarate yields NADPH, a reducing agent that is used in processes that protect cells from oxidative damage. Knockdown of IDH2 sensitises tumour cells to apoptosis in response to treatment with several anti-cancer drugs e.g. doxorubicin and it was hypothesised that this knockdown could also impact on HIF-1α protein levels. Suppression of IDH2 in PC3 cells via RNAi targeting resulted in suppressed HIF-1α protein levels (Kim *et al.,* 2010). This suggests that loss of, or suppression of some TCA cycle enzymes may not lead to tumourigenesis. However, the results observed in PC3 cells could have been a cell type specific response. This is also true of the results observed as a result of SDH B suppression in Hep G2 cells (figures 4.25, 4.26, 4.29 and 4.30); particularly as Hep G2 and PC3 cells are not representative of the cell types that harbour *SDH* mutations. IDH2 suppression in PC3 cells resulted in HIF-1α protein suppression which was accompanied by a decrease in HIF-1α mRNA. This appeared to be mediated via the PI3K/ Akt pathway and was not a result of an off target effect of the RNAi. These results are in marked contrast to those obtained from SDH B suppression, where

there was no apparent knockdown of HIF-1α mRNA (figure 4.31). However, in contrast to the results described, experiments carried out by Selak *et al.,* in HEK 293 cells, a non-representative cell type of pheochromocytoma or paraganglioma, appear to have produced a mechanistic model of what happens as a result of SDH mutation i.e. upregulation of HIF as a result of SDH D suppression. These observations highlight the complexity that exists in determining the mode of action of tumourigenesis from mutations in TCA cycle enzymes.

### *4.4.5 siRNA methods.*

The approaches used to design the siRNAs used in this study were based on the thought that siRNA targeting was specific and non-immunostimulatory (Elbashir *et al.,* 2001). However, in practice unmodified siRNAs such as the ones used in this study have some limitations. Unmodified siRNAs are susceptible to nuclease attack, have been shown to have off target effects as a result of interference in natural miRNA pathways and are potent triggers of the innate immune response (Gavrilov and Saltzman, 2012)

Off target effects of unmodified siRNAs were shown in expression profiling studies carried out by Jackson *et al.,* (2003), using siRNAs designed to the standard selection rules of Elbashir *et al.,* (2001). Sequence analysis of several off target transcripts revealed there was only partial complementarity between the siRNA and the off target transcript (Jackson *et al.,* 2003). Further research revealed that guide strand (the strand of siRNA incorporated into RISC) off targeting effects were the result of complementarity between the seed region of siRNA (positions 1-8 of the 5' end of the strand) and the 3' untranslated region (3' UTR) of mRNA (Jackson *et al.,* 2006). MicroRNAs (miRNAs) are endogenous and regulate gene expression via incomplete hybridisation of their seed region with 3'UTRs. This results in gene suppression by translational inhibition and deadenylation. 3'UTR sequences can be shared by mRNAs, therefore a single miRNA can regulate hundreds of gene siRNAs and miRNAs share the same silencing machinery and therefore it is thought siRNA off target silencing occurs as a result of the siRNA entering the miRNA pathway and causing miRNA-like effects thus downregulating off-target genes (Kanasty *et al.,*

2012). Other causes of off target effects can also be caused by as little as 11 nucleotides of continuous sequence of homology in coding regions (Jackson *et al.,* 2006) or passenger strand incorporation into RISC. The strand selection process of RISC is dependent on several factors including duplex thermodynamics where the least tightly bound 5' end of the duplex is normally incorporated into the complex (Khvorova *et al.,* 2003; Schwarz *et al.,* 2003), a 5' phosphate required for RISC binding and the sequence located at the 5' end of the guide strand as it appears argonaute-2 prefers A and U nucleotides over G and C (Deleavey and Damha., 2012).To avoid miRNA like off target effects siRNA design algorithms have been developed that attempt to select sequences with minimum seed complementarity to 3'UTR regions (Naito *et al.,* 2009).

Chemical modifications can also be introduced to limit miRNA like off target effects, increase stability and prolong the half-life of the siRNA. The most common modifications in siRNAs are the 2' modifications to the ribose ring and these include 2'-*O*-Methyl, 2' – fluoro and 2' –*O*- deoxymethymethoxyethl modifications. Linked nucleic acids (LNAs) which introduce a methylene bridge between the 2' oxygen and 4'carbon of the ribose ring are a further modification that can be introduced to the 2' site of the ribose ring (Shukla *et al.,* 2012). Backbone modifications of siRNAs can provide further resistance to nuclease attack and these include modifying backbone with phosphothioate or boranophosphate. Both of these modifications can enhance nuclease resistance of the siRNA (Gavrilov and Saltzman, 2012). Nuclease degradation of the SDH B siRNA used in this study may have affected its potency and could account for the differences in knockdown that are shown in western blots. It is also possible that a true signature of SDH B gene silencing was not observed in this study due to off target gene silencing by the SDH B siRNA. Alternatively, the control siRNA could equally have been responsible for an off target effect and the levels of HIF-1α observed in control treated samples (figure 4.30) was actually up-regulation due to a target effect of the siRNA.

Studies carried out by Reynolds *et al.,* (2004) and Ui-Tei *et al.,* (2008) have identified positional preferences an A or U is preferred at position 1 of the antisense strand, G or C is preferred at position 19, an A or U is favoured at position 10 (the cleavage site of argonaute-2) and A-U richness in positions 1-7 is favourable. These

positional preferences result in highly functional siRNAs and are also important for guide strand entry into RISC (Ui-Tei *et al.,* 2008). In both control and SDH B siRNAs an A or U is present at position 1 of the anti-sense strand, AU richness was also present in positions 1-7. However, an A or U was not present at position 10 of the siRNA and this could have affected the action of argonaute-2. Only the control siRNA had a G or C at position 19, thus indicating the SDH B siRNA used in this study may not be highly functional.

Original experiments using siRNAs suggested they were non-immunostimulatory (Elbashir *et al.,* 2001). However, it was subsequently shown that siRNAs can provoke the innate immune system via Toll like receptors (TLRs). TLRs are nucleic acid responsive with TLRs 7 and 8 thought to mediate the dominant immune response *in vivo*. Activation of TLR7/8 results in upregulation of type I interferons and cytokines (Samuel-Abraham and Leonard, 2010). HIF-1α can be upregulated by TLR7/8 ligands and therefore it is possible that up-regulation of HIF-1α seen in control targeted samples could be sue to provocation of an immune response by siRNA transfection (Nicholas and Sumbayev, 2009).

Further developments in RNA interference have resulted in the generation of vectors containing RNA polymerase II or III promotors. The RNAi trigger can be expressed as an miRNA of short hairpin RNA (shRNA). These are then cleaved into small siRNAs by Dicer before entry into RISC. Development of these vectors allows for stable long-term knockdown of the target transcript (Paddison *et al.,* 2002).

# Chapter 5: Discussion

# 5. Discussion

Hypoxia, the result of low levels of oxygen concentration in tissue, causes cells to activate several adaptive responses to match $O_2$ supply with metabolic, bioenergetic and redox demands. These events are co-ordinated by several processes including the unfolded protein response and mTOR signalling (Wouters and Koritzinsky, 2008). However, transcription regulation in hypoxia by hypoxia inducible factors is recognised as one of the key processes in a cell's adaptation to low oxygen levels.

HIF function has been identified as a major contributory factor in several major diseases including pulmonary hypertension, ischaemia, angiogenesis and tumourigenesis. HIF has also been identified as having a specific involvement in asthma, inflammatory bowel disease, coeliac disease and haematological malignancies such as leukaemia (Hirota *et al.,* 2009 and Konopleva *et al.,* 2009). Therefore, the development of therapeutic strategies capable of modulating HIF function is an attractive prospect. Current research strategies involve the development of targeted small molecules that result in HIF-1 up-regulation for ischaemic disease therapy or the inhibition of HIF-1 activity for cancer-therapy (figure 5.1, Li *et al.,* 2005; Hewitson and Schofield, 2004; Semenza, 2003; Belozerov and Van Meir, 2005).

The involvement of HIF signalling in disease outlines the importance of developing therapeutics to HIF, whether to inhibit or regulate its activity. Currently, very few therapeutics that specifically target HIF are used clinically. However, many novel anti-cancer drugs which specifically target other regulatory pathways also have anti-angiogenic effects largely due to their ability to inhibit HIF-1. For example, the anthracyclines e.g. doxorubicin and daunorubicin decrease HIF-1 DNA binding, EGFR inhibitors, microtubule inhibitors, mTOR inhibitors and topoisomerase inhibitors decrease HIF-1a synthesis, proteasome and histone deacetylases decrease HIF-1a transactivation and finally histone deacetylases and HSP90 inhibitors increase HIF-1a degradation (Semenza, 2010). In the case of HSP90 inhibitors, this is due to an oxygen and PHD independent ubiquitin mediated degradation (Liu *et al.,* 2007).

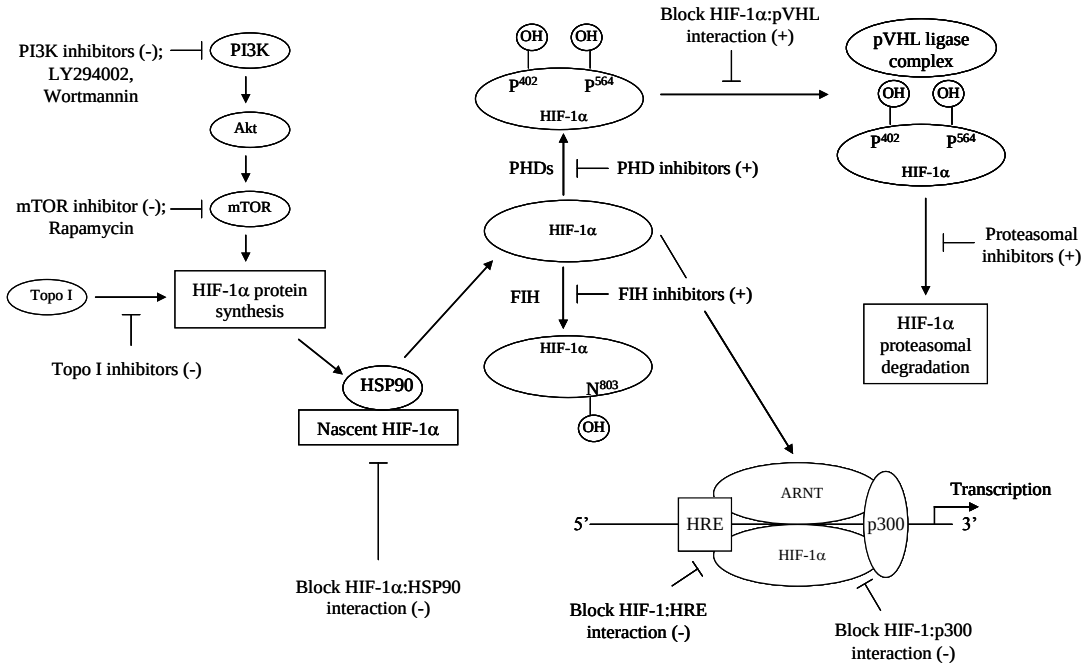


**Figure 5.1 Potential therapeutic target sites in the HIF pathway.**

An overview of the potential points of therapeutic intervention in the HIF pathway either to increase (+) or decrease (-) the levels of HIF-1α.

**Key:** ARNT, aryl hydrocabonreceptor nuclear translocator; FIH, factor inhibiting HIF; HIF-1α, hypoxia inducible factor; HRE, hypoxia response element; HSP90, heat shock protein 90; 1-α mTOR, mammalian target of rapamycin; N, asparagine; P, proline; PHDs, prolyl hydorxylases; PI3K, phosphatidylinositol 3-kinase; pVHL, von-Hippel Lindau protein; OH, hydroxyl; TOPO I, topoisomerase I.

The development of RNA aptamers as novel therapeutics provides another avenue of exploration for HIF inhibitors/up-regulators. Pegaptanib sodium also known commercially as Macugen, is an anti-VEGF RNA aptamer which is used for the treatment of all types of neovasular age related macular degeneration. It is the first aptamer to be approved for clinical use (Ng *et al.*, 2006). Other RNA aptamers have also reached the clinical trial phase. Of particular importance for cancer therapy is AS1411, the first RNA aptamer to enter oncology clinical trials. AS1411 is an RNA aptamer that specifically targets nucleolin, a protein that is found on the surface of many cancer cells, including cancer cells associated with acute myeloid leukaemia and renal cell carcinoma. AS1411 is systemically administered and its internalisation

results in a decrease in several cancer related mRNAs which results in reduced cell proliferation (Soundararajan *et al*, 2009 and Reyes-Reyes *et al.,* 2010).

The REG 1 anticoagulation system is also in clinical trials and represents an aptamer-antidote pair to coagulation factor IXa (FIXa). RB006 is the active aptamer drug that binds FIXa and RB007 is the antidote which is an oligonucleotide controlling agent that is complementary to a portion of RB006 and when bound neutralises the anti-FIXa activity of RB006. This drug is particularly useful in the treatment of thrombotic disease and represents a highly specific and controllable drug (Povsic *et al.,* 2010).

The level of HIF involvement in disease and the advantages of RNA aptamers such as high target specificity, high target affinity, in vitro development and low immunogenicity led to the development of RNA aptamers targeted to the HIF oxygen dependent degradation domain. The hoped for outcome was blockage of ubiquitin mediated degradation resulting in increased HIF-1α protein levels and a subsequent increase in HIF signalling. It was hoped that these results would be useful in potentially developing a therapeutic agent for the use in HIF related diseases, for example in ischaemic disease. Although no conclusive results could be drawn from this study, it is possible that the RNA aptamer developed against the HIF-ODDD suppressed HIF function (figure 3.17). A more robust test assay would be required to assess this (section 3.5). However, aptamers developed towards HIF that decrease HIF signalling would potentially be useful in the treatment of cancer. HIF exerts its affects on cancer progression by activating target genes involved in angiogenesis, cell survival, chemotherapy and radiation resistance, genetic instability, immortalisation, immune evasion, invasion and metastasis, proliferation, metabolism and pH regulation (reviewed by Semenza, 2010). Development of a specific anti-HIF RNA aptamer would be useful as this could prevent tumour angiogenesis and metastasis.

Further developments in the RNA aptamer field have resulted in a fusion of technologies such as RNA aptamer delivery by siRNAs and RNA aptamer delivery by nanobiotechnology particles. RNA aptamer hybrids have also been developed and this would be a useful area for further study in the case of a HIF-1α RNA aptamer

(reviewed by Guo *et al.*, 2008). This is because HIF-1α is a cytoplasmic and nuclear protein, therefore any RNA aptamer targeting HIF-1α would need to be delivered to the cell type of interest and internalised before it could act. Therefore, development of a cell type specific RNA aptamer and hybridisation with a HIF-1α aptamer could provide a delivery mechanism.

The involvement of HIF in intratumour hypoxia is well documented however, alterations resulting in oncogene gain of function or tumour suppressor loss of function (as is the case for SDH B), often lead to increased HIF-1 activity, suggesting increased HIF-1 activity represents a common pathway in cancer pathogenesis. One of the most studied cancer syndromes known to exhibit de-regulation of the HIF pathway is von Hippel Lindau disease (section 1.6.5). Sufferers of VHL disease suffer from central nervous system and retinal hemagioblastomas, clear cell renal carcinomas and pheochromocytomas (Kim and Kaelin Jr., 2004). Similarities in the tumour type and tumour vasculature between VHL disease and paraganglionic tumours harbouring *SDH D* mutations suggested HIF involvement in tumour formation that was not solely due to the role of HIF in tumourigenesis with regards to tumour hypoxia. Germline mutations in *SDH B* also resulted in paraganglioma and pheochromocytoma. Therefore, the effect of SDH B inhibition on HIF-1 was investigated. 3-NPA, an inhibitor of complex II of the mitochondrial respiratory chain, was used to treat of Hep G2 cells in a proof of principle experiment that determined 3-NPA inhibition of complex II resulted in increased levels of HIF-1α protein (section 4.2.6). However, a more targeted approach to suppress SDH B in the form of RNA interference targeted to *SDHB* mRNA resulted in suppression of HIF-1α protein levels (figures 4.25 and 4.26). This was in marked contrast to research carried out by other groups and could possibly be due to the cell type experiments were carried out in or because the level of SDH B suppression was not great enough to induce HIF-1α protein levels (Gimenez-Roqueplo *et al.*, 2001; Selak *et al.*, 2005; Lee *et al.*, 2005; Pollard *et al.*, 2005 and Guzy *et al.*, 2008). Mutations in *SDHAF2* (the gene encoding for succinate dehydrogenase assembly factor 2), *SDH B, SDH C, SDH D, FH, IDH1* and *IDH2* have all been shown to cause up-regulation of HIF-1α protein levels resulting in the up-regulation of HIF regulated target genes (Kantorovich *et al*, 2010; Pollard *et al.*, 2007 and Gaal *et al*, 2009). This suggests that the results achieved in this study were not indicative of the tumour

mechanism for *SDH B* mutation. Until recently, no genetic link between SDH A and paraganglioma/pheochromocytoma syndromes had been identified. However, a germline mutation in SDH A has been identified in a patient suffering from an abdominal catecholamine secreting paraganglioma. This mutation resulted in a pseudo-hypoxic response which is also observed in other tumours caused by mutation of TCA cycle intermediates. Loss of heterozygocity at the *SDH A* loci in the tumour tissue identifies SDH A as a tumour suppressor gene (Burnichon *et al.,* 2010).

Several facets in the regulation of HIF have recently been described. These mechanisms could provide further therapeutic targets for HIF regulation. Under hypoxic conditions stimulated sphingosine kinase 1 (SphK1) converts sphingosine to sphingosine 1-phosphate resulting in the up-regulation of HIF-1α via an Akt/GSK3β pathway (Ader *et al.,* 2009). microRNAs have also been identified that can regulate HIF-1 both under hypoxic conditions (where the microRNA is referred to as a hypoxamir) and independently of hypoxia. For example, the hypoxamir miR20b suppresses HIF-1α expression in MCF-7 breast cancer cells whereas the hypoxamir miR424 targets CUL2 in the pVHL ubiquitin ligase complex resulting in impaired prolyl hydroxylation of HIF-1α and a subsequent stabilisation of HIF-1α protein levels. Independently of hypoxia c-MYC induces the miR17-92 cluster which suppresses expression of HIF-1α in lung cancer cells whereas miR31 targets FIH resulting in the stabilisation of HIF-1α (Loscalzo, 2010 and Loboda *et al.,* 2010).

The involvement of HIF in so many types of cancer e.g pheochromocytoma/paraganglioma syndromes, lymphoma and leukaemia, and also in several different diseases such as ischaemia, highlights the importance of developing therapeutics specifically targeted towards HIF, whether as HIF inhibitors or as HIF up-regulators. As our knowledge of the mechanisms which regulate HIF and the roles the HIF family of proteins are involved in grow so does the opportunity for development of novel HIF specific therapeutics.

# Chapter 6: Bibliography

Ackrell, B. A. (2000). Progress in understanding structure-function relationships in respiratory chain complex II. *FEBS Lett.* 466, 1-5.

Ackrell, B. A. (2002). Cytopathies involving mitochondrial complex II. *Mol. Aspects Med.* 23, 369-384.

Ader, I., Malavaud, B. and Cuvillier, O. (2009). When the sphingosine kinase 1/sphingosine 1-phosphate pathway meets hypoxia signaling: New targets for cancer therapy. *Cancer Res.* 69, 3723-3726.

Adjei, A. A. (2001). Blocking oncogenic ras signaling for cancer therapy. *J. Natl. Cancer Inst.* 93, 1062-1074.

Alam, N. A., Rowan, A. J., Wortham, N. C., Pollard, P. J., Mitchell, M., Tyrer, J. P., Barclay, E., Calonje, E., Manek, S., Adams, S. J. et al. (2003). Genetic and functional analyses of FH mutations in multiple cutaneous and uterine leiomyomatosis, hereditary leiomyomatosis and renal cancer, and fumarate hydratase deficiency. *Hum. Mol. Genet.* 12, 1241-1252.

Alfranca, A., Gutierrez, M. D., Vara, A., Aragones, J., Vidal, F. and Landazuri, M. O. (2002). c-jun and hypoxia-inducible factor 1 functionally cooperate in hypoxia-induced gene transcription. *Mol. Cell. Biol.* 22, 12-22.

Alston, T. A., Mela, L. and Bright, H. J. (1977). 3-nitropropionate, the toxic substance of indigofera, is a suicide inactivator of succinate dehydrogenase. *Proc. Natl. Acad. Sci. U. S. A.* 74, 3767-3771.

Appelhoff, R. J., Tian, Y. M., Raval, R. R., Turley, H., Harris, A. L., Pugh, C. W., Ratcliffe, P. J. and Gleadle, J. M. (2004). Differential function of the prolyl hydroxylases PHD1, PHD2, and PHD3 in the regulation of hypoxia-inducible factor. *J. Biol. Chem.* 279, 38458-38465.

Arany, Z., Huang, L. E., Eckner, R., Bhattacharya, S., Jiang, C., Goldberg, M. A., Bunn, H. F. and Livingston, D. M. (1996). An essential role for p300/CBP in the cellular response to hypoxia. *Proc. Natl. Acad. Sci. U. S. A.* 93, 12969-12973.

Astuti, D., Douglas, F., Lennard, T. W., Aligianis, I. A., Woodward, E. R., Evans, D. G., Eng, C., Latif, F. and Maher, E. R. (2001). Germline SDHD mutation in familial phaeochromocytoma. *Lancet* 357, 1181-1182.

Astuti, D., Latif, F., Dallol, A., Dahia, P. L., Douglas, F., George, E., Skoldberg, F., Husebye, E. S., Eng, C. and Maher, E. R. (2001). Gene mutations in the succinate dehydrogenase subunit SDHB cause susceptibility to familial pheochromocytoma and to familial paraganglioma. *Am. J. Hum. Genet.* 69, 49-54.

ATCC. Passage effects in cell lines; technical bulletin no. 7.
http://www.atcc.org/Portals/1/Pdf/tb07.pdf

Badenhop, R. F., Cherian, S., Lord, R. S., Baysal, B. E., Taschner, P. E. and Schofield, P. R. (2001). Novel mutations in the SDHD gene in pedigrees with familial carotid body paraganglioma and sensorineural hearing loss. *Genes Chromosomes Cancer* 31, 255-263.

Baek, J. H., Liu, Y. V., McDonald, K. R., Wesley, J. B., Hubbi, M. E., Byun, H. and Semenza, G. L. (2007). Spermidine/spermine-N1-acetyltransferase 2 is an essential component of the ubiquitin ligase complex that regulates hypoxia-inducible factor 1alpha. *J. Biol. Chem.* 282, 23572-23580.

Baek, J. H., Mahon, P. C., Oh, J., Kelly, B., Krishnamachary, B., Pearson, M., Chan, D. A., Giaccia, A. J. and Semenza, G. L. (2005). OS-9 interacts with hypoxia-inducible factor 1alpha and prolyl hydroxylases to promote oxygen-dependent degradation of HIF-1alpha. *Mol. Cell* 17, 503-512.

Bardos, J. I. and Ashcroft, M. (2004). Hypoxia-inducible factor-1 and oncogenic signalling. *Bioessays* 26, 262-269.

Bardos, J. I. and Ashcroft, M. (2005). Negative and positive regulation of HIF-1: A complex network. *Biochim. Biophys. Acta* 1755, 107-120.

Bartel, D. P. (2004). MicroRNAs: Genomics, biogenesis, mechanism, and function. *Cell* 116, 281-297.

Baysal, B. E. (2003). On the association of succinate dehydrogenase mutations with hereditary paraganglioma. *Trends Endocrinol. Metab.* 14, 453-459.

Baysal, B. E., Ferrell, R. E., Willett-Brozick, J. E., Lawrence, E. C., Myssiorek, D., Bosch, A., van der Mey, A., Taschner, P. E., Rubinstein, W. S., Myers, E. N. et al. (2000). Mutations in SDHD, a mitochondrial complex II gene, in hereditary paraganglioma. *Science* 287, 848-851.

Baysal, B. E., Willett-Brozick, J. E., Lawrence, E. C., Drovdlic, C. M., Savul, S. A., McLeod, D. R., Yee, H. A., Brackmann, D. E., Slattery, W. H.,3rd, Myers, E. N. et al. (2002). Prevalence of SDHB, SDHC, and SDHD germline mutations in clinic patients with head and neck paragangliomas. *J. Med. Genet.* 39, 178-183.

Belozerov, V. E. and Van Meir, E. G. (2005). Hypoxia inducible factor-1: A novel target for cancer therapy. *Anticancer Drugs* 16, 901-909.

Berchner-Pfannschmidt, U., Yamac, H., Trinidad, B. and Fandrey, J. (2007). Nitric oxide modulates oxygen sensing by hypoxia-inducible factor 1-dependent induction of prolyl hydroxylase 2. *J. Biol. Chem.* 282, 1788-1796.

Berra, E., Benizri, E., Ginouves, A., Volmat, V., Roux, D. and Pouyssegur, J. (2003). HIF prolyl-hydroxylase 2 is the key oxygen sensor setting low steady-state levels of HIF-1alpha in normoxia. *EMBO J.* 22, 4082-4090.

Berra, E., Ginouves, A. and Pouyssegur, J. (2006). The hypoxia-inducible-factor hydroxylases bring fresh air into hypoxia signalling. *EMBO Rep.* 7, 41-45.

Bhattacharya, S. and Ratcliffe, P. J. (2003). ExCITED about HIF. *Nat. Struct. Biol.* 10, 501-503.

Bhattacharya, S., Michels, C. L., Leung, M. K., Arany, Z. P., Kung, A. L. and Livingston, D. M. (1999). Functional role of p35srj, a novel p300/CBP binding protein, during transactivation by HIF-1. *Genes Dev.* 13, 64-75.

Blagosklonny, M. V., An, W. G., Romanova, L. Y., Trepel, J., Fojo, T. and Neckers, L. (1998). P53 inhibits hypoxia-inducible factor-stimulated transcription. *J. Biol. Chem.* 273, 11995-11998.

Blouw, B., Song, H., Tihan, T., Bosze, J., Ferrara, N., Gerber, H. P., Johnson, R. S. and Bergers, G. (2003). The hypoxic response of tumors is dependent on their microenvironment. *Cancer. Cell.* 4, 133-146.

Boast, K., Binley, K., Iqball, S., Price, T., Spearman, H., Kingsman, S., Kingsman, A. and Naylor, S. (1999). Characterization of physiologically regulated vectors for the treatment of ischemic disease. *Hum. Gene Ther.* 10, 2197-2208.

Bouis, D., Kusumanto, Y., Meijer, C., Mulder, N. H. and Hospers, G. A. (2006). A review on pro- and anti-angiogenic factors as targets of clinical intervention. *Pharmacol. Res.* 53, 89-103.

Bourgeron, T., Rustin, P., Chretien, D., Birch-Machin, M., Bourgeois, M., Viegas-Pequignot, E., Munnich, A. and Rotig, A. (1995). Mutation of a nuclear succinate dehydrogenase gene results in mitochondrial respiratory chain deficiency. *Nat. Genet.* 11, 144-149.

Brown, J. M. (2002). Tumor microenvironment and the response to anticancer therapy. *Cancer. Biol. Ther.* 1, 453-458.

Bruening, W., Giasson, B., Mushynski, W. and Durham, H. D. (1998). Activation of stress-activated MAP protein kinases up-regulates expression of transgenes driven by the cytomegalovirus immediate/early promoter. *Nucleic Acids Res.* 26, 486-489.

Bruick, R. K. and McKnight, S. L. (2001). A conserved family of prolyl-4-hydroxylases that modify HIF. *Science* 294, 1337-1340.

Brusselmans, K., Compernolle, V., Tjwa, M., Wiesener, M. S., Maxwell, P. H., Collen, D. and Carmeliet, P. (2003). Heterozygous deficiency of hypoxia-inducible factor-2alpha protects mice against pulmonary hypertension and right ventricular dysfunction during prolonged hypoxia. *J. Clin. Invest.* 111, 1519-1527.

Bryant, J., Farmer, J., Kessler, L. J., Townsend, R. R. and Nathanson, K. L. (2003). Pheochromocytoma: The expanding genetic differential diagnosis. *J. Natl. Cancer Inst.* 95, 1196-1204.

Burnichon, N., Briere, J. J., Libe, R., Vescovo, L., Riviere, J., Tissier, F., Jouanno, E., Jeunemaitre, X., Benit, P., Tzagoloff, A. et al. (2010). SDHA is a tumor suppressor gene causing paraganglioma. *Hum. Mol. Genet.* 19, 3011-3020.

Capaldi, R. A. and Aggeler, R. (2002). Mechanism of the F(1)F(0)-type ATP synthase, a biological rotary motor. *Trends Biochem. Sci.* 27, 154-160.

Carmeliet, P. (2005). Angiogenesis in life, disease and medicine. *Nature* 438, 932-936.

Carrero, P., Okamoto, K., Coumailleau, P., O'Brien, S., Tanaka, H. and Poellinger, L. (2000). Redox-regulated recruitment of the transcriptional coactivators CREB-binding protein and SRC-1 to hypoxia-inducible factor 1alpha. *Mol. Cell. Biol.* 20, 402-415.

Castanotto, D. and Rossi, J. J. (2009). The promises and pitfalls of RNA-interference-based therapeutics. *Nature* 457, 426-433.

Cecchini, G. (2003). Function and structure of complex II of the respiratory chain. *Annu. Rev. Biochem.* 72, 77-109.

Chalhoub, N. and Baker, S. J. (2009). PTEN and the PI3-kinase pathway in cancer. *Annu. Rev. Pathol.* 4, 127-150.

Chan, D. A., Sutphin, P. D., Denko, N. C. and Giaccia, A. J. (2002). Role of prolyl hydroxylation in oncogenically stabilized hypoxia-inducible factor-1alpha. *J. Biol. Chem.* 277, 40112-40117.

Chandel, N. S., McClintock, D. S., Feliciano, C. E., Wood, T. M., Melendez, J. A., Rodriguez, A. M. and Schumacker, P. T. (2000). Reactive oxygen species generated at mitochondrial complex III stabilize hypoxia-inducible factor-1alpha during hypoxia: A mechanism of O2 sensing. *J. Biol. Chem.* 275, 25130-25138.

Chang, L. and Karin, M. (2001). Mammalian MAP kinase signalling cascades. *Nature* 410, 37-40.

Chapman-Smith, A., Lutwyche, J. K. and Whitelaw, M. L. (2004). Contribution of the Per/Arnt/Sim (PAS) domains to DNA binding by the basic helix-loop-helix PAS transcriptional regulators. *J. Biol. Chem.* 279, 5353-5362.

Chelliserrykattil, J. and Ellington, A. D. (2004). Evolution of a T7 RNA polymerase variant that transcribes 2'-O-methyl RNA. *Nat. Biotechnol.* 22, 1155-1160.

Chen, C., Pore, N., Behrooz, A., Ismail-Beigi, F. and Maity, A. (2001). Regulation of glut1 mRNA by hypoxia-inducible factor-1. interaction between H-ras and hypoxia. *J. Biol. Chem.* 276, 9519-9525.

Chilov, D., Camenisch, G., Kvietikova, I., Ziegler, U., Gassmann, M. and Wenger, R. H. (1999). Induction and nuclear translocation of hypoxia-inducible factor-1 (HIF-1): Heterodimerization with ARNT is not necessary for nuclear accumulation of HIF-1alpha. *J. Cell. Sci.* 112 ( Pt 8), 1203-1212.

Chun, Y. S., Choi, E., Yeo, E. J., Lee, J. H., Kim, M. S. and Park, J. W. (2001). A new HIF-1 alpha variant induced by zinc ion suppresses HIF-1-mediated hypoxic responses. *J. Cell. Sci.* 114, 4051-4061.

Clifford, S. C., Cockman, M. E., Smallwood, A. C., Mole, D. R., Woodward, E. R., Maxwell, P. H., Ratcliffe, P. J. and Maher, E. R. (2001). Contrasting effects on HIF-1alpha regulation by disease-causing pVHL mutations correlate with patterns of tumourigenesis in von hippel-lindau disease. *Hum. Mol. Genet.* 10, 1029-1038.

Cockman, M. E., Masson, N., Mole, D. R., Jaakkola, P., Chang, G. W., Clifford, S. C., Maher, E. R., Pugh, C. W., Ratcliffe, P. J. and Maxwell, P. H. (2000). Hypoxia inducible factor-alpha binding and ubiquitylation by the von hippel-lindau tumor suppressor protein. *J. Biol. Chem.* 275, 25733-25741.

Coles, C. J., Edmondson, D. E. and Singer, T. P. (1979). Inactivation of succinate dehydrogenase by 3-nitropropionate. *J. Biol. Chem.* 254, 5161-5167.

Conrad, P. W., Freeman, T. L., Beitner-Johnson, D. and Millhorn, D. E. (1999). EPAS1 trans-activation during hypoxia requires p42/p44 MAPK. *J. Biol. Chem.* 274, 33709-33713.

Corn, P. G., McDonald, E. R.,3rd, Herman, J. G. and El-Deiry, W. S. (2003). Tat-binding protein-1, a component of the 26S proteasome, contributes to the E3 ubiquitin ligase function of the von hippel-lindau protein. *Nat. Genet.* 35, 229-237.

Cosma, M. P. (2002). Ordered recruitment: Gene-specific mechanism of transcription activation. *Mol. Cell* 10, 227-236.

Czyzyk-Krzeska, M. F. and Meller, J. (2004). Von hippel-lindau tumor suppressor: Not only HIF's executioner. *Trends Mol. Med.* 10, 146-149.

D'Angio, C. T. and Finkelstein, J. N. (2000). Oxygen regulation of gene expression: A study in opposites. *Mol. Genet. Metab.* 71, 371-380.

Dann, C. E.,3rd, Bruick, R. K. and Deisenhofer, J. (2002). Structure of factor-inhibiting hypoxia-inducible factor 1: An asparaginyl hydroxylase involved in the hypoxic response pathway. *Proc. Natl. Acad. Sci. U. S. A.* 99, 15351-15356.

de Smidt, P. C., Le Doan, T., de Falco, S. and van Berkel, T. J. (1991). Association of antisense oligonucleotides with lipoproteins prolongs the plasma half-life and modifies the tissue distribution. *Nucleic Acids Res.* 19, 4695-4700.

del Peso, L., Castellanos, M. C., Temes, E., Martin-Puig, S., Cuevas, Y., Olmos, G. and Landazuri, M. O. (2003). The von hippel Lindau/hypoxia-inducible factor (HIF) pathway regulates the transcription of the HIF-proline hydroxylase genes in response to low oxygen. *J. Biol. Chem.* 278, 48690-48695.

Deleavey, GF., Damha, MJ., (2012) Designing chemically modified oligonucleotides for targeted gene silencing. *Chem Biol.* 19(8),937-54.

Doronzo, G., Russo, I., Mattiello, L., Riganti, C., Anfossi, G. and Trovati, M. (2006). Insulin activates hypoxia-inducible factor-1alpha in human and rat vascular smooth muscle cells via phosphatidylinositol-3 kinase and mitogen-activated protein kinase pathways: Impairment in insulin resistance owing to defects in insulin signalling. *Diabetologia* 49, 1049-1063.

Douwes Dekker, P. B., Hogendoorn, P. C., Kuipers-Dijkshoorn, N., Prins, F. A., van Duinen, S. G., Taschner, P. E., van der Mey, A. G. and Cornelisse, C. J. (2003). SDHD mutations in head and neck paragangliomas result in destabilization of complex II in the mitochondrial respiratory chain with loss of enzymatic activity and abnormal mitochondrial morphology. *J. Pathol.* 201, 480-486.

Drutel, G., Kathmann, M., Heron, A., Schwartz, J. C. and Arrang, J. M. (1996). Cloning and selective expression in brain and kidney of ARNT2 homologous to the ah receptor nuclear translocator (ARNT). *Biochem. Biophys. Res. Commun.* 225, 333-339.

Duan, D. R., Pause, A., Burgess, W. H., Aso, T., Chen, D. Y., Garrett, K. P., Conaway, R. C., Conaway, J. W., Linehan, W. M. and Klausner, R. D. (1995). Inhibition of transcription elongation by the VHL tumor suppressor protein. *Science* 269, 1402-1406.

Elbashir, S. M., Harborth, J., Lendeckel, W., Yalcin, A., Weber, K. and Tuschl, T. (2001). Duplexes of 21-nucleotide RNAs mediate RNA interference in cultured mammalian cells. *Nature* 411, 494-498.

Elbashir, S. M., Harborth, J., Weber, K. and Tuschl, T. (2002). Analysis of gene function in somatic mammalian cells using small interfering RNAs. *Methods* 26, 199-213.

Elder, E. E., Elder, G. and Larsson, C. (2005). Pheochromocytoma and functional paraganglioma syndrome: No longer the 10% tumor. *J. Surg. Oncol.* 89, 193-201.

Elson, D. A., Thurston, G., Huang, L. E., Ginzinger, D. G., McDonald, D. M., Johnson, R. S. and Arbeit, J. M. (2001). Induction of hypervascularity without leakage or inflammation in transgenic mice overexpressing hypoxia-inducible factor-1alpha. *Genes Dev.* 15, 2520-2532.

Ema, M., Taya, S., Yokotani, N., Sogawa, K., Matsuda, Y. and Fujii-Kuriyama, Y. (1997). A novel bHLH-PAS factor with close sequence similarity to hypoxia-inducible factor 1alpha regulates the VEGF expression and is potentially involved in lung and vascular development. *Proc. Natl. Acad. Sci. U. S. A.* 94, 4273-4278.

Epstein, A. C., Gleadle, J. M., McNeill, L. A., Hewitson, K. S., O'Rourke, J., Mole, D. R., Mukherji, M., Metzen, E., Wilson, M. I., Dhanda, A. et al. (2001). C. elegans EGL-9 and mammalian homologs define a family of dioxygenases that regulate HIF by prolyl hydroxylation. *Cell* 107, 43-54.

Esteban, M. A. and Maxwell, P. H. (2005). HIF, a missing link between metabolism and cancer. *Nat. Med.* 11, 1047-1048.

Evans, A. R., Limp-Foster, M. and Kelley, M. R. (2000). Going APE over ref-1. *Mutat. Res.* 461, 83-108.

Famulok, M. (1994). Molecular recognition of amino acids by RNA-aptamers: An L-citrulline binding RNA motif and its evolution into and L-arginine binder. *J. Am. Chem. Soc.* 116, 1698-1706.

Fang, J. Y. and Richardson, B. C. (2005). The MAPK signalling pathways and colorectal cancer. *Lancet Oncol.* 6, 322-327.

Farr, A. and Roman, A. (1992). A pitfall of using a second plasmid to determine transfection efficiency. *Nucleic Acids Res.* 20, 920.

Feldser, D., Agani, F., Iyer, N. V., Pak, B., Ferreira, G. and Semenza, G. L. (1999). Reciprocal positive regulation of hypoxia-inducible factor 1alpha and insulin-like growth factor 2. *Cancer Res.* 59, 3915-3918.

Flashman, E., McDonough, M. A. and Schofield, C. J. (2005). OS-9: Another piece in the HIF complex story. *Mol. Cell* 17, 472-473.

Fox, S. B., Braganca, J., Turley, H., Campo, L., Han, C., Gatter, K. C., Bhattacharya, S. and Harris, A. L. (2004). CITED4 inhibits hypoxia-activated transcription in cancer cells, and its cytoplasmic location in breast cancer is associated with elevated expression of tumor cell hypoxia-inducible factor 1alpha. *Cancer Res.* 64, 6075-6081.

Frede, S., Stockmann, C., Freitag, P. and Fandrey, J. (2006). Bacterial lipopolysaccharide induces HIF-1 activation in human monocytes via p44/42 MAPK and NF-kappaB. *Biochem. J.* 396, 517-527.

Freedman, S. J., Sun, Z. Y., Kung, A. L., France, D. S., Wagner, G. and Eck, M. J. (2003). Structural basis for negative regulation of hypoxia-inducible factor-1alpha by CITED2. *Nat. Struct. Biol.* 10, 504-512.

Freedman, S. J., Sun, Z. Y., Poy, F., Kung, A. L., Livingston, D. M., Wagner, G. and Eck, M. J. (2002). Structural basis for recruitment of CBP/p300 by hypoxia-inducible factor-1 alpha. *Proc. Natl. Acad. Sci. U. S. A.* 99, 5367-5372.

Fresno Vara, J. A., Casado, E., de Castro, J., Cejas, P., Belda-Iniesta, C. and Gonzalez-Baron, M. (2004). PI3K/Akt signalling pathway and cancer. *Cancer Treat. Rev.* 30, 193-204.

Friedrich, C. A. (2001). Genotype-phenotype correlation in von hippel-lindau syndrome. *Hum. Mol. Genet.* 10, 763-767.

Fry, M. J. (2001). Phosphoinositide 3-kinase signalling in breast cancer: How big a role might it play? *Breast Cancer Res.* 3, 304-312.

Fukuda, T., Kiuchi, K. and Takahashi, M. (2002). Novel mechanism of regulation of rac activity and lamellipodia formation by RET tyrosine kinase. *J. Biol. Chem.* 277, 19114-19121.

Gaal, J., Burnichon, N., Korpershoek, E., Roncelin, I., Bertherat, J., Plouin, P. F., de Krijger, R. R., Gimenez-Roqueplo, A. P. and Dinjens, W. N. (2010). Isocitrate dehydrogenase mutations are rare in pheochromocytomas and paragangliomas. *J. Clin. Endocrinol. Metab.* 95, 1274-1278.

Gao, N., Ding, M., Zheng, J. Z., Zhang, Z., Leonard, S. S., Liu, K. J., Shi, X. and Jiang, B. H. (2002). Vanadate-induced expression of hypoxia-inducible factor 1 alpha and vascular endothelial growth factor through phosphatidylinositol 3-kinase/Akt pathway and reactive oxygen species. *J. Biol. Chem.* 277, 31963-31971.

Gao, N., Jiang, B. H., Leonard, S. S., Corum, L., Zhang, Z., Roberts, J. R., Antonini, J., Zheng, J. Z., Flynn, D. C., Castranova, V. et al. (2002). p38 signaling-mediated hypoxia-inducible factor 1alpha and vascular endothelial growth factor induction by cr(VI) in DU145 human prostate carcinoma cells. *J. Biol. Chem.* 277, 45041-45048.

Gavrilov, K., Saltzman, W. M.,(2012). Therapeutic siRNA: Principles, challenges, and strategies. *Yale Journal of Biology amd Medicine.* 85, 187-200.

Gekakis, N., Staknis, D., Nguyen, H. B., Davis, F. C., Wilsbacher, L. D., King, D. P., Takahashi, J. S. and Weitz, C. J. (1998). Role of the CLOCK protein in the mammalian circadian mechanism. *Science* 280, 1564-1569.

Giaccia, A. J. and Kastan, M. B. (1998). The complexity of p53 modulation: Emerging patterns from divergent signals. *Genes Dev.* 12, 2973-2983.

Giles, R. H., Peters, D. J. and Breuning, M. H. (1998). Conjunction dysfunction: CBP/p300 in human disease. *Trends Genet.* 14, 178-183.

Gimenez-Roqueplo, A. P., Favier, J., Rustin, P., Mourad, J. J., Plouin, P. F., Corvol, P., Rotig, A. and Jeunemaitre, X. (2001). The R22X mutation of the SDHD gene in hereditary paraganglioma abolishes the enzymatic activity of complex II in the mitochondrial respiratory chain and activates the hypoxia pathway. *Am. J. Hum. Genet.* 69, 1186-1197.

Gimenez-Roqueplo, A. P., Favier, J., Rustin, P., Rieubland, C., Crespin, M., Nau, V., Khau Van Kien, P., Corvol, P., Plouin, P. F., Jeunemaitre, X. et al. (2003). Mutations in the SDHB gene are associated with extra-adrenal and/or malignant phaeochromocytomas. *Cancer Res.* 63, 5615-5621.

Gimenez-Roqueplo, A. P., Favier, J., Rustin, P., Rieubland, C., Kerlan, V., Plouin, P. F., Rotig, A. and Jeunemaitre, X. (2002). Functional consequences of a SDHB gene mutation in an apparently sporadic pheochromocytoma. *J. Clin. Endocrinol. Metab.* 87, 4771-4774.

Gimm, O., Armanios, M., Dziema, H., Neumann, H. P. and Eng, C. (2000). Somatic and occult germ-line mutations in SDHD, a mitochondrial complex II gene, in nonfamilial pheochromocytoma. *Cancer Res.* 60, 6822-6825.

Glickman, M. H. and Ciechanover, A. (2002). The ubiquitin-proteasome proteolytic pathway: Destruction for the sake of construction. *Physiol. Rev.* 82, 373-428.

Gold, L., Polisky, B., Uhlenbeck, O. and Yarus, M. (1995). Diversity of oligonucleotide functions. *Annu. Rev. Biochem.* 64, 763-797.

Goodman, R. H. and Smolik, S. (2000). CBP/p300 in cell growth, transformation, and development. *Genes Dev.* 14, 1553-1577.

Goyal, P., Weissmann, N., Grimminger, F., Hegel, C., Bader, L., Rose, F., Fink, L., Ghofrani, H. A., Schermuly, R. T., Schmidt, H. H. et al. (2004). Upregulation of NAD(P)H oxidase 1 in hypoxia activates hypoxia-inducible factor 1 via increase in reactive oxygen species. *Free Radic. Biol. Med.* 36, 1279-1288.

Grabko, V. I., Chistyakova, L. G., Lyapustin, V. N., Korobko, V. G. and Miroshnikov, A. I. (1996). Reverse transcription, amplification and sequencing of poliovirus RNA by taq DNA polymerase. *FEBS Lett.* 387, 189-192.

Gradin, K., Takasaki, C., Fujii-Kuriyama, Y. and Sogawa, K. (2002). The transcriptional activation function of the HIF-like factor requires phosphorylation at a conserved threonine. *J. Biol. Chem.* 277, 23508-23514.

Gray, M. J., Zhang, J., Ellis, L. M., Semenza, G. L., Evans, D. B., Watowich, S. S. and Gallick, G. E. (2005). HIF-1alpha, STAT3, CBP/p300 and ref-1/APE are components of a transcriptional complex that regulates src-dependent hypoxia-induced expression of VEGF in pancreatic and prostate carcinomas. *Oncogene* 24, 3110-3120.

Green, L. S., Jellinek, D., Bell, C., Beebe, L. A., Feistner, B. D., Gill, S. C., Jucker, F. M. and Janjic, N. (1995). Nuclease-resistant nucleic acid ligands to vascular permeability factor/vascular endothelial growth factor. *Chem. Biol.* 2, 683-695.

Griffiths, J. R., McSheehy, P. M., Robinson, S. P., Troy, H., Chung, Y. L., Leek, R. D., Williams, K. J., Stratford, I. J., Harris, A. L. and Stubbs, M. (2002). Metabolic changes detected by in vivo magnetic resonance studies of HEPA-1 wild-type tumors and tumors deficient in hypoxia-inducible

factor-1beta (HIF-1beta): Evidence of an anabolic role for the HIF-1 pathway. *Cancer Res.* 62, 688-695.

Gu, Y. Z., Hogenesch, J. B. and Bradfield, C. A. (2000). The PAS superfamily: Sensors of environmental and developmental signals. *Annu. Rev. Pharmacol. Toxicol.* 40, 519-561.

Gu, Y. Z., Moran, S. M., Hogenesch, J. B., Wartman, L. and Bradfield, C. A. (1998). Molecular characterization and chromosomal localization of a third alpha-class hypoxia inducible factor subunit, HIF3alpha. *Gene Expr.* 7, 205-213.

Gunton, J. E., Kulkarni, R. N., Yim, S., Okada, T., Hawthorne, W. J., Tseng, Y. H., Roberson, R. S., Ricordi, C., O'Connell, P. J., Gonzalez, F. J. et al. (2005). Loss of ARNT/HIF1beta mediates altered gene expression and pancreatic-islet dysfunction in human type 2 diabetes. *Cell* 122, 337-349.

Guo, K. T., Ziemer, G., Paul, A. and Wendel, H. P. (2008). CELL-SELEX: Novel perspectives of aptamer-based therapeutics. *Int. J. Mol. Sci.* 9, 668-678.

Guzy, R. D., Sharma, B., Bell, E., Chandel, N. S. and Schumacker, P. T. (2008). Loss of the SdhB, but not the SdhA, subunit of complex II triggers reactive oxygen species-dependent hypoxia-inducible factor activation and tumorigenesis. *Mol. Cell. Biol.* 28, 718-731.

Haddad, J. J. and Land, S. C. (2001). A non-hypoxic, ROS-sensitive pathway mediates TNF-alpha-dependent regulation of HIF-1alpha. *FEBS Lett.* 505, 269-274.

Hara, S., Hamada, J., Kobayashi, C., Kondo, Y. and Imura, N. (2001). Expression and characterization of hypoxia-inducible factor (HIF)-3alpha in human kidney: Suppression of HIF-mediated gene expression by HIF-3alpha. *Biochem. Biophys. Res. Commun.* 287, 808-813.

Hartmann-Petersen, R., Seeger, M. and Gordon, C. (2003). Transferring substrates to the 26S proteasome. *Trends Biochem. Sci.* 28, 26-31.

Harvey, A. J. and Crompton, M. R. (2003). Use of RNA interference to validate brk as a novel therapeutic target in breast cancer: Brk promotes breast carcinoma cell proliferation. *Oncogene* 22, 5006-5010.

Heutink, P., van der Mey, A. G., Sandkuijl, L. A., van Gils, A. P., Bardoel, A., Breedveld, G. J., van Vliet, M., van Ommen, G. J., Cornelisse, C. J. and Oostra, B. A. (1992). A gene subject to genomic imprinting and responsible for hereditary paragangliomas maps to chromosome 11q23-qter. *Hum. Mol. Genet.* 1, 7-10.

Hewitson, K. S. and Schofield, C. J. (2004). The HIF pathway as a therapeutic target. *Drug Discov. Today* 9, 704-711.

Hewitson, K. S., McNeill, L. A., Riordan, M. V., Tian, Y. M., Bullock, A. N., Welford, R. W., Elkins, J. M., Oldham, N. J., Bhattacharya, S., Gleadle, J. M. et al. (2002). Hypoxia-inducible factor (HIF) asparagine hydroxylase is identical to factor inhibiting HIF (FIH) and is related to the cupin structural family. *J. Biol. Chem.* 277, 26351-26355.

Hirose, K., Morita, M., Ema, M., Mimura, J., Hamada, H., Fujii, H., Saijo, Y., Gotoh, O., Sogawa, K. and Fujii-Kuriyama, Y. (1996). cDNA cloning and tissue-specific expression of a novel basic helix-loop-helix/PAS factor (Arnt2) with close sequence similarity to the aryl hydrocarbon receptor nuclear translocator (arnt). *Mol. Cell. Biol.* 16, 1706-1713.

Hirota, S. A., Beck, P. L. and MacDonald, J. A. (2009). Targeting hypoxia-inducible factor-1 (HIF-1) signaling in therapeutics: Implications for the treatment of inflammatory bowel disease. *Recent. Pat. Inflamm. Allergy Drug Discov.* 3, 1-16.

Hirst, J., Carroll, J., Fearnley, I. M., Shannon, R. J. and Walker, J. E. (2003). The nuclear encoded subunits of complex I from bovine heart mitochondria. *Biochim. Biophys. Acta* 1604, 135-150.

Ho, Y. S., Lee, H. M., Chang, C. R. and Lin, J. K. (1999). Induction of bax protein and degradation of lamin A during p53-dependent apoptosis induced by chemotherapeutic agents in human cancer cell lines. *Biochem. Pharmacol.* 57, 143-154.

Hoffman, M. A., Ohh, M., Yang, H., Klco, J. M., Ivan, M. and Kaelin, W. G.,Jr. (2001). Von hippel-lindau protein mutants linked to type 2C VHL disease preserve the ability to downregulate HIF. *Hum. Mol. Genet.* 10, 1019-1027.

Hogenesch, J. B., Chan, W. K., Jackiw, V. H., Brown, R. C., Gu, Y. Z., Pray-Grant, M., Perdew, G. H. and Bradfield, C. A. (1997). Characterization of a subset of the basic-helix-loop-helix-PAS superfamily that interacts with components of the dioxin signaling pathway. *J. Biol. Chem.* 272, 8581-8593.

Hogenesch, J. B., Gu, Y. Z., Moran, S. M., Shimomura, K., Radcliffe, L. A., Takahashi, J. S. and Bradfield, C. A. (2000). The basic helix-loop-helix-PAS protein MOP9 is a brain-specific heterodimeric partner of circadian and hypoxia factors. *J. Neurosci.* 20, RC83.

Hopkins, N. and McLoughlin, P. (2002). The structural basis of pulmonary hypertension in chronic lung disease: Remodelling, rarefaction or angiogenesis? *J. Anat.* 201, 335-348.

http://www.promega.com/~/media/Files/Resources/Protocols/Technical%20Bulletins/101/pRL%20Renilla%20Luciferase%20Reporter%20Vectors%20Protocol.ashx

Huang, L. E., Gu, J., Schau, M. and Bunn, H. F. (1998). Regulation of hypoxia-inducible factor 1alpha is mediated by an O2-dependent degradation domain via the ubiquitin-proteasome pathway. *Proc. Natl. Acad. Sci. U. S. A.* 95, 7987-7992.

Huang, L. E., Willmore, W. G., Gu, J., Goldberg, M. A. and Bunn, H. F. (1999). Inhibition of hypoxia-inducible factor 1 activation by carbon monoxide and nitric oxide. implications for oxygen sensing and signaling. *J. Biol. Chem.* 274, 9038-9044.

Hudson, C. C., Liu, M., Chiang, G. G., Otterness, D. M., Loomis, D. C., Kaper, F., Giaccia, A. J. and Abraham, R. T. (2002). Regulation of hypoxia-inducible factor 1alpha expression and function by the mammalian target of rapamycin. *Mol. Cell. Biol.* 22, 7004-7014.

Hughes, P., Marshall, D., Reid, Y., Parkes, H. and Gelber, C. (2007). The costs of using unauthenticated, over-passaged cell lines: How much more data do we need? *BioTechniques* 43, 575, 577-8, 581-2 passim.

Hunte, C., Palsdottir, H. and Trumpower, B. L. (2003). Protonmotive pathways and mechanisms in the cytochrome bc1 complex. *FEBS Lett.* 545, 39-46.

Ikeda, M. and Nomura, M. (1997). cDNA cloning and tissue-specific expression of a novel basic helix-loop-helix/PAS protein (BMAL1) and identification of alternatively spliced variants with alternative translation initiation site usage. *Biochem. Biophys. Res. Commun.* 233, 258-264.

Ikeda, M., Yu, W., Hirai, M., Ebisawa, T., Honma, S., Yoshimura, K., Honma, K. I. and Nomura, M. (2000). cDNA cloning of a novel bHLH-PAS transcription factor superfamily gene, BMAL2: Its mRNA expression, subcellular distribution, and chromosomal localization. *Biochem. Biophys. Res. Commun.* 275, 493-502.

Iliopoulos, O., Kibel, A., Gray, S. and Kaelin, W. G.,Jr. (1995). Tumour suppression by the human von hippel-lindau gene product. *Nat. Med.* 1, 822-826.

Iliopoulos, O., Ohh, M. and Kaelin, W. G.,Jr. (1998). pVHL19 is a biologically active product of the von hippel-lindau gene arising from internal translation initiation. *Proc. Natl. Acad. Sci. U. S. A.* 95, 11661-11666.

Imamura, T., Kikuchi, H., Herraiz, M. T., Park, D. Y., Mizukami, Y., Mino-Kenduson, M., Lynch, M. P., Rueda, B. R., Benita, Y., Xavier, R. J. et al. (2009). HIF-1alpha and HIF-2alpha have divergent roles in colon cancer. *Int. J. Cancer* 124, 763-771.

Isaacs, J. S., Jung, Y. J., Mole, D. R., Lee, S., Torres-Cabala, C., Chung, Y. L., Merino, M., Trepel, J., Zbar, B., Toro, J. et al. (2005). HIF overexpression correlates with biallelic loss of fumarate hydratase in renal cancer: Novel role of fumarate in regulation of HIF stability. *Cancer. Cell.* 8, 143-153.

Ishii, T., Yasuda, K., Akatsuka, A., Hino, O., Hartman, P. S. and Ishii, N. (2005). A mutation in the SDHC gene of complex II increases oxidative stress, resulting in apoptosis and tumorigenesis. *Cancer Res.* 65, 203-209.

Ishizawar, R. and Parsons, S. J. (2004). c-src and cooperating partners in human cancer. *Cancer. Cell.* 6, 209-214.

Ivan, M. and Kaelin, W. G.,Jr. (2001). The von hippel-lindau tumor suppressor protein. *Curr. Opin. Genet. Dev.* 11, 27-34.

Ivan, M., Kondo, K., Yang, H., Kim, W., Valiando, J., Ohh, M., Salic, A., Asara, J. M., Lane, W. S. and Kaelin, W. G.,Jr. (2001). HIFalpha targeted for VHL-mediated destruction by proline hydroxylation: Implications for O2 sensing. *Science* 292, 464-468.

Iwai, K., Yamanaka, K., Kamura, T., Minato, N., Conaway, R. C., Conaway, J. W., Klausner, R. D. and Pause, A. (1999). Identification of the von hippel-lindau tumor-suppressor protein as part of an active E3 ubiquitin ligase complex. *Proc. Natl. Acad. Sci. U. S. A.* 96, 12436-12441.

Iyer, N. V., Kotch, L. E., Agani, F., Leung, S. W., Laughner, E., Wenger, R. H., Gassmann, M., Gearhart, J. D., Lawler, A. M., Yu, A. Y. et al. (1998). Cellular and developmental control of O2 homeostasis by hypoxia-inducible factor 1 alpha. *Genes Dev.* 12, 149-162.

Jaakkola, P., Mole, D. R., Tian, Y. M., Wilson, M. I., Gielbert, J., Gaskell, S. J., Kriegsheim, A., Hebestreit, H. F., Mukherji, M., Schofield, C. J. et al. (2001). Targeting of HIF-alpha to the von hippel-lindau ubiquitylation complex by O2-regulated prolyl hydroxylation. *Science* 292, 468-472.

Jackson, AL., Bartz, SR., Schelter J, Kobayashi SV., Burchard J., Mao M., Li B., Cavet G., Linsley PS., (2003) Expression profiling reveals off-target gene regulation by RNAi. *Nat Biotechnol*. 21(6),635-7.
Jackson, AL., Burchard, J., Leake, D., Reynolds, A., Schelter, J., Guo, J., Johnson, JM., Lim, L., Karpilow, J., Nichols, K., Marshall, W., Khvorova, A., Linsley, PS., (2006). Position-specific chemical modification of siRNAs reduces "off-target" transcript silencing. *RNA.* 12(7),1197-205.

Jackson, P. K., Eldridge, A. G., Freed, E., Furstenthal, L., Hsu, J. Y., Kaiser, B. K. and Reimann, J. D. (2000). The lore of the RINGs: Substrate recognition and catalysis by ubiquitin ligases. *Trends Cell Biol.* 10, 429-439.

Jeong, J. W., Bae, M. K., Ahn, M. Y., Kim, S. H., Sohn, T. K., Bae, M. H., Yoo, M. A., Song, E. J., Lee, K. J. and Kim, K. W. (2002). Regulation and destabilization of HIF-1alpha by ARD1-mediated acetylation. *Cell* 111, 709-720.

Jeong, S., Han, S. R., Lee, Y. J. and Lee, S. W. (2010). Selection of RNA aptamers specific to active prostate-specific antigen. *Biotechnol. Lett.* 32, 379-385.

Jiang, B. H. and Liu, L. Z. (2009). PI3K/PTEN signaling in angiogenesis and tumorigenesis. *Adv. Cancer Res.* 102, 19-65.

Jiang, B. H., Jiang, G., Zheng, J. Z., Lu, Z., Hunter, T. and Vogt, P. K. (2001). Phosphatidylinositol 3-kinase signaling controls levels of hypoxia-inducible factor 1. *Cell Growth Differ.* 12, 363-369.

Jiang, B. H., Rue, E., Wang, G. L., Roe, R. and Semenza, G. L. (1996). Dimerization, DNA binding, and transactivation properties of hypoxia-inducible factor 1. *J. Biol. Chem.* 271, 17771-17778.

Kaelin, W. G. (2007). Von hippel-lindau disease. *Annu. Rev. Pathol.* 2, 145-173.

Kageyama, Y., Koshiji, M., To, K. K., Tian, Y. M., Ratcliffe, P. J. and Huang, L. E. (2004). Leu-574 of human HIF-1alpha is a molecular determinant of prolyl hydroxylation. *FASEB J.* 18, 1028-1030.

Kalkhoven, E. (2004). CBP and p300: HATs for different occasions. *Biochem. Pharmacol.* 68, 1145-1155.

Kallio, P. J., Okamoto, K., O'Brien, S., Carrero, P., Makino, Y., Tanaka, H. and Poellinger, L. (1998). Signal transduction in hypoxic cells: Inducible nuclear translocation and recruitment of the CBP/p300 coactivator by the hypoxia-inducible factor-1alpha. *EMBO J.* 17, 6573-6586.

Kallio, P. J., Pongratz, I., Gradin, K., McGuire, J. and Poellinger, L. (1997). Activation of hypoxia-inducible factor 1alpha: Posttranscriptional regulation and conformational change by recruitment of the arnt transcription factor. *Proc. Natl. Acad. Sci. U. S. A.* 94, 5667-5672.

Kamura, T., Koepp, D. M., Conrad, M. N., Skowyra, D., Moreland, R. J., Iliopoulos, O., Lane, W. S., Kaelin, W. G.,Jr, Elledge, S. J., Conaway, R. C. et al. (1999). Rbx1, a component of the VHL tumor suppressor complex and SCF ubiquitin ligase. *Science* 284, 657-661.

Kamura, T., Sato, S., Iwai, K., Czyzyk-Krzeska, M., Conaway, R. C. and Conaway, J. W. (2000). Activation of HIF1alpha ubiquitination by a reconstituted von hippel-lindau (VHL) tumor suppressor complex. *Proc. Natl. Acad. Sci. U. S. A.* 97, 10430-10435.

Kanasty, RL., Whitehead, KA., Vegas, AJ., Anderson, DG., (2012). Action and reaction: the biological response to siRNA and its delivery vehicles. *Mol Ther.* 20(3),513-24.

Kang, M. R., Kim, M. S., Oh, J. E., Kim, Y. R., Song, S. Y., Seo, S. I., Lee, J. Y., Yoo, N. J. and Lee, S. H. (2009). Mutational analysis of IDH1 codon 132 in glioblastomas and other common cancers. *Int. J. Cancer* 125, 353-355.

Kantorovich, V., King, K. S. and Pacak, K. (2010). SDH-related pheochromocytoma and paraganglioma. *Best Pract. Res. Clin. Endocrinol. Metab.* 24, 415-424.

Karni, R., Dor, Y., Keshet, E., Meyuhas, O. and Levitzki, A. (2002). Activated pp60c-src leads to elevated hypoxia-inducible factor (HIF)-1alpha expression under normoxia. *J. Biol. Chem.* 277, 42919-42925.

Kasuno, K., Takabuchi, S., Fukuda, K., Kizaka-Kondoh, S., Yodoi, J., Adachi, T., Semenza, G. L. and Hirota, K. (2004). Nitric oxide induces hypoxia-inducible factor 1 activation that is dependent on MAPK and phosphatidylinositol 3-kinase signaling. *J. Biol. Chem.* 279, 2550-2558.

Katsoulidis, E., Li, Y., Mears, H. and Platanias, L. C. (2005). The p38 mitogen-activated protein kinase pathway in interferon signal transduction. *J. Interferon Cytokine Res.* 25, 749-756.

Ke, Q. and Costa, M. (2006). Hypoxia-inducible factor-1 (HIF-1). *Mol. Pharmacol.* 70, 1469-1480.

Kewley, R. J., Whitelaw, M. L. and Chapman-Smith, A. (2004). The mammalian basic helix-loop-helix/PAS family of transcriptional regulators. *Int. J. Biochem. Cell Biol.* 36, 189-204.

Kibel, A., Iliopoulos, O., DeCaprio, J. A. and Kaelin, W. G.,Jr. (1995). Binding of the von hippel-lindau tumor suppressor protein to elongin B and C. *Science* 269, 1444-1446.

Kietzmann, T. and Gorlach, A. (2005). Reactive oxygen species in the control of hypoxia-inducible factor-mediated gene expression. *Semin. Cell Dev. Biol.* 16, 474-486.

Kim, S. Y. and Park, J. W. (2010). Modulation of hypoxia-inducible factor-1alpha expression by mitochondrial NADP+-dependent isocitrate dehydrogenase. *Biochimie* 92, 1908-1913.

Kim, W. and Kaelin, W. G.,Jr. (2003). The von hippel-lindau tumor suppressor protein: New insights into oxygen sensing and cancer. *Curr. Opin. Genet. Dev.* 13, 55-60.

Kim, W. Y. and Kaelin, W. G. (2004). Role of VHL gene mutation in human cancer. *J. Clin. Oncol.* 22, 4991-5004.

Kimoto, M., Sakamoto, K., Shirouzu, M., Hirao, I. and Yokoyama, S. (1998). RNA aptamers that specifically bind to the ras-binding domain of raf-1. *FEBS Lett.* 441, 322-326.

Kinoshita, A., Kobayashi, D., Hibino, Y., Isago, T., Uchino, K., Yagi, K., Hirai, M., Saitoh, Y. and Komada, F. (2008). Regulation of CMV promoter-driven exogenous gene expression with doxorubicin in genetically modified cells. *J. Pharm. Pharmacol.* 60, 1659-1665.

Knowles, H. J. and Harris, A. L. (2001). Hypoxia and oxidative stress in breast cancer. hypoxia and tumourigenesis. *Breast Cancer Res.* 3, 318-322.

Koivunen, P., Hirsila, M., Remes, A. M., Hassinen, I. E., Kivirikko, K. I. and Myllyharju, J. (2007). Inhibition of hypoxia-inducible factor (HIF) hydroxylases by citric acid cycle intermediates: Possible links between cell metabolism and stabilization of HIF. *J. Biol. Chem.* 282, 4524-4532.

Kondo, K. and Kaelin, W. G.,Jr. (2001). The von hippel-lindau tumor suppressor gene. *Exp. Cell Res.* 264, 117-125.

Konopleva, M., Tabe, Y., Zeng, Z. and Andreeff, M. (2009). Therapeutic targeting of microenvironmental interactions in leukemia: Mechanisms and approaches. *Drug Resist Updat* 12, 103-113.

Kotch, L. E., Iyer, N. V., Laughner, E. and Semenza, G. L. (1999). Defective vascularization of HIF-1alpha-null embryos is not associated with VEGF deficiency but with mesenchymal cell death. *Dev. Biol.* 209, 254-267.

Kung, A. L., Wang, S., Klco, J. M., Kaelin, W. G. and Livingston, D. M. (2000). Suppression of tumor growth through disruption of hypoxia-inducible transcription. *Nat. Med.* 6, 1335-1340.

Kung, A. L., Zabludoff, S. D., France, D. S., Freedman, S. J., Tanner, E. A., Vieira, A., Cornell-Kennon, S., Lee, J., Wang, B., Wang, J. et al. (2004). Small molecule blockade of transcriptional coactivation of the hypoxia-inducible factor pathway. *Cancer. Cell.* 6, 33-43.

Kuznetsova, A. V., Meller, J., Schnell, P. O., Nash, J. A., Ignacak, M. L., Sanchez, Y., Conaway, J. W., Conaway, R. C. and Czyzyk-Krzeska, M. F. (2003). Von hippel-lindau protein binds hyperphosphorylated large subunit of RNA polymerase II through a proline hydroxylation motif and targets it for ubiquitination. *Proc. Natl. Acad. Sci. U. S. A.* 100, 2706-2711.

Lancaster, C. R. (2003). Wolinella succinogenes quinol:Fumarate reductase and its comparison to E. coli succinate:Quinone reductase. *FEBS Lett.* 555, 21-28.

Lando, D., Peet, D. J., Gorman, J. J., Whelan, D. A., Whitelaw, M. L. and Bruick, R. K. (2002). FIH-1 is an asparaginyl hydroxylase enzyme that regulates the transcriptional activity of hypoxia-inducible factor. *Genes Dev.* 16, 1466-1471.

Lando, D., Peet, D. J., Whelan, D. A., Gorman, J. J. and Whitelaw, M. L. (2002). Asparagine hydroxylation of the HIF transactivation domain a hypoxic switch. *Science* 295, 858-861.

Latif, F., Tory, K., Gnarra, J., Yao, M., Duh, F. M., Orcutt, M. L., Stackhouse, T., Kuzmin, I., Modi, W. and Geil, L. (1993). Identification of the von hippel-lindau disease tumor suppressor gene. *Science* 260, 1317-1320.

Lee, C., Kim, S. J., Jeong, D. G., Lee, S. M. and Ryu, S. E. (2003). Structure of human FIH-1 reveals a unique active site pocket and interaction sites for HIF-1 and von hippel-lindau. *J. Biol. Chem.* 278, 7558-7563.

Lee, S. R., Yang, K. S., Kwon, J., Lee, C., Jeong, W. and Rhee, S. G. (2002). Reversible inactivation of the tumor suppressor PTEN by H2O2. *J. Biol. Chem.* 277, 20336-20342.

Lee, S., Nakamura, E., Yang, H., Wei, W., Linggi, M. S., Sajan, M. P., Farese, R. V., Freeman, R. S., Carter, B. D., Kaelin, W. G.,Jr et al. (2005). Neuronal apoptosis linked to EglN3 prolyl hydroxylase and familial pheochromocytoma genes: Developmental culling and cancer. *Cancer. Cell.* 8, 155-167.

Leger, C., Heffron, K., Pershad, H. R., Maklashina, E., Luna-Chavez, C., Cecchini, G., Ackrell, B. A. and Armstrong, F. A. (2001). Enzyme electrokinetics: Energetics of succinate oxidation by fumarate reductase and succinate dehydrogenase. *Biochemistry* 40, 11234-11245.

Leonardi, E., Murgia, A. and Tosatto, S. C. (2009). Adding structural information to the von hippel-lindau (VHL) tumor suppressor interaction network. *FEBS Lett.* 583, 3704-3710.

Li, J., Post, M., Volk, R., Gao, Y., Li, M., Metais, C., Sato, K., Tsai, J., Aird, W., Rosenberg, R. D. et al. (2000). PR39, a peptide regulator of angiogenesis. *Nat. Med.* 6, 49-55.

Li, L., Lin, X., Staver, M., Shoemaker, A., Semizarov, D., Fesik, S. W. and Shen, Y. (2005). Evaluating hypoxia-inducible factor-1alpha as a cancer therapeutic target via inducible RNA interference in vivo. *Cancer Res.* 65, 7249-7258.

Li, Z., Wang, D., Na, X., Schoen, S. R., Messing, E. M. and Wu, G. (2003). The VHL protein recruits a novel KRAB-A domain protein to repress HIF-1alpha transcriptional activity. *EMBO J.* 22, 1857-1867.

Linke, S., Stojkoski, C., Kewley, R. J., Booker, G. W., Whitelaw, M. L. and Peet, D. J. (2004). Substrate requirements of the oxygen-sensing asparaginyl hydroxylase factor-inhibiting hypoxia-inducible factor. *J. Biol. Chem.* 279, 14391-14397.

Lisy, K. and Peet, D. J. (2008). Turn me on: Regulating HIF transcriptional activity. *Cell Death Differ.* 15, 642-649.

Lisztwan, J., Imbert, G., Wirbelauer, C., Gstaiger, M. and Krek, W. (1999). The von hippel-lindau tumor suppressor protein is a component of an E3 ubiquitin-protein ligase activity. *Genes Dev.* 13, 1822-1833.

Liu, Y. V., Baek, J. H., Zhang, H., Diez, R., Cole, R. N. and Semenza, G. L. (2007). RACK1 competes with HSP90 for binding to HIF-1alpha and is required for O(2)-independent and HSP90 inhibitor-induced degradation of HIF-1alpha. *Mol. Cell* 25, 207-217.

Loboda, A., Jozkowicz, A. and Dulak, J. (2010). HIF-1 and HIF-2 transcription factors--similar but not identical. *Mol. Cells* 29, 435-442.

Loscalzo, J. (2010). The cellular response to hypoxia: Tuning the system with microRNAs. *J. Clin. Invest.* 120, 3815-3817.

Lu, H., Forbes, R. A. and Verma, A. (2002). Hypoxia-inducible factor 1 activation by aerobic glycolysis implicates the warburg effect in carcinogenesis. *J. Biol. Chem.* 277, 23111-23115.

Luo, J. C. and Shibuya, M. (2001). A variant of nuclear localization signal of bipartite-type is required for the nuclear translocation of hypoxia inducible factors (1alpha, 2alpha and 3alpha). *Oncogene* 20, 1435-1444.

MacKenzie, E. D., Selak, M. A., Tennant, D. A., Payne, L. J., Crosby, S., Frederiksen, C. M., Watson, D. G. and Gottlieb, E. (2007). Cell-permeating alpha-ketoglutarate derivatives alleviate pseudohypoxia in succinate dehydrogenase-deficient cells. *Mol. Cell. Biol.* 27, 3282-3289.

Maher, E. R. and Eng, C. (2002). The pressure rises: Update on the genetics of phaeochromocytoma. *Hum. Mol. Genet.* 11, 2347-2354.

Mahon, P. C., Hirota, K. and Semenza, G. L. (2001). FIH-1: A novel protein that interacts with HIF-1alpha and VHL to mediate repression of HIF-1 transcriptional activity. *Genes Dev.* 15, 2675-2686.

Maier-Woelfle, M., Brandle, M., Komminoth, P., Saremaslani, P., Schmid, S., Locher, T., Heitz, P. U., Krull, I., Galeazzi, R. L., Schmid, C. et al. (2004). A novel succinate dehydrogenase subunit B gene mutation, H132P, causes familial malignant sympathetic extraadrenal paragangliomas. *J. Clin. Endocrinol. Metab.* 89, 362-367.

Makino, Y., Cao, R., Svensson, K., Bertilsson, G., Asman, M., Tanaka, H., Cao, Y., Berkenstam, A. and Poellinger, L. (2001). Inhibitory PAS domain protein is a negative regulator of hypoxia-inducible gene expression. *Nature* 414, 550-554.

Makino, Y., Kanopka, A., Wilson, W. J., Tanaka, H. and Poellinger, L. (2002). Inhibitory PAS domain protein (IPAS) is a hypoxia-inducible splicing variant of the hypoxia-inducible factor-3alpha locus. *J. Biol. Chem.* 277, 32405-32408.

Maltepe, E., Keith, B., Arsham, A. M., Brorson, J. R. and Simon, M. C. (2000). The role of ARNT2 in tumor angiogenesis and the neural response to hypoxia. *Biochem. Biophys. Res. Commun.* 273, 231-238.

Maltepe, E., Schmidt, J. V., Baunoch, D., Bradfield, C. A. and Simon, M. C. (1997). Abnormal angiogenesis and responses to glucose and oxygen deprivation in mice lacking the protein ARNT. *Nature* 386, 403-407.

Mandavilli, B. S., Boldogh, I. and Van Houten, B. (2005). 3-nitropropionic acid-induced hydrogen peroxide, mitochondrial DNA damage, and cell death are attenuated by bcl-2 overexpression in PC12 cells. *Brain Res. Mol. Brain Res.* 133, 215-223.

Marshall, K. A. and Ellington, A. D. (1999). Molecular parasites that evolve longer genomes. *J. Mol. Evol.* 49, 656-663.

Marshall, K. A. and Ellington, A. D. (1999). Training ribozymes to switch. *Nat. Struct. Biol.* 6, 992-994.

Marshall, K. A. and Ellington, A. D. (2000). In vitro selection of RNA aptamers. *Methods Enzymol.* 318, 193-214.

Marshall, K. A., Robertson, M. P. and Ellington, A. D. (1997). A biopolymer by any other name would bind as well: A comparison of the ligand-binding pockets of nucleic acids and proteins. *Structure* 5, 729-734.

Masson, N., Willam, C., Maxwell, P. H., Pugh, C. W. and Ratcliffe, P. J. (2001). Independent function of two destruction domains in hypoxia-inducible factor-alpha chains activated by prolyl hydroxylation. *EMBO J.* 20, 5197-5206.

Mateo, J., Garcia-Lecea, M., Cadenas, S., Hernandez, C. and Moncada, S. (2003). Regulation of hypoxia-inducible factor-1alpha by nitric oxide through mitochondria-dependent and -independent pathways. *Biochem. J.* 376, 537-544.

Mates, J. M., Segura, J. A., Campos-Sandoval, J. A., Lobo, C., Alonso, L., Alonso, F. J. and Marquez, J. (2009). Glutamine homeostasis and mitochondrial dynamics. *Int. J. Biochem. Cell Biol.* 41, 2051-2061.

Maxwell, P. H., Wiesener, M. S., Chang, G. W., Clifford, S. C., Vaux, E. C., Cockman, M. E., Wykoff, C. C., Pugh, C. W., Maher, E. R. and Ratcliffe, P. J. (1999). The tumour suppressor protein VHL targets hypoxia-inducible factors for oxygen-dependent proteolysis. *Nature* 399, 271-275.

Maynard, M. A., Evans, A. J., Hosomi, T., Hara, S., Jewett, M. A. and Ohh, M. (2005). Human HIF-3alpha4 is a dominant-negative regulator of HIF-1 and is down-regulated in renal cell carcinoma. *FASEB J.* 19, 1396-1406.

Maynard, M. A., Qi, H., Chung, J., Lee, E. H., Kondo, Y., Hara, S., Conaway, R. C., Conaway, J. W. and Ohh, M. (2003). Multiple splice variants of the human HIF-3 alpha locus are targets of the von hippel-lindau E3 ubiquitin ligase complex. *J. Biol. Chem.* 278, 11032-11040.

Mazure, N. M., Brahimi-Horn, M. C., Berta, M. A., Benizri, E., Bilton, R. L., Dayan, F., Ginouves, A., Berra, E. and Pouyssegur, J. (2004). HIF-1: Master and commander of the hypoxic world. A pharmacological approach to its regulation by siRNAs. *Biochem. Pharmacol.* 68, 971-980.

McNeill, L. A., Hewitson, K. S., Gleadle, J. M., Horsfall, L. E., Oldham, N. J., Maxwell, P. H., Pugh, C. W., Ratcliffe, P. J. and Schofield, C. J. (2002). The use of dioxygen by HIF prolyl hydroxylase (PHD1). *Bioorg. Med. Chem. Lett.* 12, 1547-1550.

Meister, G. and Tuschl, T. (2004). Mechanisms of gene silencing by double-stranded RNA. *Nature* 431, 343-349.

Metzen, E., Berchner-Pfannschmidt, U., Stengel, P., Marxsen, J. H., Stolze, I., Klinger, M., Huang, W. Q., Wotzlaw, C., Hellwig-Burgel, T., Jelkmann, W. et al. (2003). Intracellular localisation of human HIF-1 alpha hydroxylases: Implications for oxygen sensing. *J. Cell. Sci.* 116, 1319-1326.

Metzen, E., Wolff, M., Fandrey, J. and Jelkmann, W. (1995). Pericellular PO2 and O2 consumption in monolayer cell cultures. *Respir. Physiol.* 100, 101-106.

Metzen, E., Zhou, J., Jelkmann, W., Fandrey, J. and Brune, B. (2003). Nitric oxide impairs normoxic degradation of HIF-1alpha by inhibition of prolyl hydroxylases. *Mol. Biol. Cell* 14, 3470-3481.

Miller, J. and Gordon, C. (2005). The regulation of proteasome degradation by multi-ubiquitin chain binding proteins. *FEBS Lett.* 579, 3224-3230.

Milunsky, J. M., Maher, T. A., Michels, V. V. and Milunsky, A. (2001). Novel mutations and the emergence of a common mutation in the SDHD gene causing familial paraganglioma. *Am. J. Med. Genet.* 100, 311-314.

Moeller, B. J., Cao, Y., Li, C. Y. and Dewhirst, M. W. (2004). Radiation activates HIF-1 to regulate vascular radiosensitivity in tumors: Role of reoxygenation, free radicals, and stress granules. *Cancer. Cell.* 5, 429-441.

Mylonis, I., Chachami, G., Samiotaki, M., Panayotou, G., Paraskeva, E., Kalousi, A., Georgatsou, E., Bonanou, S. and Simos, G. (2006). Identification of MAPK phosphorylation sites and their role in the localization and activity of hypoxia-inducible factor-1alpha. *J. Biol. Chem.* 281, 33095-33106.

Na, X., Duan, H. O., Messing, E. M., Schoen, S. R., Ryan, C. K., di Sant'Agnese, P. A., Golemis, E. A. and Wu, G. (2003). Identification of the RNA polymerase II subunit hsRPB7 as a novel target of the von hippel-lindau protein. *EMBO J.* 22, 4249-4259.

Naito, Y., Yoshimura, J., Morishita, S., Ui-Tei, K., (2009). siDirect 2.0: updated software for designing functional siRNA with reduced seed-dependent off-target effect. *BMC Bioinformatics.* 10; 392.

Nakayama, K., Frew, I. J., Hagensen, M., Skals, M., Habelhah, H., Bhoumik, A., Kadoya, T., Erdjument-Bromage, H., Tempst, P., Frappell, P. B. et al. (2004). Siah2 regulates stability of prolyl-hydroxylases, controls HIF1alpha abundance, and modulates physiological responses to hypoxia. *Cell* 117, 941-952.

Navon, A. and Ciechanover, A. (2009). The 26 S proteasome: From basic mechanisms to drug targeting. *J. Biol. Chem.* 284, 33713-33718.

Neumann, H. P., Bausch, B., McWhinney, S. R., Bender, B. U., Gimm, O., Franke, G., Schipper, J., Klisch, J., Altehoefer, C., Zerres, K. et al. (2002). Germ-line mutations in nonsyndromic pheochromocytoma. *N. Engl. J. Med.* 346, 1459-1466.

Ng, E. W., Shima, D. T., Calias, P., Cunningham, E. T.,Jr, Guyer, D. R. and Adamis, A. P. (2006). Pegaptanib, a targeted anti-VEGF aptamer for ocular vascular disease. *Nat. Rev. Drug Discov.* 5, 123-132.

Nicholas,S., Sumbayev, V., (2009). The involvement of hypoxia-inducible factor 1 alpha in Toll-like receptor 7/8-mediated inflammatory response. *Cell Research* 19,973-983.

Niemann, S. and Muller, U. (2000). Mutations in SDHC cause autosomal dominant paraganglioma, type 3. *Nat. Genet.* 26, 268-270.

North, S., Moenner, M. and Bikfalvi, A. (2005). Recent developments in the regulation of the angiogenic switch by cellular stress factors in tumors. *Cancer Lett.* 218, 1-14.

O'Donnell, V. B., Spycher, S. and Azzi, A. (1995). Involvement of oxidants and oxidant-generating enzyme(s) in tumour-necrosis-factor-alpha-mediated apoptosis: Role for lipoxygenase pathway but not mitochondrial respiratory chain. *Biochem. J.* 310 ( Pt 1), 133-141.

Ohh, M., Park, C. W., Ivan, M., Hoffman, M. A., Kim, T. Y., Huang, L. E., Pavletich, N., Chau, V. and Kaelin, W. G. (2000). Ubiquitination of hypoxia-inducible factor requires direct binding to the beta-domain of the von hippel-lindau protein. *Nat. Cell Biol.* 2, 423-427.

Okano, T., Sasaki, M. and Fukada, Y. (2001). Cloning of mouse BMAL2 and its daily expression profile in the suprachiasmatic nucleus: A remarkable acceleration of Bmal2 sequence divergence after bmal gene duplication. *Neurosci. Lett.* 300, 111-114.

Olenyuk, B. Z., Zhang, G. J., Klco, J. M., Nickols, N. G., Kaelin, W. G.,Jr and Dervan, P. B. (2004). Inhibition of vascular endothelial growth factor with a sequence-specific hypoxia response element antagonist. *Proc. Natl. Acad. Sci. U. S. A.* 101, 16768-16773.

Oostveen, F. G., Au, H. C., Meijer, P. J. and Scheffler, I. E. (1995). A chinese hamster mutant cell line with a defect in the integral membrane protein CII-3 of complex II of the mitochondrial electron transport chain. *J. Biol. Chem.* 270, 26104-26108.

O'Rourke, J. F., Tian, Y. M., Ratcliffe, P. J. and Pugh, C. W. (1999). Oxygen-regulated and transactivating domains in endothelial PAS protein 1: Comparison with hypoxia-inducible factor-1alpha. *J. Biol. Chem.* 274, 2060-2071.

Paddison, PJ., Caudy, AA., Hannon, GJ. (2002). Stable suppression of gene expression by RNAi in mammalian cells. *Proc Natl Acad Sci U S A.* 99(3), 1443-8.

Pajusola, K., Kunnapuu, J., Vuorikoski, S., Soronen, J., Andre, H., Pereira, T., Korpisalo, P., Yla-Herttuala, S., Poellinger, L. and Alitalo, K. (2005). Stabilized HIF-1alpha is superior to VEGF for angiogenesis in skeletal muscle via adeno-associated virus gene transfer. *FASEB J.* 19, 1365-1367.

Paltoglou, S. M. and Roberts, B. J. (2005). Role of the von hippel-lindau tumour suppressor protein in the regulation of HIF-1alpha and its oxygen-regulated transactivation domains at high cell density. *Oncogene* 24, 3830-3835.

Parfait, B., Chretien, D., Rotig, A., Marsac, C., Munnich, A. and Rustin, P. (2000). Compound heterozygous mutations in the flavoprotein gene of the respiratory chain complex II in a patient with leigh syndrome. *Hum. Genet.* 106, 236-243.

Park, Y. K., Ahn, D. R., Oh, M., Lee, T., Yang, E. G., Son, M. and Park, H. (2008). Nitric oxide donor, (+/-)-S-nitroso-N-acetylpenicillamine, stabilizes transactive hypoxia-inducible factor-1alpha by inhibiting von hippel-lindau recruitment and asparagine hydroxylation. *Mol. Pharmacol.* 74, 236-245.

Pause, A., Lee, S., Worrell, R. A., Chen, D. Y., Burgess, W. H., Linehan, W. M. and Klausner, R. D. (1997). The von hippel-lindau tumor-suppressor gene product forms a stable complex with human CUL-2, a member of the Cdc53 family of proteins. *Proc. Natl. Acad. Sci. U. S. A.* 94, 2156-2161.

Pecina, P., Houstkova, H., Hansikova, H., Zeman, J. and Houstek, J. (2004). Genetic defects of cytochrome c oxidase assembly. *Physiol. Res.* 53 Suppl 1, S213-23.

Peng, J., Zhang, L., Drysdale, L. and Fong, G. H. (2000). The transcription factor EPAS-1/hypoxia-inducible factor 2alpha plays an important role in vascular remodeling. *Proc. Natl. Acad. Sci. U. S. A.* 97, 8386-8391.

Pickart, C. M. (2000). Ubiquitin in chains. *Trends Biochem. Sci.* 25, 544-548.

Pollard, P. J., Briere, J. J., Alam, N. A., Barwell, J., Barclay, E., Wortham, N. C., Hunt, T., Mitchell, M., Olpin, S., Moat, S. J. et al. (2005). Accumulation of krebs cycle intermediates and over-expression of HIF1alpha in tumours which result from germline FH and SDH mutations. *Hum. Mol. Genet.* 14, 2231-2239.

Pollard, P. J., Spencer-Dene, B., Shukla, D., Howarth, K., Nye, E., El-Bahrawy, M., Deheragoda, M., Joannou, M., McDonald, S., Martin, A. et al. (2007). Targeted inactivation of fh1 causes proliferative renal cyst development and activation of the hypoxia pathway. *Cancer. Cell.* 11, 311-319.

Pore, N., Jiang, Z., Shu, H. K., Bernhard, E., Kao, G. D. and Maity, A. (2006). Akt1 activation can augment hypoxia-inducible factor-1alpha expression by increasing protein translation through a mammalian target of rapamycin-independent pathway. *Mol. Cancer. Res.* 4, 471-479.

Povsic, T. J., Sullenger, B. A., Zelenkofske, S. L., Rusconi, C. P. and Becker, R. C. (2010). Translating nucleic acid aptamers to antithrombotic drugs in cardiovascular medicine. *J. Cardiovasc. Transl. Res.* 3, 704-716.

Powis, G. and Kirkpatrick, L. (2004). Hypoxia inducible factor-1alpha as a cancer drug target. *Mol. Cancer. Ther.* 3, 647-654.

Promega Corporation. Promega technical bulletin: PRL *renilla* luciferase reporter vectors. Source

Przybyla-Zawislak, B. D., Kim, C. S., Ali, S. F., Slikker, W.,Jr and Binienda, Z. K. (2005). The differential JunB responses to inhibition of succinate dehydrogenase in rat hippocampus and liver. *Neurosci. Lett.* 381, 354-357.

Pugh, C. W. and Ratcliffe, P. J. (2003). The von hippel-lindau tumor suppressor, hypoxia-inducible factor-1 (HIF-1) degradation, and cancer pathogenesis. *Semin. Cancer Biol.* 13, 83-89.

Qian, D., Lin, H. Y., Wang, H. M., Zhang, X., Liu, D. L., Li, Q. L. and Zhu, C. (2004). Normoxic induction of the hypoxic-inducible factor-1 alpha by interleukin-1 beta involves the extracellular signal-regulated kinase 1/2 pathway in normal human cytotrophoblast cells. *Biol. Reprod.* 70, 1822-1827.

Rational siRNA design for RNA interference. *Nat Biotechnol*. 22(3):326-30.

Ravi, R., Mookerjee, B., Bhujwalla, Z. M., Sutter, C. H., Artemov, D., Zeng, Q., Dillehay, L. E., Madan, A., Semenza, G. L. and Bedi, A. (2000). Regulation of tumor angiogenesis by p53-induced degradation of hypoxia-inducible factor 1alpha. *Genes Dev.* 14, 34-44.

Rey, S. and Semenza, G. L. (2010). Hypoxia-inducible factor-1-dependent mechanisms of vascularization and vascular remodelling. *Cardiovasc. Res.* 86, 236-242.

Reyes-Reyes, E. M., Teng, Y. and Bates, P. J. (2010). A new paradigm for aptamer therapeutic AS1411 action: Uptake by macropinocytosis and its stimulation by a nucleolin-dependent mechanism. *Cancer Res.* 70, 8617-8629.

Reynolds, A., Leake, D., Boese, Q., Scaringe, S., Marshall, WS., Khvorova, A., (2004).

Richard, D. E., Berra, E. and Pouyssegur, J. (2000). Nonhypoxic pathway mediates the induction of hypoxia-inducible factor 1alpha in vascular smooth muscle cells. *J. Biol. Chem.* 275, 26765-26771.

Richard, D. E., Berra, E., Gothie, E., Roux, D. and Pouyssegur, J. (1999). p42/p44 mitogen-activated protein kinases phosphorylate hypoxia-inducible factor 1alpha (HIF-1alpha) and enhance the transcriptional activity of HIF-1. *J. Biol. Chem.* 274, 32631-32637.

Richter, O. M. and Ludwig, B. (2003). Cytochrome c oxidase--structure, function, and physiology of a redox-driven molecular machine. *Rev. Physiol. Biochem. Pharmacol.* 147, 47-74.

Rosenberger, C., Mandriota, S., Jurgensen, J. S., Wiesener, M. S., Horstrup, J. H., Frei, U., Ratcliffe, P. J., Maxwell, P. H., Bachmann, S. and Eckardt, K. U. (2002). Expression of hypoxia-inducible factor-1alpha and -2alpha in hypoxic and ischemic rat kidneys. *J. Am. Soc. Nephrol.* 13, 1721-1732.

Ruas, J. L., Poellinger, L. and Pereira, T. (2005). Role of CBP in regulating HIF-1-mediated activation of transcription. *J. Cell. Sci.* 118, 301-311.

Rustin, P. and Rotig, A. (2002). Inborn errors of complex II--unusual human mitochondrial diseases. *Biochim. Biophys. Acta* 1553, 117-122.

Ryan, H. E., Poloni, M., McNulty, W., Elson, D., Gassmann, M., Arbeit, J. M. and Johnson, R. S. (2000). Hypoxia-inducible factor-1alpha is a positive factor in solid tumor growth. *Cancer Res.* 60, 4010-4015.

Ryu, J. K., Nagai, A., Kim, J., Lee, M. C., McLarnon, J. G. and Kim, S. U. (2003). Microglial activation and cell death induced by the mitochondrial toxin 3-nitropropionic acid: In vitro and in vivo studies. *Neurobiol. Dis.* 12, 121-132.

Safran, M. and Kaelin, W. G.,Jr. (2003). HIF hydroxylation and the mammalian oxygen-sensing pathway. *J. Clin. Invest.* 111, 779-783.

Salceda, S. and Caro, J. (1997). Hypoxia-inducible factor 1alpha (HIF-1alpha) protein is rapidly degraded by the ubiquitin-proteasome system under normoxic conditions. its stabilization by hypoxia depends on redox-induced changes. *J. Biol. Chem.* 272, 22642-22647.

Sambucetti, L. C., Cherrington, J. M., Wilkinson, G. W. and Mocarski, E. S. (1989). NF-kappa B activation of the cytomegalovirus enhancer is mediated by a viral transactivator and by T cell stimulation. *EMBO J.* 8, 4251-4258.

Sandau, K. B., Fandrey, J. and Brune, B. (2001). Accumulation of HIF-1alpha under the influence of nitric oxide. *Blood* 97, 1009-1015.

Sandau, K. B., Zhou, J., Kietzmann, T. and Brune, B. (2001). Regulation of the hypoxia-inducible factor 1alpha by the inflammatory mediators nitric oxide and tumor necrosis factor-alpha in contrast to desferroxamine and phenylarsine oxide. *J. Biol. Chem.* 276, 39805-39811.

Sang, N., Fang, J., Srinivas, V., Leshchinsky, I. and Caro, J. (2002). Carboxyl-terminal transactivation activity of hypoxia-inducible factor 1 alpha is governed by a von hippel-lindau protein-independent, hydroxylation-regulated association with p300/CBP. *Mol. Cell. Biol.* 22, 2984-2992.

Sauer, H., Wartenberg, M. and Hescheler, J. (2001). Reactive oxygen species as intracellular messengers during cell growth and differentiation. *Cell. Physiol. Biochem.* 11, 173-186.

Schoenfeld, A. R., Davidowitz, E. J. and Burk, R. D. (2000). Elongin BC complex prevents degradation of von hippel-lindau tumor suppressor gene products. *Proc. Natl. Acad. Sci. U. S. A.* 97, 8507-8512.

Schoenfeld, A., Davidowitz, E. J. and Burk, R. D. (1998). A second major native von hippel-lindau gene product, initiated from an internal translation start site, functions as a tumor suppressor. *Proc. Natl. Acad. Sci. U. S. A.* 95, 8817-8822.

Selak, M. A., Armour, S. M., MacKenzie, E. D., Boulahbel, H., Watson, D. G., Mansfield, K. D., Pan, Y., Simon, M. C., Thompson, C. B. and Gottlieb, E. (2005). Succinate links TCA cycle dysfunction to oncogenesis by inhibiting HIF-alpha prolyl hydroxylase. *Cancer. Cell.* 7, 77-85.

Semenza, G. (2002). Signal transduction to hypoxia-inducible factor 1. *Biochem. Pharmacol.* 64, 993-998.

Semenza, G. L. (2000). HIF-1 and human disease: One highly involved factor. *Genes Dev.* 14, 1983-1991.

Semenza, G. L. (2001). Hypoxia-inducible factor 1: Oxygen homeostasis and disease pathophysiology. *Trends Mol. Med.* 7, 345-350.

Semenza, G. L. (2002). HIF-1 and tumor progression: Pathophysiology and therapeutics. *Trends Mol. Med.* 8, S62-7.

Semenza, G. L. (2004). O2-regulated gene expression: Transcriptional control of cardiorespiratory physiology by HIF-1. *J. Appl. Physiol.* 96, 1173-7; discussion 1170-2.

Semenza, G. L. (2010). Oxygen homeostasis. *Wiley Interdiscip. Rev. Syst. Biol. Med.* 2, 336-361.

Semenza, G. L. and Wang, G. L. (1992). A nuclear factor induced by hypoxia via de novo protein synthesis binds to the human erythropoietin gene enhancer at a site required for transcriptional activation. *Mol. Cell. Biol.* 12, 5447-5454.

Semenza, G. L., Nejfelt, M. K., Chi, S. M. and Antonarakis, S. E. (1991). Hypoxia-inducible nuclear factors bind to an enhancer element located 3' to the human erythropoietin gene. *Proc. Natl. Acad. Sci. U. S. A.* 88, 5680-5684.

Senoo-Matsuda, N., Yasuda, K., Tsuda, M., Ohkubo, T., Yoshimura, S., Nakazawa, H., Hartman, P. S. and Ishii, N. (2001). A defect in the cytochrome b large subunit in complex II causes both superoxide anion overproduction and abnormal energy metabolism in caenorhabditis elegans. *J. Biol. Chem.* 276, 41553-41558.

Shannon, A. M., Bouchier-Hayes, D. J., Condron, C. M. and Toomey, D. (2003). Tumour hypoxia, chemotherapeutic resistance and hypoxia-related therapies. *Cancer Treat. Rev.* 29, 297-307.

Sharp, F. R. and Bernaudin, M. (2004). HIF1 and oxygen sensing in the brain. *Nat. Rev. Neurosci.* 5, 437-448.

Sheline, C., Zhu, J., Zhang, W., Shi, C., Cai, A. (2013). Mitochondrial inhibitor models of Huntington's Disease and Parkinson's Disease induce zinc accumulation and are attenuated by inhibition of zinc neurotoxicity in vitro or in vivo. *Neurodegener Dis.* 11,49–58.

Sheta, E. A., Trout, H., Gildea, J. J., Harding, M. A. and Theodorescu, D. (2001). Cell density mediated pericellular hypoxia leads to induction of HIF-1alpha via nitric oxide and Ras/MAP kinase mediated signaling pathways. *Oncogene* 20, 7624-7634.

Shukla, S., Sumaria, CS., Pradeepkumar, PI. (2012). Exploring chemical modifications for siRNA therapeutics: a structural and functional outlook. *ChemMedChem*. 5(3):328-349.

Sodhi, A., Montaner, S., Patel, V., Zohar, M., Bais, C., Mesri, E. A. and Gutkind, J. S. (2000). The kaposi's sarcoma-associated herpes virus G protein-coupled receptor up-regulates vascular endothelial growth factor expression and secretion through mitogen-activated protein kinase and p38 pathways acting on hypoxia-inducible factor 1alpha. *Cancer Res.* 60, 4873-4880.

Soilleux, E. J., Turley, H., Tian, Y. M., Pugh, C. W., Gatter, K. C. and Harris, A. L. (2005). Use of novel monoclonal antibodies to determine the expression and distribution of the hypoxia regulatory factors PHD-1, PHD-2, PHD-3 and FIH in normal and neoplastic human tissues. *Histopathology* 47, 602-610.

Soundararajan, S., Wang, L., Sridharan, V., Chen, W., Courtenay-Luck, N., Jones, D., Spicer, E. K. and Fernandes, D. J. (2009). Plasma membrane nucleolin is a receptor for the anticancer aptamer AS1411 in MV4-11 leukemia cells. *Mol. Pharmacol.* 76, 984-991.

Stebbins, C. E., Kaelin, W. G.,Jr and Pavletich, N. P. (1999). Structure of the VHL-ElonginC-ElonginB complex: Implications for VHL tumor suppressor function. *Science* 284, 455-461.

Stoltenburg, R., Reinemann, C. and Strehlitz, B. (2007). SELEX--a (r)evolutionary method to generate high-affinity nucleic acid ligands. *Biomol. Eng.* 24, 381-403.

Storgaard, J., Kornblit, B. T., Zimmer, J. and Gramsbergen, J. B. (2000). 3-nitropropionic acid neurotoxicity in organotypic striatal and corticostriatal slice cultures is dependent on glucose and glutamate. *Exp. Neurol.* 164, 227-235.

Sudarshan, S., Sourbier, C., Kong, H. S., Block, K., Valera Romero, V. A., Yang, Y., Galindo, C., Mollapour, M., Scroggins, B., Goode, N. et al. (2009). Fumarate hydratase deficiency in renal cancer induces glycolytic addiction and hypoxia-inducible transcription factor 1alpha stabilization by glucose-dependent generation of reactive oxygen species. *Mol. Cell. Biol.* 29, 4080-4090.

Sulis, M. L. and Parsons, R. (2003). PTEN: From pathology to biology. *Trends Cell Biol.* 13, 478-483.

Svensson, R. U., Barnes, J. M., Rokhlin, O. W., Cohen, M. B. and Henry, M. D. (2007). Chemotherapeutic agents up-regulate the cytomegalovirus promoter: Implications for bioluminescence imaging of tumor response to therapy. *Cancer Res.* 67, 10445-10454.

Takahata, S., Sogawa, K., Kobayashi, A., Ema, M., Mimura, J., Ozaki, N. and Fujii-Kuriyama, Y. (1998). Transcriptionally active heterodimer formation of an arnt-like PAS protein, Arnt3, with HIF-1a, HLF, and clock. *Biochem. Biophys. Res. Commun.* 248, 789-794.

Tanahashi, N., Suzuki, M., Fujiwara, T., Takahashi, E., Shimbara, N., Chung, C. H. and Tanaka, K. (1998). Chromosomal localization and immunological analysis of a family of human 26S proteasomal ATPases. *Biochem. Biophys. Res. Commun.* 243, 229-232.

Tanimoto, K., Makino, Y., Pereira, T. and Poellinger, L. (2000). Mechanism of regulation of the hypoxia-inducible factor-1 alpha by the von hippel-lindau tumor suppressor protein. *EMBO J.* 19, 4298-4309.

Taschner, P. E., Jansen, J. C., Baysal, B. E., Bosch, A., Rosenberg, E. H., Brocker-Vriends, A. H., van Der Mey, A. G., van Ommen, G. J., Cornelisse, C. J. and Devilee, P. (2001). Nearly all hereditary paragangliomas in the netherlands are caused by two founder mutations in the SDHD gene. *Genes Chromosomes Cancer* 31, 274-281.

Thomas, D. D., Espey, M. G., Ridnour, L. A., Hofseth, L. J., Mancardi, D., Harris, C. C. and Wink, D. A. (2004). Hypoxic inducible factor 1alpha, extracellular signal-regulated kinase, and p53 are regulated by distinct threshold concentrations of nitric oxide. *Proc. Natl. Acad. Sci. U. S. A.* 101, 8894-8899.

Tian, H., McKnight, S. L. and Russell, D. W. (1997). Endothelial PAS domain protein 1 (EPAS1), a transcription factor selectively expressed in endothelial cells. *Genes Dev.* 11, 72-82.

Tomlinson, I. P., Alam, N. A., Rowan, A. J., Barclay, E., Jaeger, E. E., Kelsell, D., Leigh, I., Gorman, P., Lamlum, H., Rahman, S. et al. (2002). Germline mutations in FH predispose to dominantly inherited uterine fibroids, skin leiomyomata and papillary renal cell cancer. *Nat. Genet.* 30, 406-410.

Ui-Tei, K., Nishi, K., Takahashi, T., Nagasawa, T., (2012). Thermodynamic Control of Small RNA-Mediated Gene Silencing. *Front Genet*.3,101.

van den Heuvel, L. and Smeitink, J. (2001). The oxidative phosphorylation (OXPHOS) system: Nuclear genes and human genetic diseases. *Bioessays* 23, 518-525.

van der Mey, A. G., Maaswinkel-Mooy, P. D., Cornelisse, C. J., Schmidt, P. H. and van de Kamp, J. J. (1989). Genomic imprinting in hereditary glomus tumours: Evidence for new genetic theory. *Lancet* 2, 1291-1294.

Vanharanta, S., Buchta, M., McWhinney, S. R., Virta, S. K., Peczkowska, M., Morrison, C. D., Lehtonen, R., Januszewicz, A., Jarvinen, H., Juhola, M. et al. (2004). Early-onset renal cell carcinoma as a novel extraparaganglial component of SDHB-associated heritable paraganglioma. *Am. J. Hum. Genet.* 74, 153-159.

Wang, G. L., Jiang, B. H., Rue, E. A. and Semenza, G. L. (1995). Hypoxia-inducible factor 1 is a basic-helix-loop-helix-PAS heterodimer regulated by cellular O2 tension. *Proc. Natl. Acad. Sci. U. S. A.* 92, 5510-5514.

Wang, J., Green, P. S. and Simpkins, J. W. (2001). Estradiol protects against ATP depletion, mitochondrial membrane potential decline and the generation of reactive oxygen species induced by 3-nitroproprionic acid in SK-N-SH human neuroblastoma cells. *J. Neurochem.* 77, 804-811.

Weber, K., Ridderskamp, D., Alfert, M., Hoyer, S. and Wiesner, R. J. (2002). Cultivation in glucose-deprived medium stimulates mitochondrial biogenesis and oxidative metabolism in HepG2 hepatoma cells. *Biol. Chem.* 383, 283-290.

Wei, G., Hough, C. J. and Sarvey, J. M. (2004). The mitochondrial toxin, 3-nitropropionic acid, induces extracellular Zn2+ accumulation in rat hippocampus slices. *Neurosci. Lett.* 370, 118-122.

Weiss, W., Taylor, S., Shokat, K. (2007). Recognizing and exploiting differences between RNAi and smallmolecule inhibitors. *Nat. Chem. Biol.* 3(12), 739–744.

Wenger, R. H., Stiehl, D. P. and Camenisch, G. (2005). Integration of oxygen signaling at the consensus HRE. *Sci. STKE* 2005, re12.

Wiesener, M. S., Turley, H., Allen, W. E., Willam, C., Eckardt, K. U., Talks, K. L., Wood, S. M., Gatter, K. C., Harris, A. L., Pugh, C. W. et al. (1998). Induction of endothelial PAS domain protein-1 by hypoxia: Characterization and comparison with hypoxia-inducible factor-1alpha. *Blood* 92, 2260-2268.

Wilkinson, K. D., Ventii, K. H., Friedrich, K. L. and Mullally, J. E. (2005). The ubiquitin signal: Assembly, recognition and termination. symposium on ubiquitin and signaling. *EMBO Rep.* 6, 815-820.

Willam, C., Masson, N., Tian, Y. M., Mahmood, S. A., Wilson, M. I., Bicknell, R., Eckardt, K. U., Maxwell, P. H., Ratcliffe, P. J. and Pugh, C. W. (2002). Peptide blockade of HIFalpha degradation modulates cellular metabolism and angiogenesis. *Proc. Natl. Acad. Sci. U. S. A.* 99, 10423-10428.

Woodward, E. R. and Maher, E. R. (2006). Von hippel-lindau disease and endocrine tumour susceptibility. *Endocr. Relat. Cancer* 13, 415-425.

Wouters, B. G. and Koritzinsky, M. (2008). Hypoxia signalling through mTOR and the unfolded protein response in cancer. *Nat. Rev. Cancer.* 8, 851-864.

Xu, J. and Li, Q. (2003). Review of the in vivo functions of the p160 steroid receptor coactivator family. *Mol. Endocrinol.* 17, 1681-1692.

Yamakuchi, M., Lotterman, C. D., Bao, C., Hruban, R. H., Karim, B., Mendell, J. T., Huso, D. and Lowenstein, C. J. (2010). P53-induced microRNA-107 inhibits HIF-1 and tumor angiogenesis. *Proc. Natl. Acad. Sci. U. S. A.* 107, 6334-6339.

Yankovskaya, V., Horsefield, R., Tornroth, S., Luna-Chavez, C., Miyoshi, H., Leger, C., Byrne, B., Cecchini, G. and Iwata, S. (2003). Architecture of succinate dehydrogenase and reactive oxygen species generation. *Science* 299, 700-704.

Yano, T. (2002). The energy-transducing NADH: Quinone oxidoreductase, complex I. *Mol. Aspects Med.* 23, 345-368.

Yasinska, I. M. and Sumbayev, V. V. (2003). S-nitrosation of cys-800 of HIF-1alpha protein activates its interaction with p300 and stimulates its transcriptional activity. *FEBS Lett.* 549, 105-109.

Yin, Z., Haynie, J., Yang, X., Han, B., Kiatchoosakun, S., Restivo, J., Yuan, S., Prabhakar, N. R., Herrup, K., Conlon, R. A. et al. (2002). The essential role of Cited2, a negative regulator for HIF-1alpha, in heart development and neurulation. *Proc. Natl. Acad. Sci. U. S. A.* 99, 10488-10493.

Yoo, Y. G., Oh, S. H., Park, E. S., Cho, H., Lee, N., Park, H., Kim, D. K., Yu, D. Y., Seong, J. K. and Lee, M. O. (2003). Hepatitis B virus X protein enhances transcriptional activity of hypoxia-inducible factor-1alpha through activation of mitogen-activated protein kinase pathway. *J. Biol. Chem.* 278, 39076-39084.

Yu, A. Y., Shimoda, L. A., Iyer, N. V., Huso, D. L., Sun, X., McWilliams, R., Beaty, T., Sham, J. S., Wiener, C. M., Sylvester, J. T. et al. (1999). Impaired physiological responses to chronic hypoxia in mice partially deficient for hypoxia-inducible factor 1alpha. *J. Clin. Invest.* 103, 691-696.

Yu, B., Miao, Z. H., Jiang, Y., Li, M. H., Yang, N., Li, T. and Ding, J. (2009). c-jun protects hypoxia-inducible factor-1alpha from degradation via its oxygen-dependent degradation domain in a nontranscriptional manner. *Cancer Res.* 69, 7704-7712.

Yu, F., White, S. B., Zhao, Q. and Lee, F. S. (2001). HIF-1alpha binding to VHL is regulated by stimulus-sensitive proline hydroxylation. *Proc. Natl. Acad. Sci. U. S. A.* 98, 9630-9635.

Zagorska, A. and Dulak, J. (2004). HIF-1: The knowns and unknowns of hypoxia sensing. *Acta Biochim. Pol.* 51, 563-585.

Zhang, J. G., Wang, J. J., Zhao, F., Liu, Q., Jiang, K. and Yang, G. H. (2010). MicroRNA-21 (miR-21) represses tumor suppressor PTEN and promotes growth and invasion in non-small cell lung cancer (NSCLC). *Clin. Chim. Acta* 411, 846-852.

Zhang, X. D., Wang, Y., Wu, J. C., Lin, F., Han, R., Han, F., Fukunaga, K. and Qin, Z. H. (2009). Down-regulation of bcl-2 enhances autophagy activation and cell death induced by mitochondrial dysfunction in rat striatum. *J. Neurosci. Res.* 87, 3600-3610.

Zhao, S., Lin, Y., Xu, W., Jiang, W., Zha, Z., Wang, P., Yu, W., Li, Z., Gong, L., Peng, Y. et al. (2009). Glioma-derived mutations in IDH1 dominantly inhibit IDH1 catalytic activity and induce HIF-1alpha. *Science* 324, 261-265.

Zhong, H., Chiles, K., Feldser, D., Laughner, E., Hanrahan, C., Georgescu, M. M., Simons, J. W. and Semenza, G. L. (2000). Modulation of hypoxia-inducible factor 1alpha expression by the epidermal growth factor/phosphatidylinositol 3-kinase/PTEN/AKT/FRAP pathway in human prostate cancer cells: Implications for tumor angiogenesis and therapeutics. *Cancer Res.* 60, 1541-1545.

Zhou, J. and Brune, B. (2005). NO and transcriptional regulation: From signaling to death. *Toxicology* 208, 223-233.

Zhou, J., Schmid, T., Frank, R. and Brune, B. (2004). PI3K/Akt is required for heat shock proteins to protect hypoxia-inducible factor 1alpha from pVHL-independent degradation. *J. Biol. Chem.* 279, 13506-13513.

Zhou, Q., Liu, L. Z., Fu, B., Hu, X., Shi, X., Fang, J. and Jiang, B. H. (2007). Reactive oxygen species regulate insulin-induced VEGF and HIF-1alpha expression through the activation of p70S6K1 in human prostate cancer cells. *Carcinogenesis* 28, 28-37.

Zuker, M. (2003). Mfold web server for nucleic acid folding and hybridization prediction. *Nucleic Acids Res.* 31, 3406-3415.

Zundel, W., Schindler, C., Haas-Kogan, D., Koong, A., Kaper, F., Chen, E., Gottschalk, A. R., Ryan, H. E., Johnson, R. S., Jefferson, A. B. et al. (2000). Loss of PTEN facilitates HIF-1-mediated gene expression. *Genes Dev.* 14, 391-396.